AVANCES EN SISTEMAS INTERACTIVOS PARA PERSONAS CON PARÁLISIS CEREBRAL

Leticia Peña Carrodeguas

UNIVERSITAT ROVIRA i VIRGILI

Synthesis of Biobased Polymers derived from Terpenes

Leticia Peña Carrodeguas

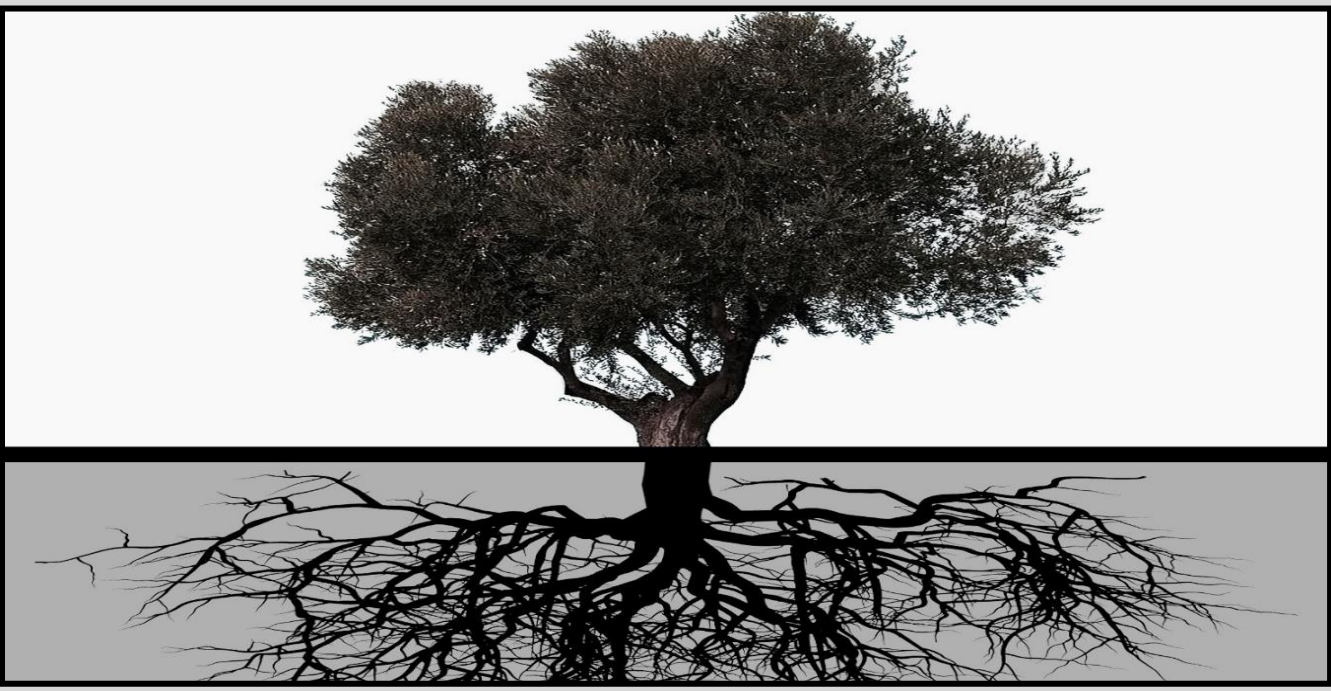

DOCTORAL THESIS
2017

UNIVERSITAT ROVIRA I VIRGILI
AVANCES EN SISTEMAS INTERACTIVOS PARA PERSONAS CON PARÁLISIS CEREBRAL
Leticia Peña Carrodeguas

UNIVERSITAT ROVIRA I VIRGILI
AVANCES EN SISTEMAS INTERACTIVOS PARA PERSONAS CON PARÁLISIS CEREBRAL
Leticia Peña Carrodeguas

PhD Thesis

Synthesis of Biobased polymers derived from Terpenes

Leticia Peña Carrodeguas

Supervised by Prof. Dr. Arjan W. Kleij

Tarragona

June 2017

UNIVERSITAT ROVIRA I VIRGILI
AVANCES EN SISTEMAS INTERACTIVOS PARA PERSONAS CON PARÁLISIS CEREBRAL
Leticia Peña Carrodeguas

UNIVERSITAT ROVIRA i VIRGILI

ICIQ

Prof. Dr. Arjan W. Kleij, Group Leader at the Institute of Chemical Research of Catalonia (ICIQ) and Research Professor of the Catalan Institution for Research and Advanced Studies (ICREA),

I STATE that the present study, entitled "Synthesis of Biobased Polymers derived from Terpenes" presented by Leticia Peña Carrodeguas for the award of the degree of Doctor, has been carried out under my supervision at Institute of Chemical Research of Catalonia (ICIQ)

Tarragona, June 2017

Doctoral Thesis Supervisor
Prof. Dr. Arjan W. Kleij

UNIVERSITAT ROVIRA I VIRGILI
AVANCES EN SISTEMAS INTERACTIVOS PARA PERSONAS CON PARÁLISIS CEREBRAL
Leticia Peña Carrodeguas

“Quote”

UNIVERSITAT ROVIRA I VIRGILI
AVANCES EN SISTEMAS INTERACTIVOS PARA PERSONAS CON PARÁLISIS CEREBRAL
Leticia Peña Carrodeguas

Table of Contents

General introduction

UNIVERSITAT ROVIRA I VIRGILI
AVANCES EN SISTEMAS INTERACTIVOS PARA PERSONAS CON PARÁLISIS CEREBRAL
Leticia Peña Carrodeguas

Prologue

Polymers can considered highly useful commodity chemicals to increase the quality of our everyday life and find applications in a vast and diverse range of consumer products including clothing, construction and automotive materials, medicine and diagnostics, among others. Furthermore, polymers are extensively used for separation, purification and increased energy efficient processes. Given the broad scope of polymers, only 6 % of the oil produced worldwide is used for polymer manufacture; nevertheless, there are increasing environmental and health concerns associated to both the raw materials used for polymer synthesis and their end-to-life fate.[1]

Use of renewable based raw materials to produce "green" plastics is increasingly considered a feasible and desirable strategy to loosen the grip on depleting resources such as oil, while developing new monomers and materials retaining or improving the characteristics of commonly employed plastics. There are some key factors to take into account in order to pursue a smooth transition towards renewable based plastics: (a) *bio-refinery integration*: the term "biorefinery" defines a facility that integrates biomass conversion process and equipment to produce fuels, power and chemicals in an analogous manner to known oil refinery. Not only bio-refineries will need to be integrated within the existing oil refinery technology, but the impact of the use of renewable based raw materials on food and feed production should be carefully considered and modeled; (b) *choice of raw materials*: for example, biopolymers such as cellulose, hemicellulose and lignin represent the most abundant source of carbon available on Earth. Development of reliable and efficient physico-chemical strategies to depolymerise and/or functionalise these biopolymers would represent a key milestone in the development of renewable base plastics. Another class of interesting and renewable based monomers are long- and short-chain organic acids, which can be directly obtained from forestry and agriculture waste and/or by microorganism fermentation. These materials can be precisely engineered at a molecular level into renewable polymers in a way similar to some of the plastics derived from petroleum chemicals. A notable example is represented by poly(lactic acid) (PLA) which has been commercially used for over 50 years. The use of terpene, terpenoids and rosins is potentially relevant to the development of rigid and stiff plastics, therefore access to and preparation of new monomers and polymerisation processes based on this class of cyclic aliphatic compounds would represent a step forward in the preparation of high-end renewable based plastics.[2]

I.1 Thermoplastics in everyday life

Thermoplastics are widely used in modern life. Depending on their density, optic properties, glass transition and/or decomposition temperature, thermoplastics are used in specific applications including (but not limited to) vehicle parts, glass substitutes, electronics, fiber clothing, furniture and coatings. The properties of thermoplastics are characterized by the starting monomer(s) which are converted to polymers (e.g. polyethylene, polystyrene and polylactic acid). When more than one monomer is used and/or additional functionalities are added during the polymerization process, the resulting copolymer is named after the new functionality embedded in the polymer chain: for example, polyesters and polyurethanes, are copolymers containing esters and carbamates repeating units, respectively.

Polystyrene[3] is one of the most commonly used thermoplastics, formed via homo-polymerization of styrene, a cheap and readily available aromatic monomer, resulting in a rigid homo-polymers. Because of these properties, polystyrene is the default choice for many commonly employed plastic products (such as disposable containers and thermal and acoustic insulation). Styrene is also widely used as a co-monomer in thermoplastic terpolymers, for example acrylonitrile butadiene styrene (ABS), where styrene is polymerized with acrylonitrile in the presence of polybutadiene. While the cost of producing ABS is roughly twice the cost of producing polystyrene, it is considered a superior polymer for its hardness, gloss, toughness, and electrical insulation properties. Moreover, easy ABS injection molding and extrusion render it extremely useful for manufacturing pipes, golf club heads, car components or LEGO® bricks. Poly-alkenes are another class of widely employed thermoplastics in which the polyalkene units are held together via C–C bonds. Polyethylene (PE), polypropylene (PP), polyvinyl chlorides (PVC) and polyacrylates are typical examples of alkene homo-polymerization products, and commonly employed materials. Notably, PP, PS and PVC represent approximately 70% of the worldwide production and consumption of thermoplastic materials.

Other relevant thermoplastics are polyamides, polycarbonates, polyesters and polyurethanes. These materials are copolymers formed by the copolymerization of two monomers which are differentiated from each other by the overall functionalities (*i.e*, amide, carbonate, ester or carbamate units, respectively). Polyurethanes are the most widely employed, accounting for approximately 5% of the global plastic production.

I.2 Polyesters and polycarbonates

These two classes of polymers are characterized by the presence of ester (-CO_2-) or carbonate (-CO_3-) fragments, respectively. Although some commercially available biodegradable homo-polymers such as polylactic acid (PLA) or polyglycolic acid (PGA) are considered as polyesters, generally the term "polyesters" refers to *co*-polymers obtained from the condensation of a diacid and a polyol in a step-growth polymerization process.[4] Polyesters are widely used in clothing and as a "finisher" in high-quality wood products such as guitars, pianos or decorative objects.

The most commonly employed and commercially available polyester is polyethylene terephthalate (PET).[3] The monomer bis-(2-hydroxyethyl) terephthalate can be synthesized by the esterification reaction between terephthalic acid and ethylene glycol with water as by-product, or by a transesterification reaction between ethylene glycol and dimethyl terephthalate, obtaining methanol as byproduct. In the latter process, dimethyl terephthalate and an excess of ethylene glycol are melted at 150–200 °C in the presence of a basic catalyst. The high temperatures associated to this process have a dual effect: (a) to ensure that the reaction mixture is homogeneous; (b) to remove the volatile by-product(s), water or methanol, that are formed. Excess ethylene glycol is distilled off at a higher temperature under reduced pressure. The second transesterification step proceeds at 270–280 ºC, with continuous distillation of ethylene glycol.

Scheme I.1 PET industrial synthesis.

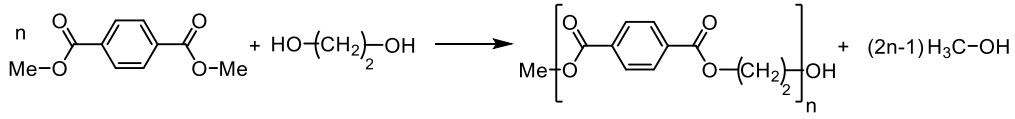

Nevertheless, terephthalic acid and ethylene glycol are non-renewable, fossil fuel based materials. In particular, the diacid is obtained by oxidation of xylene, while ethylene glycol is prepared via oxidation of ethene to ethylene oxide followed by a ring opening reaction with water as the nucleophile. Considering the environmental issues associated to fossil fuel dependency and non-renewable feedstock depletion, there is widespread academic and industrial interest in developing alternative ways to produce polyesters and the requisite monomers.

Polycarbonates,[3] on the other hand, are stiff, tough materials characterized by optical transparency. From a material properties point of view, polycarbonates combine several useful

features including temperature resistance and desirable optical properties such as transparency, which position them between commodity plastics and engineering plastics. The main commercially exploited polycarbonate material is produced by reaction of bisphenol-A (BPA) and phosgene ($COCl_2$).

Scheme I.2 Polycarbonate industrial synthesis.

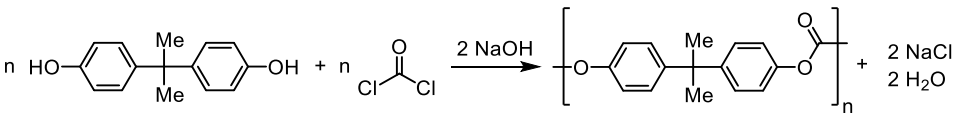

The first step of the synthesis involves treatment of deprotonation of the phenolic groups on bisphenol-A with NaOH. The resulting anion reacts with phosgene to yield a chloroformate, which subsequently is attacked by another phenoxide resulting in growth of the polycarbonate chain. Approximately one billion kilograms of polycarbonate is produced annually using this methodology. The use of phosgene is associated to health and safety concerns, as well as severe toxicity hazards and environmental issues, hence its synthesis and usage is subject to strict regulations. Therefore, the development of alternative greener methods based on alternative "carbonylation" sources is a highly relevant research topic. For example, at an industrial level, diphenyl carbonate has been used to some extent as a greener phosgene replacement as it forms polycarbonates by transesterification with dialcohol monomers in a melt polymerization process.[5]

There is an increasing need to develop sustainable, alternative methodologies for the preparation of commercially relevant polymers according to the 12 principles of Green Chemistry.[6] This can eventually contribute in reducing fossil fuel dependence while, where possible, replace hazardous processes with more environmentally benign and safer ones. Many efforts have been devoted to this aim, and, in the next section we will discuss selected examples of state-of-the-art sustainable alternatives for the preparation of polyesters and polycarbonates.

I.3 Alternative synthesis: ROP and ROCOP

As has been mentioned before, the most common route for polyester synthesis is the step-growth polymerization of diacids or diesters with diols.[4] This method has several important drawbacks: (1) formation of stoichiometric amounts of byproduct (water or alcohol) which need

to be removed at high temperatures and/or low pressures; (2) broad polydispersity (*Đ*) of the resulting polymer chains (*Đ* >2) resulting from the inability to control accurately the molecular weight of the polymers, and (3) high monomer conversion required to achieve high molecular weight (M_n) polymers. The most promising alternative route is represented by chain-growth polymerization. In contrast to step-growth polymerization, no by-products are formed during this type of polymerization reaction. Additionally, polymers with high molecular weights (M_n) and low polydispersity (*Đ*) can be obtained even at low monomer conversions.

Due to these advantages, there has been great interest in developing chain-growth polymerization methods. Two of the most effective strategies towards polyesters and polycarbonates through chain-growth polymerization are the ring-opening polymerization (ROP) of cyclic esters or carbonates, and the ring-opening copolymerization (ROCOP) of epoxides with cyclic anhydrides or carbon dioxide.

Scheme I.3 Generic ROP and ROCOP reactions to prepare polyesters and polycarbonates.

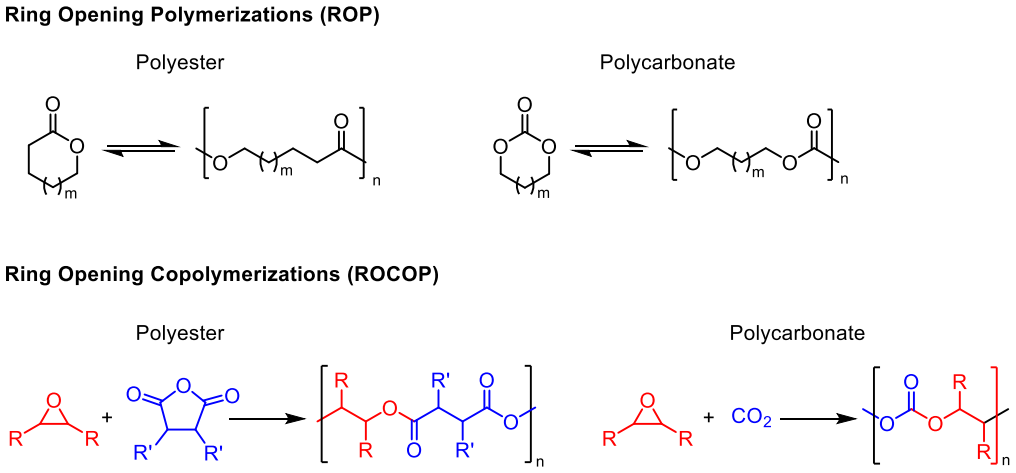

I.3.1 Ring opening polymerization (ROP)

The ring opening polymerization (ROP) of lactones and cyclic carbonates is an attractive method to prepare aliphatic polyesters and polycarbonates, respectively. The reaction occurs via living polymerization in which the terminal end of a polymer chain acts as a reactive center where further cyclic monomers (carbonates or lactones) are inserted through ring opening to form a longer polymer chain. The thermodynamic driving force for these polymerization

reactions is the relief of the ring strain in the monomer. Accordingly, noticeable differences in reactivity are noted among this type of monomers depending on the nature of the cyclic monomer. ROP, especially of lactones, has been widely studied and a broad variety of initiators such as organocatalysts, metal alkoxides and metal complexes have been explored.[7]

The first step in the ROP mechanism is the anionic, cationic or coordination–insertion initiation. The most common initiators in polyester and polycarbonate synthesis are anionic (e.g. Cl^-, Br^- or MeO^-). The reaction proceeds in the presence of a Lewis acid catalyst and a nucleophilic co-catalyst. The Lewis acid catalyst coordinates the carbonyl oxygen atom and activates the cyclic monomer. The ROP process is then triggered by the nucleophilic attack of the initiator to the electrophilic carbon atom in the cyclic monomer, forming a metal alkoxide intermediate that acts as a nucleophile and attacks a second monomer unit and upon repetition of this sequence, a polymer is obtained. Scheme I.4 shows the mechanism for ROP of a lactide monomer in which initially the nucleophilic (metal alkoxide or amide) co-catalyst is coordinated by a labile bond to the Lewis acid catalyst (*i.e.*, initiation occurs by coordination-insertion).

Scheme I.4 Coordination-insertion mechanism for lactide ROP.

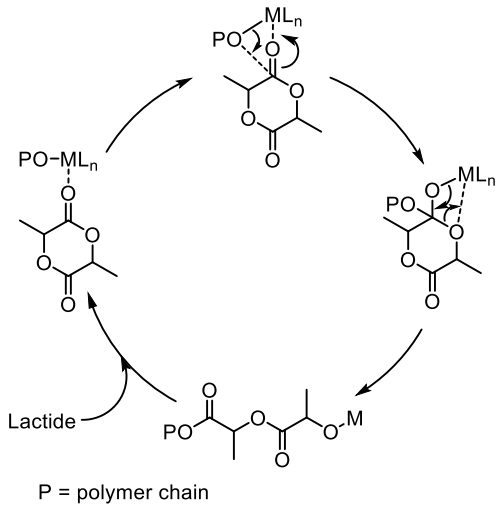

Several reviews have already covered the selection and range of initiators tested.[7–18] The most explored class of cyclic monomers are those derived from ε-caprolactone (with substitution at the 3-, 4- or 5-position in the monomer) and lactide to form poly(lactic acid) PLA. Among the available selection of biodegradable polymers for biomedical applications and large-scale replacement of oil-based commodity plastics synthesized from renewable resources, PLA is

certainly the most promising polymer today. While the synthesis of PLA can be realized by either polycondensation of lactic acid or ring-opening polymerization (ROP) of lactide, ROP enables a higher degree of control over the polymer output parameters. This increased control leads to lower polydispersities, and higher molecular weight in comparison to polycondensation reactions.

Nevertheless, the ROP of lactones and cyclic carbonates has some important limitations. Side reactions such as transesterification are common, particularly at high conversion. Also, since only one type of monomer is used, the resulting polymers have a limited range of properties due to the lack of functional diversity in the available monomers. For instance, PLA has a T_g of approximately 60 ºC which is quite low and limits its usage in cooking applications and food storage. Additionally, synthesis of functionalized monomers for ROP can be challenging and there are no guarantees that the chemical elaboration/modification of the lactone or cyclic carbonate will allow polymerization to occur at all.[19] As a result of the modification of the lactone or carbonate, the ring strain is often reduced reducing the thermodynamic driving force for the polymerization reaction to occur. One of the mayor drawbacks of ROP for the synthesis of polyesters and polycarbonates is the limitation in the production of polymers containing aromatic groups in the polymer backbone, a desirable goal to increase thermal and mechanical properties.

I.3.2 Ring opening copolymerization (ROCOP)

An alternative chain-growth route to both aliphatic and semi-aromatic[20–25] polymers is represented by ring opening co-polymerizations (ROCOP). ROCOP reactions are used to produce polyesters and polycarbonates by an alternative method, which relies on the co-polymerization of two different monomers: epoxide and cyclic anhydrides in the case of polyesters, and epoxides and CO_2 for the synthesis of polycarbonates.

Scheme I.5 Epoxide co-polymerizations towards polyesters and polycarbonates.

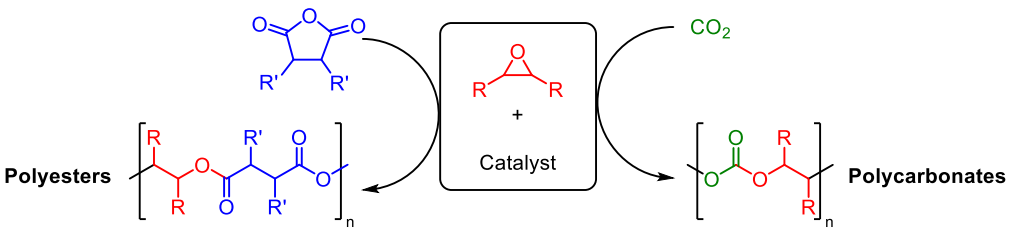

In contrast to ROP, ROCOP chain-growth polymerization has received far less attention. The major advantage of ROCOP in comparison with ROP is that the use of two different sets of monomers allows for the facile tuning of the properties of the resulting materials by the substitution of just one of the monomers.[26][27] Furthermore, the monomers (epoxides, anhydrides and CO_2) are easily accessible and many are commercially available or relatively straightforward to prepare from olefins or dicarboxylic acids. As a consequence, a wide range of monomers has been used in the synthesis of polyesters and polycarbonates, including bio-based epoxides and anhydrides and waste materials such as CO_2.[A]

Epoxide/anhydride ROCOP mechanism

ROCOP polymerizations require a 'catalyst' or, more accurately, an initiator. This species is often a single site metal complex of general form "LMX" (

Scheme I.**6**), where L is a ligand, M is the metal site at which catalysis occurs and X is the initiating group. In other cases, the metal catalyst M does not incorporate the initiating group X, and is then referred to as a binary system catalytic system (metal catalyst [M] plus nucleophilic initiator [X])

Scheme I.6 Generic steps proposed during epoxide/anhydride ROCOP

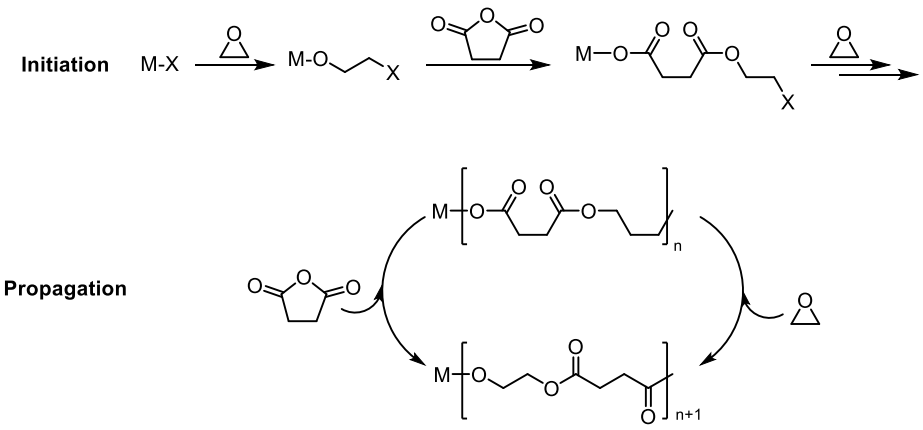

The *initiation* reaction involves monomer activation by coordination to the metal center of the MX Lewis acid catalyst. Subsequent nucleophilic attack of the initiator X generates a metal

[A] See section I.3.3 "*Renewable monomer scope*" in this chapter for further information.

alkoxide intermediate. The initiating group is commonly a carboxylate, alkoxide or halide group. The *propagation* reaction occurs as monomers are sequentially enchained, involving the sequential formation of metal-alkoxide and carboxylate intermediates. The metal alkoxide intermediate attacks the anhydride to generate the metal carboxylate intermediate, which attacks and ring-opens the epoxide co-monomer to regenerate a metal alkoxide species. The *termination* of the polymerization is typically controlled by manipulating the conditions (reducing temperature or monomer removal) or by addition of water or acids to stop the reaction.

Epoxide/carbon dioxide ROCOP mechanism

The mechanism of the ROCOP of epoxide and CO_2 is rather similar to the one proposed for the ROCOP of epoxide and cyclic anhydride. Similar to the previous case, the Lewis acid metal complex initiates the copolymerization by coordinating the epoxide monomer, which is then attacked by the nucleophilic group X leading to epoxide ring-opening and formation of a metal bound alkoxide. The metal alkoxide is able to undergo CO_2 insertion to form a metal carbonate.

Scheme I.7 Proposed catalytic cycle for the ring-opening copolymerization of CO_2 and epoxides.

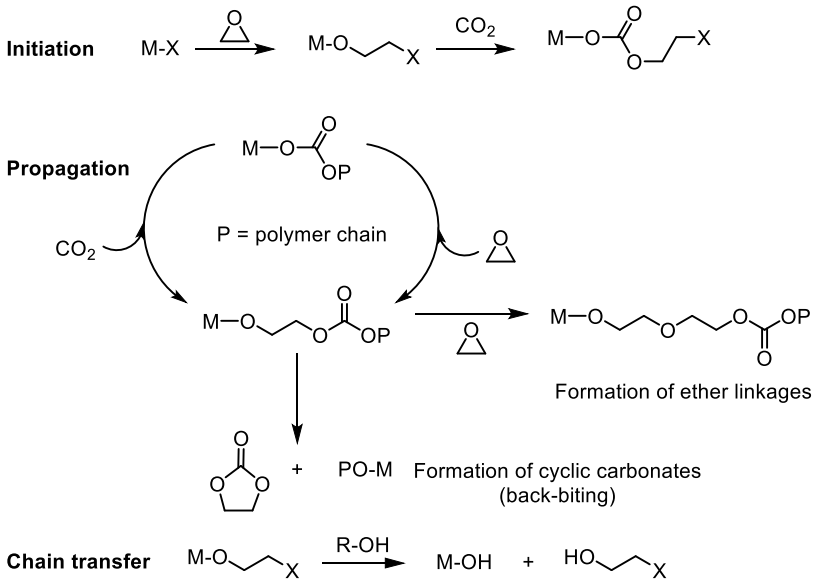

In principle this mechanism should lead to a copolymer with only carbonate linkages (or ester linkages in the case of ROCOP of epoxide and anhydride), however some catalysts also

induce homo-coupling of epoxides (ether linkage formation). For this type of mechanism, it is also possible that the propagation suffers from chain transfer via two possible routes: (a) intramolecular backbiting, and (b) reaction with a protic agent such as an alcohol, water or diacid.[B] Backbiting reactions occur when the metal alkoxide chain end attacks a carbonate linkage on the copolymer chain forming a cyclic carbonate by-product and regenerating a metal alkoxide/X species. The resulting back-biting products, five membered ring cyclic carbonates, are thermodynamically stable and do not undergo any further ring-opening polymerization therefore they are often detected as undesired by-products.

I.3.3 Renewable monomer scope

As we have mentioned before, one of the major advantages of ROCOP in comparison with ROP is the wide scope of available monomers potentially reactive towards the formation of polycarbonates and polyesters.

Epoxide and anhydride scope

To date, more than 20 epoxides and 20 anhydrides have been studied as monomers for the preparation of aliphatic and semi-aromatic polyesters. So far, the most widely studied epoxide monomers are cyclohexene oxide (CHO) and propylene oxide (PO), whereas phthalic anhydride (PA) is the commonly used anhydride monomer. All used epoxides and anhydrides reported to date are shown in Scheme I.8 and Scheme I.9, respectively.

Scheme I.8 Most commonly used anhydride monomers.

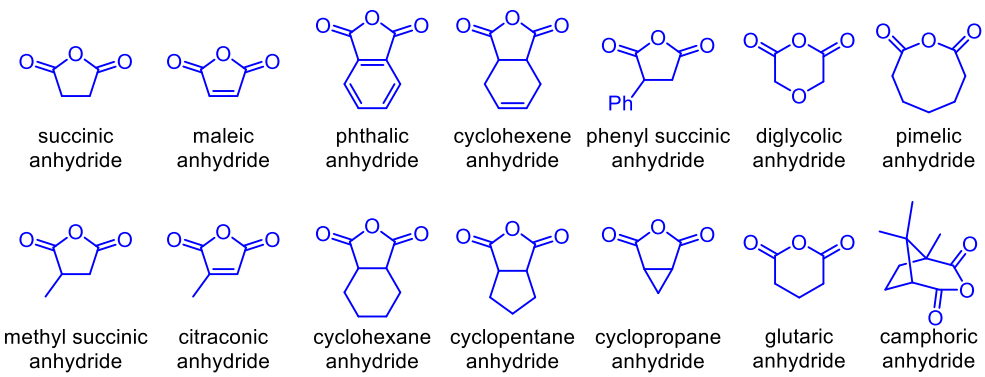

[B] Chain transfer will be discussed in detail in Chapter 2 of this thesis. Chain transfer agents can be useful to control the polymer properties (M_n, $Đ$) *a priori*.

Scheme I.9 Most commonly used epoxide monomers.

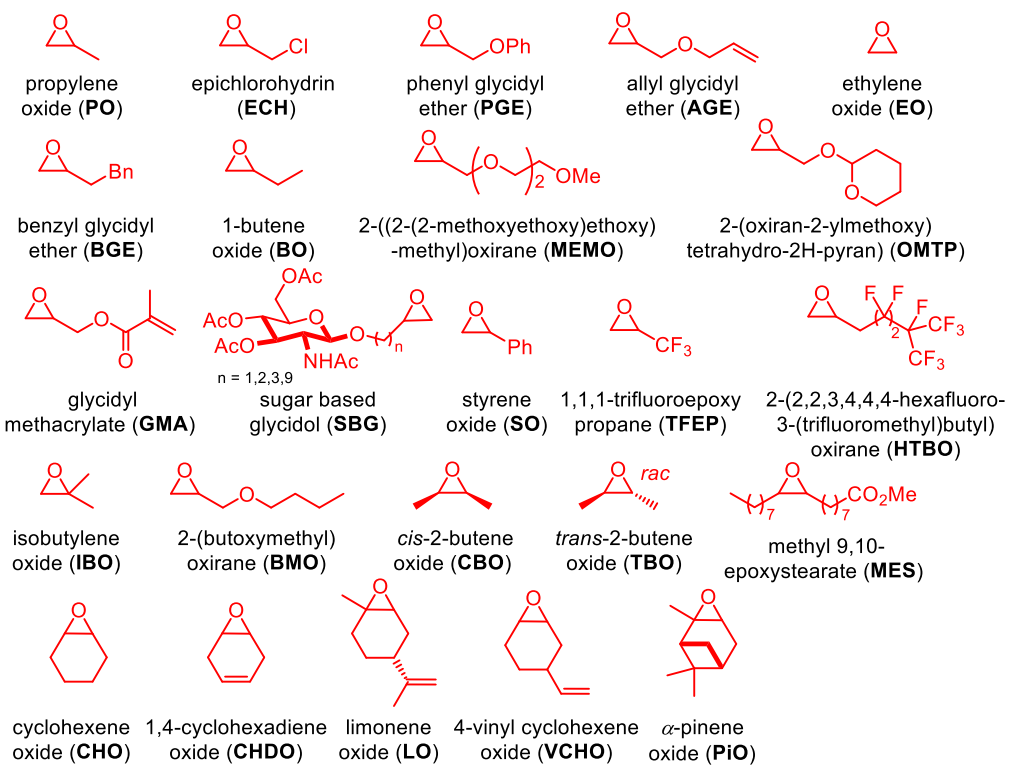

Polymers obtained from renewable sources have recently attracted considerable interest as alternatives to fossil-fuel-based polymers.[28–31] Succinic anhydride (which can be readily obtained from a renewable feedstock such as succinic acid) was the first renewable monomer tested for the synthesis of a well-defined alternating polyester from an epoxide/anhydride ROCOP, as reported by Maeda et al.[32] Since then, succinic anhydride has been commonly used in ROCOP polymerizations: for example, in 2005 Takusu and co-workers polymerized succinic anhydride with a renewable epoxide obtained from a sugar-based glycidol (SBG) to yield fully renewable polyesters.[33] Although the molecular weight of these polymers was low, it showed the potential of using renewable based monomers in polymer synthesis paving the way to future development towards renewable polymeric materials. Duchateau and co-workers[34] showed that succinic anhydride could be copolymerized with styrene oxide (SO) generating partially renewable, semi-aromatic polyesters. In the same report, they also polymerized styrene oxide with another renewable anhydride, citraconic anhydride, which can be obtained from itaconic acid. Itaconic acid is produced by fermentation of carbohydrates such as glucose.[35] Coates and

co-workers also copolymerized succinic anhydride with 4-vinylcyclohexene oxide and CHO[36] and at a later stage, they reported the synthesis of a renewable, "stereo-complexed" polyester of PO and succinic anhydride.[37] DiCiccio and Coates also reported in 2011 the use of several renewable glycidol-based epoxides[38] used in combination with maleic anhydride.

One of the most studied renewable based epoxide for ROCOP is a terpene derivative: limonene oxide. Terpenes and terpenoids are components of essential oils that are derived from plants and are characterized by the presence of isoprene unit(s) within their chemical structure.[39] The best-known example of a poly-terpene is natural rubber. Other terpenes are increasingly investigated as monomers for polymer production although on a much smaller scale. These studies includes limonene, which is extracted from the peel of citrus fruits.[39] In 2004, Coates and co-workers reported the first example of the copolymerization of limonene oxide and CO_2[40] to yield a fully renewable polycarbonate.[C] Limonene oxide was also employed in the ROCOP with cyclic anhydride monomers to yield semi-renewable polyesters. The group of Coates in particular studied the copolymerization of limonene oxide with diglycolic anhydride and maleic anhydride,[36] while Duchateau reported on the synthesis of semi-aromatic polyesters obtained by ROCOP of limonene oxide and phthalic anhydride.[34] In 2011, Thomas and co-workers[41] reported the use of limonene oxide and α-pinene oxide in the ROCOP using renewable anhydrides obtained by tandem synthesis of linear anhydrides from dicarboxylic acids. Four of the anhydrides used in this work were renewable (succinic anhydride, glutaric anhydride, pimelic anhydride and camphoric anhydride) affording several polymers resulting from a combination of completely renewable monomers. Finally, Coates and co-workers used the terpenes α-phellandrene and α-terpinene to generate, through a Diels-Alder reaction, tricyclic anhydrides for copolymerization with PO.[42,43]

The extensive range of renewable monomers that have been employed so far for ROCOP shows the diversity of functionality and renewable structures that can be incorporated into polymers.

Carbon dioxide

One advantage of using ROCOP for the synthesis of polycarbonates is the possibility of incorporating CO_2 into the polymer chain. CO_2 is a waste product from combustion of fossil fuels and as such, it is abundant, virtually renewable and characterized by low toxicity. Because CO_2 is characterized by a high degree of kinetic inertness, it has been a long-standing goal of

[C] This contribution will be discussed in more detail in Chapter 1 of this thesis.

synthetic chemists to develop catalyst and processes which activate and convert it into value-added products.[44–46] So far, polycarbonates produced from CO_2 do not have the same chemico-physical properties of conventional polycarbonates; however, they have been proposed as alternatives for commodity applications, including packaging, engineering polymers and elastomers.[45]

I.3.4 Catalyst

Many metal complexes have been investigated as catalysts for the ring opening copolymerization of epoxide and anhydrides or epoxides and carbon dioxide, including those based on zinc,[47–56] magnesium,[50,52,57] chromium,[20,24,34,41,52,58–64] cobalt,[20,34,37,41,52,56,59,60] manganese,[20,41,65–67] iron,[68] aluminum[20,33,41,43,59,60,69–71] and nickel[56] complexes. Many of these catalysts show higher activity upon the addition of a nucleophilic co-catalyst. A diverse array of co-catalysts has been used including bis(triphenylphosphine)-iminium salts (PPN-X), 4-dimethylaminopyridine (DMAP) and ammonium salts, with PPNX and DMAP being generally most effective. The most important metal complexes active towards ROCOP copolymerization will be briefly discussed in the next section.

Metalloporphyrins

Aida and Inoue reported the first well-controlled polymerization of PO with phthalic anhydride in 1985[69,70] using a catalytic system based on porphyrinato aluminum complexes and quaternary ammonium/phosphonium co-catalyst. The resulting polyesters were characterized by low molecular weights ($2.3 < M_n < 3$ kg/mol), but the narrow polydispersities ($Đ = 1.1$) hinted to a controlled polymerization process. However, the catalytic system displayed low activity as quantitative conversion of PO and phthalic anhydride was only achieved after prolonged reaction times (4–7 days) at room temperature. Inoue[72] and co-workers also reported in 1978 the use of similar metalloporphyrins for the copolymerization of PO and CHO with CO_2, using Al and Zn as the active metal centers. Since then, catalyst development in this field has resulted in multiple contributions reporting exceptional activity. Porphyrin systems have been widely investigated and this has led to the discovery of several related catalysts, including other aluminum derivatives,[60,70] as well as chromium,[24,60,61] cobalt,[60] iron[65] and manganese[65] based complexes. Porphyrin complexes have also been widely used for ROCOP by Chisholm and coworkers[73–75] in particular using Al, Cr and Co complexes for the copolymerization of PO and CO_2.

Scheme I.10 Porphyrin and corrole based catalysts used for ROCOP

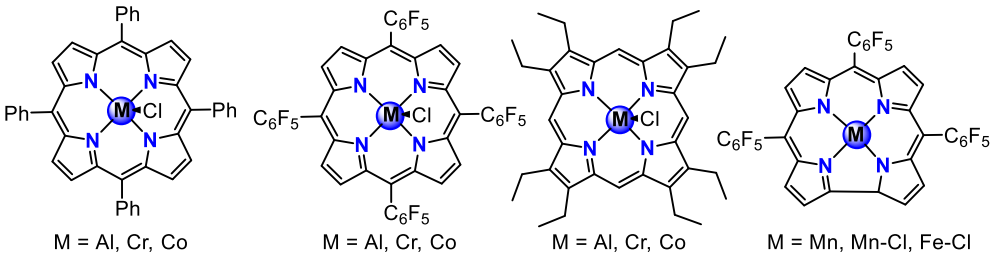

β-Diiminate (BDI) zinc complexes

Another major breakthrough was achieved by Coates and coworkers with the use of *β*-diiminate zinc or (BDI)Zn complexes. These complexes showed to be highly active catalysts for a range of epoxide/CO_2 co-polymerizations (CHO and PO).[40,76–79] The general structure of these complexes comprises a Zn metal center confined within a sterically demanding environment in which the sterically encumbered BDI ligand enforces a low-coordinate metal center useful for catalytic activation. Steric and electronic variations in the BDI ligand had a dramatic impact on the catalyst activity. In 2001, Coates and coworkers reported[77] an unprecedented catalytic activity for CHO/CO_2 co-polymerization yielding a polycarbonate with a molecular weight up to 39.4 kg/mol and narrow polydispersity of 1.09. In 2004, Coates used the same type of system for the first copolymerization of limonene oxide and CO_2.[40]

Scheme I.11 Structure of a *β* -diiminate zinc catalyst.

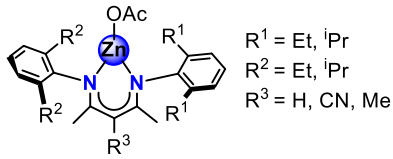

Furthermore, (BDI)Zn complexes showed high activity for the ROCOP of cyclic anhydrides and epoxides. The earliest report of a BDI-based catalyst active towards epoxide/anhydride ROCOP was published by Coates and coworkers in 2007[36] using CHO, PO, LO and other monomers, and DGA as the cyclic anhydride, affording perfectly alternating polyesters characterized by a high molar mass (M_n > 55 kg/mol).

Metal salen and salan complexes

Metal salen systems represent the most widely studied homogeneous catalytic systems for epoxide/CO_2 ROCOP, and have been applied in many ROCOP processes during the last decades. Darensbourg,[23,80–85] Coates,[86–90] Lu,[91–96] Li,[97] Nozaki,[98–102] Lee,[103–109] Rieger[110–114] and others have reported on various ROCOP-active [salenMX] complexes where M typically stands for Cr(III), Co(III) or Al(III). The cheap and simple synthetic preparation, excellent thermal and chemical stability and high polymer selectivity as well as excellent regioselectivity are just a few advantages associated to the use metal salen complexes. Moreover, copolymerization reactions with salen-based catalysts generally proceed under relatively mild temperatures and pressures. All these factors make salen complexes among the most popular catalysts active towards epoxide/CO_2 copolymerization as well as ring opening copolymerization of epoxides and anhydride. When using salen complexes, many parameters can be fine-tuned and optimized including the active metal center, nature of the axial group X, type of diamine backbone and nature of the co-catalyst.[59,87,115] The sub-class of chiral cobalt salen catalysts has been extensively investigated by a number of groups and exhibit outstanding levels of regio- and stereochemical control.[87,116,117] Notably, chiral salen complexes have been applied in the preparation of new classes of "stereocomplexed" polycarbonates starting from racemic mixtures of epoxides.[89–91,101] Salen structures have also been widely used in epoxide/anhydride ROCOP[59,67] as well as ligands with different backbones including *N,N'*-bis(salicylidene)-phenylenediamine (salphen)[20,24,34,42,59,67,68,118] and *N,N'*-bis(salicylidene)-cyclohexanediamine (salcy).[41,64] Chiral (salcy)MX type salen complexes have become some of the most widely used complexes for epoxide/anhydride copolymerization since they are highly active which allows to prepare stereoregular polymers, and notable systems are based on chromium,[41,52,58,59,63,64] colbalt,[37,41,52,59,64,119,120] aluminum,[41,59] manganese,[41,67] and iron[68] complexes.

Dinuclear complexes

A series of zinc anilidoaldimine complexes **cat-I1** (

Scheme I.13 I.13) was reported by Lee and coworkers in 2005.[121] These complexes exhibited very high activity towards the production of poly(cyclohexene)carbonate (PCHC) resulting in high molecular weights (M_n = 90,000–280,000 g/mol) and relatively narrow $Đ$ values ranging from 1.3 to 1.7.[121] These catalysts were the first discrete zinc complexes to yield copolymers of such high molecular weight. In the same year, Xiao *et al*. reported a bimetallic zinc complex **cat-I2** (

Scheme I.13 I.13) based on a "Trost" type phenolate ligand and showed moderate activity for CHO/CO_2 copolymerization. In 2009, Williams and coworkers reported on a series of bimetallic complexes **cat-I3** (

Scheme I.13 I.13), based on a novel type of macrocyclic Robson ligand.[122] These complexes exhibited high activity for CHO copolymerization under mild conditions at only 1 bar of CO_2. The macrocyclic ligand environment and bimetallic structure were both shown to be essential toward the high activity of the catalyst, as 'open' and monometallic analogues (which are active for lactide polymerization) showed almost no activity for CHO/CO_2 copolymerization under these conditions.

Scheme I.12 Salcy, salphen and salen more used ligands.

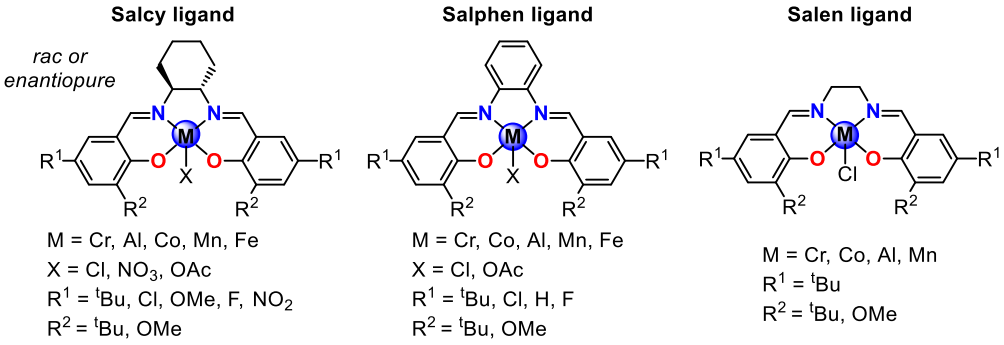

Scheme I.13 Di- and tri-metallic zinc complexes.

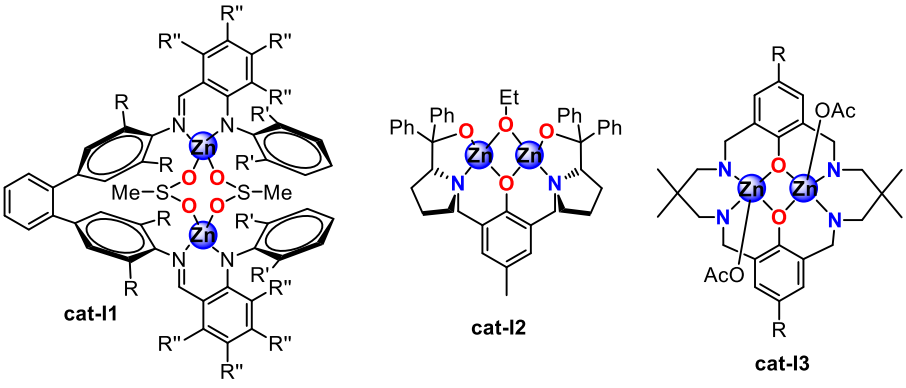

Given the recent success with dinuclear catalysts for epoxide/CO_2 ROCOP, investigating such dinuclear catalysts for anhydride/epoxide polymerization was a logical step. Multinuclear zinc and magnesium catalysts have been studied extensively by Williams and co-workers,[50,52–55,123] Ko and co-workers,[56] and Lü and co-workers.[47,48,51] Each of these catalysts had unique features, and the diversity in catalysts allowed for the synthesis of polyesters with a wide range of properties.

Aminotriphenolates complexes

A new family of homogeneous metal catalysts based on amino triphenolate scaffolds have shown excellent activity in the conversion of a range of epoxides and oxetanes to cyclic carbonates under mild conditions and using tetrabutylammonium salts or PPNX as co-catalysts.[124–130] This type of complexes are readily accessible and they have modular properties towards electronic and steric tuning. These characteristics, associated with a threefold symmetry and tetradentate nature of the system offers opportunities for new catalyst development in ROCOP processes. The main advantage of this ligand is the high thermodynamic stability of the corresponding metal complexes, which also ensures catalyst integrity at low catalyst loadings and under harsh reaction conditions. These aminotriphenolate ligands can coordinate both transition and main group metal ions, and they usually bind the metal in a tetradentate manner:[130] the three anionic oxygen donor atoms typically occupy equatorial positions and the tertiary amine one of the axial positions. Metal such as Ti(IV), V(V), Fe(III) and Al(III) afford mononuclear complexes with approximate trigonal bipyramidal (TBP) geometries. Furthermore, aminotriphenolate complexes have shown activity in diverse polymerization processes. Ti, Zr and Ge-aminotriphenolate complexes are able to catalyze the ring opening polymerization (ROP) of *rac*-lactide[8,9,31,32] to form poly(lactic acid) which, as mentioned before, is of interest due to its degradability and bio-origin. Iron(III) aminotriphenolate complexes were shown to be excellent catalysts for the ROCOP reaction of cyclohexene oxide with CO_2.[131] The use of environmentally friendly and inexpensive iron as the metal center makes such a catalyst highly attractive in the context of green chemistry and in view of potential large-scale applications.

Scheme I.14 General structure of metal-aminotriphenolate catalysts.

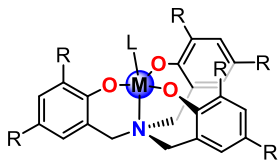

M = Ti, Zr, V, Fe, Al
L = THF, OR
R= Me, H, ^{t}Bu, Cl

I.4 Thesis aims and outline

The initially defined main objectives of the work described in this thesis were (a) the development of precursors based on renewable sources such as terpenes or fatty acids for the preparation of biopolymers, and (b) the synthesis of (semi-)renewable polycarbonates, aliphatic polyesters and semi-aromatic polyesters using aminotriphenolate complexes (M = Al, Fe) and a nucleophile as a binary catalytic system. Furthermore, a third main objective was (c) a detailed study on the polymer microstructure and thermal properties through various techniques such as MALDI-TOF-MS, NMR, GPC, TGA and DSC.

Chapter 1 describes the use of amino-triphenolate derived Al(III) complexes combined with suitable nucleophiles as binary catalysts for the coupling of limonene oxide and carbon dioxide to afford alternating polycarbonates. Detailed computational studies (DFT) revealed unique features of the binary catalysts system, among which is the preferred nucleophilic attack on the quaternary carbon center in the limonene oxide substrate, and the potential the binary catalyst has to produce virtually stereo-regular poly(limonene)carbonate with a relatively high glass transition (T_g) of 112 ºC.

In *Chapter 2*, the synthesis of semi-renewable aliphatic polyesters is reported to provide potential alternatives for conventional polyesters that show limitations in terms of accessible glass transitions. The newly reported epoxide/anhydride copolymerizations allow for tuning of the polymer properties through two distinct monomer sets. Six partially or fully renewable tricyclic anhydrides were copolymerized with either propylene oxide (PO) or cyclohexene oxide (CHO). By varying both the epoxide and the anhydride monomer, the T_g of the resulting polyesters could be tuned over a nearly 120 °C range up to 182 ºC.

In *Chapter 3* the use of terpene derived epoxides (limonene oxide, carene oxide, limonene dioxide and menthene oxide) is discussed in the context of the ring-opening copolymerization (ROCOP) using various aromatic cyclic anhydrides. These copolymerization reactions were mostly performed under mild reaction conditions using a binary catalyst comprising of a Fe(III) based aminotriphenolate complex and PPNCl (bis(triphenylphosphine)iminium chloride) providing partially bio-based, semi-aromatic polyesters. The copolymerization reactions proceed with excellent selectivity towards fully alternating polyesters with modular thermal properties (T_g´s up to 243 ºC) that depend on the nature of the terpene oxide and anhydride monomers used, and are potentially useful towards the development of new coating and thermoset materials.

In *Chapter 4*, an efficient catalytic method for the preparation of a series of fatty acid derived biocarbonates is dislosed with the use of a binary Al-complex/PPNCl catalyst being key to control the properties and yield of mono-, di- and tri-cyclic carbonates. The catalyst system allows to convert fatty acid derived epoxides under comparatively mild reaction conditions while maintaining high levels of diastereo-specificity. Comparative catalysis data obtained for the reactions catalyzed only by the nucleophilic halide shows that the presence of the Al-complex is crucial for retention of the original stereochemistry. The di- and tri-cyclic carbonates are potentially useful towards the development of new polyurethane formulations obviating the use of conventionally applied isocyanate reagents.

I.5 References

[1] Y. Zhu, C. Romain, C. K. Williams, *Nature* **2016**, *540*, 354.

[2] P. A. Wilbon, F. Chu, C. Tang, *Macromol. Rapid Commun.* **2013**, *34*, 8–37.

[3] H. Köpnick, M. Schmidt, W. Brügging, J. Rüter, W. Kaminsky, in *Ullmann's Encycl. Ind. Chem.*, Wiley-VCH Verlag GmbH & Co. KGaA, **2000**.

[4] G. Odian, in *Princ. Polym.*, John Wiley & Sons, Inc., **2004**.

[5] O. Haba, I. Itakura, M. Ueda, S. Kuze, *J. Polym. Sci. Part A Polym. Chem.* **1999**, *37*, 2087–2093.

[6] P. . Anastas, J. C. Warner, *Green Chemistry: Theory and Practice*, Oxford University Press, New York, **1998**.

[7] P. Lecomte, C. Jérôme, in *Synth. Biodegrad. Polym.* (Eds.: B. Rieger, A. Künkel, G.W. Coates, R. Reichardt, E. Dinjus, T.A. Zevaco), Springer Berlin Heidelberg, Berlin, Heidelberg, **2012**, pp. 173–217.

[8] C. K. Williams, *Chem. Soc. Rev.* **2007**, *36*, 1573.

[9] C. M. Thomas, J. F. Lutz, *Angew. Chem. Int. Ed.* **2011**, *50*, 9244–9246.

[10] M. J. Stanford, A. P. Dove, *Chem. Soc. Rev.* **2010**, *39*, 486–494.

[11] N. Ajellal, J.-F. Carpentier, C. Guillaume, S. M. Guillaume, M. Helou, V. Poirier, Y. Sarazin, A. Trifonov, *Dalton Trans.* **2010**, *39*, 8363.

[12] D. B. Odile Dechy-Cabaret , B. Martin-Vaca, *J. Am. Chem. Soc.* **2004**, *104*, 6147–6176.

[13] P. J. Dijkstra, H. Du, J. Feijen, *Polym. Chem.* **2011**, *2*, 520–527.

[14] C. G. Jaffredo, S. M. Guillaume, *Polym. Chem.* **2014**, *5*, 4168.

[15] L. Mespouille, O. Coulembier, M. Kawalec, A. P. Dove, P. Dubois, *Prog. Polym. Sci.* **2014**, *39*, 1144–1164.

[16] K. Yao, C. Tang, *Macromolecules* **2013**, *46*, 1689–1712.

[17] S. Dutta, W.-C. Hung, B.-H. Huang, C.-C. Lin, in *Synth. Biodegrad. Polym.* (Eds.: B. Rieger, A. Künkel, G.W. Coates, R. Reichardt, E. Dinjus, T.A. Zevaco), Springer Berlin Heidelberg, Berlin, Heidelberg, **2012**, pp. 219–283.

[18] M. A. Hillmyer, W. B. Tolman, *Acc. Chem. Res.* **2014**, *47*, 2390–2396.

[19] C. K. Williams, *Chem. Soc. Rev.* **2007**, *36*, 1573.

[20] E. H. Nejad, A. Paoniasari, C. G. W. Van Melis, C. E. Koning, R. Duchateau, *Macromolecules* **2013**, *46*, 631–637.

[21] E. Hosseini Nejad, A. Paoniasari, C. E. Koning, R. Duchateau, *Polym. Chem.* **2012**, *3*, 1308.

[22] C. E. Koning, R. J. Sablong, E. Hosseini Nejad, R. Duchateau, P. Buijsen, *Prog. Org. Coatings* **2013**, *76*, 1704–1711.

[23] D. J. Darensbourg, S. J. Wilson, *Macromolecules* **2013**, *46*, 5929–5934.

[24] S. Huijser, E. Hosseininejad, R. Sablong, C. De Jong, C. E. Koning, R. Duchateau, *Macromolecules* **2011**, *44*, 1132–1139.

[25] D. J. Darensbourg, S. J. Wilson, *J. Am. Chem. Soc.* **2011**, *133*, 18610–18613.

[26] S. Paul, Y. Zhu, C. Romain, R. Brooks, P. K. Saini, C. K. Williams, *Chem. Commun.* **2015**, *51*, 6459–6479.

[27] B. Han, L. Zhang, B. Liu, X. Dong, I. Kim, Z. Duan, P. Theato, *Macromolecules* **2015**, *48*, 3431–3437.

[28] A. J. Ragauskas, C. K. Williams, B. H. Davison, G. Britovsek, J. Cairney, C. A. Eckert, W. J. Frederick Jr., J. P. Hallett, D. J. Leak, C. L. Liotta, et al., *Science* **2006**, *311*, 484–489.

[29] R. A. Gross, B. Kalra, C. Bastoli, R. A. Gross, J.-D. Gu, D. Eberiel, S. P. McCarthy, C. M. Buchanan, B. G. Pearcy, A. W. White, et al., *Science* **2002**, *297*, 803–7.

[30] A. Gandini, *Green Chem.* **2011**, *13*, 1061.

[31] S. Mecking, *Angew. Chem. Int. Ed.* **2004**, *43*, 1078–1085.

[32] Y. Maeda, A. Nakayama, N. Kawasaki, K. Hayashi, S. Aiba, N. Yamamoto, *Polymer* **1997**, *38*, 4719–4725.

[33] A. Takasu, T. Bando, Y. Morimoto, Y. Shibata, T. Hirabayashi, *Biomacromolecules* **2005**, *6*, 1707–1712.

[34] E. Hosseini Nejad, A. Paoniasari, C. E. Koning, R. Duchateau, *Polym. Chem.* **2012**, *3*, 1308–1313.

[35] H. Hajian, W. Mohtar, W. Yusoff, *Curr. Res. J. Biol. Sci.* **2015**, *7*, 37–42.

[36] R. C. Jeske, A. M. DiCiccio, G. W. Coates, *J. Am. Chem. Soc.* **2007**, *129*, 11330–11331.

[37] J. M. Longo, A. M. Diciccio, G. W. Coates, *J. Am. Chem. Soc.* **2014**, *136*, 15897–15900.

[38] A. M. Diciccio, G. W. Coates, *J. Am. Chem. Soc.* **2011**, *133*, 10724–10727.

[39] M. Winnacker, B. Rieger, *ChemSusChem* **2015**, *8*, 2455–2471.

[40] C. M. Byrne, S. D. Allen, E. B. Lobkovsky, G. W. Coates, *J. Am. Chem. Soc.* **2004**, *126*, 11404–11405.

[41] C. Robert, F. de Montigny, C. M. Thomas, *Nat. Commun.* **2011**, *2*, 586.

[42] N. J. Van Zee, M. J. Sanford, G. W. Coates, *J. Am. Chem. Soc.* **2016**, *138*, 2755–2761.

[43] N. J. Van Zee, G. W. Coates, *Angew. Chem. Int. Ed.* **2015**, *54*, 2665–2668.

[44] H. Arakawa, M. Aresta, J. N. Armor, M. A. Barteau, E. J. Beckman, A. T. Bell, J. E. Bercaw, C. Creutz, E. Dinjus, D. A. Dixon, et al., *Chem. Rev.* **2001**, *101*, 953–996.

[45] M. Aresta, A. Dibenedetto, *Dalton Trans.* **2007**, 2975.

[46] T. Sakakura, J. C. Choi, H. Yasuda, *Chem. Rev.* **2007**, *107*, 2365–2387.

[47] L. Zhu, D. Liu, L. Wu, W. Feng, X. Zhang, J. Wu, D. Fan, X. Lü, R. Lu, Q. Shi, *Inorg. Chem. Commun.* **2013**, *37*, 182–185.

[48] D. Steiner, L. Ivison, C. T. Goralski, R. B. Appell, J. R. Gojkovic, B. Singaram, *Tetrahedron Asymmetry* **2002**, *13*, 2359–2363.

[49] Y. Liu, M. Xiao, S. Wang, L. Xia, D. Hang, G. Cui, Y. Meng, *RSC Adv.* **2014**, *4*, 9503–9508.

[50] P. K. Saini, C. Romain, Y. Zhu, C. K. Williams, *Polym. Chem.* **2014**, *5*, 6068–6075.

[51] L. Y. Wu, D. Di Fan, X. Q. Lü, R. Lu, *Chinese J. Polym. Sci. (English Ed.)* **2014**, *32*, 768–777.

[52] M. Winkler, C. Romain, M. A. R. Meier, C. K. Williams, *Green Chem.* **2015**, *17*, 300–306.

[53] Y. Zhu, C. Romain, C. K. Williams, *J. Am. Chem. Soc.* **2015**, *137*, 12179–12182.

[54] A. Thevenon, J. A. Garden, A. J. P. White, C. K. Williams, *Inorg. Chem.* **2015**, *54*, 11906–11915.

[55] J. A. Garden, P. K. Saini, C. K. Williams, *J. Am. Chem. Soc.* **2015**, *137*, 15078–15081.

[56] C.-Y. Yu, H.-J. Chuang, B.-T. Ko, *Catal. Sci. Technol.* **2016**, *6*, 1779–1791.

[57] A. Takasu, M. Ito, Y. Inai, T. Hirabayashi, Y. Nishimura, *Polym. J.* **1999**, *31*, 961–969.

[58] D. J. Darensbourg, R. R. Poland, C. Escobedo, *Macromolecules* **2012**, *45*, 2242–2248.

[59] E. Hosseini Nejad, C. G. W. Van Melis, T. J. Vermeer, C. E. Koning, R. Duchateau, *Macromolecules* **2012**, *45*, 1770–1776.

[60] A. Bernard, C. Chatterjee, M. H. Chisholm, *Polym. (United Kingdom)* **2013**, *54*, 2639–2646.

[61] N. D. Harrold, Y. Li, M. H. Chisholm, *Macromolecules* **2013**, *46*, 692–698.

[62] J. Liu, Y.-Y. Bao, Y. Liu, W.-M. Ren, X.-B. Lu, *Polym. Chem.* **2013**, *4*, 1439–1444.

[63] U. Biermann, A. Sehlinger, M. A. R. Meier, J. O. Metzger, *Eur. J. Lipid Sci. Technol.* **2016**, *118*, 104–110.

[64] A. M. DiCiccio, G. W. Coates, *J. Am. Chem. Soc.* **2011**, *133*, 10724–10727.

[65] C. Robert, T. Ohkawara, K. Nozaki, *Chem. - A Eur. J.* **2014**, *20*, 4789–4795.

[66] D.-F. Liu, L.-Q. Zhu, J. Wu, L.-Y. Wu, X.-Q. Lü, *RSC Adv.* **2015**, *5*, 3854–3859.

[67] D. Liu, Z. Zhang, X. Zhang, X. Lü, *Aust. J. Chem.* **2016**, *69*, 47–55.

[68] R. Mundil, Z. Hošťálek, I. Šeděnková, J. Merna, *Macromol. Res.* **2015**, *23*, 161–166.

[69] T. Aida, S. Inoue, *J. Am. Chem. Soc.* **1985**, *107*, 1358–1364.

[70] T. Aida, K. Sanuki, S. Inoue, *Macromolecules* **1985**, *18*, 1049–1055.

[71] N. J. Van Zee, M. J. Sanford, G. W. Coates, *J. Am. Chem. Soc.* **2016**, *138*, 2755–2761.

[72] N. Takeda, S. Inoue, *Die Makromol. Chemie* **1978**, *179*, 1377–1381.

[73] C. Chatterjee, M. H. Chisholm, *Inorg. Chem.* **2012**, *51*, 12041–12052.

[74] A. Bernard, C. Chatterjee, M. H. Chisholm, *Polym. (United Kingdom)* **2013**, *54*, 2639–2646.

[75] P. Chen, M. H. Chisholm, J. C. Gallucci, X. Zhang, Z. Zhou, *Inorg. Chem.* **2005**, *44*, 2588–2595.

[76] M. Cheng, E. B. Lobkovsky, G. W. Coates, *J. Am. Chem. Soc.* **1998**, *120*, 11018–11019.

[77] M. Cheng, D. R. Moore, J. J. Reczek, B. M. Chamberlain, E. B. Lobkovsky, G. W. Coates, *J. Am. Chem. Soc.* **2001**, *123*, 8738–8749.

[78] S. D. Allen, D. R. Moore, E. B. Lobkovsky, G. W. Coates, *J. Am. Chem. Soc.* **2002**, *124*, 14284–14285.

[79] D. R. Moore, M. Cheng, E. B. Lobkovsky, G. W. Coates, *J. Am. Chem. Soc.* **2003**, *125*, 11911–11924.

[80] D. J. Darensbourg, *Chem. Rev.* **2007**, *107*, 2388–2410.

[81] D. J. Darensbourg, A. I. Moncada, S. H. Wei, *Macromolecules* **2011**, *44*, 2568–2576.

[82] D. J. Darensbourg, in *Synth. Biodegrad. Polym.* (Eds.: B. Rieger, A. Künkel, G.W. Coates, R. Reichardt, E. Dinjus, T.A. Zevaco), Springer Berlin Heidelberg, Berlin, Heidelberg, **2012**, pp. 1–

27.

[83] D. J. Darensbourg, A. D. Yeung, *Polym. Chem.* **2015**, *6*, 1103–1117.

[84] D. J. Darensbourg, W. C. Chung, *Polyhedron* **2013**, *58*, 139–143.

[85] D. J. Darensbourg, A. I. Moncada, W. Choi, J. H. Reibenspies, *J. Am. Chem. Soc.* **2008**, *130*, 6523–6533.

[86] G. W. Coates, D. R. Moore, *Angew. Chem. Int. Ed.* **2004**, *43*, 6618–6639.

[87] C. T. Cohen, T. Chu, G. W. Coates, *J. Am. Chem. Soc.* **2005**, *127*, 10869–10878.

[88] Z. Qin, C. M. Thomas, S. Lee, G. W. Coates, *Angew. Chem. Int. Ed.* **2003**, *42*, 5484–5487.

[89] F. Auriemma, C. De Rosa, M. R. Di Caprio, R. Di Girolamo, W. C. Ellis, G. W. Coates, *Angew. Chem. Int. Ed.* **2015**, *54*, 1215–1218.

[90] F. Auriemma, C. De Rosa, M. R. Di Caprio, R. Di Girolamo, G. W. Coates, *Macromolecules* **2015**, *48*, 2534–2550.

[91] Y. Liu, W. M. Ren, M. Wang, C. Liu, X. B. Lu, *Angew. Chem. Int. Ed.* **2015**, *54*, 2241–2244.

[92] Y. Liu, W.-M. Ren, K.-K. He, X.-B. Lu, *Nat. Commun.* **2014**, *5*, 5687.

[93] G. P. Wu, Y. P. Zu, P. X. Xu, W. M. Ren, X. B. Lu, *Chem. Asian J.* **2013**, *8*, 1854–1862.

[94] G. P. Wu, P. X. Xu, Y. P. Zu, W. M. Ren, X. B. Lu, *J. Polym. Sci. Part A Polym. Chem.* **2013**, *51*, 874–879.

[95] G. Wu, P. Xu, X. Lu, Y. Zu, S. Wei, W. Ren, D. J. Darensbourg, *Macromolecules* **2013**, *46*, 2128–2133.

[96] Y. Liu, W. M. Ren, J. Liu, X. B. Lu, *Angew. Chem. Int. Ed.* **2013**, *52*, 11594–11598.

[97] Y. Niu, H. Li, *Colloid Polym. Sci.* **2013**, *291*, 2181–2189.

[98] K. Nakano, M. Nakamura, K. Nozaki, *Macromolecules* **2009**, *42*, 6972–6980.

[99] K. Nakano, T. Kamada, K. Nozaki, *Angew. Chem. Int. Ed.* **2006**, *45*, 7274–7277.

[100] T. Ohkawara, K. Suzuki, K. Nakano, S. Mori, K. Nozaki, *J. Am. Chem. Soc.* **2014**, *136*, 10728–10735.

[101] K. Nakano, S. Hashimoto, M. Nakamura, T. Kamada, K. Nozaki, *Angew. Chem. Int. Ed.* **2011**, *50*, 4868–4871.

[102] K. Nakano, S. Hashimoto, K. Nozaki, *Chem. Sci.* **2010**, *1*, 369.

[103] S. J. Na, S. Sujith, A. Cyriac, B. E. Kim, J. Yoo, Y. K. Kang, S. J. Han, C. Lee, B. Y. Lee, *Inorg. Chem.* **2009**, *48*, 10455–10465.

[104] E. K. Noh, S. J. Na, S. Sujith, S. W. Kim, B. Y. Lee, *J. Am. Chem. Soc.* **2007**, *129*, 8082–8083.

[105] S. S, J. K. Min, J. E. Seong, S. J. Na, B. Y. Lee, *Angew. Chem. Int. Ed.* **2008**, *47*, 7306–7309.

[106] J. Y. Jeon, J. J. Lee, J. K. Varghese, S. J. Na, S. Sujith, M. J. Go, J. Lee, M.-A. Ok, B. Y. Lee, *Dalton Trans.* **2013**, *42*, 9245–9254.

[107] J. Yoo, S. J. Na, H. C. Park, A. Cyriac, B. Y. Lee, *Dalton Trans.* **2010**, *39*, 2622.

[108] J. E. Seong, S. J. Na, A. Cyriac, B. W. Kim, B. Y. Lee, *Macromolecules* **2010**, *43*, 903–908.

[109] B. E. Kim, J. K. Varghese, Y. Han, B. Y. Lee, *Bull. Korean Chem. Soc.* **2010**, *31*, 829–834.

[110] S. Klaus, S. I. Vagin, M. W. Lehenmeier, P. Deglmann, A. K. Brym, B. Rieger, *Macromolecules* **2011**, *44*, 9508–9516.

[111] W. Xia, K. A. Salmeia, S. I. Vagin, B. Rieger, *Chem.-Eur. J.* **2015**, *21*, 4384–4390.

[112] G. A. Luinstra, G. R. Haas, F. Molnar, V. Bernhart, R. Eberhardt, B. Rieger, *Chem.-Eur. J.* **2005**, *11*, 6298–6314.

[113] S. I. Vagin, R. Reichardt, S. Klaus, B. Rieger, *J. Am. Chem. Soc.* **2010**, *132*, 14367–14369.

[114] R. Eberhardt, M. Allmendinger, B. Rieger, *Macromol. Rapid Commun.* **2003**, *24*, 194–196.

[115] D. J. Darensbourg, P. Bottarelli, J. R. Andreatta, *Macromolecules* **2007**, *40*, 7727–7729.

[116] M. I. Childers, J. M. Longo, N. J. Van Zee, A. M. LaPointe, G. W. Coates, *Chem. Rev.* **2014**, *114*, 8129–8152.

[117] K. Yu, C. W. Jones, *Organometallics* **2003**, *22*, 2571–2580.

[118] N. J. Van Zee, G. W. Coates, *Angew. Chem. Int. Ed.* **2015**, *54*, 2665–2668.

[119] Z. Duan, X. Wang, Q. Gao, L. Zhang, B. Liu, I. Kim, *J. Polym. Sci. Part A Polym. Chem.* **2014**, *52*, 789–795.

[120] J. Y. Jeon, S. C. Eo, J. K. Varghese, B. Y. Lee, *Beilstein J. Org. Chem.* **2014**, *10*, 1787–1795.

[121] B. Y. Lee, H. Y. Kwon, S. Y. Lee, S. J. Na, S. Han, H. Yun, H. Lee, Y.-W. Park, *J. Am. Chem. Soc.* **2005**, *127*, 3031–3037.

[122] M. R. Kember, P. D. Knight, P. T. R. Reung, C. K. Williams, *Angew. Chem. Int. Ed.* **2009**, *48*, 931–933.

[123] C. Romain, Y. Zhu, P. Dingwall, S. Paul, H. S. Rzepa, A. Buchard, C. K. Williams, *J. Am. Chem. Soc.* **2016**, *138*, 4120–4131.

[124] C. J. Whiteoak, N. Kielland, V. Laserna, F. Castro-Gómez, E. Martin, E. C. Escudero-Adán, C. Bo, A. W. Kleij, *Chem.-Eur. J.* **2014**, *20*, 2264–2275.

[125] C. J. Whiteoak, N. Kielland, V. Laserna, E. C. Escudero-Adán, E. Martin, A. W. Kleij, *J. Am. Chem. Soc.* **2013**, *135*, 1228–1231.

[126] V. Laserna, G. Fiorani, C. J. Whiteoak, E. Martin, E. Escudero-Adán, A. W. Kleij, *Angew. Chem. Int. Ed.* **2014**, *53*, 10416–10419.

[127] C. J. Whiteoak, E. Martin, M. M. Belmonte, J. Benet-Buchholz, A. W. Kleij, *Adv. Synth. Catal.* **2012**, *354*, 469–476.

[128] G. Fiorani, M. Stuck, C. Martín, M. M. Belmonte, E. Martin, E. C. Escudero-Adán, A. W. Kleij, *ChemSusChem* **2016**, *9*, 1304–1311.

[129] C. Miceli, J. Rintjema, E. Martin, E. C. Escudero-Adán, C. Zonta, G. Licini, A. W. Kleij, *ACS Catal.* **2017**, 2367–2373.

[130] G. Licini, M. Mba, C. Zonta, *Dalton Trans.* **2009**, 5265.

[131] M. Taherimehr, S. M. Al-Amsyar, C. J. Whiteoak, A. W. Kleij, P. P. Pescarmona, *Green Chem.* **2013**, *15*, 3083.

Chapter 1

Al^{III}-catalyzed formation of poly(limonene) carbonate

This chapter has been published in:

L. Peña Carrodeguas, J. González-Fabra, F. Castro-Gómez, C. Bo, A. W. Kleij, *Chem. A Eur. J.* **2015**, *21*, 6115–6122

This work described in this chapter was carried out in collaboration with the group of Prof. Carles Bo at ICIQ.

UNIVERSITAT ROVIRA I VIRGILI
AVANCES EN SISTEMAS INTERACTIVOS PARA PERSONAS CON PARÁLISIS CEREBRAL
Leticia Peña Carrodeguas

1.1 Introduction

Currently there is a high demand for chemical processes that enable the conversion of renewable feed stocks into value-added chemicals as to increase the overall sustainability of our societies.[1–5] In this regard, the use of carbon dioxide as a carbon resource has attracted much interest during the last decade and substantial progress has been made to use this synthon in organic synthesis.[6–12] The co-polymerization of epoxides and CO_2 is a successful and relevant example of using a renewable carbon feed stock and converting it into a material of widespread commercial and academic interest.[13–21] However, chemical processes leading to such CO_2-based materials still depend on petroleum-based feed stocks despite the impressive advancements made in this area using various types of epoxide monomers. Most reported polycarbonates are based on petroleum derived epoxide monomers such as cyclohexene oxide,[22–27] propylene oxide[28–35] and other non-renewable epoxides.[36–41] The use of bio-renewable based monomers has offered new potential for bioderived polycarbonates[42–44] and polyesters.[5,45–50]

At the moment we started working on this topic, terpenes such as limonene oxide had received far less attention, and we were aware of only a few reports dealing with the successful co-polymerization of this monomer with CO_2.[45,51,52]

Scheme 1.1 Previous work on polymerization of limonene oxide with CO_2 reported by Coates and coworkers.[45]

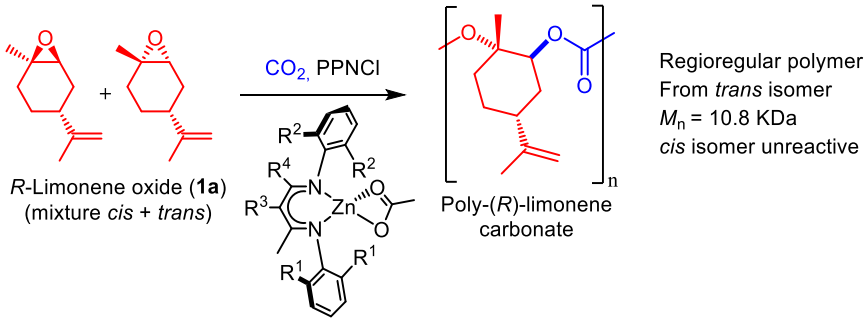

(*R*)-Limonene is a naturally occurring terpene that is available in large amounts, and the epoxidized form is commercially available at low cost as a mixture of *cis* and *trans* isomers [A] (Scheme 1.2). Its structural resemblance to cyclohexene oxide (the most widely used epoxide in copolymerization reactions with CO_2) makes it thus an ideal target to provide a cost-effective, bio-based polycarbonate from a renewable feed stock. Though, some important challenges remain to be solved: limonene oxide represents an internal, tri-substituted epoxide monomer and the kinetic barrier for its activation is significantly higher than for terminal epoxides.[53] There are only relative few reports describing the efficient conversion of internal epoxides into their respective organic carbonates,[54–66] and the development of (more) powerful catalytic systems[54–59] is thus of vital importance to solve these synthetically more challenging preparations that involve such monomers.

Scheme 1.2 Structures of the aminotriphenolate metal complexes used in this work, PPN-X cocatalyst and *cis*- and *trans*-(*R*) limonene oxide.

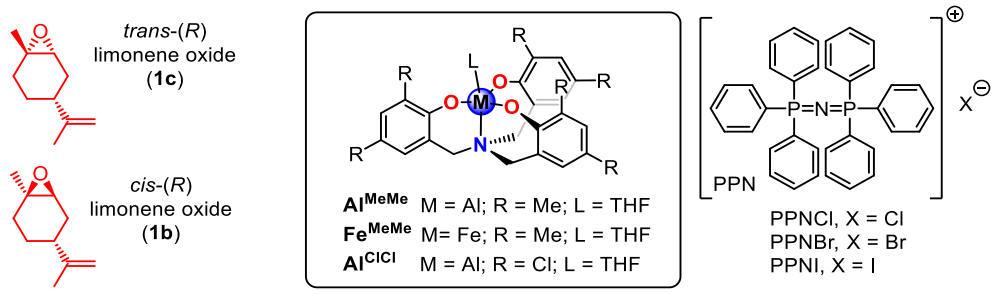

We have developed Fe(III)[60–62] and Al(III)[63–66] amino-triphenolate complexes (Scheme 1.2) that show high efficiency in the formation of functional organic carbonates from both terminal and internal epoxides. Further to this, we also found that these complexes have the intrinsic ability to switch between penta- and hexa-coordination,[65,66] a feature that may be useful in the creation of flexible coordination behavior around the metal ion in the presence of sterically more demanding substrates.[67]

In this chapter, we report a catalytic system able to mediate the efficient and stereo-selective formation of poly(limonene)carbonate, a tri-substituted oxirane monomer. In order to get more insight into the chemo- and stereo-selective features of the catalytic process, detailed computational studies (DFT) were carried out to evaluate the difference in reactivity for isomers

[A] The *cis* and *trans* nomenclature of limonene oxide refers to the relative position of the methyl group with respect to the double bond.

cis-LO (**1b**) and *trans*-LO (**1c**) providing unique insight into the operative modus of the catalyst system. Catalysts as the ones reported herein pave the way for the conversion of other naturally occurring, renewable compounds into valuable chemicals including biopolymers that are derived from epoxide/CO_2 couplings. The development of such bio-based polymers may give useful alternatives for existing, environmentally less attractive copolymers, of which bis-phenol A (BPA) based ones are most prominent.

1.2 Results and discussion

1.2.1 Screening studies

Previous results in our group using amino-triphenolate complexes as catalysts for poly(cyclohexene)carbonate synthesis[67] prompted us to evaluate their catalytic efficiencies in the copolymerization of a commercially available mixture of *cis*/*trans* (40:60 by GC) (*R*)-limonene oxide (Table 1.1).

Various combinations of catalysts (**Al^{MeMe}**, **Fe^{MeMe}** and **Al^{ClCl}** in Scheme 1.2) and co-catalysts (nucleophiles abbreviated as **Cl**, **Br** and **I**) and their relative ratios were probed in a screening phase. At 42ºC, complex **Al^{MeMe}** (Table 1.1, entry 1) gave a reasonable conversion of 20% furnishing a copolymer with high chemo-selectivity (CO_2 linkages >99%) and high *trans* incorporation (78%). In contrast to the Zn(BDI) catalyst reported by Coates,[45] **Al^{MeMe}** shows lower activity but does maintain activity throughout a long period of time (Table 1.1, entries 2-7). The presence of the Al-complex is a requisite for the synthesis of poly(limonene)carbonate as the use of co-catalyst alone (PPNCl = **Cl**; Table 1.1, entry 8) does not lead to any observable conversion.

In general, Al-complex **Al^{MeMe}** proved to be the most efficient mediator of the copolymerization reaction and co-catalyst **Cl** (PPNCl) and **Br** (PPNBr) the best co-catalysts with the former one leading to a higher percentage of *trans* units [B] in the polymer product; co-catalyst loadings required for efficient catalysis were 0.5-1.0 mol%. Longer reaction times provided higher conversion levels, but increasing temperatures (Table 1.1, entries 15 and 16) had no favorable effect on the activity/selectivity.[B] As the reaction proceeds with time (Table 1.1, entries 2-5), it can be noted that the amount of *trans* units.[B] in the polymer product stays stable around 70%.

[B] For a detailed explanation, we refer to section 1.2.3 "*Regio- and stereochemistry of the monomers*" of this chapter.

Table 1.1 Copolymerization of *cis/trans* (*R*)-limonene oxide and CO_2 using complexes **Al^{MeMe}**, **Fe^{MeMe}**, **Al^{ClCl}** and nucleophilic PPN-based cocatalyst.

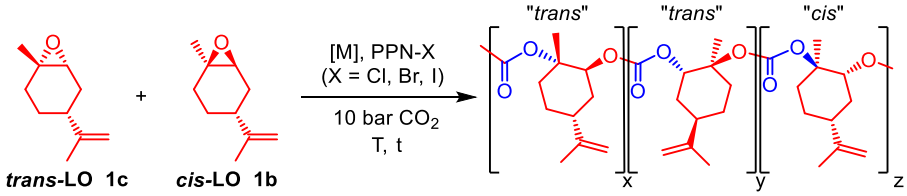

entry	complex (mol%)	cocat. (mol%)	*T* (ºC)[b]	*t* (h)	conv. (%)[c]	*trans* (%)[d]
1	**Al^{MeMe}** (0.5)	**Cl** (0.25)	42	18	20	78
2	**Al^{MeMe}** (1.0)	**Cl** (0.50)	42	4	4	77
3	**Al^{MeMe}** (1.0)	**Cl** (0.50)	42	6	16	68
4	**Al^{MeMe}** (1.0)	**Cl** (0.50)	42	24	50	72
5	**Al^{MeMe}** (1.0)	**Cl** (0.50)	42	48	60	70
6	**Al^{MeMe}** (1.0)	**Cl** (0.25)	42	48	53	74
7	**Al^{MeMe}** (0.5)	**Cl** (0.25)	42	48	47	72
8	–	**Cl** (1.0)	42	48	0	–
9	**Al^{MeMe}** (1.0)	**Cl** (0.50)	42	12	28	68
10	**Al^{MeMe}** (1.0)	**Br** (0.50)	42	12	35	74
11	**Al^{MeMe}** (1.0)	**I** (0.50)	42	12	3	97
12	**Fe^{MeMe}** (1.0)	**Cl** (0.50)	42	24	31	74
13	**Al^{ClCl}** (0.5)	**Cl** (0.25)	42	18	5	85
14	**Al^{MeMe}** (1.0)	**Cl** (1.0)	42	24	18	76
15	**Al^{MeMe}** (1.0)	**Cl** (1.0)	60	24	18	67
16	**Al^{MeMe}** (1.0)	**Cl** (1.0)	70	24	11	67
17	**Al^{MeMe}** (1.0)	**Br** (1.0)	45	24	23	77

[a] Reaction conditions: *cis*/*trans* (*R*)-limonene oxide (1.0 g, 6.57 mmol), metal complex (quantity indicated), co-catalyst (quantity indicated), 10 bar initial CO_2 pressure, 30 mL autoclave, neat. [b] Temperature inside the autoclave. [c] Determined by ^{1}H NMR of the crude reaction mixture with amount of carbonate linkages >99%. [d] Total % of *trans* repeat units in the copolymer determined by ^{1}H NMR using signal integration

This result suggests that both *cis* and *trans* (*R*)-limonene oxide are converted by the binary catalyst system **Al^{MeMe}/Cl**. Interestingly, the ^{1}H NMR spectra of the isolated polymer samples display three separate peaks (δ = 5.05, 5.08 and 5.12 ppm, respectively, see Scheme 1.3) for the C*H* groups located near the carbonate linkages (colored blue in the Scheme 1.3). The peaks at 5.05 and 5.12 ppm were previously assigned to different regio-related *trans* units in the poly(limonene)carbonate (Scheme 1.3),[45,51] whereas the signal at 5.08 ppm was tentatively assigned to the presence of *cis* units (Scheme 1.3).

Scheme 1.3 (a) Expansion (4.30-5.30 ppm region) of a typical ^{1}H NMR spectrum of an isolated sample of poly(limonene)carbonate containing two types of *trans* units as well as one *cis* unit.[C] (b) Comparative ^{1}H NMR trace for a copolymer obtained from pure *cis* limonene oxide.[D] Note that the peaks at δ = 5.05, 5.08 and 5.13 ppm relate to the blue-colored H´s in the polymer figure.

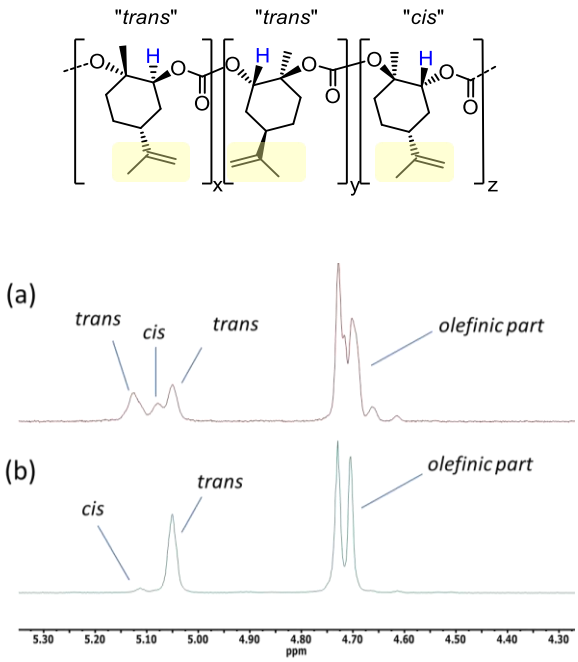

This screening study shows that aminotriphenolate complex **Al^{MeMe}** in combination with a suitable nucleophile additive (PPNCl) affords active and robust catalyst systems for limonene oxide/CO_2 couplings with high selectivity for the copolymer.

[C] Reaction conditions: complex **Al^{MeMe}** (1.0 mol%), PPNCl (0.5 mol%), 42ºC, 18 h, p(CO_2) = 10 bar, **1a** (mixture of **1b** and **1c**) as substrate.
[D] For reaction conditions see Table 1.2, entry 8.

1.2.2 Optimization of the copolymerization reaction

In order to get a better understanding of the origin of the presence of *trans* and *cis* units in the isolated poly(limonene)carbonates, we then used pure *trans* (**1c**) and *cis* (*R*)-limonene oxide (**1b**) and investigated their behavior separately in the copolymerization with CO_2, and compared the results with those obtained for the commercial mixture of *cis*/*trans* limonene oxide **1a** (Table 1.2).

Table 1.2 Copolymerization of pure **1b**, pure **1c** or a mixture of *cis/trans* (*R*)-limonene oxide (**1a**) and CO_2 using complex $\mathbf{Al^{MeMe}}$ and PPNCl (**Cl**).

entry	epoxide	Cl (mol%)	*T* (h)	conv(%)[b]	*trans* (%)[c]	M_n (kg/mol)[d]	$Đ$[d]
1	**1a**	0.50	12	37	75	2.9	1.33
2	**1a**	0.50	24	47	74	3.1	1.38
3	**1a**	0.50	48	60	70	2.4	1.49
4[e]	**1a**	0.25	48	53	76	6.7	1.55
5[e]	**1a**	0.50	24	31	75	5.2	1.42
6[e]	**1a**	0.50	87	54	74	5.5	1.47
7	**1c**	0.50	60	59	73	3.1	1.28
8	**1b**	0.50	24	67	93	7.0	1.32
9[e]	**1b**	0.50	24	71	98	5.9	1.40
10[e]	**1b**	0.25	48	53	91	5.8	1.43
11[e]	**1b**	0.50	8	27	96	4.8	1.35
12[e,f]	**1b**	0.50	24	54	95	9.1	1.48
13[e,f]	**1b**	0.50	24	49	96	10.6	1.43
14[g]	**1a**	3.0	34	42	>95	n.a.	n.a
15[g]	**1c**	3.0	64	29	>95	n.a.	n.a
16[g]	**1b**	3.0	64	3	n.d.	n.a.	n.a

[a] Reaction conditions: *cis/trans*, *cis* or *trans* (*R*)-limonene oxide (1.0 g, 6.57 mmol), Al-complex $\mathbf{Al^{MeMe}}$ (1 mol%), co-catalyst (quantity indicated in mol%), 10 bar initial CO_2 pressure, 30 mL autoclave, 42ºC, neat. [b] Determined by ^{1}H NMR of the crude reaction mixture with amount of carbonate linkages >99%. [c] Total % *trans* in copolymer determined by ^{1}H NMR using signal integration. [d] Determined by GPC, in THF, at 30 °C, calibrated with polystyrene standards. [e] Reaction carried out in a Fischer-Porter reactor at 5 bar and 45ºC. [f] A different stirring technique was applied.[E] [g] Only co-catalyst PPNCl used at 90ºC; only cyclic limonene carbonate observed. N.a. = not applicable, n.d. = not determined.

[E] See section 1.4.3 "*General copolymerization procedures*" (Figure 1.4) of this chapter for more information.

The copolymerization of a commercial mixture of *trans* and *cis* limonene oxide (**1a**) with CO_2 in a conventional autoclave reactor furnishes poly(limonene)carbonate with relatively low molecular weight (Table 1.2, entries 1-3; M_n around 3.0 Kg·mol^{-1}) and the total reaction time seems to have little effect on the polymer properties (*cf*, Table 1.2, entries 1-3 and 5-6), although some depolymerization of the formed polycarbonate cannot be ruled out completely. The total amount of *trans* units in the formed polycarbonate was followed in time and showed a stable progress in time amounting to about 70-75%. Interestingly, when more strict anhydrous conditions were used (Table 1.2, entries 4-6; Fischer-Porter reactor)[E] the molecular weight values increased up to 6.7 Kg·mol^{-1}, indicating that chain transfer reactions by trace amounts of water are likely responsible for this difference.[68] This assumption was supported by end-group inspection of the MALDI-TOF spectra recorded for these polymers.[F] In all cases where the commercial mixture **1a** of limonene oxide was used as substrate, the stereo-regularity of the produced copolymer was similar.

Then, pure **1c** and **1b** limonene oxide were probed under similar polymerization conditions (entries 7-13) to assess whether the type of substrate has any influence. Remarkably, whereas the use of pure **1c** (Table 1.2, entry 7) results in the formation of a low molecular weight copolymer, the use of the pure *cis* isomer **1b** gives substantially higher molecular weight material (Table 1.2, entry 8) and its conversion is significantly faster. Moreover, the resultant copolymer based on pure **1b** shows a higher degree of stereo-regularity (92% *trans* units, one type) compared with the copolymer based on pure *trans* **1c** (73% *trans* units, two types). This implies that the coupling of pure *cis* limonene oxide is more stereo-selective and suggests that nucleophilic attack of the chloride is surprisingly favored on the most substituted carbon center of the oxirane unit in **1b**. The use of more strict anhydrous conditions failed to give improved polymer properties when using pure **1b** as substrate (Table 1.2, entries 9-11) despite varying both the co-catalyst concentration and reaction time. However, when a different stirring technique (Figure 1.4, section 1.4.3 "*General experimental procedures*")[G] was applied in the reactor (**Table 1.2**, entries 12 and 13), improved molecular weights of the resultant copolymers could be achieved up to an appreciable 10.6 Kg·mol^{-1} while maintaining similar polydispersities (*Đ*) around 1.4. Finally, attempts were done to convert limonene oxide (**1a**) being either a mixture of isomers or a single isomer (Table 1.2. entries 14-16) in the absence of catalyst **Al^{MeMe}**.

[F] See section 1.2.4 "MALDI-TOF-MS analysis" of this chapter for more information.
[G] The influence of the stirring technique suggests that the increasing viscosity of the mixtures observed during the course of the copolymerization reaction (in particular at high conversion levels) strongly affects the mass transfer properties.

The highest conversion was achieved with the commercial mixture of limonene oxide (at 90ºC), whereas the use of pure **1c** (29%) and pure **1b** gave much lower conversion. In these latter reactions full selectivity for the cyclic limonene carbonate was noted, emphasizing the crucial role of catalyst **Al^{MeMe}** to form the copolymer under much milder conditions.

Our results contrast in some aspects with those reported by Coates *et al*.[45] in the sense that (1) lower activities are noted for the binary catalyst **Al^{MeMe}/Cl**, (2) in the presence of this latter binary catalyst system the *cis*-isomer of limonene oxide reacts significantly faster than the *trans* one, whereas for the Coates system this isomer could not be converted, and (3) the use of the *cis*-isomer **1b** results in a stereo-regular, virtually all *trans*-regular copolymer whereas the Coates catalyst is selective towards stereo-regular poly(limonene)carbonate based on the conversion of *trans* isomer **1c**.

1.2.3 Regio- and stereochemistry of the monomers

The Lewis acid catalyst typically coordinates the epoxide after which ring-opening can more easily take place in the presence of a nucleophile to form a corresponding metal alkoxide. This metal alkoxide then can insert a CO_2 molecule and evolve either into a cyclic carbonate or a polycarbonate. Nucleophilic attack may occur in both the *alpha* and *beta* position of both limonene oxide isomers, and thus there are (theoretically) four possible different carbonate repeat units present in the polymer depending on the position where the nucleophilic attack takes place (Scheme 1.4). If the nucleophilic attack occurs at the *alpha* position of the *cis* isomer, a *trans* repeat unit is produced in the growing polymer chain due the inversion of configuration at the *alpha* stereocenter. In contrast, if the nucleophilic attack in the *cis* limonene oxide takes place in the *beta* position, the resulting repeat unit will have a *cis* configuration with retention of the original stereochemistry of the limonene oxide monomer. In case of the *trans* limonene oxide, when the nucleophilic attack occurs at the *alpha* position of *trans* limonene oxide, a *cis* repeat unit is incorporated into the polymer chain, whereas a nucleophilic attack at the *beta* carbon of *trans* limonene oxide generates a *trans* unit in the copolymer. It is important to note here that the *trans* units (Table 1.1and Table 1.2) present in the polymers refer to the total amount of monomers incorporated to the polymer chain with a *trans* configuration and *not* the total amount of *trans* limonene oxide monomer that has reacted. *Trans* repeat units monomers in the polymer are the result of a nucleophilic attack at the *alpha* position of the *cis* limonene oxide isomer and in the *beta* position of the *trans* limonene oxide isomer, respectively.

Scheme 1.4 Different manifolds for the nucleophilic attack in both *cis* and *trans* isomers of limonene oxide. P stands for the polymer backbone.

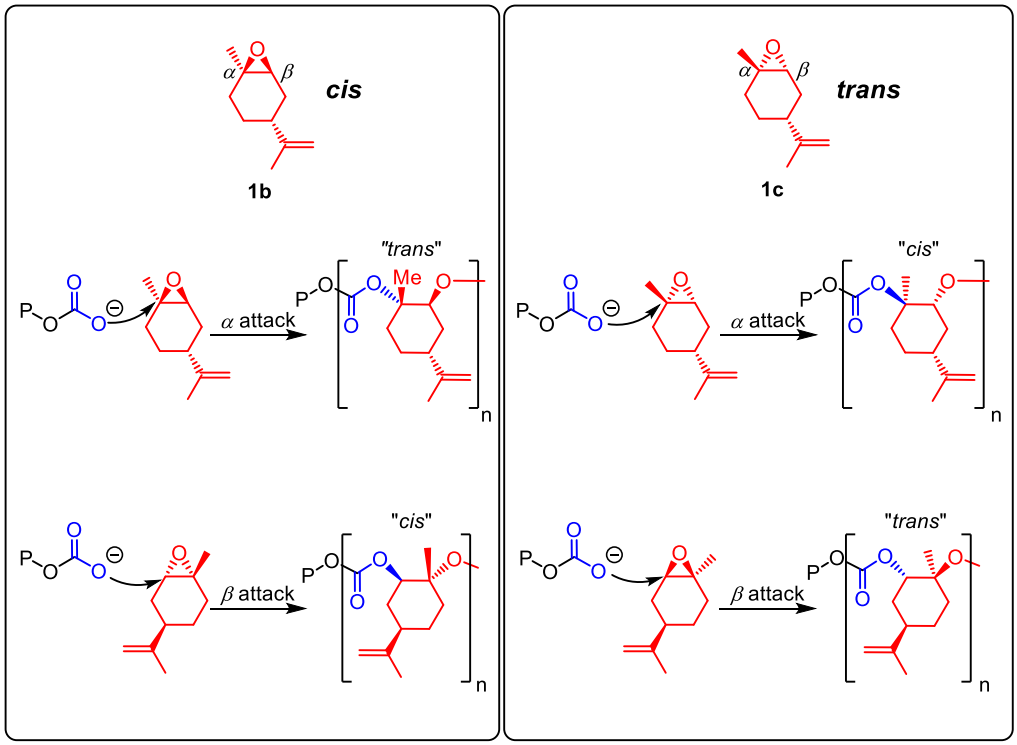

1.2.4 MALDI-TOF-MS analysis

A representative MALDI-TOF-MS spectra for poly(limonene)carbonate is shown Figure 1.1 and Figure 1.2. This poly(limonene)carbonate showed four different distributions. One of these is assigned to a polymer having α,ω-Cl,OH (Figure 1.1 and Figure 1.2 in green) terminal groups which support some degree of Cl-initiation. Other observed distributions were assigned to polymers without a chloride end group (ω-OH, Figure 1.1 and Figure 1.2 in purple). In agreement with previous work reported by Duchateau[69,70] we propose that Meerwein–Ponndorf–Verley–Oppenauer (MPVO) type reactions are responsible for the formation of limonene oxide based alcohols that can acts as initiators. It should be noted that the endgroup in these polymeric structures could be either saturated or unsaturated,[69] though the resolution of these MALDI-TOF measurements was too low to determinate this accurately. The formation of limonene oxide based alcohol initiators through a MPVO reaction is shown in Scheme 1.5.

Figure 1.1 MALDI-TOF mass spectrum of the poly(limonene)carbonate product of Table 1.2 (entry 3) and the assignment of the peaks observed.

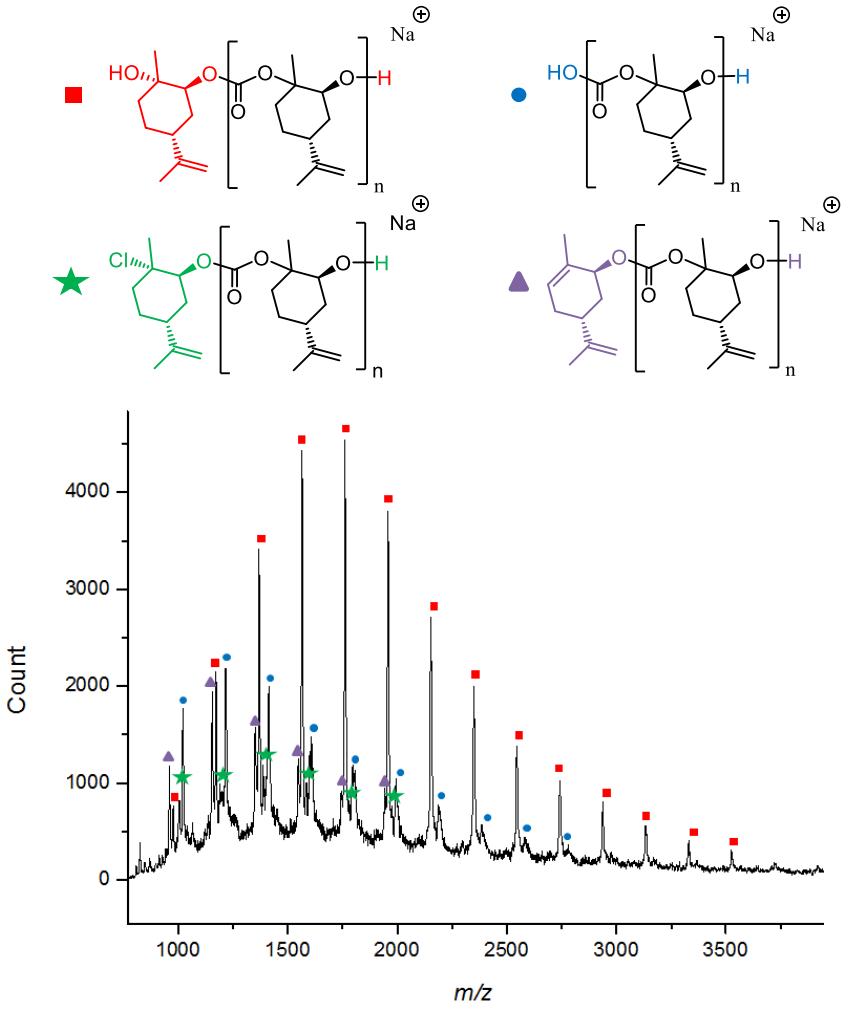

Figure 1.2 Amplification of part of the MALDI-TOF mass spectrum of the poly(limonene)carbonate product of Table 1.2 (entry 3) and the proposed assignment of the peaks observed.

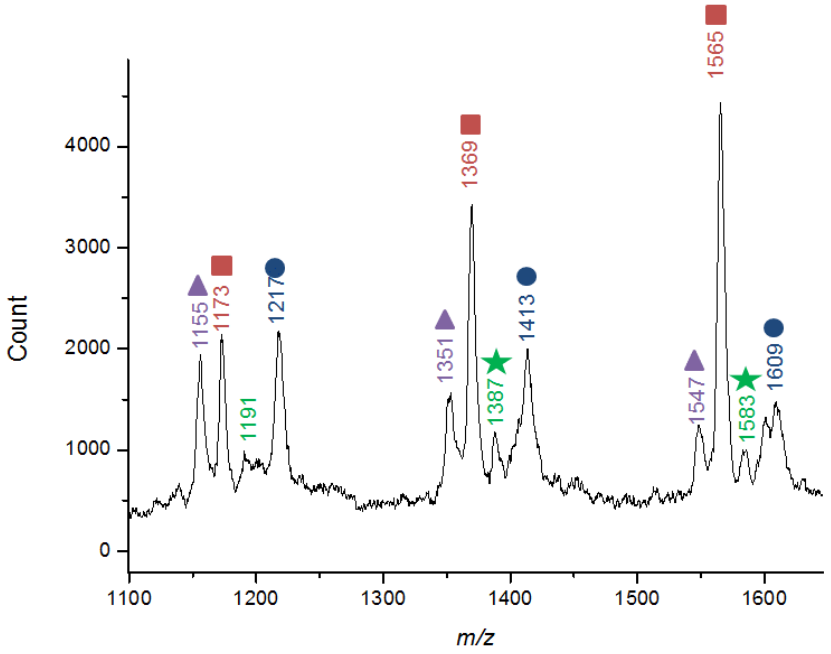

Scheme 1.5 Formation of a limonene oxide based alcohol (inside the blue box) via a MPVO reaction.

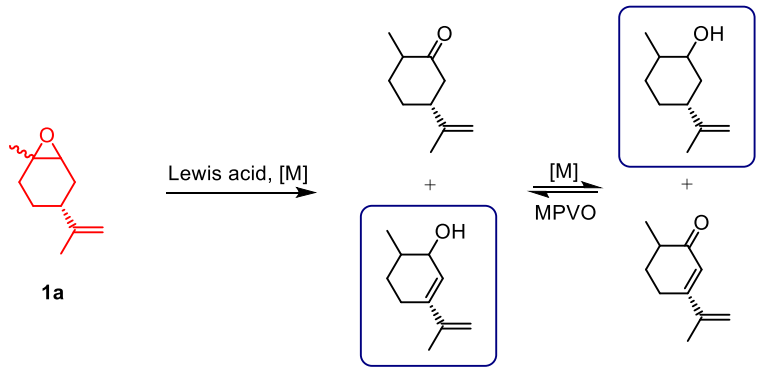

Also, two other distributions were observed with α,ω-OH,OH terminal groups (Figure 1.1 and Figure 1.2; red and blue colored polymers). Due the absence of signals corresponding to polymers having α,ω-Cl,Cl terminal groups, we discard a transesterification reaction as the origin of *α,ω*-OH,OH terminal groups, but rather assign these end-groups as the result of diol initiated chains. In this case, a metal hydroxide can be generated from a metal alkoxide chain

which may react with adventitious water present during the reaction. This metal hydroxide can either attack a carbon dioxide (Figure 1.1 and Figure 1.2 in blue) or react with a limonene oxide molecule (Figure 1.1 and Figure 1.2 in red) to generate a diol.[H] The presence of adventitious water in the reaction and the generation of alcohol groups during the polymerization process results in an increase in the number of initiators, and therefore in a decrease in the observed molecular weight.

1.2.5 Computational studies

Considering a bimetallic[I] mechanism,[71] we further investigated the alternating copolymerization of (*R*)-limonene oxide and CO_2 by using density functional theory (DFT) methods at the B97D3/6-311G**/LANL2DZ level of theory. Both initiation and propagation reactions comprising the Al-catalyst **Al^{MeMe}** were studied as described below giving important and unique insight in the chemo and stereo-selectivities observed experimentally.

Table 1.3 NBO population analysis and activation energies for the epoxide ring-opening step by nucleophilic attack of Cl^- and Br^-.

Substrate	Carbon	NBO population analysis[a]	TS ring-opening (kcal·mol^{-1})[b]	
			Cl$^-$	**Br$^-$**
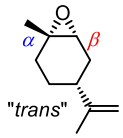	*α*	0.27 (0.31)	2.8	8.9
	β	0.10 (0.12)	4.7	10.2
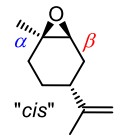	*α*	0.27 (0.31)	0.7	6.1
	β	0.11 (0.13)	3.8	9.1

[a] The first value corresponds to the charge obtained for isolated epoxide; whereas the second (in parenthesis), for the activated substrate due to coordination with the Al-catalyst **Al^{MeMe}**. [b] Ring-opening barriers calculated from the energy difference between the transition state TS and initial complex coordination. Cl- and Br- were used as nucleophilic reagent.

Initiation step

The ring opening of the *trans* (*R*)-limonene oxide **1c** and *cis* (*R*)-limonene oxide **1b** was first evaluated in the presence of chloride as well as bromide nucleophiles. This step usually

[H] For a detailed explanation we refer to section 2.2.4: "*Comparison of GPC traces*" of Chapter 2 where the mechanism of this reaction is explained in detail.
[I] A monometallic mechanism was also investigated for the alternating copolymerization of CO_2 and epoxides, affording higher free-energy barriers for the propagation reaction.

involves a concerted transition state (**TS1** in Scheme 1.6) which is characterized by the breaking of the $C_{\alpha/\beta}$–O epoxide bond and the simultaneous formation of a $C_{\alpha/\beta}$–Cl/Br, leading to the formation of an alkoxide intermediate (**Int-1** in Scheme 1.6).[53,65]

Scheme 1.6 Free-energy profiles for the initiation reaction of copolymerization between *cis*/*trans*-(*R*)-limonene oxide and CO_2 catalyzed by the Al-complex **Al^{MeMe}/Cl** binary system, and considering nucleophilic attack on the *α* and *β* positions resulting in four different pathways.[J]

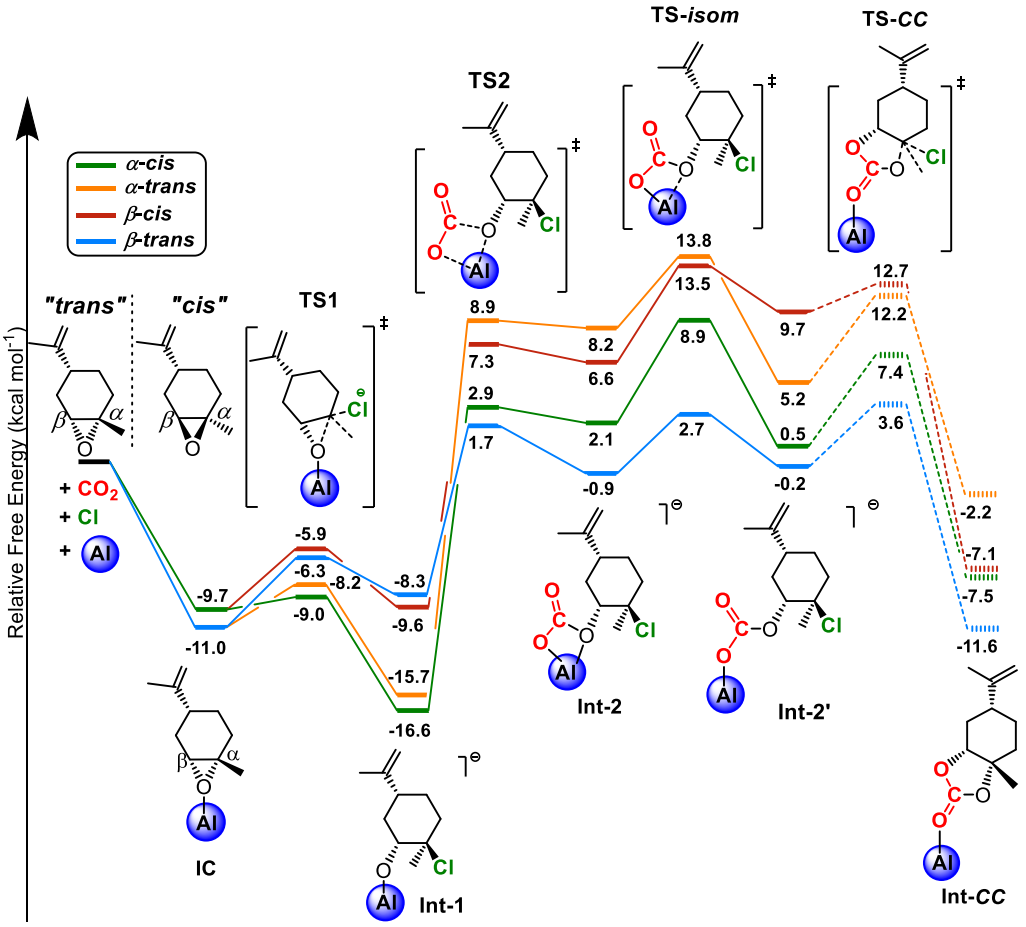

[J] As solvent, 1-hexanol was evaluated at 25 ºC. Barriers for the backbiting reactions appear in dashed lines. Note that only for the pathway involving the *trans* substrate **1c** (α attack) accompanying schematic structures are provided.

The nucleophilic attack can occur at the α carbon (most substituted carbon) or the β carbon (least substituted carbon) atoms of the *cis*/*trans* limonene oxide, and therefore eight possible ways of epoxide ring opening should be considered. The fourth and fifth columns of Table 1.3 collect the activation free-energies calculated for this step, once the epoxide is activated by the Lewis acidic aluminum center in complex **Al^{MeMe}**. In general, barriers for the chloride attack are much lower than those obtained for the bromide attack. In all the cases, the α attack is favored over the β one, as supported by the NBO population analysis included also in Table 1.3. It is commonly thought that the most substituted α carbon is less reactive than the least hindered because of the electronic effects induced by the methyl group. In contrast, the α attack was found to be more feasible, with the *cis* isomer being preferred over the *trans* one by 2.1 kcal·mol^{-1}. Alternatively, for the β attack, this energy difference is less marked (0.9 kcal·mol^{-1}) although the *cis* isomer still remains favored. Because of the better results obtained using the chloride nucleophile, the latter was selected as co-catalyst for the alternating copolymerization, and thus decreasing the number of possible pathways to study. Scheme 1.6 illustrates the free-energy profiles for the Al-complex **Al^{MeMe}**/chloride catalyzed initiation of the copolymerization of *cis/trans*-(*R*)-limonene oxide and CO_2, taking into account the nucleophilic attack by chloride on the α and β positions of both epoxides. The starting point is the assembly of the isolated reactants, i.e. the Al-complex **Al^{MeMe}**, chloride, *cis*/*trans* epoxide and CO_2 for which the total free energy is set to 0.0 kcal·mol^{-1}. Then, the catalytic cycle begins with the coordination of each epoxide to the Al(III) center of complex **Al^{MeMe}** (allowing for epoxide activation) yielding two different complexes **IC**. This step is exergonic by 9.7 kcal·mol^{-1} for the *cis*-coordinated (trace in green) complex and 11.0 kcal·mol^{-1} for the *trans* one (trace in blue), showing thus a (slight) preference towards formation of the latter complex.

As indicated above, the ring-opening step leads to formation of the metal-alkoxide **Int-1**. It can be observed that the intermediates obtained by nucleophilic attack at the α position are energetically more stable than those involving the β attack; the α carbon is more electrophilic than the β one, as explained before by the NBO population analysis (Table 1.3). It is worth noting that the α carbon is a stereogenic center; consequently the nucleophilic attack of chloride on this carbon center evolves with inversion of configuration. Thus, the *cis*-coordinated epoxide evolves into the most stable *trans*-product **Int-1** (trace in green) and the *trans* one is converted into the *cis* metal-alkoxide intermediate (trace in orange). For the β attack, retention of configuration holds since the nucleophilic attack does not involve a stereogenic carbon center.

Following the epoxide ring opening by the nucleophilic chloride, CO_2 is inserted into the Al–O alkoxide bond of **Int–1** *via* transition state **TS2**. The intermolecular CO_2 insertion was located to be less energetically demanding for the *β-trans* and *α-cis* pathways, with relative barriers of 1.7 and 2.9 kcal·mol^{-1}, respectively. The highest barrier was calculated for the *α-trans* pathway, having an activation energy of 24.6 kcal·mol^{-1}. This step affords the hemi-carbonates **Int-2**, which are coordinated by two oxygen atoms to the Al(III) center. These intermediates follow the same stability trends as the preceding **TS2**, and could suffer isomerization (through **TS-isom**) to form the linear hemi-carbonate **Int-2'**. In this case, the *β-trans* and *α-cis* pathways still lead to the most stable intermediates. The isomerization of **Int-2** is rate-determining for the *α-trans*, *β-cis* and *α-cis* profiles, with activation barriers (calculated from the alkoxide intermediate **Int-1**) of 29.5, 23.1 and 25.5 kcal·mol^{-1}, respectively. In the case of the *β-trans* profile, this is valid if the reaction is evaluated only until formation of the intermediate **Int-2'** (rather than taking into account the subsequent backbiting reaction as further discussed below) involving an activation barrier of 13.7 kcal·mol^{-1}, which is calculated from the most stable complex **IC**.

Having reached this point, two possible routes can be followed by these intermediate; the backbiting of the linear hemi-carbonate **Int-2'** yielding the (undesired) cyclic carbonate, or consecutive addition of new epoxide and CO_2 monomers allowing for propagation towards an alternating copolymer. The backbiting reaction is shown in Scheme 1.6 and goes through **TS-CC**. The latter displays features of a classical S_N2 type transition state similar to the epoxide ring opening with intramolecular ring-closing and concomitant release of the chloride nucleophile. This step requires slightly lower barriers than that involved in the isomerization reaction, with the *β-trans* profile being the only exception with relative barrier of 3.6 kcal·mol^{-1}. The alternating propagation reaction is separately discussed in the next section and will explain why there is a preference for polycarbonate formation from limonene oxide and CO_2 using Al complex **Al^{MeMe}**/PPNCl as catalyst system.

Propagation step

Once the linear hemi-carbonate **Int-2'** is formed in the initiation process, several attack routes can be followed.[K] The carbonyl oxygen of the four resulting **Int-2'** species serve as nucleophiles for attacking two different epoxide conformations (*cis* or *trans*) on two different carbon atoms (α or β). This situation generates sixteen possible profiles to investigate (Scheme 1.7).

Scheme 1.7 Sixteen possible pathways for the copolymerization of *cis*/*trans*-(*R*)-limonene oxide and CO_2 catalyzed by the Al-complex **Al^{MeMe}**/chloride binary system.

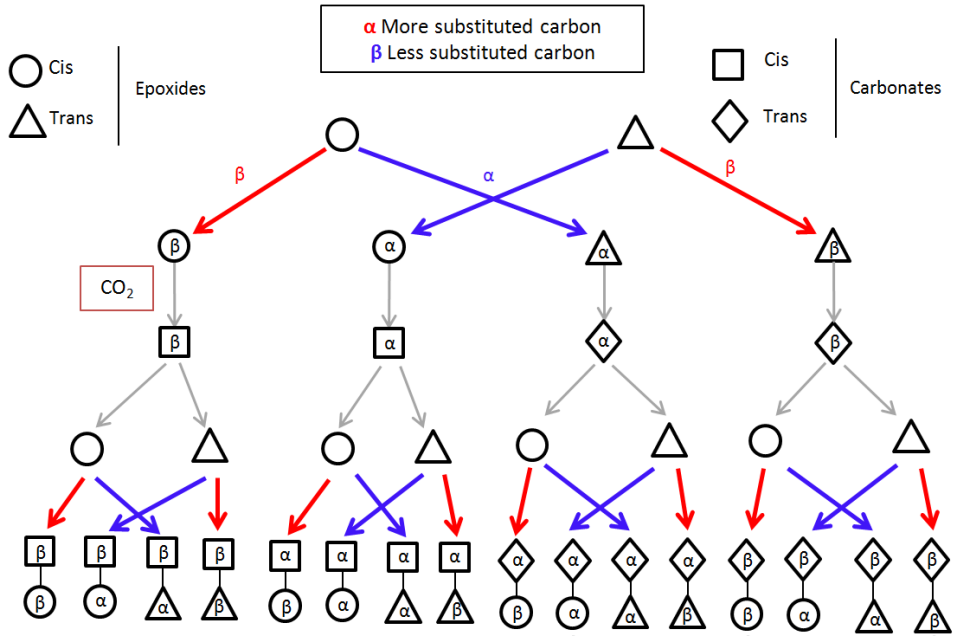

In order to decrease the computational efforts, we decided to study the most feasible pathways based on the outcome from the initiation reaction. Thus, the number of pathways was reduced to four by considering the attack by the most stable *α-cis* and *β-trans* hemi-carbonates on the α carbon (the most electrophilic atom) of the *cis* and *trans* epoxides. The free-energy

[K] Note that the formulation *cis-cis* (for instance) for a dimeric carbonate unit refers to initial conversion of a *cis*-limonene oxide monomer followed by the insertion (through an S_N2 like pathway, **TS-*p*** in Scheme **1.8**) of a second *cis*-limonene oxide monomer to afford a *trans-trans* dimeric carbonate unit. Alternatively, the conversion of two *trans* limonene oxide monomers in a similar way also leads to a *trans-trans* dimeric carbonate intermediate (cf., **Int-*p´*** in Scheme **1.8**).

profiles for the alternating propagation step of *cis*/*trans*-(*R*)-limonene oxide and CO_2, taking into account the previous considerations, are illustrated in

Scheme **1.8**.

Scheme 1.8 Free-energy profiles for the propagation of the bimetallic copolymerization between CO_2 and *cis*/*trans*-(*R*)-limonene oxide mediated by the Al-complex **Al^{MeMe}**/chloride binary system, and considering the nucleophilic attack by the carbonyl oxygen (O[2]) on the *α* carbon of the epoxides.[L]

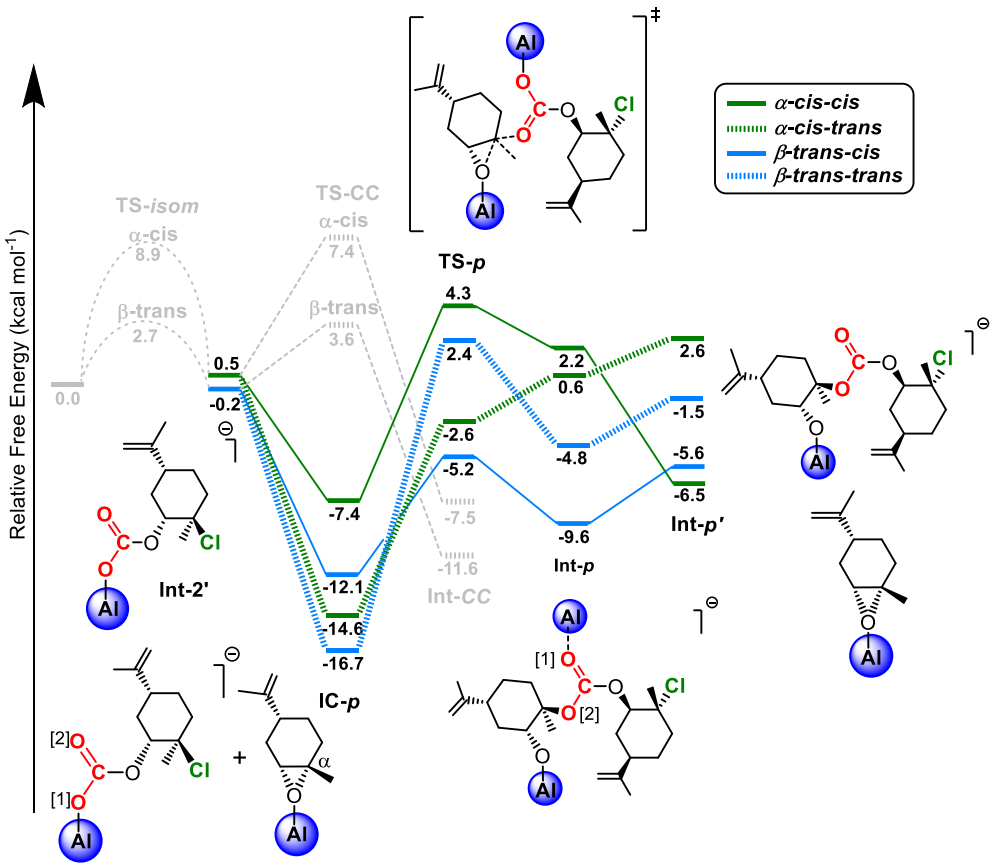

[L] As solvent, 1-hexanol was evaluated at 25 ˚C. The barriers for the isomerization and the backbiting reactions of the initiation process (affording cyclic carbonates) appear in grey dashed lines. Note that only for the pathway involving the *trans* substrate **1b** (α attack) accompanying schematic structures are given (*i.e.*, formation of a *cis*-*cis* dimer).

The propagation step requires two aluminum centers (bimetallic mechanism[M]).[71,72] First the formation of a very stable adduct is observed between the intermediate **Int-2'** and the complex having a new epoxide substrate coordinated to another Al-complex **cat2** (**IC-p**). Natural bond orbital (NBO) population analysis on this complex shows small difference in the value of the charge assigned to the oxygen atoms of the carbonate **Int-2'**. The oxygen atom labeled O[1] bound to the Al center in

Scheme **1.8** exhibits a charge of -0.83, whereas for the carbonyl oxygen (O[2]) a value of -0.69 was obtained. Although the oxygen O[1] is slightly more nucleophilic than the carbonyl oxygen O[2], reaction progress through O[1] leads to the higher barriers for subsequent steps of the free-energy profile (Scheme 1.9). In all cases, a substantial lower energy between the formed **IC-p** and the transition state of the backbiting reaction (**TS-CC**; Scheme 1.6 and grey traces in

Scheme **1.8**) was found. Thus, for instance, the resulting complexes between the *α-cis* **Int-2'** and the coordinated *cis* and *trans* epoxides (*i.e.*, *α-cis-cis* and *α-cis-trans* dimers in

Scheme **1.8**) were found to be more stable than their corresponding **TS-CC** by 14.8 and 22.0 kcal·mol^{-1}, respectively. In the case of the *β-trans* carbonate **Int-2'** forming an initial adduct with each (coordinated) substrate attached to a second Al complex **Al^{MeMe}**, this energy difference becomes 15.7 kcal·mol^{-1} combining with the *cis*-epoxide and 20.3 kcal·mol^{-1} with the *trans* one that would result in dimers *α-trans-cis* and *α-trans-trans*.

Following the reaction coordinate, the next step is the epoxide ring opening, which is the result from a nucleophilic attack of the carbonyl oxygen labeled O[2] (

Scheme **1.8**) on the most substituted carbon (*α*) of each epoxide isomer bound to one of the Al(III) centers in **IC-p**. Similar to the initiation step, in the propagation step the epoxide ring-opening is characterized by a concerted transition state **TS-p**. The *α-cis-cis* profile shows the highest activation barrier being 20.9 kcal·mol^{-1} (having a relative energy of 4.3 kcal·mol^{-1}), calculated from the most stable intermediate of the initiation process **Int-1** with a relative energy of –16.6 kcal·mol^{-1} (Scheme 1.6). In contrast, the **TS-p** for the *β-trans-cis* pathway involves an activation barrier of only 6.9 kcal·mol^{-1} (estimated from the adduct **IC-p**). In the case of the *β-trans-trans* and *α-cis-trans* profiles, these barriers were obtained in a similar way as described for the previous pathways, and lead to values of 19.1 and 14.0 kcal·mol^{-1}, respectively.

[M] Williams *et al.* have recently described a bimetallic Zn catalyst that is active in CO_2/CHO copolymerization, and computational efforts have also demonstrated the necessity of two metal centres for efficient copolymerization.

Once passing through the barrier for **TS-p**, the formation of the intermediate **Int-p** occurs which has both Al complexes still coordinated. However, the strength of interaction between the oxygen from the alkoxide and the Al center is much stronger than that observed for the oxygen O[1] of the coordinated carbonate and the Al(III) center from **Int-2'**. Hence, it is proposed that **Int-p** can evolve into intermediate **Int–p'** by releasing the Al complex from the carbonate and allowing for coordination of a new *trans*-(*R*)-limonene oxide monomer.

Scheme 1.9 Free-energy profiles of the nucleophilic attack by both oxygen atoms[1] and [2] of the carbonate on the epoxide for the copolymerization of *cis*/*trans*-(*R*)-limonene oxide and CO_2 catalyzed by the Al-complex **Al^{MeMe}**/chloride binary system. Two options (*cis-cis* and *cis-trans*) were considered for comparison. As solvent, 1-hexanol was evaluated at 25 °C. Barriers for the backbiting and isomerization reactions for the initiation process appear in grey and dashed line.

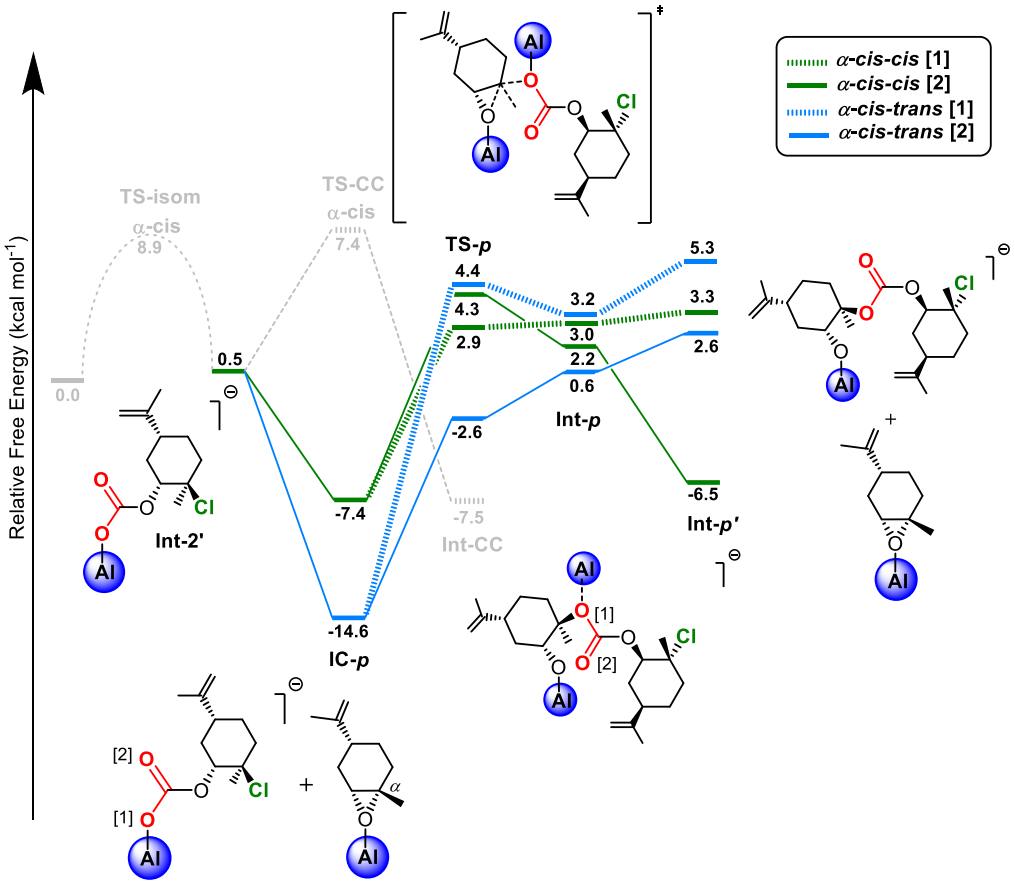

This reaction is endergonic by 2.6 kcal·mol^{-1} for the *α-cis-trans* profile. The remaining processes are slightly exergonic, with a release of -1.5, -5.6 and -6.5 kcal·mol^{-1} in the case of the *β-trans-trans*, *β-trans-cis* and *α-cis-cis* pathways, respectively. Interestingly, both the energetically most stable dimeric units **Int-p'** resulting from the *β-trans-cis* and *α-cis-cis* profiles will contain merely trans units in their backbone,[71] which is overall well in line with the experimental results. The current catalytic process based on Al complex **Al^{MeMe}**/PPNCl shows two main features: (1) a clear preference for the faster conversion of *cis* (*R*)-limonene oxide **1b**, and (2) the resulting copolymers contain a significant higher amount of *trans* versus *cis* units (up to 98:2, Table 1.2) where the use of pure *cis*-limonene oxide will result in the formation of a nearly stereo-regular all-*trans* polycarbonate.

1.3 Conclusions

This work showcases the rare but efficient conversion of a tri-substituted oxirane (limonene oxide) and CO_2 into a 100% bio-based polycarbonate using an Al(III)amino-trisphenolate/PPNCl binary catalyst under mild reaction conditions (42ºC, 5-10 bar). The typical features of this process involve a catalyst system based on an earth-abundant metal and modular, cheap and easily accessible ligand systems. The catalyst is highly robust as testified by the high conversion levels that can be attained (>70%) of the limonene oxide under neat reaction conditions. The poly(limonene)carbonates can be produced in a stereo-regular fashion (when pure *cis*-limonene oxide is used) and its copolymer exhibits a T_g value of around 112ºC potentially useful in the context of finding bio-alternatives for CHO-derived polycarbonates.

The DFT results show unique and important insight into the chemo- and stereo-selectivity of the limonene oxide/CO_2 coupling reaction mediated by Al complex **Al^{MeMe}**/PPNCl. This information is highly valuable to develop other types of bio-based poly(carbonates) and/or polyesters. These types of bio-based polymers are expected to grow significantly in importance in the forthcoming development of new, sustainable alternative thermoplastics for the specialty polymer industries. Taking into account the favorable characteristics of the presented Al(III) amino-triphenolate complex and their reactivity and robustness, we are currently planning to widen the scope of accessible CO_2-based polymers. In this context, several other relevant contributions have been reported after publication of our work, including the synthesis of poly(limonene)carbonate by Rieger and coworkers.[73] Greiner and coworkers reported in 2016 the synthesis[74] and post-modification[75] of poly(limonene)carbonate, and post-modification of poly(limonene)dicarbonate has also been studied by Sablong, Koning *et al*.[76,77]

1.4 Experimental section

1.4.1 General information and instrumentation

^{1}H NMR and ^{13}C NMR spectra were recorded at ambient conditions on Bruker AV-400 or AV-500 spectrometers and referenced to the residual deuterated solvent signals. All reported NMR values are given in parts per million (ppm). Assignment of the signals in the NMR spectra of all polyesters was based on 2D NMR experiments.

Matrix-assisted laser desorption/ionization time-of-flight mass spectrometry (MALDI) were performed by the Research Support Group at ICIQ on a BRUKER Autoflex spectrometer using dithranol as a matrix and CF_3COONa as an additive. Other mass spectrometric analyses were done using a Micro TOF II (Bruker Daltonics) HPLC-MS-TOF equipment.

Glass transition temperatures (T_g) were measured using a Mettler Toledo apparatus, model DSC822e. Samples (~ 7 mg) were weighed into 40 μL aluminum crucibles and subjected to two heating cycles. The measures were carried out under N_2 atmosphere. The first cycle covered the range from -80 °C to 200 °C at 5 °C/min and was cooled back to -80 °C at -5 °C/min. Midpoint T_g data was obtained from the second heating cycle which ranged from -80 °C to 200 °C at a heating rate of 5 °C/min. Thermo-gravimetric analyses were recorded under a N_2 atmosphere using a Mettler Toledo apparatus (model TGA/SDTA851) with a heating rate of 10 °C/min.

Gel permeation chromatography measurements were performed in tetrahydrofuran at 40 °C at a flow rate of 1 mL·min^{-1}. Samples were analyzed at a concentration of 3 mg·mL^{-1} after filtration through a 0.45 μm pore-size membrane. The separation was carried out on three polystyrene/divinylbenzene columns from Agilent: PLgel 5 μm MIXED-C, 300 × 7.5 mm. The setup (Viscotek TDA305) was equipped with a refractive index (RI) detector (λ = 670 nm). M_n, M_w and $Đ$ were derived from the RI signal by a calibration curve based on polystyrene standards (PS from Polymer Standards Service) for the analysis of the polymers. GPC measurements for the polymers were performed by the LCPP Team at CPE Lyon.

Gas chromatogram (GC) analysis was performed on a GC-MS Agilent equipped; model 6890N (GC) 5973 (MSD) using a HP-5MS chromatography column (30 m × 0.25 mm × 0.25 μm). The sample (2 mg·mL^{-1} in dichloromethane) was analyzed under the following conditions: T_{inj}-aux: 280 °C, rate: 1.5 mL/min, split 100:1 (0.2 μL), isothermal 60 °C.

1.4.2 Synthesis of complexes

Synthesis of amino triphenolate ligand H_3L^{Me}

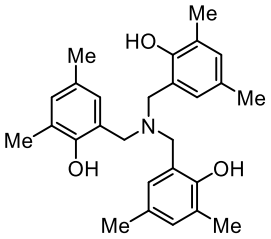

H_3L^{Me} was prepared according to a literature procedure:[78] A mixture of hexamethylenetetramine (2.58 g, 18.4 mmol, 1 equiv.), 2,4-dimethylphenol (10 mL, 82.8 mmol, 4.5 equiv.) and p-toluenesulfonic acid hydrate (70 mg, 0.36 mmol,0.02 equiv.) was stirred and heated with an oil bath at 110 °C for 20 h. Then an additional quantity of 2,4-dimethylphenol (3.4 mL, 27.6 mmol, 1.5 equiv.) was added and heated for a further period of 20 h. Once the time was over, the reaction was cooled down to room temperature and 20 mL of MeOH were added to the yellow slurry. The solution was sonicated until a pale yellow solid crashed out of solution. The solid was filtered off, washed with cold MeOH and dried under vacuum. The compound was recrystallized from acetone. Spectroscopic characterization was consistent with the reported data in the literature.

^{1}H NMR (400 MHz, $CDCl_3$) δ 6.87 (d, *J* = 1.9 Hz, 3H), 6.74 (d, *J* = 1.9Hz, 3H), 3.63 (s, 6H), 2.22 (s, 18H).
^{13}C NMR (101 MHz, $CDCl_3$) δ 151.10, 131.28, 129.12, 128.85, 124.56, 121.83, 56.53, 20.39, 15.90.

Synthesis of amino triphenolate ligand H_3L^{Cl}

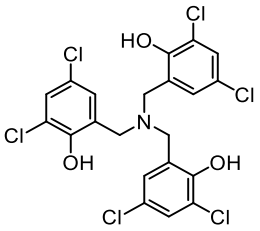

H_3L^{Cl}: 2,4-dichlorophenol (4.0 g, 24.5 mmol) and hexamethylene tetramine (HMTA; 1.2 g, 8.5 mmol) were heated at 110 ºC for 2.5 h. Once the time was over, the reaction was cooled down to room temperature and 20 mL of MeOH were added to the yellow slurry. The solution was sonicated until a pale yellow solid crashed out of solution. The solid was filtered off and washed with cold MeOH. Then, 100 mL of distilled water was added to the solid forming a suspension, which was slowly basified by adding dropwise 1 M NaOH until all the solid had

dissolved. Once the solid was dissolved, the solution was neutralized with 1 M HCl. A white precipitate formed which was filtered off and dissolved in 10 mL of CH_2Cl_2, and after the addition of hexane the product precipitated. The white powder was filtered off and dried under vacuum. Spectroscopic characterization was consistent with that reported in the literature.[63]

^{1}H NMR (500 MHz, $CDCl_3$) δ 7.26 (d, *J* = 2.5Hz, 3H), 7.05 (d, *J* = 2.5Hz, 3H), 3.75 (s, 6H).
^{13}C NMR (125 MHz, $CDCl_3$) δ 149.83, 129.10, 128.54, 124.84, 124.72, 121.09 and 55.35 ppm

Synthesis of ion complex **Fe^{MeMe}**

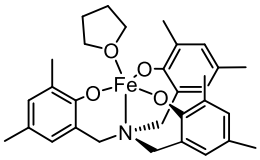

Fe^{MeMe} was prepared according to a reported literature procedure:[62] To a suspension of sodium hydride (85.6 mg, 3.57 mmol, 3 equiv.) in tetrahydrofuran (10 mL) was slowly added a solution of H_3L^{Me} (500 mg, 1.19 mmol, 1 equiv.) in tetrahydrofuran (10 mL). The mixture was stirred for 18 h and after this time it was added to a solution of anhydrous iron(III) chloride (193 mg, 1.19 mmol, 1 equiv.) in tetrahydrofuran (10 mL). The mixture was stirred for a further 4 h and then filtered through a path of Celite. Hereafter, the solvent was evaporated to yield a brown residue, which was subsequently dissolved in dichloromethane, filtered and the solvent removed under reduced pressure to yield a brown powder.

Synthesis of aluminium complex **Al^{MeMe}**

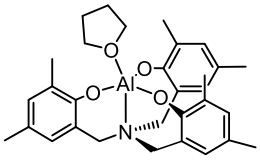

[Al Me_3] (2 M in heptane, 1.19 mL, 2.38 mmol) was slowly added to a solution of ligand **H_3L^{Me}** (1.0 g, 2.38 mmol) in THF (20 mL). The solution was stirred at rt for 2 h and then concentrated. Hexane was added to the residue resulting in the precipitation of the desired complex, which was isolated by filtration and further dried under vacuum to yield a white powder. Spectroscopic characterization was consistent with that reported in the literature.[65]

^{1}H NMR (300 MHz, $CDCl_3$) δ 6.87 (d, *J* = 2.3 Hz, 1H), 6.61 (d, *J* = 2.3 Hz, 1H), 4.26 (d, *J* = 13.8 Hz, 1H), 2.83 (d, *J* = 13.8 Hz, 1H), 2.20 (s, 5H), 2.19 (s, 7H).
^{13}C NMR (101 MHz, $CDCl_3$) δ 154.25, 131.01, 126.95, 125.84, 120.63, 58.66, 25.60, 20.39.

Synthesis of aluminium complex **Al^{ClCl}**

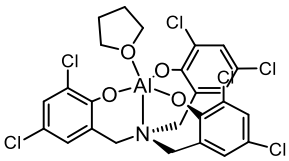

Al-complex **Al^{ClCl}** was synthesized according to a reported literature procedure:[63] To a solution of **H$_3$L^{Cl}** (800 mg, 1.47 mmol) in tetrahydrofuran (20 mL) was slowly added $AlMe_3$ (2 M in heptane, 735 μL, 1.47 mmol). The solution was stirred at rt for an additional 2 h and then concentrated. Hexane was added to the residue resulting in the precipitation of the desired complex, which was isolated by filtration and dried under vacuum to yield a white powder. Spectroscopic characterization was consistent with that reported in the literature.[63]

^{1}H NMR (400 MHz, $CDCl_3$) δ 7.33 (d, *J* = 2.6 Hz, 3H), 6.90 (d, *J* = 2.6 Hz, 3H), 4.74 – 4.63 (m, 4H), 4.17 (d, *J* = 13.7 Hz, 3H), 2.94 (d, *J* = 14.1 Hz, 3H), 2.26 – 2.19 (m, 4H).
^{13}C NMR (101 MHz, $CDCl_3$) δ 152.46, 129.75, 127.13, 124.68, 123.08, 122.16, 72.38, 58.26, 25.48.

1.4.3 General copolymerization procedures

Copolymerization of limonene oxide with carbon dioxide

Typical conditions: (*R*)-limonene oxide (1.0 g, 6.57 mmol), the Al catalyst (0.5-1.0 mol %) and co-catalyst (the respective chloride or bromide, 0.25-2.5 mol %) were placed in a 30 mL stainless steel reactor with a stirring bar. Three cycles of pressurization and depressurization with carbon dioxide were applied (pCO_2 = 5 bar) before finally stabilizing the pressure at 10 bar. The reactor was then heated to the required temperature for the chosen time. After that, the reactor was cooled down to rt before depressurizing. After this time, the conversion and selectivity was calculated using ^{1}H NMR analysis ($CDCl_3$) of an aliquot of the reaction mixture.

The starting material was removed from the reaction mixture *in vacuo*. The poly(limonene)carbonates were further purified by dissolving the reaction mixture into a small amount of dichloromethane followed by precipitation of the products by addition of acidic methanol (HCl, 1 M in methanol). After that, the polymer was filtered off and dried *in vacuo* followed by, depending on the sample, a combination of NMR, MALDI-TOF, GPC, TGA and DSC analyses.

Figure 1.3 Stainless steel reactor used for the copolymerization reactions.

Figure 1.4 Schlenk reactor vessel and stirring bar used: **Left**: stirring bar used in the polymerization of limonene oxide and carbon dioxide. **Right**: stirring bar used in Table 1.2 entry 12 and entry 13.

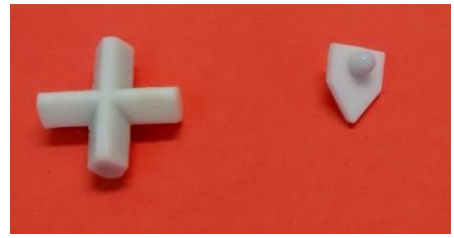

Copolymerization of limonene oxide with carbon dioxide under anhydrous conditions

Reactions under more rigorously dry conditions were conducted in a Fischer-Porter (Schlenk type reactor; Figure 1.4 left). Typically, (*R*)-limonene oxide (*cis*/*trans* mixture) and pure *cis*-(*R*)-limonene oxide were each distilled from calcium hydride under reduced pressure following three cycles (30 min each) of vacuum-N_2 purging, and stored in a glove box. The

catalyst and co-catalyst were dried by three cycles (30 min each) of vacuum-N_2 purging in a silicon bath at 70ºC. The Fisher-Porter reactor was filled inside the glove box and closed. After one cycle of pressurization and depressurization with carbon dioxide (pCO_2 = 3 bar) the reactor was pressurized at 5 bar and heated in a silicon bath at 45 ºC for the chosen time. The reaction mixture was then dissolved in dichloromethane and the poly(limonene)carbonate was precipitated by addition of acidic methanol (HCl, 1 M in methanol). Analysis was done as reported for the other poly(carbonate) samples.

1.4.4 Cyclic limonene carbonate formation

(*R*)-Limonene oxide was introduced in a 30 mL stainless steel reactor with the appropriate loading of co-catalyst (PPNCl, 3 mol%) and MEK (1 mL). After 64 h, the reaction was stopped and the product was purified through column chromatography and analyzed by ^{1}H NMR ($CDCl_3$).

1.4.5 Kinetic resolution of *cis*- and *trans*- 1,2-limonene oxide

Cis and *trans*-(*R*)-limonene oxide were isolated according to literature procedures.[79]

Cis-(*R*)-limonene oxide (**1b**)

Pyrrolidine (8.35 mL, 0.10 mol), (*R*)-(+)-limonene oxide (16.4 mL, 0.10 mol), and water (1.5 mL, 0.08 mol) were added to a 50 mL round-bottom flask equipped with a magnetic stir bar and a reflux condenser. The reaction mixture was heated to reflux, 100 °C, and stirred under reflux for 48 h. The contents of the round-bottom flask were transferred to a separation funnel containing pentane (50 mL). The organic layer was extracted with water (2 × 50 mL). The pentane layer was dried over anhydrous magnesium sulfate and gravity filtered into a 100 mL round-bottom flask. The pentane was removed *in vacuo* (rotary evaporator). The *cis*-(*R*)-(+)-limonene oxide was then purified by silica gel chromatography using EtOAc/hexanes (1:9) as eluent giving 5.10 g of product (84%).

Trans-(*R*)-limonene oxide (**1c**)

A 50 mL round-bottom flask equipped with a magnetic stir bar and a reflux condenser was charged with (*R*)-(+)-limonene oxide (4.57 g, 0.03 mol), pyrazole (0.34 g, 0.005 mol), and deionized water (16.2 mL). The mixture was heated to 100 °C (reflux) and heated under reflux for 5 h. The reaction mixture was placed in a water bath heated to approximately 80 °C. The

mixture was then transferred to a separation funnel and extracted with warm (80 °C) deionized water (2 × 30 mL) to remove the diol. The aqueous layer was then placed in a refrigerator wherein the diol precipitated upon cooling. Excess pentane was then added to the separation funnel containing the organic layer and a slurry of white solid formed immediately. The mixture was vacuum filtered to remove the solid and further solid formed upon evaporative cooling from the vacuum. The mixture was filtered for a second time removing the remainder of 1,2-limonene diol. The clear pentane phase that remained clear was dried over anhydrous magnesium sulfate and gravity filtered into a 100 mL round-bottom flask. The pentane was removed *in vacuo* (rotary evaporator) leaving *trans-R*-(+)-limonene oxide (1.50 g, 55%).

Scheme 1.10 Kinetic resolution of *cis*- and *trans*-limonene oxides

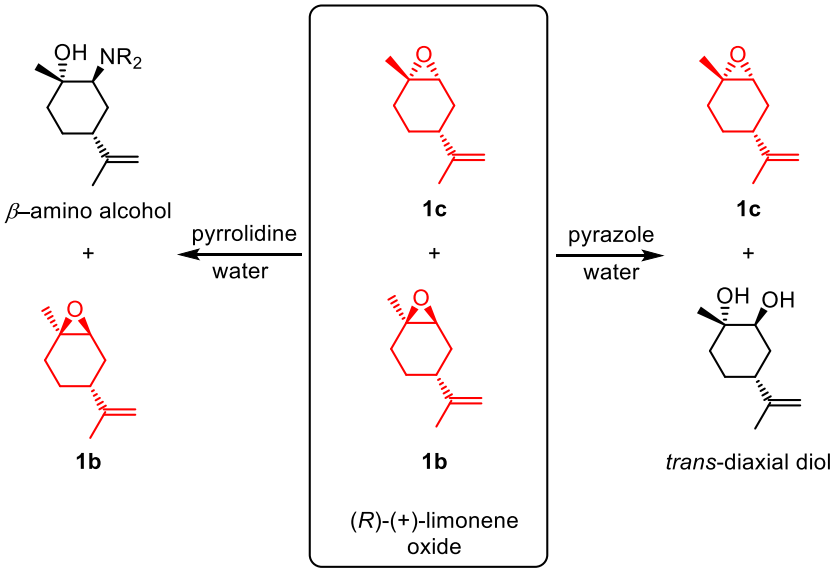

1.4.6 Computational details

All calculations in this study were carried out using the Gaussian 09 package.[N] The B97D3 functional was employed, which includes empirical dispersion energy corrections as introduced by Grimme.[80,81] The standard 6-311G(d,p) basis set was used to describe the H, C, N and O atoms. The relativistic effective core pseudo potential LANL2DZ was used for Al, Br and Cl atoms together with its associated basis set. Full geometry optimizations were performed without constrains. The nature of the stationary points encountered was characterized either as minima or transition states by means of harmonic vibrational frequencies analysis. Gibbs free energies were calculated at standard conditions (T = 298 K, p = 1 bar). In order to introduce solvent effects, single point calculations were performed on the gas-phase optimized structures by using the polarizable continuum model (PCM). The dielectric constant (ε) of the polarizable medium was set to the value reported for the simplest epoxide, ethylene oxide (ε = 12.42)[82] as the reaction takes place in the limonene oxide rich phase. The 1-hexanol solvent was used for this purpose (ε = 12.51), as implemented in Gaussian.

[N] Gaussian, Revision D.01, M. J. Frisch, G. W. Trucks, H. B. Schlegel, G. E. Scuseria, M. A. Robb, J. R. Cheeseman, G. Scalmani, V. Barone, B. Mennucci, G. A. Petersson, H. Nakatsuji, M. Caricato, X. Li, H. P. Hratchian, A. F. Izmaylov, J. Bloino, G. Zheng, J. L. Sonnenberg, M. Hada, M. Ehara, K. Toyota, R. Fukuda, J. Hasegawa, M. Ishida, T. Nakajima, Y. Honda, O. Kitao, H. Nakai, T. Vreven, J. A. Montgomery, Jr., J. E. Peralta, F. Ogliaro, M. Bearpark, J. J. Heyd, E. Brothers, K. N. Kudin, V. N. Staroverov, R. Kobayashi, J. Normand, K. Raghavachari, A. Rendell, J. C. Burant, S. S. Iyengar, J. Tomasi, M. Cossi, N. Rega, N. J. Millam, M. Klene, J. E. Knox, J. B. Cross, V. Bakken, C. Adamo, J. Jaramillo, R. Gomperts, R. E. Stratmann, O. Yazyev, A. J. Austin, R. Cammi, C. Pomelli, J. W. Ochterski, R. L. Martin, K. Morokuma, V. G. Zakrzewski, G. A. Voth, P. Salvador, J. J. Dannenberg, S. Dapprich, A. D. Daniels, Ö. Farkas, J. B. Foresman, J. V. Ortiz, J. Cioslowski and D. J. Fox, **2013**, Gaussian, Inc., Wallingford CT.

1.4.7 ^{1}H and ^{13}C NMR spectra of isolated cyclic limonene carbonate

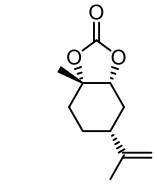

^{1}H NMR (500 MHz, $CDCl_3$): δ 4.69 (s, 1H), 4.66 (s, 1H), 4.33 (dd, , $^{3}J_{HH}$ = 9.5 Hz, $^{3}J_{HH}$ = 7.0 Hz, 1H), 1.87 (tt, $^{3}J_{HH}$ = 11.9 Hz, $^{3}J_{HH}$ = 2.9 Hz, 1H), 1.65 (s, 3H), 1.64 – 1.55 (m, 2H), 1.40 (s, 3H), 1.38 – 1.31 (m, 2H).

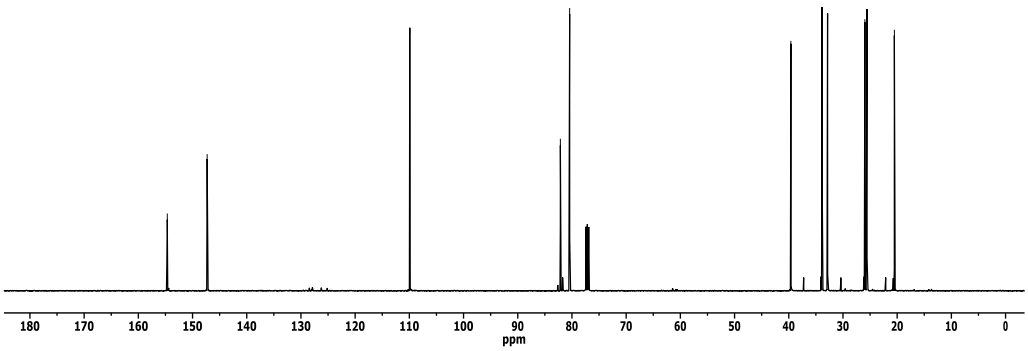

^{13}C NMR (125 MHz, $CDCl_3$): δ 152.66 (CO_2=O), 147.31 ($R_2\underline{C}$=CH_2), 109.92 (R_2C=$\underline{C}H_2$), 82.14 (R-(RCO_2O)$\underline{C}$(CH_3)-R), 80.43 (R-(RCO_2O)$\underline{C}$H-R), 39.61 (R-(CH_3C=CH_2)$\underline{C}$H-R), 33.86 (R-$\underline{C}H_2$($COCO_2$R)), 32.84 (R-$\underline{C}H_2$((CH_3)$COCO_2$R)), 25.96 ($\underline{C}H_3$(R$\underline{C}$=$CH\underline{2}$)), 25.57 (R-$\underline{C}H_2$(CH_2((CH_3)$COCO_2$R)), 20.52 ($\underline{C}H_3$($COCO_2$R)).

HRMS (APCI+, CH_3OH): *m/z* calcd. 219.0992 $(M+Na)^+$, found: 219.0990.

1.4.8 ^{1}H and ^{13}C NMR spectra of pure *cis* and *trans* (*R*)-limonene oxide

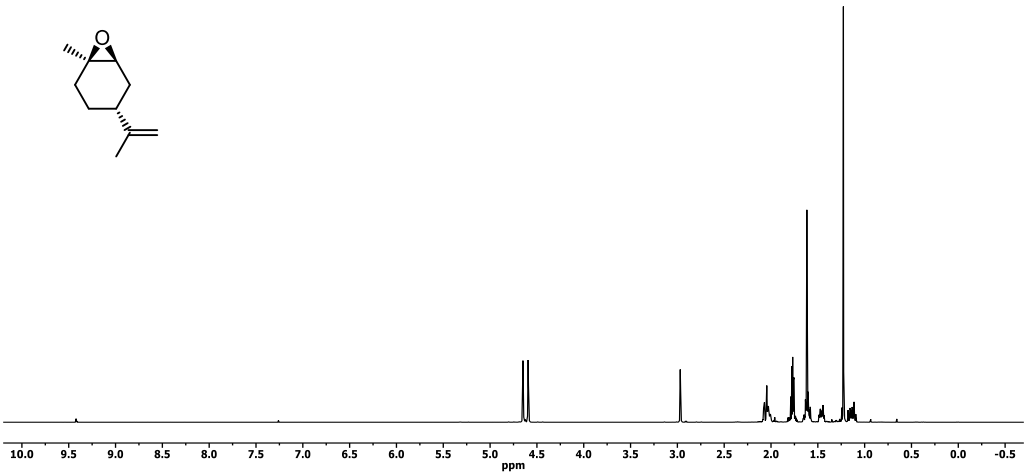

^{1}H NMR (500 MHz, $CDCl_3$): δ 4.65 (s, 1H), 4.59 (s, 1H), 2.97 (s, 1H), 2.07 (m, 1H), 2.03 (m, 1H), 1.77 (m, 2H), 1.65 – 1.58 (m, 1H), 1.62 (s, 3H), 1.46 (m, 1H), 1.23 (s, 3H), 1.14 (m, 1H).

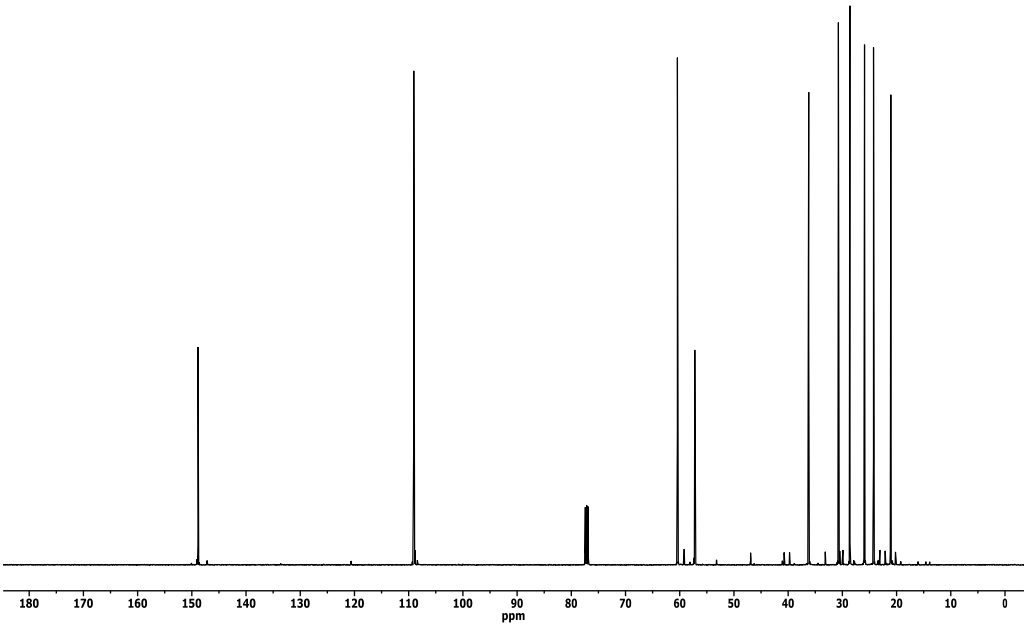

^{13}C NMR (125 MHz, $CDCl_3$): δ 148.86 ($R_2\underline{C}=CH_2$), 109.06 ($R_2C=\underline{C}H_2$), 60.43 (R-(RO)$\underline{C}$H-R), 57.22 (R-(RO)$\underline{C}(CH_3)$-R), 36.21 (R-($CH_3C=CH_2$)$\underline{C}$H-R), 30.73 (R-$\underline{C}H_2((CH_3)COR)$), 28.61 (R-$\underline{C}H_2(COR)$), 25.91 (R-$\underline{C}H_2(CH_2((CH_3)COR))$, 24.25 ($\underline{C}H_3(COR)$), 21.04 ($\underline{C}H_3(RC=CH_2)$).

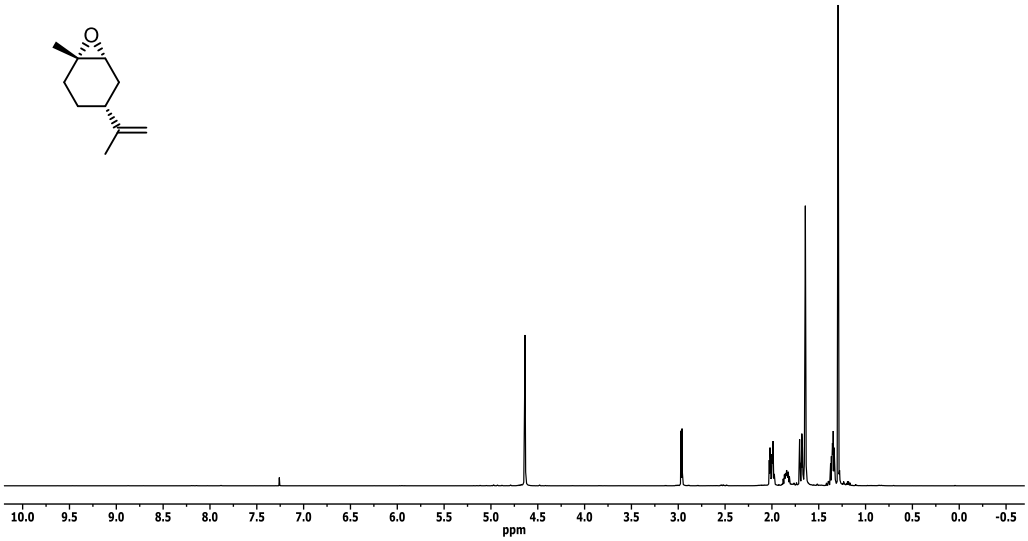

^{1}H NMR (500 MHz, $CDCl_3$): δ 4.64 (s, 2H), 2.97 (d, $^{3}J_{HH}$ = 5.4 Hz, 1H), 2.01 (m, 2H), 1.84 (m, 1H), 1.68 (m, 2H), 1.64 (s, 3H), 1.35 (m, 2H), 1.29 (s, 3H).

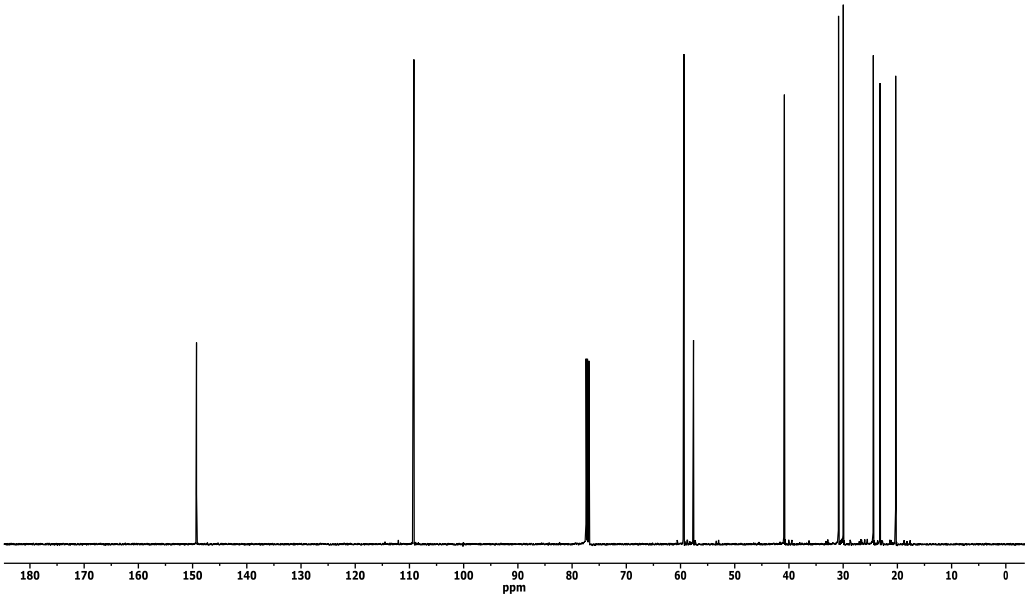

^{13}C NMR (125 MHz, $CDCl_3$): δ 149.28 ($R_2\underline{C}=CH_2$), 109.18 ($R_2C=\underline{C}H_2$), 59.37 (R-(RO)$\underline{C}$H-R), 57.60 (R-(RO)$\underline{C}(CH_3)$-R), 40.84 (R-($CH_3C=CH_2$)$\underline{C}$H-R), 30.85 (R-$\underline{C}H_2((CH_3)COR)$), 29.98 (R-$\underline{C}H_2(COR)$), 24.44 (R-$\underline{C}H_2(CH_2((CH_3)COR))$, 23.19 ($\underline{C}H_3(COR)$), 20.32 ($\underline{C}H_3(RC=CH_2)$).

1.4.9 Assigned ^{1}H and ^{13}C NMR spectra of polymers

Assignation of ^{1}H and ^{13}C NMR peaks of polymers

Starting material *cis* (*R*)-limonene oxide **1b** (Table 1.2, entry 8)

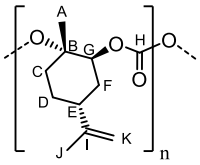

Group	^{1}H (δ, ppm)	^{13}C (δ, ppm)
A	1.50	21.68
B	-	82.00
C	2.39, 1.76	30.77
D	1.61, 1.37	25.94
E	2.24	37.59
F	1.89-1.76	31.01
G	5.05	75.45
H	-	152.08
I	-	148.78
J	1.70	20.83
K	4.73, 4.70	109.43

Starting material *trans* (*R*)-limonene oxide **1c** (Table 1.2, entry 7)

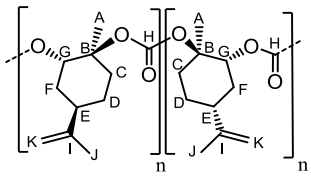

Group	^{1}H (δ, ppm)	^{13}C (δ, ppm)
A	1.50	21.78, 21.68
B	-	81.99, 81.64
$B_{terminal}$	-	70.05
C	2.39, 1.77	30.86, 30.77
D	1.61, 1.37	26.16, 25.94
E	2.24	37.98, 37.60
F	1.95 - 1.72	31.20, 31.00
G	5.08, 5.05	76.36, 75.46
$G_{terminal}$	4.61	78.80
H	-	153.78, 152.46, 152.09
I	-	149.12, 148.64
J	1.70	21.08, 20.33
K	4.73, 4.70	109.43, 109.25

Starting material *cis*/*trans* mixture of (*R*)-limonene oxide **1a** (Table 1.2, entry 1)

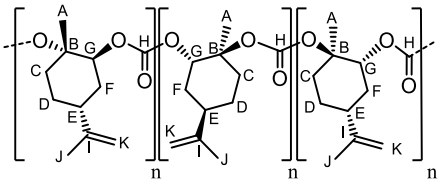

Group	1H (δ, ppm)	13C (δ, ppm)
A	1.50	21.71, 21.67
B	-	81.95, 81.33
$B_{terminal}$	-	69.96
C	2.40, 1.77	30.76, 30.63
D	1.60, 1.37	26.08, 25.93
E	2.22	38.04, 37.65
F	1.92 - 1.72	31.19, 30.99
G	5.12, 5.08, 5.05	75.46, 75.18
$G_{terminal}$	4.66, 4.61	79.60, 78.83
H	-	153.77, 152.69, 152.07
I	-	149.10, 148.76
J	1.70	21.03, 20.81
K	4.74 - 4.67	109.44, 109.25

^{1}H and ^{13}C NMR spectra of polymers

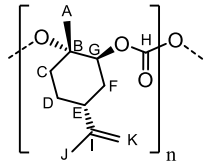

^{1}H NMR (500 MHz, $CDCl_3$): δ 5.13 – 5.02 (m, 1H), 4.72 (d, $^{2}J_{HH}$ = 10.0 Hz, 2H), 2.39 (d, $^{3}J_{HH}$ = 13.3 Hz, 1H), 2.24 (t, $^{3}J_{HH}$ = 12.1 Hz, 1H), 1.90 – 1.71 (m, 3H), 1.70 (br s, 3H), 1.61 (m, 1H), 1.50 (br s, 3H), 1.37 (m, 1H).

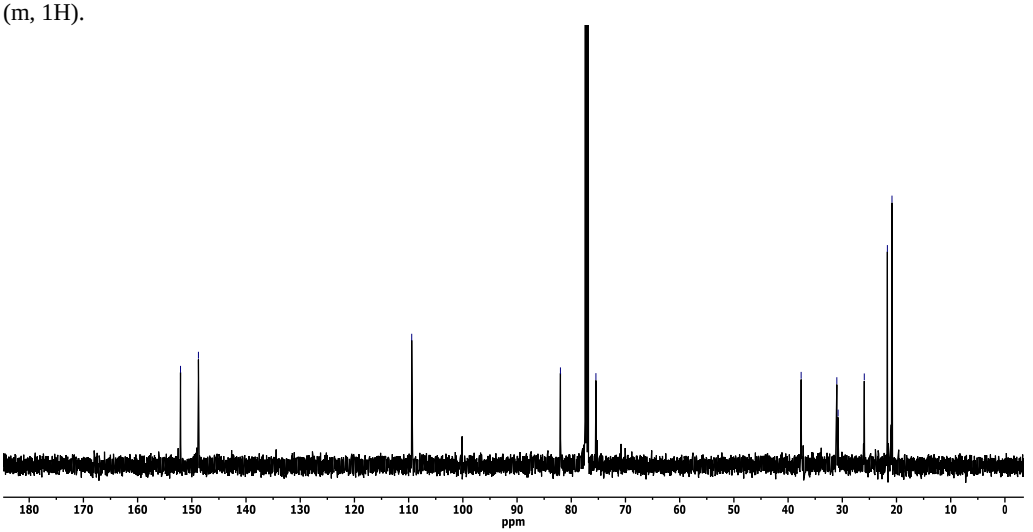

^{13}C NMR (125 MHz, $CDCl_3$): δ 152.08 (CO_2=O), 148.78 ($R_2\underline{C}$=CH_2), 109.43 (R_2C=$\underline{C}H_2$), 82.00 (R-(RCO_2O)$\underline{C}$(CH_3)-R), 75.45 (R-(RCO_2O)$\underline{C}$H-R), 37.59 (R-(CH_3C=CH_2)$\underline{C}$H-R), 31.01 (R-$\underline{C}H_2$($COCO_2R$)), 30.77 (R-$\underline{C}H_2$((CH_3)$COCO_2R$)), 25.94 (R-$\underline{C}H_2$(CH_2((CH_3)$COCO_2R$)), 21.68 ($\underline{C}H_3$($COCO_2R$)), 20.83 ($\underline{C}H_3$($R\underline{C}$=$CH\underline{2}$)).

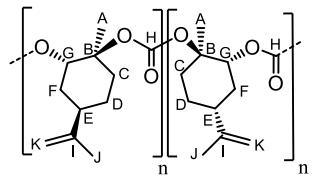

For the polymer: ^{1}H NMR (500 MHz, $CDCl_3$): δ 5.14 – 5.03 (m, 1H), 4.73 (br s, 1H), 4.70 (br s, 1H), 2.39 (br d, $^{3}J_{HH}$ = 14.3 Hz, 1H), 2.24 (m, 1H), 1.95 – 1.72 (m, 3H), 1.70 (br s, 3H), 1.61 (m, 1H), 1.50 (br s, 3H), 1.37 (m, 1H).
For the terminal units: δ 4.61 (0.15H).

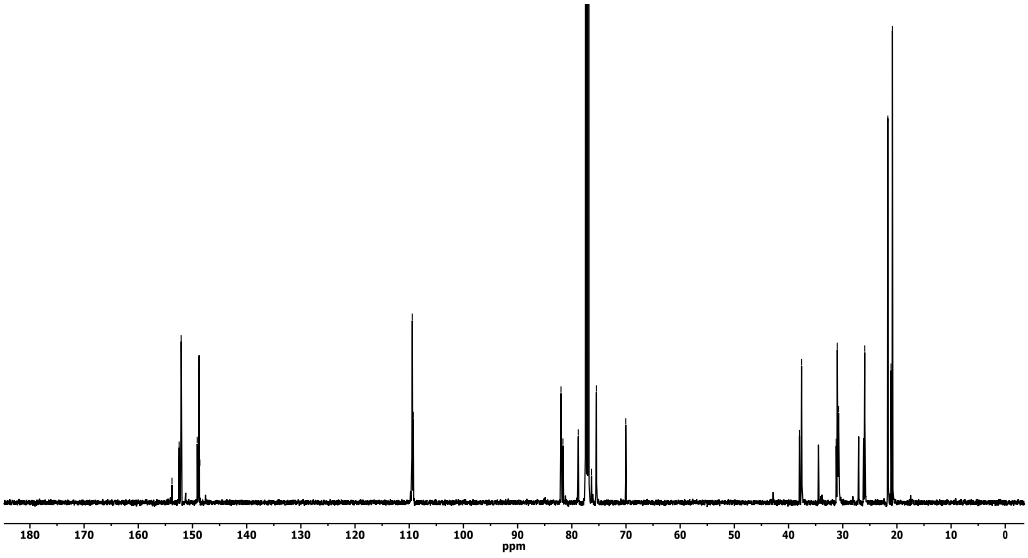

For the polymer: ^{13}C NMR (125 MHz, $CDCl_3$): δ 153.78, 152.46, 152.09 (CO_2=O), 149.12, 148.64 ($R_2\underline{C}$=CH_2), 109.43, 109.25 (R_2C=$\underline{C}H_2$), 81.99, 81.64, (R-(RCO_2O)$\underline{C}$(CH_3)-R), 76.36, 75.46, (R-(RCO_2O)$\underline{C}$H-R), 37.98, 37.60 (R-(CH_3C=CH_2)$\underline{C}$H-R), 31.20, 31.00 (R-$\underline{C}H_2$($COCO_2$R)), 30.86, 30.77 (R-$\underline{C}H_2$((CH_3)$COCO_2$R)), 26.16, 25.94 (R-$\underline{C}H_2$(CH_2((CH_3)$COCO_2$R)), 21.72, 21.68 ($\underline{C}H_3$($COCO_2$R)), 21.08, 20.83 ($\underline{C}H_3$(R$\underline{C}$=CH_2)).
Terminal units: δ 78.80 (R-(RCO_2O)$\underline{C}$H-OH), 70.05 (R-(RCO_2O)$\underline{C}$(CH_3)-OH).
Ether linkages: δ 34.04, 27.06.

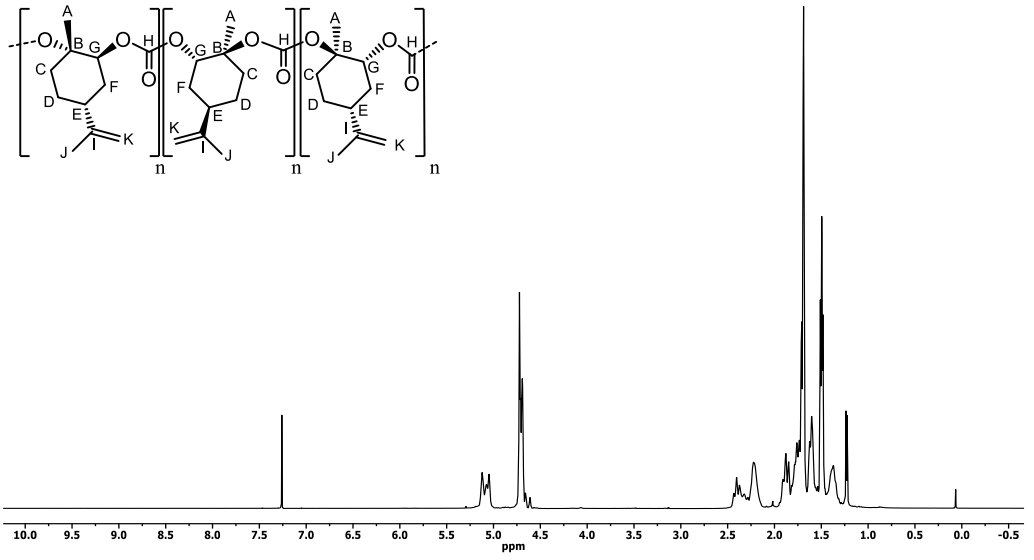

For the polymer: ^{1}H NMR (500 MHz, $CDCl_3$): δ 5.15 – 5.03 (m, 1H), 4.74 – 4.67 (m, 2H), 2.40 (m, 1H), 2.22 (m, 1H), 1.94 - 1.72 (m, 3H), 1.70 (br s, 3H), 1.60 (m, 1H), 1.50 (m, 3H), 1.37 (m, 1H).
Terminal units: δ 4.66 (0.15H), 4.61 (0.05H).

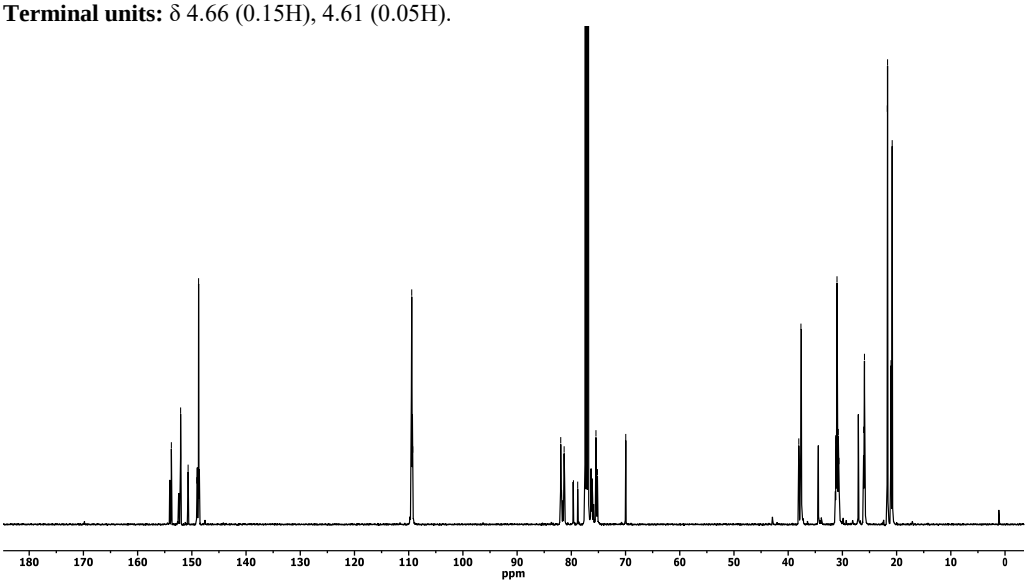

For the polymer: ^{13}C NMR (125 MHz, $CDCl_3$): δ 153.77, 152.07, 150.69 (CO_2=O), 149.10, 148.76 ($R_2\underline{C}$=CH_2), 109.44, 109.25 (R_2C=$\underline{C}H_2$), 81.95, 81.33, (R-(RCO_2O)$\underline{C}$(CH_3)-R), 75.46, 75.18, (R-(RCO_2O)$\underline{C}$H-R), 38.04, 37.65 (R-(CH_3C=CH_2)$\underline{C}$H-R), 31.19, 31.99 (R-$\underline{C}H_2$(COCO_2R)), 30.76, 30.63 (R-$\underline{C}H_2$((CH_3)COCO_2R)), 26.08, 25.93 (R-$\underline{C}H_2$(CH_2((CH_3)COCO_2R)), 21.71, 21.67 ($\underline{C}H_3$(COCO_2R)), 21.03, 20.81 ($\underline{C}H_3$(RC=CH_2)).
Terminal units: δ 79.60, 78.83 (R-(RCO_2O)$\underline{C}$H-OH), 69.96 (R-(RCO_2O)$\underline{C}$(CH_3)-OH). **Ether linkages:** δ 34.44, 27.06.

1.5 References

[1] R. A. Sheldon, *Green Chem.* **2014**, *16*, 950–963.

[2] M. Poliakoff, P. Anastas, *Nature* **2001**, *413*, 257.

[3] M. Poliakoff, J. M. Fitzpatrick, T. R. Farren, P. T. Anastas, *Science* **2002**, *297*, 807–810.

[4] R. Ciriminna, M. Lomeli-Rodriguez, P. Demma Carà, J. A. Lopez-Sanchez, M. Pagliaro, *Chem. Commun.* **2014**, *50*, 15288–15296.

[5] M. Winkler, C. Romain, M. A. R. Meier, C. K. Williams, *Green Chem.* **2015**, *17*, 300–306.

[6] M. Cokoja, C. Bruckmeier, B. Rieger, W. A. Herrmann, F. E. Kühn, *Angew. Chem. Int. Ed.* **2011**, *50*, 8510–8537.

[7] A. Decortes, A. M. Castilla, A. W. Kleij, *Angew. Chem. Int. Ed.* **2010**, *49*, 9822–9837.

[8] N. Kielland, C. J. Whiteoak, A. W. Kleij, *Adv. Synth. Catal.* **2013**, *355*, 2115–2138.

[9] M. Mikkelsen, M. Jørgensen, F. C. Krebs, *Energy Environ. Sci.* **2010**, *3*, 43–81.

[10] M. Aresta, A. Dibenedetto, A. Angelini, *Chem. Rev.* **2014**, *114*, 1709–1742.

[11] Y. Tsuji, T. Fujihara, *Chem. Commun.* **2012**, *48*, 9956–64.

[12] C. Maeda, Y. Miyazaki, T. Ema, *Catal. Sci. Technol.* **2014**, *4*, 1482.

[13] M. R. Kember, A. Buchard, C. K. Williams, *Chem. Commun.* **2011**, *47*, 141–163.

[14] D. J. Darensbourg, *Chem. Rev.* **2007**, *107*, 2388–2410.

[15] K. Nozaki, *Pure Appl. Chem.* **2004**, *76*, 541–546.

[16] X.-B. Lu, D. J. Darensbourg, *Chem. Soc. Rev.* **2012**, *41*, 1462.

[17] G. W. Coates, D. R. Moore, *Angew. Chem. Int. Ed.* **2004**, *43*, 6618–6639.

[18] S. Klaus, M. W. Lehenmeier, C. E. Anderson, B. Rieger, *Coord. Chem. Rev.* **2011**, *255*, 1460–1479.

[19] X. B. Lu, W. M. Ren, G. P. Wu, *Acc. Chem. Res.* **2012**, *45*, 1721–1735.

[20] M. I. Childers, J. M. Longo, N. J. Van Zee, A. M. Lapointe, G. W. Coates, *Chem. Rev.* **2014**, *114*, 8129–8152.

[21] S. Paul, Y. Zhu, C. Romain, R. Brooks, P. K. Saini, C. K. Williams, *Chem. Commun.* **2015**, *51*, 6459–6479.

[22] M. R. Kember, P. D. Knight, P. T. R. Reung, C. K. Williams, *Angew. Chem. Int. Ed.* **2009**, *48*, 931–933.

[23] K. Nozaki, K. Nakano, T. Hiyama, *J. Am. Chem. Soc.* **1999**, *121*, 11008–11009.

[24] F. Jutz, A. Buchard, M. R. Kember, S. B. Fredriksen, C. K. Williams, *J. Am. Chem. Soc.* **2011**, *133*, 17395–17405.

[25] M. W. Lehenmeier, S. Kissling, P. T. Altenbuchner, C. Bruckmeier, P. Deglmann, A. K. Brym, B. Rieger, *Angew. Chem. Int. Ed.* **2013**, *52*, 9821–9826.

[26] Y. Liu, W. M. Ren, J. Liu, X. B. Lu, *Angew. Chem. Int. Ed.* **2013**, *52*, 11594–11598.

[27] D. J. Darensbourg, R. M. Mackiewicz, *J. Am. Chem. Soc.* **2005**, *127*, 14026–14038.

[28] C. T. Cohen, T. Chu, G. W. Coates, *J. Am. Chem. Soc.* **2005**, *127*, 10869–10878.

[29] K. Nakano, T. Kamada, K. Nozaki, *Angew. Chem. Int. Ed.* **2006**, *45*, 7274–7277.

[30] X. B. Lu, L. Shi, Y. M. Wang, R. Zhang, Y. J. Zhang, X. J. Peng, Z. C. Zhang, B. Li, *J. Am. Chem. Soc.* **2006**, *128*, 1664–1674.

[31] S. I. Vagin, R. Reichardt, S. Klaus, B. Rieger, *J. Am. Chem. Soc.* **2010**, *132*, 14367–14369.

[32] E. K. Noh, S. J. Na, S. Sujith, S. W. Kim, B. Y. Lee, *J. Am. Chem. Soc.* **2007**, *129*, 8082–8083.

[33] K. Nakano, S. Hashimoto, M. Nakamura, T. Kamada, K. Nozaki, *Angew. Chem. Int. Ed.* **2011**, *50*, 4868–4871.

[34] X. B. Lu, B. Liang, Y. J. Zhang, Y. Z. Tian, Y. M. Wang, C. X. Bai, H. Wang, R. Zhang, *J. Am. Chem. Soc.* **2004**, *126*, 3732–3733.

[35] S. M. Ahmed, A. Poater, M. I. Childers, P. C. B. Widger, A. M. LaPointe, E. B. Lobkovsky, G. W. Coates, L. Cavallo, *J. Am. Chem. Soc.* **2013**, *135*, 18901–18911.

[36] D. J. Darensbourg, S. J. Wilson, *J. Am. Chem. Soc.* **2011**, *133*, 18610–18613.

[37] G. P. Wu, S. H. Wei, W. M. Ren, X. B. Lu, T. Q. Xu, D. J. Darensbourg, *J. Am. Chem. Soc.* **2011**, *133*, 15191–15199.

[38] Y. Liu, M. Wang, W. Ren, K. He, Y. Xu, J. Liu, X. Lu, *Macromolecules* **2014**, *47*, 1269–1276.

[39] G. Wu, P. Xu, X. Lu, Y. Zu, S. Wei, W. Ren, D. J. Darensbourg, *Macromol. Res.* **2013**, *46*, 2128–2133.

[40] G.-P. Wu, S.-H. Wei, W.-M. Ren, X.-B. Lu, B. Li, Y.-P. Zu, D. J. Darensbourg, *Energy Environ. Sci.* **2011**, *4*, 5084.

[41] G. P. Wu, S. H. Wei, X. B. Lu, W. M. Ren, D. J. Darensbourg, *Macromolecules* **2010**, *43*, 9202–9204.

[42] M. Winnacker, B. Rieger, *ChemSusChem* **2015**, *8*, 2455–2471.

[43] C. Martín, A. W. Kleij, *Macromolecules* **2016**, *49*, 6285–6295.

[44] Y. Hu, L. Qiao, Y. Qin, X. Zhao, X. Chen, X. Wang, F. Wang, *Macromolecules* **2009**, *42*, 9251–9254.

[45] C. M. Byrne, S. D. Allen, E. B. Lobkovsky, G. W. Coates, *J. Am. Chem. Soc.* **2004**, *126*, 11404–11405.

[46] H. C. Quilter, M. Hutchby, M. G. Davidson, M. D. Jones, *Polym. Chem.* **2017**, 833–837.

[47] N. J. Van Zee, G. W. Coates, *Angew. Chem. Int. Ed.* **2015**, *54*, 2665–2668.

[48] J. Shin, Y. Lee, W. B. Tolman, M. A. Hillmyer, *Biomacromolecules* **2012**, *13*, 3833–3840.

[49] M. Firdaus, L. Montero de Espinosa, M. A. R. Meier, *Macromolecules* **2011**, *44*, 7253–7262.

[50] M. J. Sanford, L. Peña Carrodeguas, N. J. Van Zee, A. W. Kleij, G. W. Coates, *Macromolecules* **2016**, *49*, 6394–6400.

[51] F. Auriemma, C. De Rosa, M. R. Di Caprio, R. Di Girolamo, W. C. Ellis, G. W. Coates, *Angew. Chem. Int. Ed.* **2015**, *54*, 1215–1218.

[52] F. Auriemma, C. De Rosa, M. R. Di Caprio, R. Di Girolamo, G. W. Coates, *Macromolecules* **2015**, *48*, 2534–2550.

[53] F. Castro-Gómez, G. Salassa, A. W. Kleij, C. Bo, *Chem. - A Eur. J.* **2013**, *19*, 6289–6298.

[54] C. Beattie, M. North, P. Villuendas, C. Young, *J. Org. Chem.* **2013**, *78*, 419–426.

[55] W. J. Kruper, D. V Dellar, *J. Org. Chem.* **1996**, *60*, 725–727.

[56] M. Bähr, A. Bitto, R. Mülhaupt, *Green Chem.* **2012**, *14*, 1447–1454.

[57] J. Wu, J. A. Kozak, F. Simeon, T. A. Hatton, T. F. Jamison, *Chem. Sci.* **2014**, *5*, 1227–1231.

[58] J. Qin, P. Wang, Q. Li, Y. Zhang, D. Yuan, Y. Yao, *Chem. Commun.* **2014**, *50*, 10952–10955.

[59] T. Ema, Y. Miyazaki, J. Shimonishi, C. Maeda, J.-Y. Hasegawa, *J. Am. Chem. Soc.* **2014**, *136*, 15270–15279.

[60] C. J. Whiteoak, E. Martin, E. Escudero-Adán, A. W. Kleij, *Adv. Synth. Catal.* **2013**, *355*, 2233–2239.

[61] C. J. Whiteoak, E. Martin, M. M. Belmonte, J. Benet-Buchholz, A. W. Kleij, *Adv. Synth. Catal.* **2012**, *354*, 469–476.

[62] C. J. Whiteoak, B. Gjoka, E. Martin, M. M. Belmonte, E. C. Escudero-Adán, C. Zonta, G. Licini, A. W. Kleij, *Inorg. Chem.* **2012**, *51*, 10639–10649.

[63] C. J. Whiteoak, N. Kielland, V. Laserna, E. C. Escudero-Adán, E. Martin, A. W. Kleij, *J. Am. Chem. Soc.* **2013**, *135*, 1228–1231.

[64] C. J. Whiteoak, A. H. Henseler, C. Ayats, A. W. Kleij, M. A. Pericàs, *Green Chem.* **2014**, *16*, 1552.

[65] C. J. Whiteoak, N. Kielland, V. Laserna, F. Castro-Gómez, E. Martin, E. C. Escudero-Adán, C. Bo, A. W. Kleij, *Chem. - A Eur. J.* **2014**, *20*, 2264–2275.

[66] V. Laserna, G. Fiorani, C. J. Whiteoak, E. Martin, E. Escudero-Adán, A. W. Kleij, *Angew. Chem. Int. Ed.* **2014**, *53*, 10416–10419.

[67] M. Taherimehr, S. M. Al-Amsyar, C. J. Whiteoak, A. W. Kleij, P. P. Pescarmona, *Green Chem.* **2013**, *15*, 3083–3090.

[68] M. R. Kember, C. K. Williams, *J. Am. Chem. Soc.* **2012**, *134*, 15676–15679.

[69] E. H. Nejad, A. Paoniasari, C. G. W. Van Melis, C. E. Koning, R. Duchateau, *Macromolecules* **2013**, *46*, 631–637.

[70] W. J. Van Meerendonk, R. Duchateau, C. E. Koning, G. J. M. Gruter, *Macromolecules* **2005**, *38*, 7306–7313.

[71] K. Nakano, K. Nozaki, T. Hiyama, *J. Am. Chem. Soc.* **2003**, *125*, 5501–5510.

[72] A. Buchard, F. Jutz, M. R. Kember, A. J. P. White, H. S. Rzepa, C. K. Williams, *Macromolecules* **2012**, *45*, 6781–6795.

[73] M. Reiter, S. Vagin, A. Kronast, C. Jandl, B. Rieger, *Chem. Sci.* **2017**, *8*, 1876–1882.

[74] O. Hauenstein, M. Reiter, S. Agarwal, B. Rieger, A. Greiner, *Green Chem.* **2016**, *18*, 760–770.

[75] O. Hauenstein, S. Agarwal, A. Greiner, *Nat. Commun.* **2016**, *7*, 11862.

[76] C. Li, R. J. Sablong, C. E. Koning, *Angew. Chem. Int. Ed.* **2016**, *55*, 11572–11576.

[77] C. Li, R. J. Sablong, C. E. Koning, *Eur. Polym. J.* **2015**, *67*, 449–458.

[78] A. Chandrasekaran, R. O. Day, R. R. Holmes, *J. Am. Chem. Soc.* **2000**, *122*, 1066–1072.

[79] D. Steiner, L. Ivison, C. T. Goralski, R. B. Appell, J. R. Gojkovic, B. Singaram, *Tetrahedron Asymmetry* **2002**, *13*, 2359–2363.

[80] S. Grimme, *J. Comput. Chem.* **2006**, *27*, 1787–1799.

[81] S. Grimme, S. Ehrlich, L. Goerigk, *J. Comput. Chem.* **2011**, *32*, 1456–1465.

[82] F. CRC Handbook of Chemistry and Physics, 84th ed. (Ed.: D.R. Lide), CRC Press LLC, **2003**.

UNIVERSITAT ROVIRA I VIRGILI
AVANCES EN SISTEMAS INTERACTIVOS PARA PERSONAS CON PARÁLISIS CEREBRAL
Leticia Peña Carrodeguas

Chapter 2

Alternating copolymerization of propylene oxide and cyclohexene oxide with partially renewable tricyclic anhydrides

This chapter has been published in:

M. J. Sanford,‡ L. Peña Carrodeguas,‡ N. J. Van Zee, A. W. Kleij, G. W. Coates, *Macromolecules*, **2016**, *49*, 6394–6400.

‡ Equal contribution

This work described in this chapter was carried out in collaboration with the group of Prof. G. W. Coates Group (Cornell University, USA).

UNIVERSITAT ROVIRA I VIRGILI
AVANCES EN SISTEMAS INTERACTIVOS PARA PERSONAS CON PARÁLISIS CEREBRAL
Leticia Peña Carrodeguas

2.1 Introduction

Polymers that are produced from sustainable feedstocks such as biomass which are biodegradable have attracted considerable interest as (potential) alternatives to fossil fuel-based polymers.[1–4] In particular, aliphatic polyesters are appealing because of their numerous renewable sources,[2,4–7] facile hydrolytic degradation to benign products,[6,8–10] and general biocompatibility.[11] These features have led to aliphatic polyesters being utilized in applications ranging from specialized biomedical devices to bulk packaging.[11–17]

The most popular route to produce aliphatic polyesters is the ring-opening polymerization (ROP) of lactones and lactide.[18] Numerous initiators have been used for lactone polymerization, including organocatalysts, metal alkoxides, and various metal complexes.[11] However, the ROP of lactones can be limited by detrimental side reactions such as transesterification, especially at high conversion. The resulting polymers also have a limited range of properties, because of the limited functional diversity of the substrate scope and lack of post-polymerization functionalization on the resulting polyesters.[11,18]

There has been interest in developing higher T_g aliphatic polyesters, since commercially available poly(lactic acid) (PLA) has a relatively low T_g (approximately 60 °C). Efforts to improve the T_g of aliphatic polyesters have mainly focused on using polysaccharide derived diols,[19,20] and lactide[21] or mannitol[22] derivatives. However, the resulting polymers either show modest improvements over PLA (T_g up to 68 °C),[19,22] or require long reaction times at low temperatures (-20 °C) to reach moderate conversion.[21] An alternative synthetic route to aliphatic polyesters is the alternating copolymerization of epoxides and cyclic anhydrides. [18]

Scheme 2.1.Alternating copolymerization of epoxides and cyclic anhydrides and simplified proposed reaction mechanism.

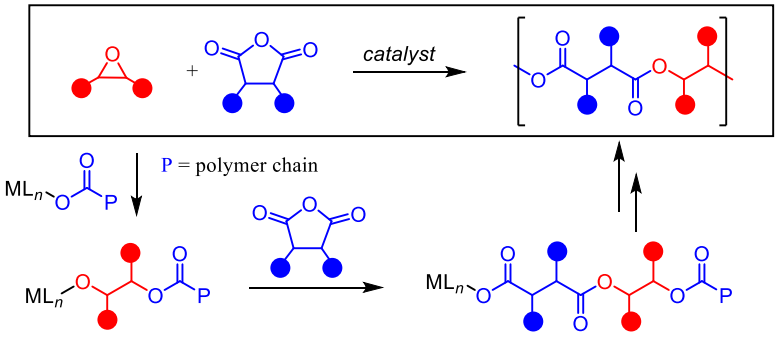

The use of two monomers allows for an easier tuning of properties, and many of the resulting polyesters can be easily functionalized by post-polymerization modification.[18,23] There is a diverse array of metal complexes reported to catalyze the copolymerization, including zinc,[24–32] magnesium,[27,29,33] chromium,[29,34–44] cobalt,[29,35,37–39,42,45] manganese,[35,42,46–48] and aluminum[35,38,39,42,49–52] complexes, including a wide range of salen- and porphyrin-type complexes which generally show markedly improved activity with the addition of a nucleophilic co-catalyst such as bis(triphenylphosphine)iminium chloride ([Ph_3P–N=PPh_3]Cl or PPNCl).

The Coates group has recently focused on the alternating copolymerization of epoxides and tricyclic anhydrides with aluminum salen complexes.[51,52] Tricyclic anhydrides are appealing monomers that are easily synthesized via the Diels-Alder reaction. The wide range of commercially available, inexpensive, biosourced dienes and dienophiles offers ample opportunities for utilizing renewable feedstocks. Additionally, the rigid nature of the resulting polymers yields materials with high glass transition temperatures (T_g). Recently, Coates at al report the chain-growth copolymerization of propylene oxide and a terpene based tricyclic anhydride, which yielded a completely amorphous aliphatic polyester with a T_g of 109 °C.[51]

Scheme 2.2. Terpene-based high-T_g polyester: copolymerization of propylene oxide and terpene-based tricyclic anhydride.[51]

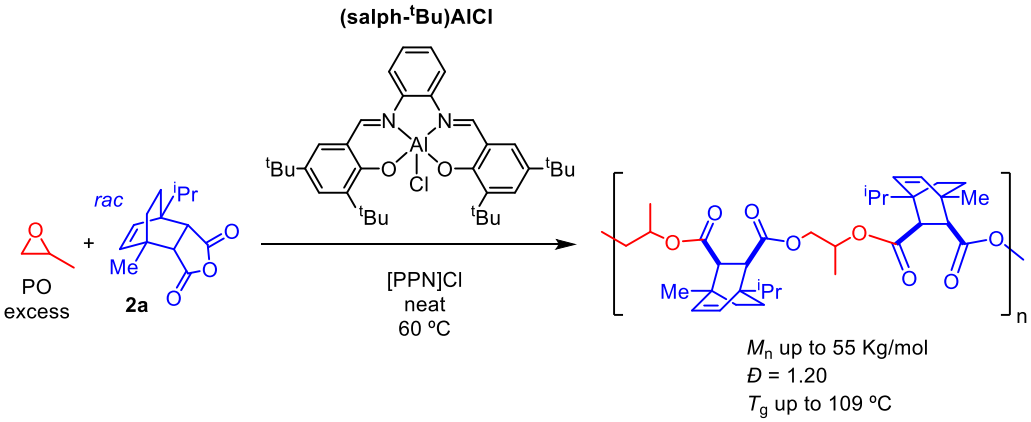

Furthermore, transesterification and epimerization (Scheme 2.3) could be suppressed even at high conversion through judicious choice of catalyst, the ratio of catalyst to co-catalyst, and the steric requirements of the monomers.[51,52]

Scheme 2.3. Side reactions commonly observed in the ring-opening co-polymerizations.[A]

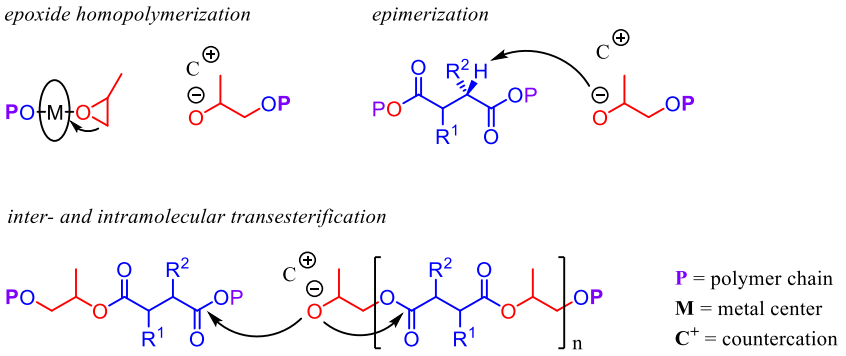

In addition to screening these (salph)AlCl catalysts for a wider range of monomers, we were also interested in exploring a geometrically more flexible[53] iron(III) aminotriphenolate complexes as they have shown potential in the copolymerization of epoxides and CO_2,[54] while other iron complexes have also been used in epoxide/anhydride copolymerizations. Recently, Merna and coworkers reported the use of (salen)FeCl complexes for the copolymerization of cyclohexene oxide and phthalic anhydride,[55] and Nozaki reported an iron corrole complex for the alternating copolymerization of propylene oxide and glutaric anhydride.[46] Iron complexes are of interest due to the high natural abundance of iron and its low toxicity. As the potential uses of aliphatic polyesters are in biomedical applications, metal catalysts with low toxicity are necessary due to the residual catalyst trapped in the polymer. Herein, we report on a series of (partially) renewable polyesters using six anhydrides and two epoxides, giving access to aliphatic polyesters with tunable and high glass transitions.

[A] For a detailed explanation of the epimerization process we refer to section 2.2.6 "*Stereochemistry of the polyester diester units*" of this chapter.

2.2 Results and discussion

2.2.1 Synthesis of partially renewable tricyclic anhydrides

On the basis on previous work,[51,52] and the range of renewable dienes and dienophiles available, we chose to focus on tricyclic anhydrides due to their well-controlled polymerization behavior and typically higher T_g values due to rigidity of the anhydride unit. We synthesized six partially or fully renewable anhydrides based on α-terpinene, α-phellandrene, 2,5-dimethylfuran and citraconic anhydride (Scheme 2.4).

Scheme 2.4. Synthesis of renewable precursors for tricyclic anhydrides.

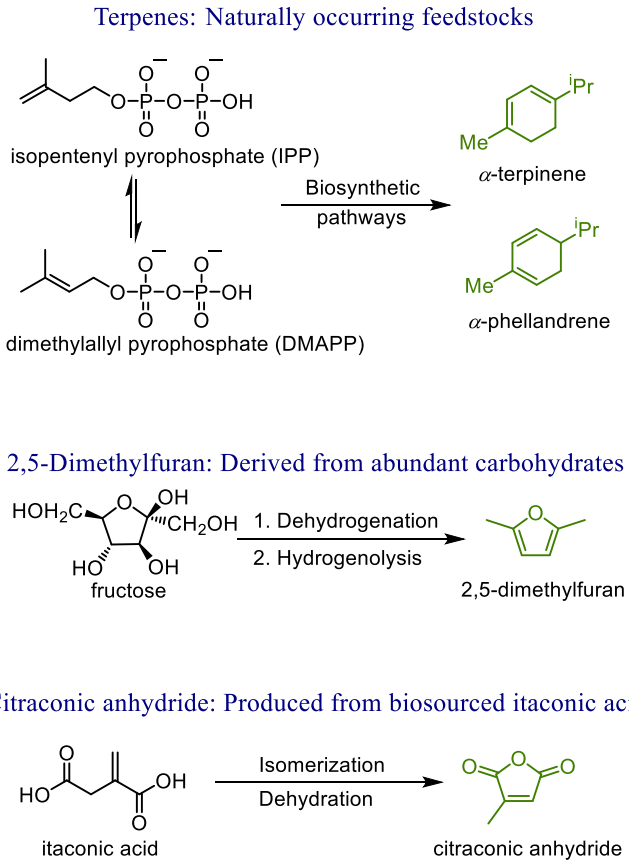

Terpenes such as α- terpinene and α-phellandrene (Scheme 2.4) are part of a class of naturally occurring molecules synthesized through biosynthetic pathways, which have been

extensively investigated as renewable building blocks.[56–60] Dehydration and subsequent hydrogenolysis of carbohydrates leads to 2,5-dimethylfuran which has been investigated as a potential renewable liquid fuel.[61–63] Citraconic anhydride is produced from the isomerization and dehydration of itaconic acid.[64] This naturally occurring acid is commonly produced industrially by fermentation of carbohydrates.[65] We used the renewable precursors in Scheme 2.4 to synthesize five tricyclic anhydrides (**2a**–**2e**) through Diels-Alder reactions, creating a series of anhydrides that are 50–63% renewable by mass (Scheme 2.5 a–c).

Scheme 2.5. Synthesis of partially renewable tricyclic anhydrides from (a) terpenes, (b) citraconic anhydride, (c) 2,5-dimethylfuran and (d) terpene and citraconic anhydride (completely renewable tricyclic anhydride).

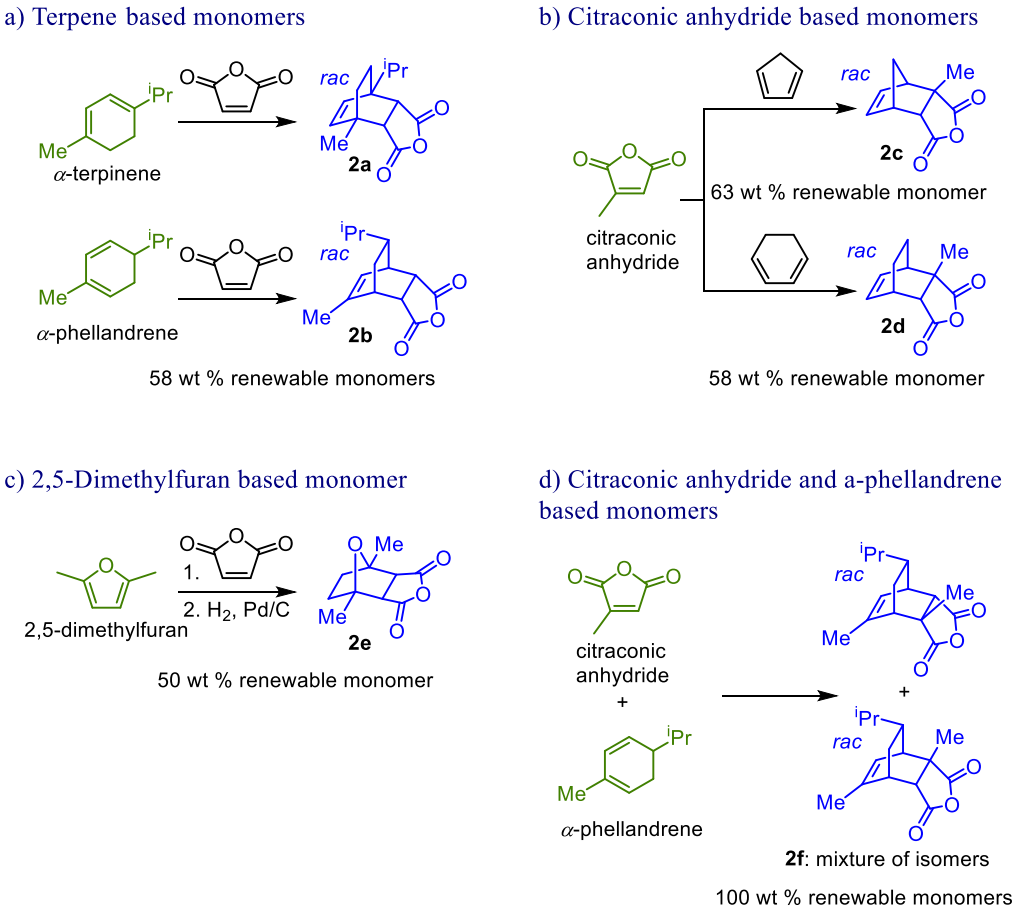

Monomer **2d** has the potential to be completely renewable, as 1,3-cyclohexadiene has been synthesized though the metathesis of plant oils.[66] The Diels-Alder adduct of maleic anhydride and 2,5-dimethylfuran undergoes a rapid retro Diels-Alder reaction in the presence of Lewis acidic catalysts, so it was saturated via catalytic hydrogenation to access an anhydride stable enough for polymerization. We also synthesized a completely renewable anhydride through the Diels-Alder reaction of citraconic anhydride and α-phellandrene. This reaction yielded an inseparable mixture of structural isomers in a 54:46 ratio (**2f**, Scheme 2.5d). Other Diels-Alder reactions between combinations of renewable dienes and dieneophiles that would have yielded completely renewable anhydrides (e.g. citraconic anhydride and α-terpinene or 2,5-dimethylfuran) were not successful under routine conditions, likely due to steric bulk hindering the reaction.

2.2.2 Copolymerization of 2a-2f with propylene oxide (PO)

We first polymerized all six anhydrides with propylene oxide (PO; Table 2.1). Previous work showed that the copolymerization of **2a** with PO yielded a polymer with a T_g up to 109 °C,[51] leading us to believe that we could achieve similarly high T_g values with the other five anhydrides reported in Scheme 2.5. Excess epoxide was used because it is easier to remove from the polymer than solid anhydride and allowed the polymerizations to be run neat, thereby increasing the polymerization rate. Since both catalytic systems had previously shown high selectivity for polyesters[51,52] or polycarbonate [54]formation, we could use excess epoxide without favoring homo-polymerization.

Table 2.1. Copolymerization of **2a-2f** with propylene oxide (PO).

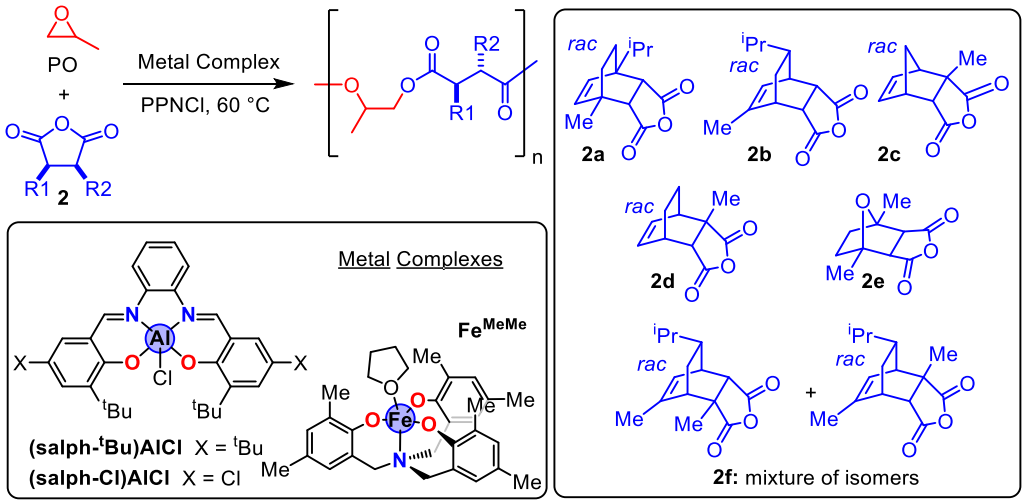

entry	anhyd.	complex	*t* (h)	conv.(%)[b]	M_n (kg/mol)[c]	$Đ$[c]	T_g (°C)[d]	% *cis*[e]
1	**2a**	(salph-^{t}Bu)AlCl	5	>99	29.2	1.10	108	>99
2	**2a**	Fe^{MeMe}	6	>99	15.3	1.13	103	>99
3	**2b**	(salph-Cl)AlCl	10	>99	30.0	1.12	91	>99
4	**2b**	Fe^{MeMe}	6	>99	17.2	1.10	91	>99
5	**2c**	(salph-^{t}Bu)AlCl	3.5	>99	32.2	1.07	79	>99
6	**2c**	Fe^{MeMe}	6	>99	11.1	1.14	74	>99
7	**2d**	(salph-^{t}Bu)AlCl	4	>99	28.1	1.12	86	>99
8	**2d**	Fe^{MeMe}	8	>99	10.5	1.11	66	>99
9	**2e**	(salph-Cl)AlCl	18	>99	29.8	1.10	92	>99
10	**2e**	Fe^{MeMe}	5.5	>99	10.4	1.28	86	36
11	**2f**	(salph-^{t}Bu)AlCl	3.5	>99	18.7	1.10	100	>99
12	**2f**	Fe^{MeMe}	7	>99	11.3	1.11	90	>99

[a] Reaction conditions: [PO]:[**2**] = 5:1, metal complex = 0.33 mol%, co-catalyst PPNCl = 0.3 mol%, 60 °C, neat. [b] Conversion of cyclic anhydride, determined by ^{1}H NMR spectroscopy. [c] Determined by GPC in THF at 30 °C calibrated with polystyrene standards. [d] Determined by DSC; reported T_g values are from the second heating run.[e] Determined by ^{1}H NMR spectroscopy of the mixture of diols obtained from the reductive degradation of the polymer using $LiAlH_4$.

With PO, the six anhydrides gave perfectly alternating copolymers with T_g values ranging from 66 to 108 °C (Table 2.1). The resulting polymers exhibited molecular weights up to 32.2 kg/mol and $Đ$ values below 1.15, with the exception of poly(PO-*alt*-**2e**) synthesized in the presence of **Fe^{MeMe}** (Table 2.1, Entry 10), which had a slightly broader dispersity ($Đ$ = 1.27). Consistent with previous work from Coates,[52] we found that an electron-withdrawing complex [**(salph-Cl)AlCl**] was necessary for the less bulky anhydrides (**2b**, **2e**) in order to avoid side-reactions at high conversion.

Bulkier anhydrides (**2a**, **2c**, **2d**, **2f**) could be copolymerized using **(salph-^{t}Bu)AlCl** without significant side reactions; these anhydrides required much longer reaction times when using the complex **(salph-Cl)AlCl**. We found that in general **Fe^{MeMe}** gave lower molecular weights than either **(salph-^{t}Bu)AlCl** or **(salph-Cl)AlCl** and that both systems gave bimodal GPC traces. We propose this could be due to the presence of adventitious water which can react with anhydrides to form diacids, or chain shuttle with a metal alkoxide ultimately forming a diol. Both processes can generate new, bifunctional, polymer chains giving rise to a second distribution which is double the molecular weight of Cl^- initiated chains. This increase in the number of chains can depress the overall molecular weight.[B] We also found that **Fe^{MeMe}** was intermediate in rate being slower than **(salph-^{t}Bu)AlCl** for monomers **2a**, **2c**, **2d**, and **2f** and faster than **(salph-Cl)AlCl** for monomers **2b** and **2e**. All of the polymers retained a high *cis*-diester content (>99%) even at full conversion with the exception of poly(PO-*alt*-**2e**) synthesized with **Fe^{MeMe}**, which had only 36% *cis*-diester linkages at full conversion (Table 2.1, Entry 10).[C]

The T_g values ranged from 66 °C for a low molecular weight sample of poly(PO-*alt*-**2d**) (Table 2.1, Entry 8), to 108 °C for the higher molecular weight sample of poly(PO-*alt*-**2a**) (Table 2.1, Entry 1). The highest T_g samples were made with the bulkiest anhydrides (**2a** and **2f**) suggesting that increased bulk along the polymer backbone increased the T_g as expected. Poly(PO-*alt*-**2a**) and poly(PO-*alt*-**2f**) are of particular interest as they have T_g values higher than or comparable to that of widely used polystyrene (T_g = 100 °C) respectively. Although there were some differences in T_g between samples synthesized with the Al complexes and Fe complex, the differences in T_g are attributable to disparities in molecular weight. In general, the

[B] For a detailed explanation we refer to section 2.2.4 "*Comparison of GPC traces*" of this chapter.
[C] For a detailed explanation we refer to section 2.2.6 "*Stereochemistry of the polyester diester units*" of this chapter.

Al and Fe complexes gave similar reactivity, although the Fe complex gave lower molecular weight materials overall.

2.2.3 Copolymerization of 2a-2f with cyclohexene oxide (CHO)

One of the advantages of epoxide/anhydride copolymerizations is that polymer properties can be tuned not only through the anhydride, but also through the epoxide. Thus, while the polymers produced with PO had T_g values up to 35 °C higher than that of PLA, we hoped to further increase the T_g by switching to a bulkier, more rigid epoxide. Cyclohexene oxide (CHO) has been shown to give high T_g polycarbonates from the alternating copolymerization of epoxides and CO_2,[67,68] which made it a promising choice. A report on the copolymerization of a similar tricyclic anhydride and CHO found that the resulting polymer had a T_g up to 129 °C.[23] Additionally, while CHO is not currently considered renewable, it could potentially be synthesized from renewable sources through metathesis of plant oils to form 1,4-cyclohexadiene and subsequent epoxidation and hydrogenation.[29,66] The initial screen with CHO was made using 5 equiv of CHO and no solvent, making these polymerizations analogous to those with PO (Table 2.1).

However, we found that while reducing the amount of CHO from 5 to 3 equiv and replacing the volume with toluene led to slower polymerizations, we could obtain higher molecular weights and narrower $Đ$ values in general. These optimized conditions are reported in Table 2.3. We propose that the higher molecular weights and narrower dispersity when a smaller amount of CHO is used are due to a reduction in the number of new alcohols generated via the MPVO reaction.[D] We screened all six anhydrides with CHO (Table 2.3) using toluene as solvent and observed a significant increase in T_g compared to the corresponding polymers synthesized using PO as monomer (Table 2.1).

[D] For a detailed explanation we refer to section 2.2.5 "*MALDI-TOF-MS analysis*" of this chapter.

Table 2.2. Copolymerization of **2a**, **2d** and **2f** with cyclohexene oxide (CHO) under neat conditions.

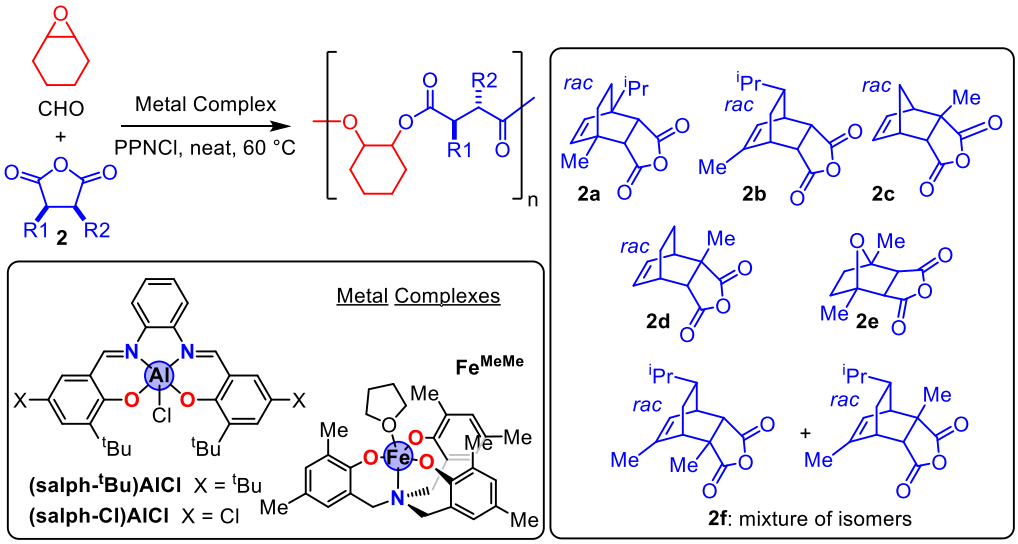

entry	anhyd.	complex	*t* (h)	conv.(%)[b]	M_n (kg/mol)[c]	$Đ$[c]
1	**2a**	(salph-^{t}Bu)AlCl	48	43	2.9	1.31
2	**2a**	Fe^{MeMe}	144	87	4.1	1.52
3	**2d**	(salph-^{t}Bu)AlCl	10	96	6.6	1.62
4	**2d**	Fe^{MeMe}	20	>99	7.6	1.57
5	**2f**	(salph-^{t}Bu)AlCl	10	91	6.1	1.36
6	**2f**	Fe^{MeMe}	15	>99	3.9	1.40

[a] Reaction conditions: [CHO]:[**2**] = 5:1, complex = 0.33 mol%, PPNCl = 0.3 mol%, 60 °C, neat. [b] Conversion of cyclic anhydride, determined by ^{1}H NMR spectroscopy. [c] Determined by GPC in THF at 30 °C calibrated with polystyrene standards.

Table 2.3. Copolymerization of **2a-2f** with cyclohexene oxide (CHO) using toluene as solvent.

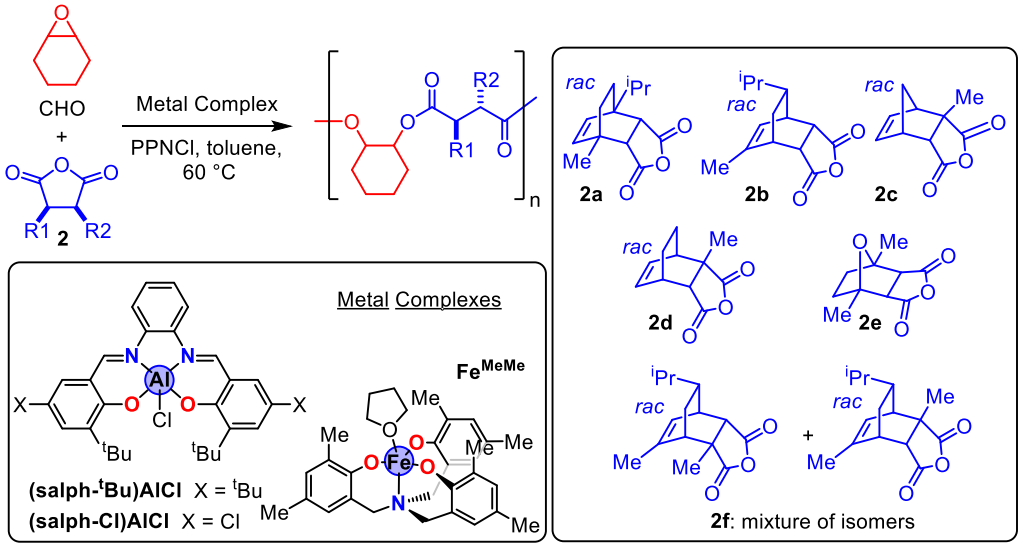

entry	anhyd.	complex	*t* (h)	conv.(%)[b]	M_n (kg/mol)[c]	$Đ$[c]	T_g (ºC)[d]	% *cis*[e]
1[f]	**2a**	(salph-^{t}Bu)AlCl	60	96	8.9	1.27	184	>99
2	**2a**	Fe^{MeMe}	168	68	4.1	1.30	162	>99
3	**2b**	(salph-^{t}Bu)AlCl	24	>99	12.2	1.40	156	>99
4	**2b**	Fe^{MeMe}	20	>99	11.6	1.37	151	>99
5	**2c**	(salph-^{t}Bu)AlCl	15	>99	10.9	1.46	149	>99
6	**2c**	Fe^{MeMe}	20	>99	8.6	1.23	149	>99
7	**2d**	(salph-^{t}Bu)AlCl	10	>99	9.4	1.40	162	>99
8	**2d**	Fe^{MeMe}	23	>99	9.9	1.58	158	>99
9	**2e**	(salph-^{t}Bu)AlCl	48	>99	7.3	1.46	128	>99
10	**2e**	Fe^{MeMe}	20	>99	9.7	1.31	124	>99
11	**2f**	(salph-^{t}Bu)AlCl	25	>99	9.5	1.24	165	>99
12	**2f**	Fe^{MeMe}	25	>99	6.4	1.36	140	>99

[a] Reaction conditions: [CHO]:[**2**] = 3:1, complex = 0.33 mol%, PPNCl = 0.3 mol%, 60 °C, toluene (0.2 mL). [b] Conversion of cyclic anhydride determined by ^{1}H NMR spectroscopy. [c] Determined by GPC in THF at 30 °C calibrated with polystyrene standards. [d] Determined by DSC; reported T_g values are from the second heating run. [e] Determined by ^{1}H NMR spectroscopy of the mixture of diols obtained from the reductive degradation of the polymer using $LiAlH_4$. [f] Polymerization reaction was carried at 70 °C.

We obtained six different polyesters with T_g values ranging from 124 to 184 °C. Similar to the PO based polymers, poly(CHO-*alt*-**2a**) and poly(CHO-*alt*-**2f**) had the highest T_g values (Table 2.3, Entries 1-2 and 11-12; up to 184 °C and 165 °C, respectively). The polymerization rates were significantly lower with CHO, likely due to the increased bulk of the epoxide and the Al and Fe complexes in general had much more comparable rates with CHO than with PO. Complex **(salph-Cl)AlCl** was markedly slower than **(salph-^{t}Bu)AlCl** with CHO, and since no epimerization was observed with **(salph-^{t}Bu)AlCl** (Table 2.3), likely due to increased steric hindrance, **(salph-^{t}Bu)AlCl** was used for all monomer sets. With **2a**, we were unable to reach high conversion using complex **(salph-^{t}Bu)AlCl** at 60 °C, even at extended reaction times. We subsequently increased the reaction temperature to 70 °C and were able to achieve 96% conversion (Table 2.3, Entry 1). Comparable to the PO based polymers we found that **Fe^{MeMe}** was slower than **(salph-^{t}Bu)AlCl** for bulky monomers **2a**, **2c**, **2d**, and faster for the less bulky monomers **2b** and **2e**. A limitation of the CHO based polymers is their relatively low molecular weights; poly(CHO-*alt*-**2b**) synthesized with complex **(salph-^{t}Bu)AlCl** had the highest molecular weight amounting to 12.2 kg/mol (Table 2.3, Entry 3).[E]

2.2.4. Comparison of GPC traces

In general, samples synthesized with complex **Fe^{MeMe}** had lower molecular weights than samples synthesized with (**salph-^{t}Bu)AlCl** or **(salph-Cl)AlCl**. We attribute this to an increased amount of adventitious water present in samples synthesized with **Fe^{MeMe}**. This is supported by the different distributions seen in the GPC traces. A representative pair of traces are shown in Figure 2.1. For Table 2.1, Entry 3, a sample of poly(PO-*alt*-**2b**) synthesized with **(salph-Cl)AlCl,** the major peak in the GPC traces is the lower molecular weight peak attributable to chains intiated by Cl^-. The smaller, high molecuar weight peak is due to chains initiated by adventitious water; by reacting with anhydride to form a diacid, or through chain shuttling, as described in more detail below, it ultimately acts as a bifunctional initatior leading to chains with double the molecuar weight of those initiated by Cl^-. However, for Table 2.1, Entry 4, a sample of poly(PO-*alt*-**2b**) synthesized with **Fe^{MeMe}**, the intensities of the two peaks are reversed and the major peak is the higher molecular weight peak, indicating that there was more adventitious water in samples synthesized with **Fe^{MeMe}** compared to those those synthesized with (**salph-^{t}Bu)AlCl** or **(salph-Cl)AlCl**. It should be noted that at the low catalyst loading used in these polymerizations (4.3

[E] For a detailed explanation we refer to section 2.2.5 "*MALDI-TOF-MS analysis*" of this chapter.

μmol catalyst and 3.8 μmol PPNCl) only a very small amount of adventitious water is necessary to significantly affect the molecular weight of the resulting polymers.

Figure 2.1. GPC traces of Table 2.1, Entry 3 and Table 2.1, Entry 4.

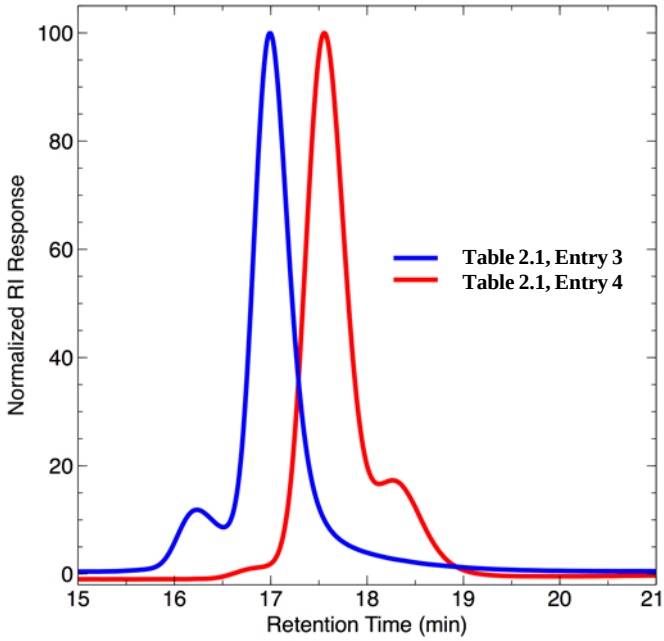

Adventitious water can initiate the polymerization, presumably through ring-opening of an anhydride leading to a diacid (Scheme 2.6b) or by chain shuttling with a metal-alkoxide followed by reaction with an epoxide to form a diol (Scheme 2.6c). In the first case, chain shuttling from a growing polymer alkoxide to the diacid allows the diacid to initiate a new polymer chain that can grow from either end leading to a 2X molecular weight distribution, and overall lowering of the molecular weight due to the increased number of initiators. In the second case, a metal alkoxide chain shuttles with water to generate a metal hydroxide species which can either attack an anhydride or react with an epoxide through a bimetallic Jacobsen-type mechanism[69] to generate a diol, which can also grow from either end giving a 2X molecular weight distribution; this lowers overall the molecular weight due to the increased number of initiators (Scheme 2.6c). In either case, due to the reversible nature of the proton transfer that gives rise to the chain shuttling, no polymer chains become permanently inactive and the process behaves as an immortal polymerization.[70] For comparison and completion, a proposed mechanism for initiation by Cl^- is also shown (Scheme 2.6a).

Scheme 2.6. Initiation by (a) chloride, (b) water or diacid, and (c) chain shuttling to form a diol.

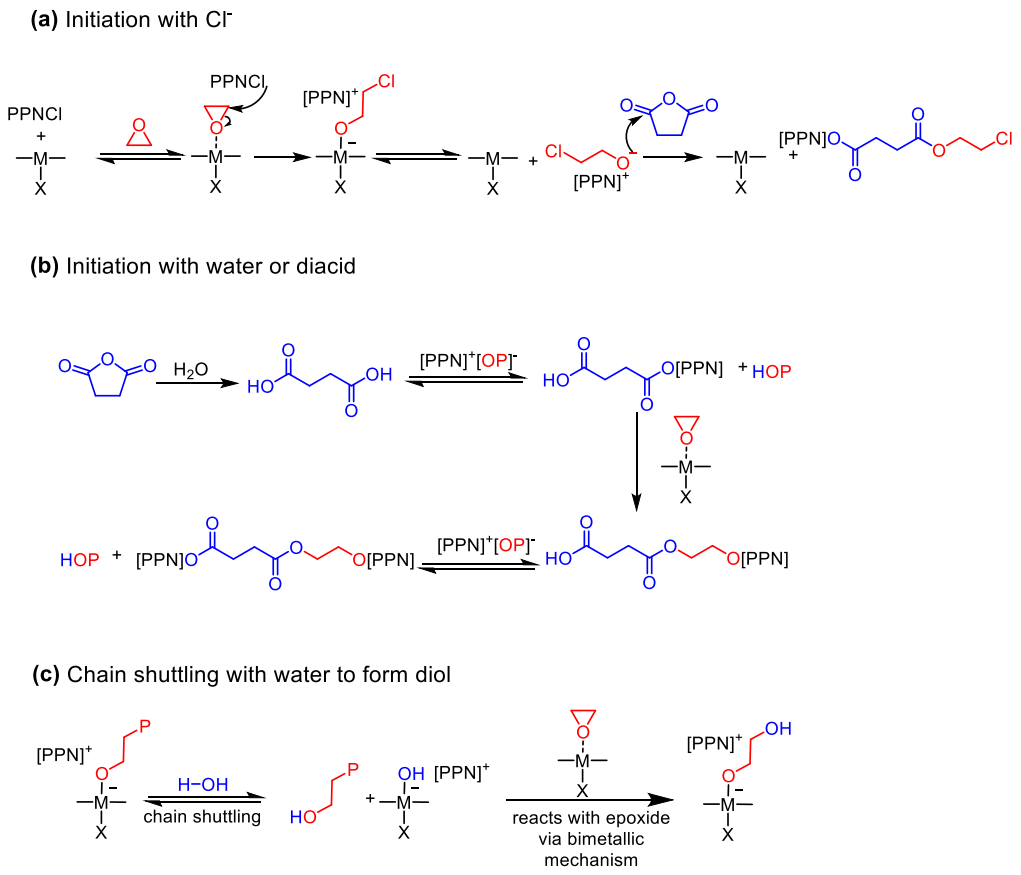

2.2.5 MALDI-TOF-MS analysis

Representative MALDI-TOF-MS spectra for the CHO-based polyesters is shown in **Error! Reference source not found.** and Figure 2.3. All PO- and CHO-based polymers showed a distribution attributable to polymer species with α,ω-Cl,OH (**Error! Reference source not found.** and Figure 2.3 in red) terminal groups which indicates that the formation of the polymer chains was initiated by Cl^-. In agreement with the results obtained by GPC analysis, the spectra of polymers synthesized using the **Fe^{MeMe}** catalyst also contained α,ω-OH,OH termini as a lower intensity but up to a high molecular weight distribution (Figure 2.3 in green). The absence of distributions with α,ω-Cl,Cl terminated polymers or cyclic polymers suggests that no transesterification occurred during the polymerization process, and that the α,ω-OH,OH signals were due solely to diacid or diol initiated chains (Scheme 2.6 b-c**Error! Reference source not**

found.). Transesterification would not only result in α,ω-OH,OH terminated polymers, but also α,ω-Cl,Cl terminated polymers and cyclic structures would have to be formed concomitantly.[52]

The CHO-based polyesters have relatively low molecular weights. We initially hypothesized that the lower molecular weights could be due to formation of cyclic polymers, theorizing that as the rate of propagation is reduced, the rate of intramolecular reactions leading to the formation of cyclic polymers could become competitive with propagation. However, MALDI-TOF-MS analysis of all samples in Table 2.3 revealed the complete absence of cyclic structures. To our surprise, there was an additional set of signals in the spectra of all CHO-based polyesters corresponding to polymers without the expected chloride end group (ω-OH) (Figure 2.2 and Figure 2.3 in blue).

Figure 2.2 MALDI-TOF-MS analysis of poly(CHO-*alt*-**2a**) synthesized with **(salph-^{t}Bu)AlCl** showing two distributions having α,ω-Cl,OH (in red) and ω-OH (in blue) end-groups.[F]

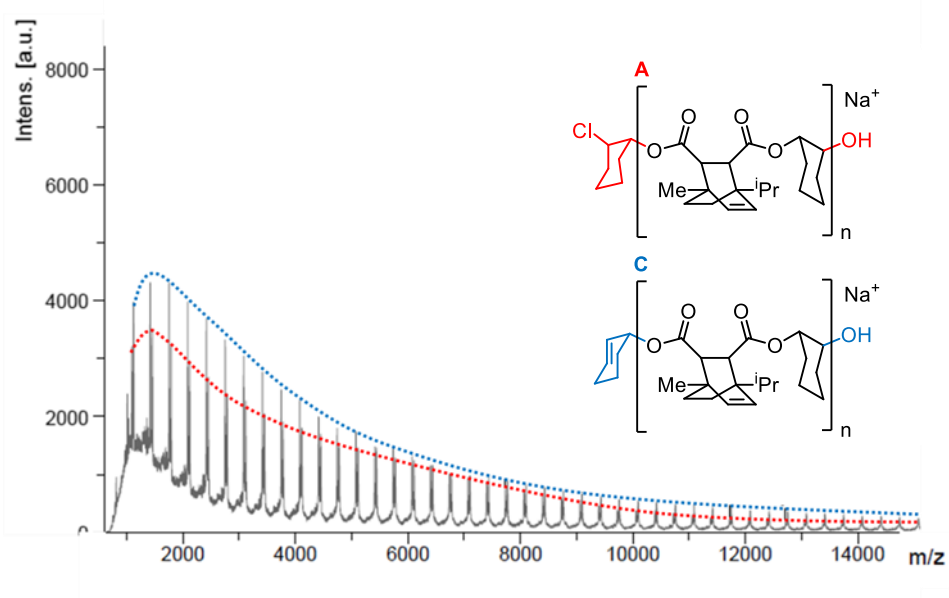

[F] The regio-regularity of anhydride insertion step was not determined.

Figure 2.3 MALDI-TOF-MS analysis of poly(CHO-*alt*-**2a**) synthesized with **Fe^{MeMe}** (Table 2.1, Entry 2) showing three distributions with α,ω-Cl,OH (in red), α,ω-OH,OH (in green) and ω-OH (in blue) end-groups.[G]

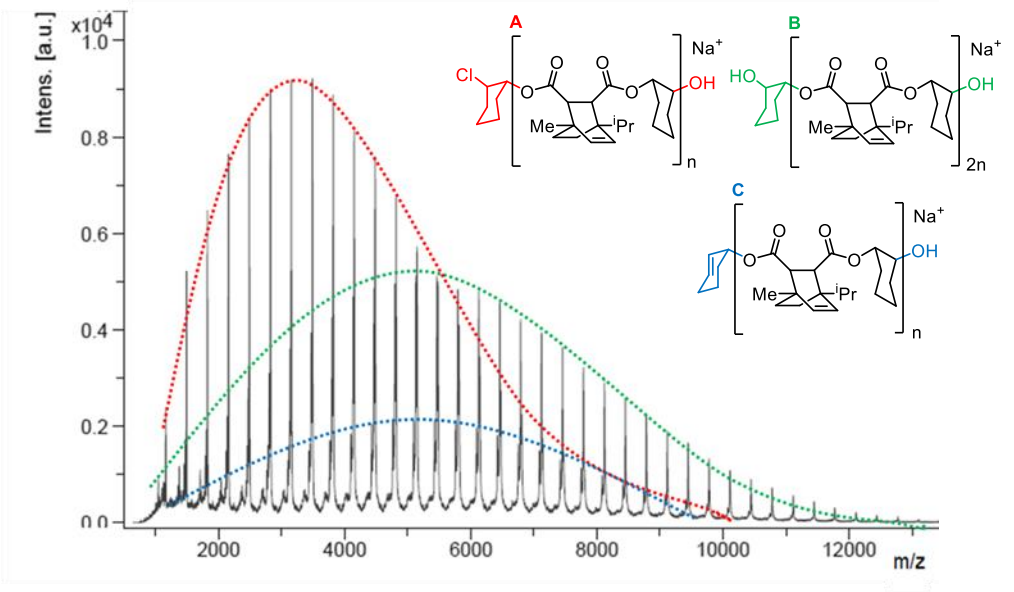

We propose that this could be due to a Meerwein–Ponndorf–Verley–Oppenauer (MPVO) type reaction occurring thereby generating CHO-based alcohols that can initiate new polymer chains as previously reported by Duchateau.[42,71] The resulting increase in the number of initiators would account for the lower molecular weights observed compared to the PO based polymers. Additionally, if alcohols are slowly being generated throughout the polymerization, new chains will be generated over the course of the polymerization leading to generally higher *Đ* values for the CHO-based polyesters (Table 2.3, *Đ* = 1.20–1.58). It should be noted that based on the work of Duchateau and co-workers, the endgroup in structure **C** (Figure 2.3) could be either saturated or unsaturated.[71] Due to the too low resolution of the MALDI-measurement, it is not possible to accurate determine this feature in the polymeric structure **C** (Figure 2.3). A general reaction scheme for the MPVO reaction is shown in Scheme 2.7**Error! Reference source not found.**a, and the formation of the cyclohexenol or cyclohexanol end-groups are shown in Scheme 2.7b.

[G] The regio-regularity of anhydride insertion step was not determined.

Scheme 2.7 (a) General MPVO reaction, and (b) formation of different end-groups via the MPVO reaction.

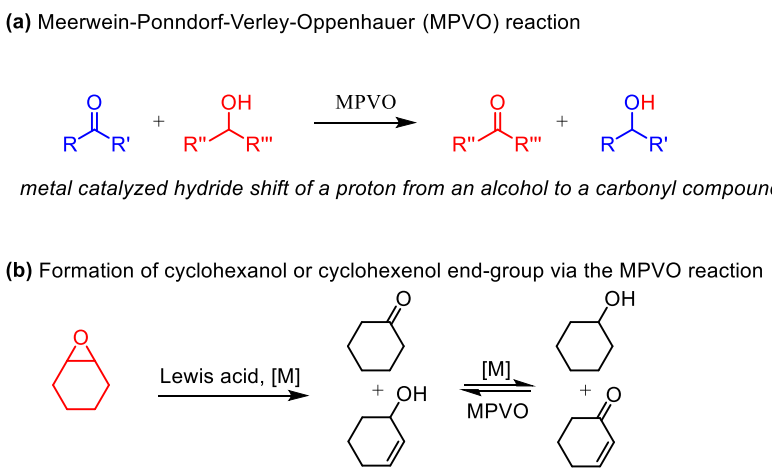

There remains another possibility for the formation of the cyclohexenol end-group. Elimination of Cl^- from α,ω-Cl,OH terminated polymers by a polymer alkoxide species would also generate the aforementioned end-group. Although we have been unable to definitively rule out this possibility, we believe that the MPVO reaction is the more likely cause of the formation of these end-groups supported by a series of control experiments. First, when a polymer sample was resubmitted to a mixture of CHO, (**salph-^{t}Bu)AlCl**, and PPNCl (conditions which should generate alkoxides and which mimic conditions near the end of the polymerization process), the ratio of end-groups remained unchanged as determined by MALDI-TOF-MS analysis. If Cl^- elimination would be the cause of the cyclohexenol end-groups then under these conditions the number of cyclohexenol end groups should have increased. Second, if Cl^- elimination would occur, the ratio of α,ω-Cl,OH to cyclohexenol end-groups should increase with decreasing molecular weight as new Cl^- initiators would be slowly generated over the course of the polymerization process, resulting in a bias towards low molecular chains having α,ω-Cl,OH end-groups but this was not observed. Finally, by reducing the amount of CHO present from 5 to 3 equiv would need to have a large impact on the polymerization (see Table 2.2) when Cl^- elimination was the source of the formation of cyclohexenol end-groups. In either case, the net effect is the same on the polymerization process, *i.e.* a slow introduction of new initiators over the course of the polymerization leading to lowered M_n values and increased $Đ$ values.

2.2.6 Stereochemistry of the polyester diester units

All tricyclic anhydrides used in this chapter have inherent *cis* stereochemistry that is retained after the ring-opening copolymerization reaction. However, epimerization processes can transform *cis*-diester units into the thermodynamically more favored *trans* configuration (Scheme 2.9). According to the mechanisms proposed by Inoue[49,50] and Chisholm[39,40] when the copolymerizations are performed with an excess of epoxide, in this case PO, the resulting species after consumption of the cyclic anhydride, are a metal alkoxide and a highly basic and nucleophilic PPN^+-based alkoxide.

Scheme 2.8. Proposed equilibria at the end of the copolymerization reaction when using an excess of epoxide and a (salphen)AlCl as catalyst.

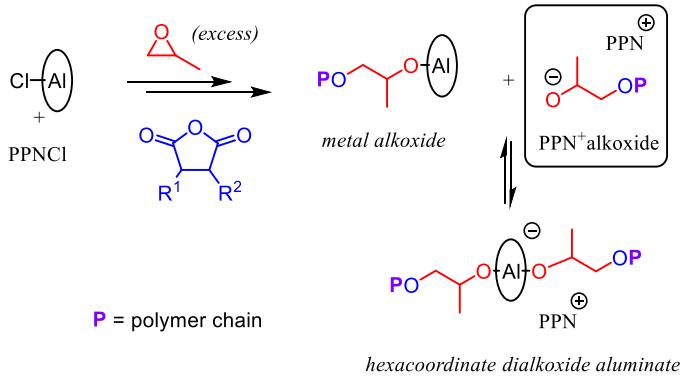

After the consumption of the cyclic anhydride monomer, this PPN^+-based alkoxide can deprotonate the α carbon adjacent to the ester group present in the repeat units of the polymer chain. The resulting structure is less strained due to the planar structure of the carbanionic intermediate which is stabilized by resonance. When the repeat unit is re-protonated, the most stable isomer will be formed with the substituents on the cyclohexene ring in a *trans* configuration to minimize steric interations. The epimerization proccess only occurs at high conversions of cyclic anhydride due to the fact that the PPN^+-based alkoxide attack is favored over the attack by the polymer (alkoxide) chain.[52]

Scheme 2.9 Epimerization of a *cis* into a *trans* diester unit in poly(PO-*alt*-**2a**).

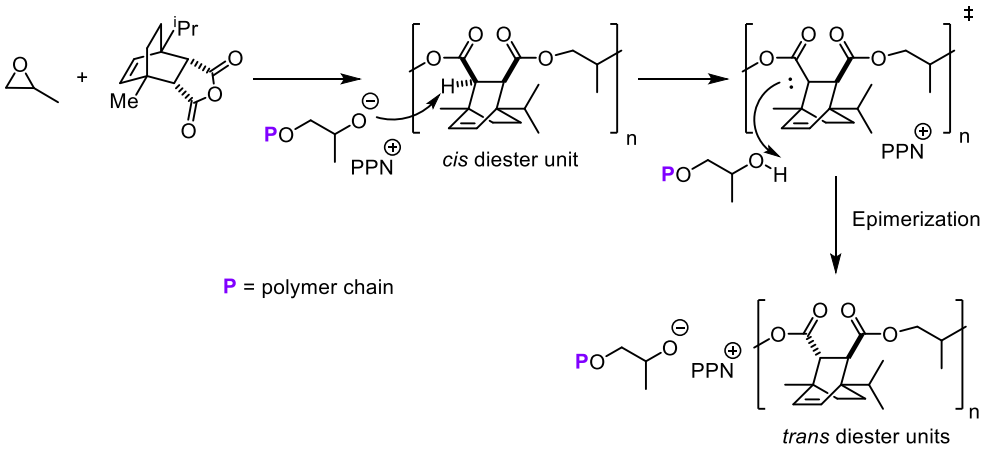

The stereochemistry of the polyester diester units was examined by carrying out degradation reactions of the polyesters, and by comparison of the degradation products with independently synthesized *cis* and *trans* diol model compounds. The polyesters were degraded to the corresponding diols using $LiAlH_4$ according to a previously published procedure.[51] All polymers were degraded after full conversion of the anhydride monomer with the exception of poly(CHO-*alt*-**2a**) (Table 2.3, Entry 1 and 2) which was degradated at the conversion shown in the table. The degraded samples were then analyzed by ^1H NMR spectroscopy and the resulting spectra compared to the spectra of the appropriate *cis* and *trans* diol reference compounds to determine the percentage of *cis* linkages in the original polyester. For some of the polymers, it was immediately apparent after the degradation reaction that no NMR signals could be assigned to *trans* diols, and since the *trans* diol model compounds in these cases were significantly harder to prepare, the degraded polymers were compared only to the *cis* model derivatives.

Comparison of ^{1}H-NMR spectrum of degraded polymers and corresponding *cis* and *trans* diols model compounds

Scheme 2.10 Comparison of the vinylic region of the ^{1}H NMR spectrum of the (a) *cis* diol model compound based on **2a**, (b) *trans* model compound based on **2a**, and (c) and (d) represent the NMR traces of the isolated materials after reductive degradation of (PO-*alt*-**2a**).

(a)

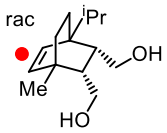

(b)

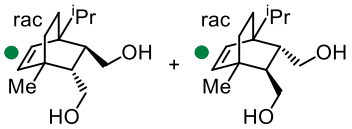

(c) Reductive degradation of (PO-*alt*-**2a**), Table 2.1, Entry 1

(d) Reductive degradation of (PO-*alt*-**2a**) Table 2.1, Entry 2

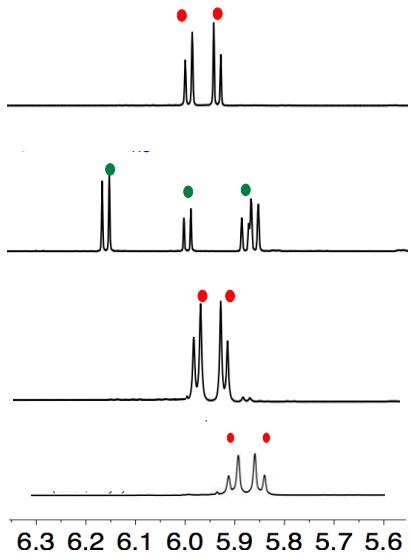

Scheme 2.11. Comparison of the vinylic region of the ^{1}H NMR spectrum of (a) *cis* diol model compound based on **2b**, and (b) and (c) represent the NMR traces of the isolated materials after reductive degradation of (PO-*alt*-**2b**).

(a)

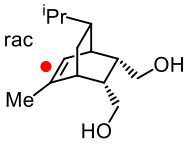

(b) Reductive degradation of (PO-*alt*-**2b**),Table 2.1, Entry 3

(c) Reductive degradation of (PO-*alt*-**2b**), Table 2.1, Entry 4

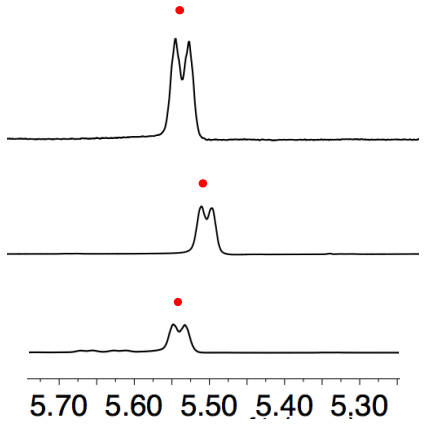

Scheme 2.12. Comparison of the vinylic region of the ^{1}H NMR spectrum of (a) *cis* diol model compound based on **2c**, (b) *trans* model compound based on **2c**, and (c) NMR trace of the isolated materials after reductive degradation of (PO-*alt*-**2c**).

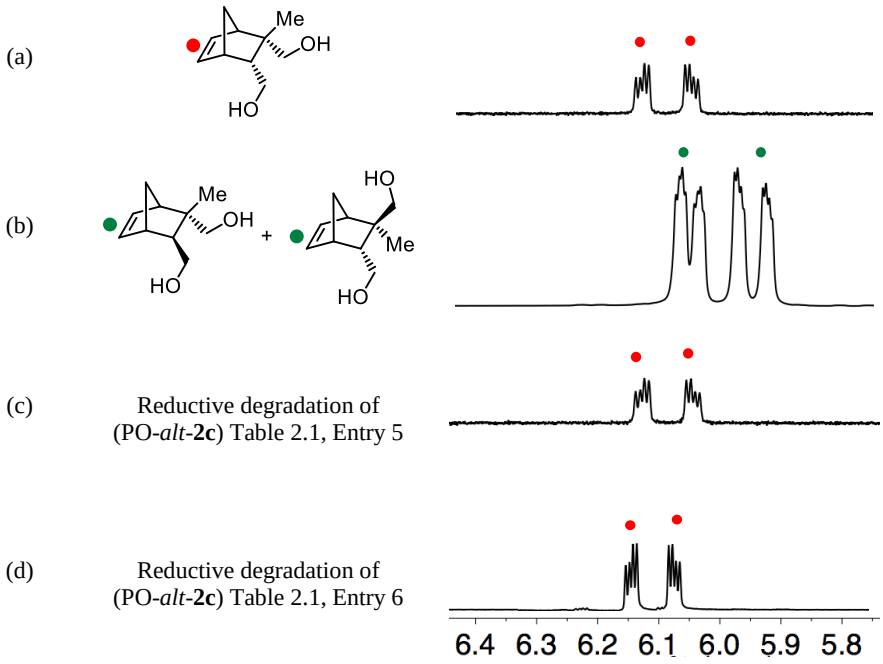

Scheme 2.13 Comparison of the vinylic region of the ^{1}H NMR spectrum of (a) *cis* diol model compound based on **2d**, and (b) and (c) are the NMR traces of the isolated materials after reductive degradation of (PO-*alt*-**2d**).

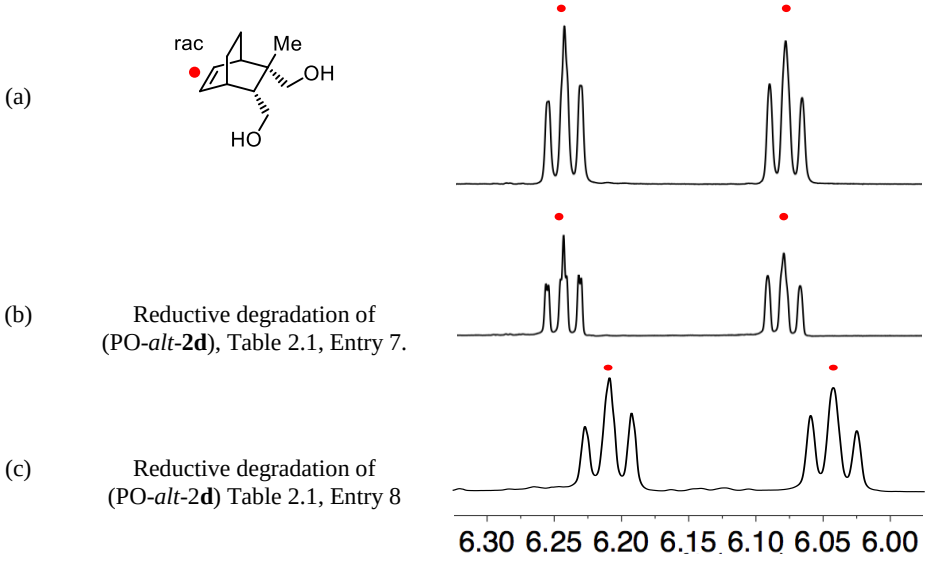

Scheme 2.14 Comparison of the diagnostic region of the ^{1}H NMR spectrum of (a) *cis* diol model compound based on **2e**, (b) *trans* model compound based on **2e**, and (c) and (d) are the NMR traces of the isolated materials after reductive degradation of (PO-*alt*-**2e**).

(a)

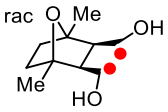

(b)

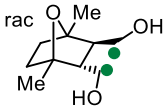

(c) Reductive degradation of (PO-*alt*-**2e**), Table 2.1, Entry 9

(d) Reductive degradation of (PO-*alt*-**2e**) Table 2.1,Entry 10

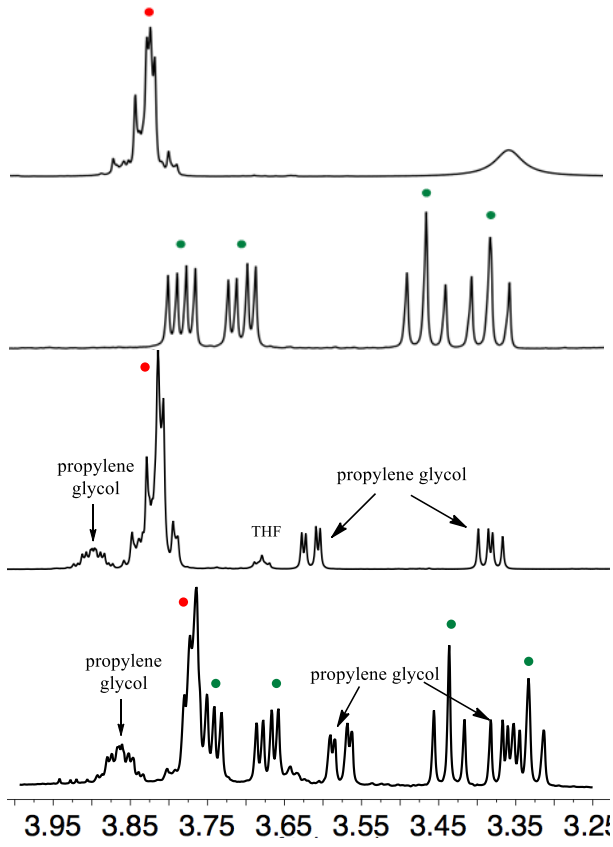

Scheme 2.15 Comparison of the vinylic region of the ^{1}H NMR spectrum of (a) *cis* diol model compound based on **2f**, and (b) and (c) represent the NMR traces of the isolated material after reductive degradation of (PO-*alt*-**2f**).

(a)

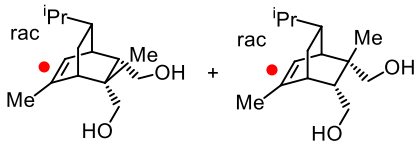

(b) Reductive degradation of (PO-*alt*-**2f**), Table 2.1, Entry 11

(c) Reductive degradation of (PO-*alt*-**2f**) (Table 2.1, Entry 12).

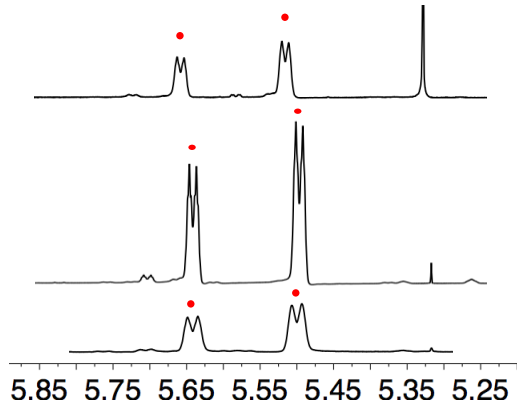

Scheme 2.16. Comparison of the vinylic region of the ^{1}H NMR spectrum of (a) *cis* diol model compound based on **2a**, (b) *trans* model compound based on **2a**, and (c) and (d) represent the NMR traces of the isolated material after reductive degradation of (CHO-*alt*-**2a**).

(a)

(b)

(c) Reductive degradation of (CHO-*alt*-**2a**) Table 2.3, Entry 1

(d) Reductive degradation of (CHO-*alt*-**2a**) Table 2.3, Entry 1

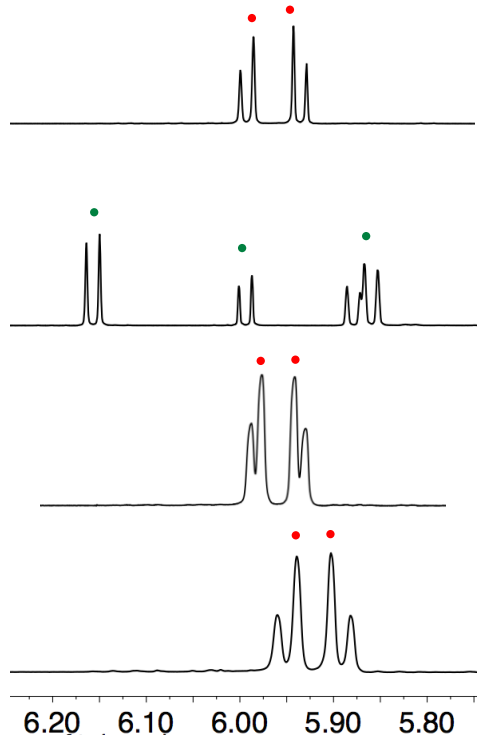

Scheme 2.17 Comparison of the vinylic region of the ^{1}H NMR spectrum of (a) *cis* diol model compound based on **2b**, and (b)+(c) are the NMR traces after reductive degradation of (CHO-*alt*-**2b**).

(a)

(b) Reductive degradation of (CHO-*alt*-**2b**) Table 2.3, Entry 3

(c) Reductive degradation of (CHO-*alt*-**2b**) Table 2.3, Entry 4

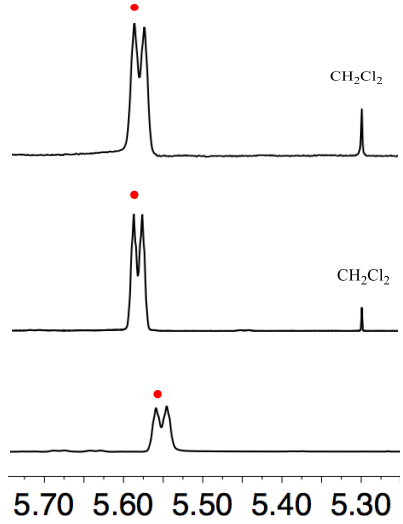

Scheme 2.18 Comparison of the vinylic region of the ^{1}H NMR spectrum of (a) *cis* diol model compound based on **2c**, (b) *trans* model compound based on **2c**, and (c) and (d) are the NMR traces of the isolated material after reductive degradation of (CHO-*alt*-**2c**).

(a) 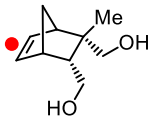

(b) 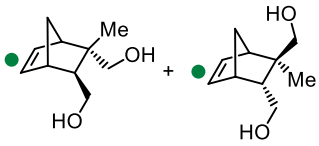

(c) Reductive degradation of (CHO-*alt*-**2**c) Table 2.3, Entry 7.

(d) Reductive degradation of (CHO-*alt*-**2c**) Table 2.3, Entry 8

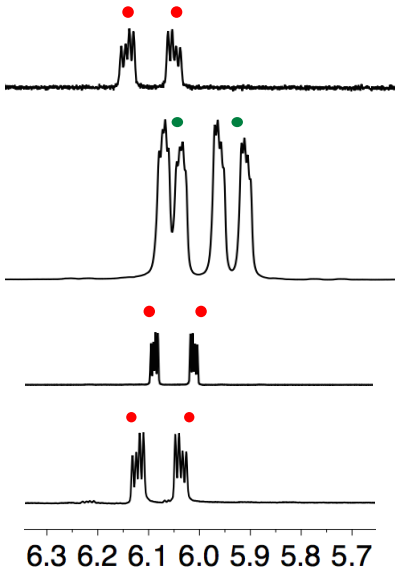

Scheme 2.19 Comparison of the vinylic region of the ^{1}H NMR spectrum of (a) *cis* diol model compound based on **2d**, and (b) and (c) are the NMR traces of the isolated material after reductive degradation of (CHO-*alt*-**2d**).

(a) 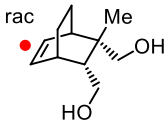

(b) Reductive degradation of CHO-*alt*-**2d**) Table 2.3, Entry 7

(c) Reductive degradation of (CHO-*alt*-**2d**) Table 2.3, Entry 8

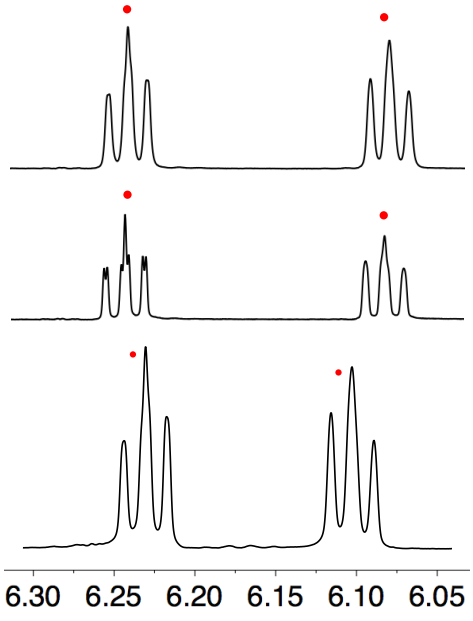

Scheme 2.20 Comparison of the diagnostic region of the ^{1}H NMR spectrum of (a) *cis* diol model compound based on **2e**, (b) *trans* model compound based on **2e**, and (c) NMR trace of the isolated material after reductive degradation of (CHO-*alt*-**2e**).

(a)

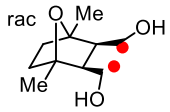

(b)

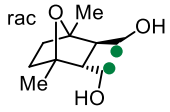

(c) Reductive degradation of (CHO-*alt*-**2e**) (Table 2.3, Entry 10)

(d) Reductive degradation of (CHO-*alt*-**2e**), Table 2.3, Entry 9

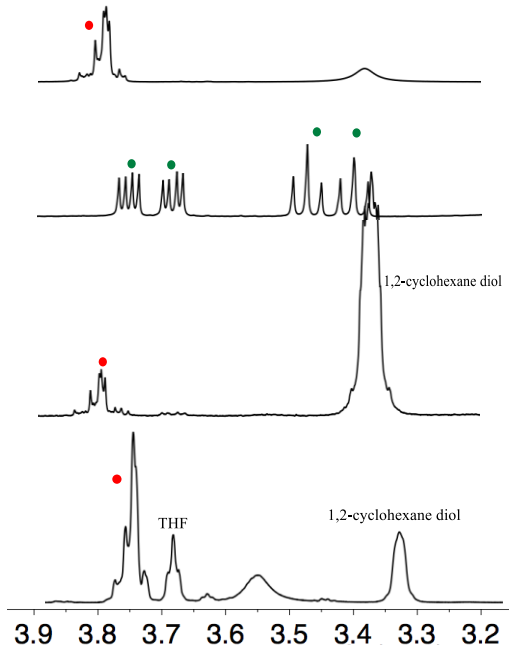

Scheme 2.21 Comparison of the vinylic region of the ^{1}H NMR spectrum of (a) *cis* diol model compound based on **2f**, and (b) and (c) are the NMR traces of the isolated material after reductive degradation of (CHO-*alt*-**2f**).

(a)

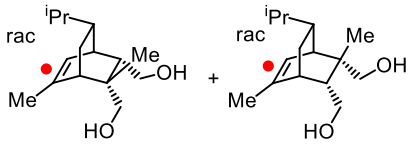

(b) Reductive degradation of (CHO-*alt*-**2f**) Table 2.3, Entry 11

(c) Reductive degradation of (CHO-*alt*-**2f**) Table 2.3, Entry 12

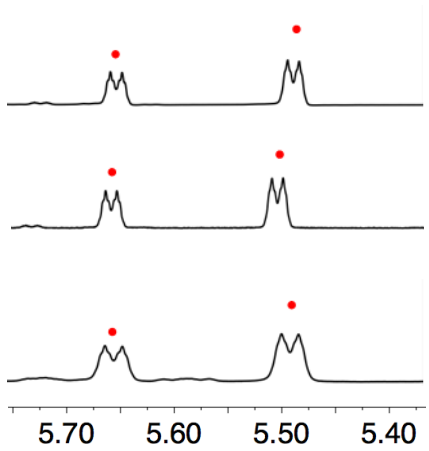

As mentioned, all of the polymers retained a high *cis*-diester content (>99%) even at full conversion with the exception of poly(PO-*alt*-**2e**) synthesized with **Fe^{MeMe}**, which had only 36% *cis*-diester linkages at full conversion (Table 2.1, Entry 10). According to bibliography[52] there are three factors that influence the rate of epimerization: the molar ratio of the metal catalyst to the nucleophilic co-catalyst, the structure of the tricyclic anhydride and the Lewis acidity of the catalyst. The ratio [complex]:[PPNCl] has a strong effect on the rate of epimerization. An excess of PPNCl with respect to the metal complex would generate larger amounts of PPN$^+$-based alkoxide at the end of the polymerization reaction, and would thus increase the epimerization reaction rate (Scheme 2.8). Since slight excess of the metal complex provides better retention of *cis*-diester stereochemistry,[52] a [complex]:[PPNCl] = 1:0.9 ratio was used for all of the polymerizations reported in Table 2.1 and Table 2.3.

The epimerization process is faster with less bulky anhydrides because the decreased steric bulk along the polymer chain facilitates deprotonation of the α carbon to the carboxylic group. This is a reasonable explanation why epimerization only affects to poly(PO-*alt*-**2e**) which is the least sterically hindered polymer.

Finally, the Lewis acidity of the catalyst plays an important role. More Lewis acidic catalysts react faster with the PPN$^+$-based alkoxide (Scheme 2.8) present at the end of the polymerization reaction and presumably it can affect the rate of epimerization. Whereas it may be difficult to compare our two catalyst systems, we hypothesize that **(salph-Cl)AlCl** catalyst (used in Table 2.1, Entry 9) is more Lewis acidic than **Fe^{MeMe}** due the smaller size of the metal center and the presence of Cl electron-withdrawing groups present in the ligand. It is also important to note that the formation of the hexacoordinate dialkoxide iron (aminotriphenolate) species will probably be less favored compared to the formation of the hexacoordinate dialkoxide aluminum (salphen) species due to the difficulty of accommodating the aminotriphenolate ligand in an octahedral geometry. Consequently, with **Fe^{MeMe}** the equilibrium would be displaced towards the pentacoordinate metal alkoxide and a free PPN$^+$-based alkoxide which would favor epimerization.

We also investigated if the epimerization of poly(PO-*alt*-**2e**) using **Fe^{MeMe}** catalyst occurred exclusively after full conversion of the anhydride **2e** or, contrary, already began before reaching this point. We synthesized a sample of poly(PO-*alt*-**2e**) and stopped the reaction at 85% conversion of the cyclic anhydride. Reductive degradation of this sample showed no signs of epimerization of diester units (by NMR) and full retention of the *cis*-diester configuration (>99%) was observed.

2.2.7 Thermogravimetric analysis of polymers

Samples prepared under the conditions given in Table 2.1 and Table 2.3 were analyzed using a Mettler Toledo Thermogravimetric Analyzer (TGA), model TGA/SDTA851. The heating program was 30 °C to 500 °C at 10 °C/min under a nitrogen atmosphere. The onset thermal decomposition temperatures are reported in Table 2.4. In general, the polyesters derived from **2a–2f** and PO or CHO display high decomposition temperatures typically >250ºC, and the polymers prepared using **Fe^{Me,Me}** generally give slightly higher T_d^{10} values.

Table 2.4. Thermal degradation data for all polymers.

Polymer	Catalyst	T_d^{10}(ºC)[a]
Poly(PO-*alt*-**2a**)	(salph-^{t}Bu)AlCl	309
	Fe^{MeMe}	315
Poly(PO-*alt*-**2b**)	(salph-Cl)AlCl	316
	Fe^{MeMe}	328
Poly(PO-*alt*-**2c**)	(salph-^{t}Bu)AlCl	242
	Fe^{MeMe}	245
Poly(PO-*alt*-**2d**)	(salph-^{t}Bu)AlCl	290
	Fe^{MeMe}	313
Poly(PO-*alt*-**2e**)	(salph-Cl)AlCl	261
	Fe^{MeMe}	325
Poly(PO-*alt*-**2f**)	(salph-^{t}Bu)AlCl	305
	Fe^{MeMe}	326
Poly(CHO-*alt*-**2a**)	(salph-^{t}Bu)AlCl	272
	Fe^{MeMe}	316
Poly(CHO-*alt*-**2b**)	(salph-^{t}Bu)AlCl	314
	Fe^{MeMe}	324
Poly(CHO-alt-**2c**)	(salph-^{t}Bu)AlCl	236
	Fe^{MeMe}	252
Poly(CHO-*alt*-**2d**)	(salph-^{t}Bu)AlCl	272
	Fe^{MeMe}	324
Poly(CHO-*alt*-**2e**)	(salph-^{t}Bu)AlCl	280
	Fe^{MeMe}	286
Poly(CHO-*alt*-**2f**)	(salph-^{t}Bu)AlCl	300
	Fe^{MeMe}	323

[a] Reported T_d data refer to T_d^{10} values at 10% wt loss.

2.3 Conclusions

We have prepared six tricyclic anhydrides that were either partially (50–63% by weight) or fully renewably sourced and successfully used them in alternating co-polymerizations with propylene oxide (PO), an inexpensive and readily available monomer, and with cyclohexene oxide (CHO), which has the potential to be renewably sourced. By varying both the epoxide and the anhydride, we were able to tune the T_g of the resulting polymers over a nearly 120 °C range from 66 °C to an exceptionally high 184 °C.

Polymers synthesized with PO had higher polymerization rates, narrower $Đ$ values, and higher molecular weights, albeit with generally lower T_g values (66–108 °C). The CHO containing polymers had significantly higher T_g values, (124–184 °C) although they had lower molecular weights, broader $Đ$ values, and substantially decreased polymerization rates. The high T_g values of these materials gives them potential for use in a variety of higher temperature applications. In addition to exploring other potential renewable monomers, we are currently investigating further catalyst development to allow access to higher molecular weight CHO based polymers, as well as examining the physical and mechanical properties of these materials.

2.4 Experimental section

2.4.1 General information and instrumentation

All manipulations of air and water sensitive compounds were carried out under nitrogen in an MBraun Labmaster glovebox or by using standard Schlenk line technique. ^{1}H NMR spectra were recorded on Varian INOVA 400 (^{1}H, 400 MHz), INOVA 500 (^{1}H, 500 MHz), or INOVA 600 (^{1}H, 600 MHz) spectrometers. Spectra were referenced to the residual chloroform (7.26 ppm) or DMSO-d_5 (2.50 ppm) signals. ^{13}C NMR spectra were recorded on a Varian INOVA 500 (^{13}C, 126 MHz) spectrometer and referenced to the residual chloroform (77.23 ppm) or DMSO-d_6 (39.50 ppm) signals. Assignment of the signals in the NMR spectra of all polyesters was based on 2D NMR experiments. HRMS analyses were performed on a Thermo Scientific Exactive Orbitrap MS system equipped with an Ion Sense DART ion source. Flash column chromatography was performed using silica gel (particle size 40–64 μm, 230–400 mesh).

Gel permeation chromatography (GPC) analyses were carried out using an Agilent 1260 Infinity GPC System equipped with a refractive index detector as well as an Agilent 1260 Infinity autosampler. The Agilent GPC system was equipped with two Agilent PolyPore columns (5

micron, 4.6 mm ID) which were eluted with THF at 30 °C at 0.3 mL/min and calibrated using monodisperse polystyrene standards. Differential scanning calorimetry (DSC) measurements of polymer samples were performed on a Mettler-Toledo Polymer DSC instrument equipped with a chiller and an auto-sampler. Samples were prepared in aluminum pans. All polyesters were analyzed using the following heating program: −70 ºC to 200 °C at 25 ºC/min, 200 to −70 ºC at 10ºC/min, and then −70 ºC to 200 ºC at 25 °C/min. Data were processed using StarE software. All reported glass transition temperatures are from the second heating cycle.

MALDI-TOF-MS analyses were performed on a BRUKER Autoflex system with a 20 Hz N_2 UV laser (337 nm) and based on a previously reported procedure.[34] Crude polymer samples were dissolved in THF at 1 mg·mL^{-1}. Sodium trifluoroacetate was used as additive and dissolved in THF at 5 mg·mL^{-1}. The matrix *trans*-2-[3-(4-*tert*-butylphenyl)-2-methyl-2-propenylidene]malononitrile (DCTB) was dissolved in THF at 40 mg·mL^{-1}. Solutions for analysis were prepared by mixing polymer, additive, and matrix solutions in a volume ratio of 80:10:40, respectively. The sample was left to air-dry after spotting on a stainless steel MALDI target plate. All spectra were recorded in linear mode. The resulting spectra were analyzed using the Flex Analysis software package.

Polymer thermal degradation experiments were performed on a Mettler Toledo Thermogravimetric Analyzer (TGA), model TGA/SDTA851. The heating program was 30 ºC to 500 ºC at 10 ºC/min under a nitrogen atmosphere. Data were processed using START software. Onset thermal decomposition temperatures were reported.

2.4.2 Materials

Solvents used for cyclic anhydride and ligand syntheses, including methanol (Macron), absolute ethanol (Koptec), methylene chloride (Fisher), hexanes (Macron), ethyl acetate (Fisher), chloroform (Fisher), and diethyl ether (J. T. Baker), were used as received. Toluene (Fisher) and hexane (Fisher) used in salicylaldehyde and complex syntheses were dried and degassed by passing them through two columns packed with neutral alumina and copper(II) oxide. α–terpinene (Aldrich, ≥89%), α-phellandrene (Aldrich, Hallal/Kosher), 1,3-cyclohexadiene (Aldrich, 97%), citraconic anhydride (Aldrich, 98%), 2,5-dimethylfuran (Aldrich, 99%) and maleic anhydride (Aldrich, ≥ 99.0%) were used as received. Hydrogen (Airgas, 99.99%) was used as received.

Propylene oxide (PO) and cyclohexene oxide (CHO) were purchased from Aldrich, stirred over freshly ground CaH_2 for one day, vacuum distilled onto a new portion of freshly ground

CaH_2 in a dry roundbottom flask with Strauss adapter, stirred one day and then vacuum distilled again before being degassed by three freeze-pump-thaw cycles.

Palladium on activated carbon (5%, reduced, dry powder, Strem) was used as received. Bis(triphenylphosphine)iminium chloride (PPNCl, 97%, Aldrich) was recrystallized by layering a saturated methylene chloride solution with diethyl ether. The resulting crystals were ground to a fine powder and then dried at 60 °C under vacuum prior to use. All other chemicals and reagents were purchased from commercial sources (Aldrich, Combi-Blocks, Strem, Acros, TCI, and Alfa Aesar) and used without further purification.

2.4.3 General copolymerization procedures

Copolymerization of propylene oxide with cyclic anhydrides

In a glovebox, the appropriate amount of metal complex (4.3 μmol) and PPNCl (2.2 mg, 3.8 μmol) were placed in an oven-dried 4-mL vial equipped with a magnetic stir bar. The appropriate amount of cyclic anhydride (1.3 mmol) was added, followed by propylene oxide (0.45 mL, 6.4 mmol). The vial was sealed with a Teflon-lined cap, removed from the glovebox, and placed in an aluminum heating block preheated to 60 °C. After the appropriate amount of time, an aliquot was taken for ^{1}H NMR spectroscopic analysis to determine conversion of the cyclic anhydride. The reaction mixture was then diluted with approximately 0.5 mL methylene chloride and precipitated into 10 mL of acidic methanol (1 M HCl in methanol) with vigorous stirring, after which the methanol was decanted. Poly(PO-*alt*-**2e**) was precipitated into hexanes due to its higher solubility in methanol. Precipitation was repeated as necessary to remove excess monomer and catalyst. The polymer was dried under vacuum at 60 °C.

Copolymerization of cyclohexene oxide with cyclic anhydrides.

In a glovebox, the appropriate amount of metal complex (4.3 μmol) and PPNCl (2.2 mg, 3.8 μmol) were placed in an oven-dried 4-mL vial equipped with a magnetic stir bar. The appropriate amount of cyclic anhydride (1.3 mmol) was added, followed by cyclohexene oxide (0.39 mL, 3.84 mmol) and dry, degassed toluene (0.2 mL). The vial was sealed with a Teflon-lined cap, removed from the glovebox, and placed in an aluminum heating block preheated to 60 °C. After the appropriate amount of time, an aliquot was taken for ^{1}H NMR spectroscopic analysis to determine conversion of the cyclic anhydride. The reaction mixture was then diluted with approximately 0.5 mL methylene chloride and precipitated into 10 mL of acidic methanol (1 M HCl in methanol) with vigorous stirring, after which the methanol was decanted.

Poly(CHO-*alt*-**2e**) was precipitated into hexanes due to its higher solubility in methanol. Precipitation was repeated as necessary to remove excess monomer and catalyst. The polymer was dried under vacuum at 60 °C.

2.4.4 Synthesis of complexes

Synthesis of 3-*tert*-butyl-5-chlorosalicylaldehyde

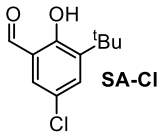

3-*tert*-butyl-5-chlorosalicylaldehyde **(SA-Cl).** Prepared according to the literature procedure:[72] A mixture of $FeCl_3$ (43.2 mg, 0.27 mmol, 0.01 equiv), 3-tert-butyl-2-hydroxybenzaldehyde (4.75 g, 26.6 mmol, 1 equiv.) and SO_2Cl_2 (2.8 mL, 35 mmol, 1.3 equiv.) was stirred at room temperature for 24 h. The resulting solid was dissolved in diethyl ether (100 mL). The organic layer was washed with water (100 mL × 3) and saturated aqueous NaCl solution (100 mL), and then dried over $MgSO_4$ After the solvent was removed by evaporation under reduced pressure; the residue dissolved in CH_2Cl_2 was passed through a short silica column using CH_2Cl_2 as eluent. The crude product after removal of the solvent was dissolved in hot methanol, and was kept at –20 °C to give the product (4.21 g, 74%). Spectroscopic characterization was consistent with that reported in the literature.[72]

^{1}H NMR (400 MHz, $CDCl_3$): δ 11.72 (s, 1H), 9.82 (s, 1H), 7.46 (d, 1H), 7.38 (d, 1H), 1.41 (s, 9H).

Synthesis of (salph)H_2 ligands

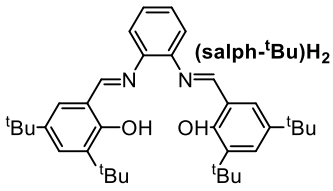

N,N'-bis(3,5-di-*tert*-butylsalicylidene)-1,2-diaminobenzene **[(salph-^{t}Bu)H_2]**. Prepared according to the literature procedure:[73] 3,5-di-*tert*-butylsalicylaldehyde (5.0 g, 21.4 mmol, 2 equiv.) was dissolved in 40 mL of ethanol. After adding 1,2-diaminobenzene (1.15 g, 10.7 mmol, 1.0 equiv.), the reaction mixture was refluxed for 4 h. The reaction mixture was then cooled to 22 °C, and the resulting precipitate was isolated by filtration. The solids were washed with small amounts of cold ethanol to give the corresponding yellow ligand after drying under vacuum at

60 °C overnight (4.51 g, 78%). Spectroscopic characterization was consistent with that reported in the literature.[73]

^{1}H NMR (400 MHz, $CDCl_3$): δ 11.64 (s, 2H,), 8.66 (s, 2H), 7.44 (d, 2H), 7.32 (m, 2H), 7.24 (m, 2H), 7.21 (d, 2H), 1.43 (s, 18H), 1.32 (s, 18H).

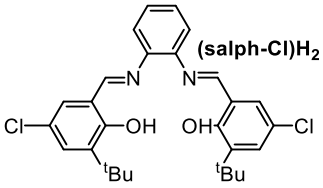

N,N'-bis(3-*tert*-butyl-5-chlorosalicylidene)-1,2-diaminobenzene **[(salph-Cl)H$_2$]**. Salicylaldehyde **SA-Cl** (0.50 g, 2.3 mmol, 2.0 equiv.) and 1,2-diaminobenzene (0.13 g, 1.2 mmol, 1.0 equiv.) were refluxed in absolute ethanol (20 mL). The reaction mixture was cooled to 22 °C, and the resulting precipitate was isolated by filtration. The solids were washed with small amounts of cold ethanol then dried under vacuum at 60 °C overnight to give **(salph-Cl)H$_2$** (0.32 g, 55%) as an orange solid.

Synthesis of aluminum complexes

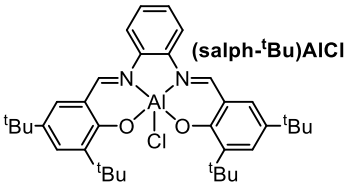

(salph-^{t}Bu)AlCl. Prepared using **(salph-^{t}Bu)H$_2$** according to the literature procedure.[52,74] In a glovebox, **(salph-^{t}Bu)H$_2$** (1.0 g, 1.85 mmol, 1.0 equiv.) was dissolved in dry, degassed toluene (30 mL) in a dry Schlenk flask. A solution of Et_2AlCl (1.0 M in toluene, 2.0 mL, 2 mmol, 1.1 equiv.) was added dropwise with stirring, resulting in the precipitation of yellow solids from the reaction mixture. After stirring at 22 °C for 5 minutes in the glovebox, the flask was sealed and removed from the glovebox. The mixture was then heated at 90 °C for 16 h. After cooling to 22 °C, the resulting solids were filtered, washed with dry, degassed hexanes, and dried under vacuum overnight yielding 0.86 g of a bright yellow solid (78%). Spectroscopic characterization was consistent with that reported in the literature.[52,74]

^{1}H NMR (300 MHz, $CDCl_3$) δ 8.97 (s, 2H), 7.77 (m, 2H), 7.66 (d, 2H), 7.41 (m, 2H), 7.24 (d, 2H), 1.59 (s, 18H), 1.34 (s, 18H).

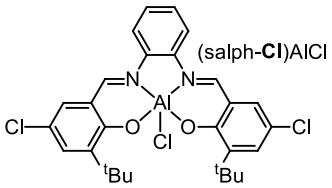

(salph-Cl)AlCl. In a glovebox, **(salph-Cl)H$_2$** (0.30 g, 0.60 mmol, 1.0 equiv.) was dissolved in approximately 20 mL dry, degassed toluene in a dry Schlenk flask. A 1.020 M solution of Et_2AlCl (0.65 mL, 0.66 mmol, 1.1 equiv.) was added dropwise with stirring, resulting in yellow solids precipitating from the reaction mixture. After stirring at 22 °C for 5 minutes in the glovebox, the flask was sealed and removed from the glovebox. The mixture was then heated at 90 °C for 16 h. After cooling to 22 °C, the resulting solid was filtered, washed with hexanes, and dried under vacuum overnight to give **(salph-Cl)AlCl** (0.19 g, 55%) as a yellow microcrystalline solid.

Synthesis of ion complex

Fe^{MeMe} was synthesized according to reported literature procedures.[53][H]

2.4.5 Synthesis of tricyclic anhydrides

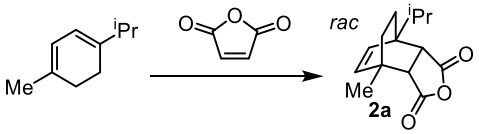

rac-cis-endo-1-isopropyl-4-methyl-bicyclo[2.2.2]oct-5-ene-2,3-dicarboxylic anhydride **[2a]:** Synthesized according to literature procedure[51]: Maleic anhydride (3.4 g, 34 mmol, 1.1 equiv.) was dissolved in 100 mL of diethyl ether in a 250-mL round bottom flask. Technical grade α-terpinene [5.0 g, 35 mmol (approximately 31.2 mmol with respect to α-terpinene), 1.0 equiv.] was then added. The mixture immediately turned yellow. The flask was fitted with a condenser, and the mixture was refluxed for 36 h. After cooling the mixture to 22 °C, the solvent was removed by rotary evaporation to give a yellow oil. The crude mixture was purified by flash column chromatography using 15% ethyl acetate/hexanes as the eluent (R_f = 0.44) to give a colorless oil that solidified upon standing; the solid was dried overnight at 22 °C (6.4 g, 87%). Spectroscopic characterization was consistent with that reported in literature.[51]

[H] For more information see section 1.4.2 "*Synthesis of complexes*" in chapter 1.

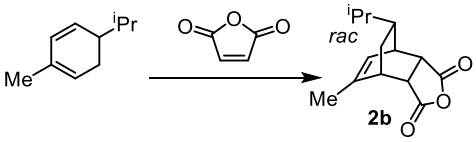

rac-cis-endo-7-Isopropyl-5-methyl-bicyclo[2.2.2]oct-5-ene-2,3-dicarboxylic anhydride **[2b]:** Synthesized according to literature procedure:[51] Maleic anhydride (3.4 g, 34 mmol, 1.1 equiv.) was dissolved in 100 mL of diethyl ether in a 250-mL round bottom flask. α-Phellandrene (4.3 g, 31 mmol, 1.0 equiv.) was then added. The flask was equipped with a condenser, and the mixture was gently refluxed for 16 h. After cooling the mixture to room temperature, the solvent was removed by rotary evaporation. The crude mixture was purified by flash column chromatography using 20% ethyl acetate/hexanes as the eluent (R_f = 0.44) to give a white solid. This product was further purified by recrystallization in hexanes to give white needles, which were dried overnight at 22 °C (4.9 g, 67%). Spectroscopic characterization was consistent with that reported in previous literature.[51]

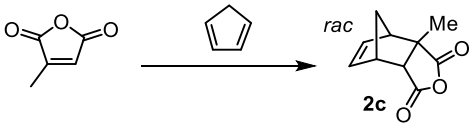

rac-cis-endo-2-methyl-bicyclo[2.2.1]hept-5-ene-2,3-dicarboxylic anhydride **[2c]**: Synthesized according to literature procedure:[75] To as solution of citraconic anhydride (14.7 g, 150 mmol, 1.0 equiv.) in chloroform (90 mL) was added freshly distilled cyclopentadiene (10.9 g, 165 mmol, 1.1 equiv.) at 0 °C. The reaction mixture was stirred overnight at room temperature and light was excluded. After evaporation of the solvent under reduced pressure and recrystallization from methanol (*rac*)-**2c** (24.6 g, 92%) was obtained as a colourless solid. Spectroscopic characterization was consistent with that reported in previous literature.[75]

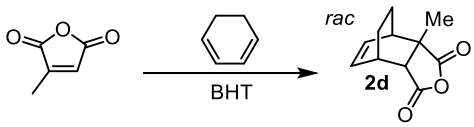

rac-cis-endo-2-methyl-bicyclo[2.2.2]hept-5-ene-2,3-dicarboxylic anhydride **[2d]:** In a 20 mL vial equipped with a magnetic stir bar and sealed with a Teflon-lined cap, 1,3-cyclohexadiene (6.00 mL, 62.8 mmol), citraconic anhydride (6.20 mL, 69.2 mmol) and 10 mg dibutylhydroxytoluene (BHT) were stirred at 60 °C for 48 h. The yellow oil was purified by column chromatography with 70:30 hexanes: ethyl acetate then crystallized from 80:20 hexanes: ethyl acetate and dried under vacuum overnight to yield 4.7 g (39 %) of a white, crystalline solid**.**

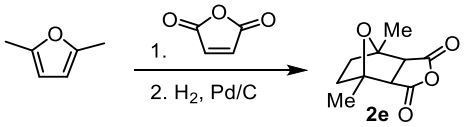

cis-exo-1,4-dimethyl-7-oxabicyclo[2.2.1]heptane-2,3-dicarboxylic anhydride **[2e]:** Maleic anhydride (5.0 g, 51.0 mmol, 1.0 equiv.) and 2,5-dimethyl furan (8.3 mL, 76.5 mmol, 1.5 equiv.) were stirred at 22 °C for 16 h. The resulting off white solid was filtered and washed with hexanes. A portion of the crude product (4.0 g, 20.5 mmol, 1.0 equiv.) was dissolved in 20 mL THF in a Parr reactor and palladium on carbon (5%, reduced, dry powder, 2.0 g) was added. The reactor was pressurized with hydrogen gas to 20 bar and the heterogeneous mixture stirred at 22 °C for 60 h. The mixture was filtered and stripped, and the product purified by crystallization in 80:20 hexanes: ethyl acetate to yield 1.98 g (49 %) of a white crystalline solid)

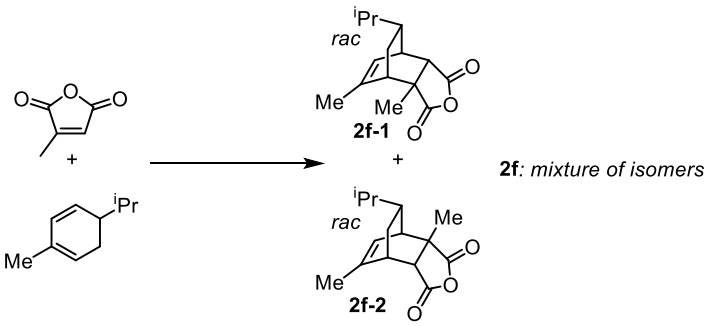

Mixture of *rac*-7-isopropyl-2,5-dimethylbicyclo[2.2.2]oct-5-ene-2,3-dicarboxylic anhydride and *rac*-8-isopropyl-2,6-dimethylbicyclo[2.2.2]oct-5-ene-2,3-dicarboxylic anhydride **[2f].** Citraconic anhydride (4.13 mL, 44.6 mmol) and α-phellandrene (6.07 g, 44.6 mmol) were combined in a 20 mL vial equipped with a magnetic stir bar and sealed with a Teflon-lined cap and stirred at 60 °C for 4 days. The yellow oil was purified by column chromatography with 90:10 hexanes: ethyl acetate then dried under vacuum overnight to yield 4.6 g (%) of a colorless oil which was found to be a 56:44 mixture of isomers **2f-1** and **2f-2** respectively.

2.4.6 Synthesis of *cis* and *trans* diol model compounds

Synthesis of *cis* diol model compound of **2a**

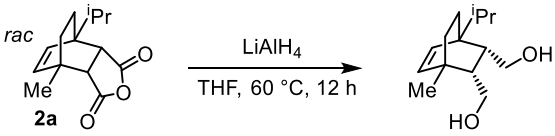

Rac-cis-endo-1-Isopropyl-4-methyl-bicyclo[2.2.2]oct-5-ene-2,3-dicarbinol was synthesized according a literature procedure:[51] 0.16 g of **2a** (0.67 mmol, 1 equiv.), 10 mL dry THF, and 0.25 g lithium aluminum hydride (6.7 mmol, 10 equiv.) were placed in a 20-mL scintillation vial equipped with a magnetic stir bar. The vial was sealed with a Teflon-lined cap and placed in an aluminum heating block preheated to 60 °C. After stirring for 12 h, the mixture was cooled to 0 °C and diluted with 20 mL diethyl ether. Excess lithium aluminum hydride was quenched by adding 0.15 mL water, then 0.15 mL 2M NaOH, and then an additional 0.60 mL water. After drying with anhydrous $MgSO_4$, the mixture was filtered through a pad of Celite and evaporated to dryness to give 0.068 g (45%) of a pale yellow viscous oil. Spectroscopic characterization was consistent with that reported in previous literature.[51]

Synthesis of t*rans* diol model compound of **2a**

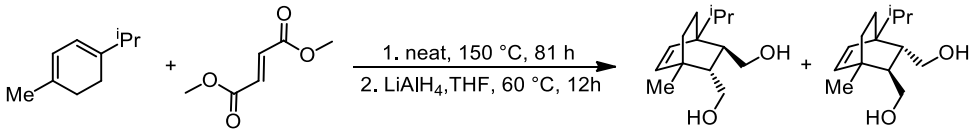

rac-trans-1-Isopropyl-4-methyl-bicyclo[2.2.2]oct-5-ene-2,3-dicarbinol (mixture of diastereomers), were synthesized according a literature procedure:[51]Technical grade *α*-terpinene (0.76 g, 5.6 mmol, 4.0 equiv.) and dimethyl fumarate (0.20 g, 1.4 mmol, 1.0 equiv.) were combined in a 25-mL Schlenk tube with a magnetic stir bar. After sealing, the tube was heated in a silicon oil bath set to 150 °C for 81 h. After cooling, the crude mixture was purified by flash column chromatography using 10% ethyl acetate/hexane as the eluent (Rf = 0.39) to give 0.32 g (82%) of a colorless oil. mixture of diastereomers, 0.15 g, 0.54 mmol, 1 equiv.). The mixture of diasteromers was reduced as described for **2a** to give 0.11 g (88%) of a pale yellow oil. The ^{1}H and ^{13}C NMR spectrum revealed that two major products were obtained in a ratio of 1.9:1.0 (*vide infra*). We were unable to chromatographically separate these two diastereo-isomers.

Synthesis of *cis* diol model compound of **2b**

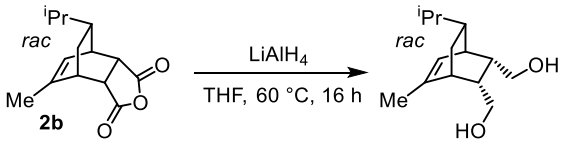

Rac-*cis*-endo-7-isopropyl-5-methylbicyclo[2.2.2]oct-5-ene-2,3-diyl)dimethanol.

Anhydride **2b** (200 mg, 0.85 mmol) and $LiAlH_4$ (324 mg, 8.54 mmol) were combined with 20 mL of dry THF in a 50-mL vial equipped with a magnetic stir bar and sealed with a Teflon-lined cap. The suspension was stirred at 60 °C for 16 h, then diluted with 20 mL of diethyl ether, cooled to 0 °C and then quenched with 0.30 mL of deionized water, 0.6 mL of 1 M NaOH, and 0.6 mL of deionized water. After drying over $MgSO_4$, the mixture was filtered through a path of Celite and the solvent was removed by rotary evaporation to yield 138 mg (72%) of a clear viscous oil.

Synthesis of *cis* diol model compound of **2c**

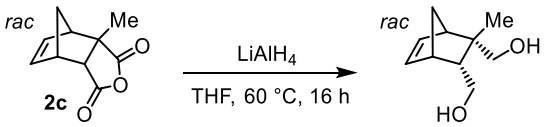

Rac-cis-endo-2-methylbicyclo[2.2.1]hept-5-ene-2,3-diyl)dimethanol. Anhydride **2c** (250 mg, 1.40 mmol) and $LiAlH_4$ (531 mg, 14 mmol) were combined with 20 mL of dry THF in a 50-mL vial equipped with a magnetic stir bar and sealed with a Teflon-lined cap. The suspension was stirred at 60 °C for 16 h, then diluted with 20 mL of diethyl ether, cooled to 0 °C and then quenched with 0.30 mL of deionized water, 0.6 mL of 1 M NaOH, and 0.6 mL of deionized water. After drying over $MgSO_4$, the mixture was filtered through a pad of Celite and the solvent was removed by rotary evaporation to yield 158 mg (67%) of a clear viscous oil.

Synthesis of *trans* diol model compound of **2c**

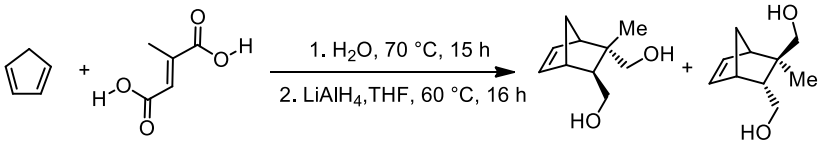

Rac-trans -2-methylbicyclo[2.2.1]hept-5-ene-2,3-diyl)dimethanol: Mesaconic acid (1 g, 7.63 mmol) was disolved in 25 mL of water in a round bottom flask with a magnetic stir bar and a reflux condenser. Under stirring, freshly distilled cyclopentadiene (600 mg, 10.08 mmol) was added dropwise. Afterwards the mixture was refluxed at 70 °C for 15 h. The reaction mixture was extracted with ethyl acetate (3x15 mL) and the organic and aqueous layers separated. The organic layers were combined, dried over anhydrous $MgSO_4$ and the solvent was removed by rotary evaporation to yield a yellow viscous oil. A portion of the crude product (500 mg, 2.54 mmol) was dissolved in dry THF without further purification and placed in a 50 mL vial equipped with a magnetic stir bar. $LiAlH_4$ (967 mg, 25 mmol) was added and the vial was sealed with a Teflon-lined cap. The suspension was stirred at 60 °C for 16 h, then diluted with 20 mL of diethyl ether, cooled to 0 °C and then quenched with 0.30 mL of deionized water, 0.6 mL of 1M NaOH, and 0.6 mL of deionized water. After drying over $MgSO_4$, the mixture was filtered through a path of Celite and the solvent was removed by rotary evaporation. The product was purified by column chromatography (silica gel, 60:40 hexanes:ethyl acetate) and then dried under vacuum to yield 346 mg (58%) of a clear viscous oil.

Synthesis of *cis* diol model compound of **2d**

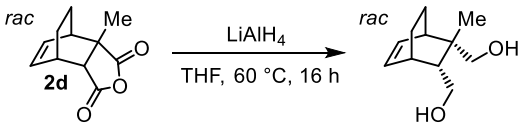

rac-2-methylbicyclo[2.2.2]oct-5-ene-2,3-diyl)dimethanol: Anhydride **2d** (63 mg, 0.33 mmol) and $LiAlH_4$ (125 mg, 3.30 mmol) were combined with 10 mL dry THF in a 20-mL vial equipped with a magnetic stir bar and sealed with a Teflon-lined cap. The suspension was stirred at 60 °C for 16 h then diluted with 20 mL diethyl ether, cooled to 0 °C, then quenched with 0.15 mL deionized water, 0.3 mL (1 M) NaOH, and 0.3 mL deionized water. After drying with $MgSO_4$, the mixture was filtered through a path of Celite and the solvent removed by rotary evaporation to yield 39 mg (65%) of a clear viscous oil.

Synthesis of *cis* diol model compound of **2e**

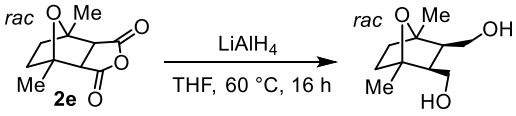

Rac-cis-endo-1,4-dimethyl-7-oxabicyclo[2.2.1]heptane-2,3-diyl)dimethanol. Anhydride **2e** (196 mg, 1 mmol) and $LiAlH_4$ (379 mg, 10 mmol) were combined with 20 mL of dry THF in a 50-mL vial equipped with a magnetic stir bar and sealed with a Teflon-lined cap. The suspension was stirred at 60 °C for 16 h, then diluted with 20 mL of diethyl ether, cooled to 0 °C and then quenched with 0.30 mL of deionized water, 0.6 mL of 1 M NaOH, and 0.6 mL of deionized water. After drying over $MgSO_4$, the mixture was filtered through a path of Celite and the solvent was removed by rotary evaporation to yield 117 mg (63%) of a clear viscous oil.

Synthesis of *trans* diol model compound of **2e**

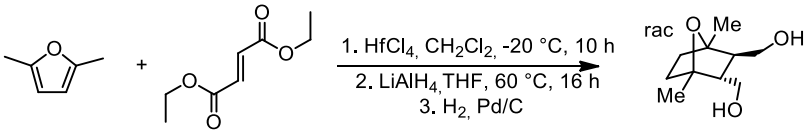

Rac-trans-1,4-dimethyl-7-oxabicyclo[2.2.1]heptane-2,3-diyl)dimethanol was synthesized according a literature procedure[76] and following for a hydrogenation using Pd/C. Diethylfumarate (220 mg, 1.28 mmol) and freshly distilled dimethylfuran (2.46 g, 25.6 mmol) were added successively at −20 °C to a suspension of $HFCl_4$ (450 mg, 1.408 mmol) in CH_2Cl_2 (1 mL) and stirred for 10 h at −20 ºC. Then, the reaction mixture was allowed to reach room

temperature and aqueous $NaHCO_3$ (10 mL) was added. After filtration of the insoluble materials, the crude was extracted with $CHCl_3$ (3 × 15 mL) and the combined organic layers were dried over anhydrous $MgSO_4$, filtered and concentrated under high vacuum to obtain a yellow oil. A portion of the crude product (166 mg, 0.61 mmol) was dissolved in dry THF without further purification and placed in a 50 mL vial equipped with a magnetic stir bar. $LiAlH_4$ (234 mg, 6.1 mmol) was added and the vial was sealed with a Teflon-lined cap. The suspension was stirred at 60 °C for 16 h, then diluted with 20 mL of diethyl ether, cooled to 0 °C and then quenched with 0.30 mL of deionized water, 0.6 mL of 1 M NaOH, and 0.6 mL of deionized water. After drying over $MgSO_4$, the mixture was filtered through a path of Celite and the solvent was removed by rotary evaporation to obtain a yellow oil. Without further purification, a portion of this oil (75 mg , 0.40 mmol) was dissolved in 15 mL of THF in a Parr reactor and palladium on carbon (5%, reduced, dry powder, 2.0 g) was added. The reactor was pressurized with hydrogen gas to 20 bar and the heterogeneous mixture was stirred at 22 °C for 24 h. The mixture was filtered,stripped and the residue was purified by column chromatography (silica gel, 60:40 hexanes:ethyl acetate) and dried under vacuum to yield 71 mg (28%) of a clear viscous oil.

Synthesis of *cis* diol model compound of **2f**

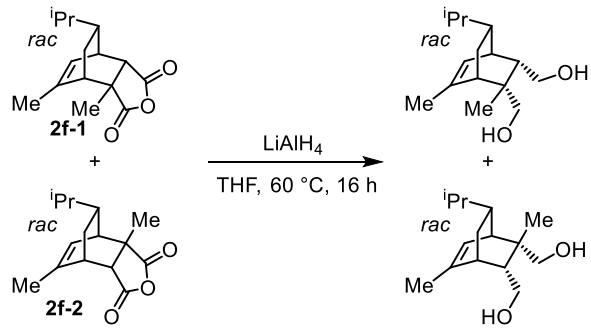

2f*: mixture of isomers*

Mixture of *rac*-7-isopropyl-2,5-dimethylbicyclo[2.2.2]oct-5-ene-2,3-diyl)dimethanol and *rac*-8-isopropyl-2,6-dimethylbicyclo[2.2.2]oct-5-ene-2,3-diyl)dimethanol: Mixture of anhydrides **2f** (82 mg, 0.33 mmol) and $LiAlH_4$ (125 mg, 3.30 mmol) were combined with 10 mL dry THF in a 20-mL vial equipped with a magnetic stir bar and sealed with a Teflon-lined cap. The suspension was stirred at 60 °C for 16 h then diluted with 20 mL diethyl ether, cooled to 0 °C then quenched with 0.15 mL deionized water, 0.3 mL (1 M) NaOH, and 0.3 mL deionized water. After drying with $MgSO_4$, the mixture was filtered through a path of Celite and the solvent removed by rotary evaporation to yield 61 mg (77%) of a clear viscous oil.

2.4.7 ^{1}H and ^{13}C NMR spectra for complexes (salph-Cl)AlCl

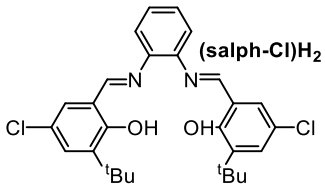

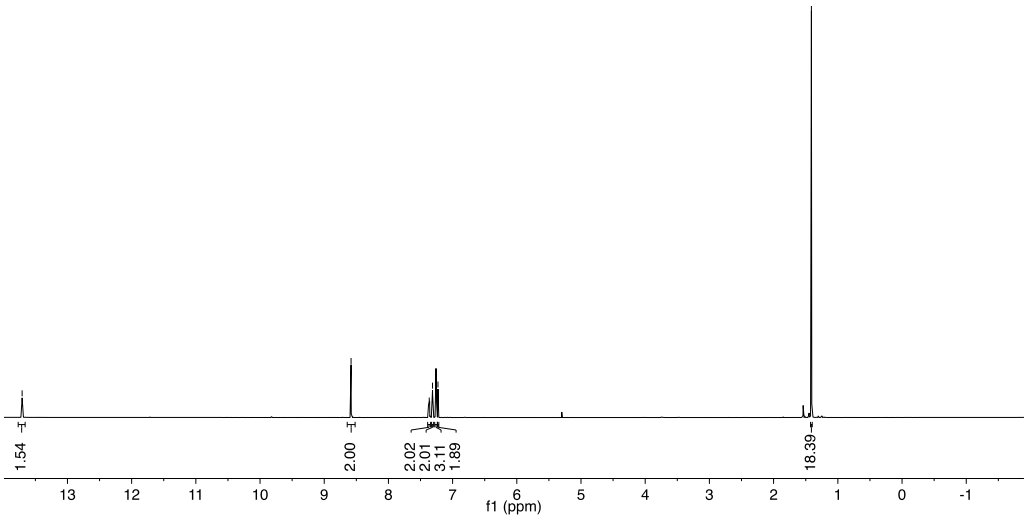

^{1}H NMR (600 MHz, $CDCl_3$): δ 13.70 (s, 2H), 8.58 (s, 2H), 7.34–7.38 (m, 2H), 7.32 (d, 2 H), 7.24–7.27 (m, 2H), 7.23 (d, 2H), 1.41 (s, 18 H).

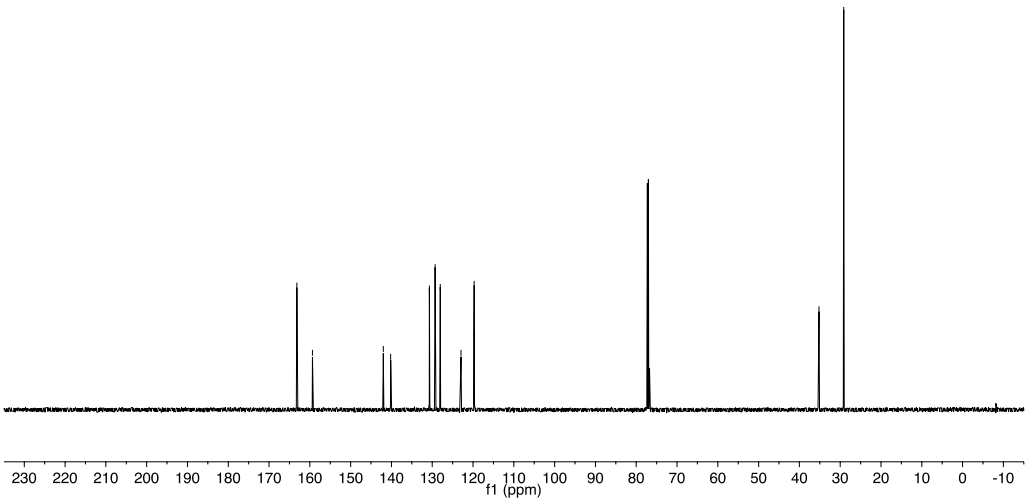

^{13}C NMR (125 MHz, $CDCl_3$): δ 163.38, 159.56, 142.20, 140.40, 130.91, 129.50, 128.23, 123.17, 119.89–119.95, 35.41, 29.33.

HRMS (DART-MS): *m/z* calculated for ($M-H^+$) 497.17571; found 497.17513.

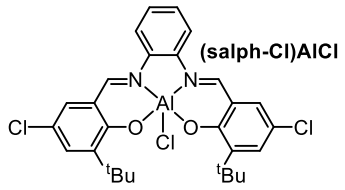

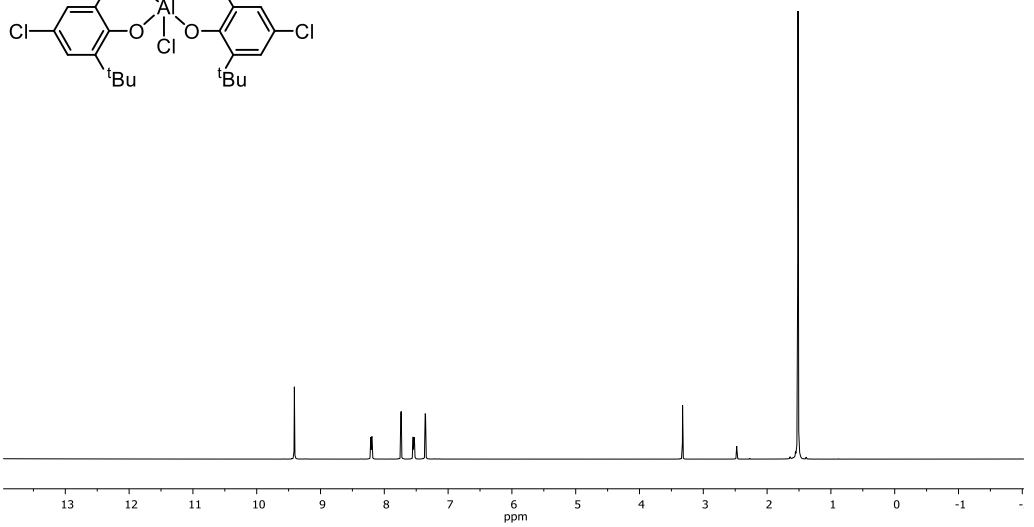

^{1}H NMR (600 MHz, DMSO-d6): δ 9.41 (s, 2H), 8.24-8.17 (m, 2H), 7.74 (d, *J* = 2.59 Hz, 2H), 7.58-7.52 (m, 2H), 7.36 (d, *J* = 2.59 Hz, 2H), 1.52 (s, 18H).

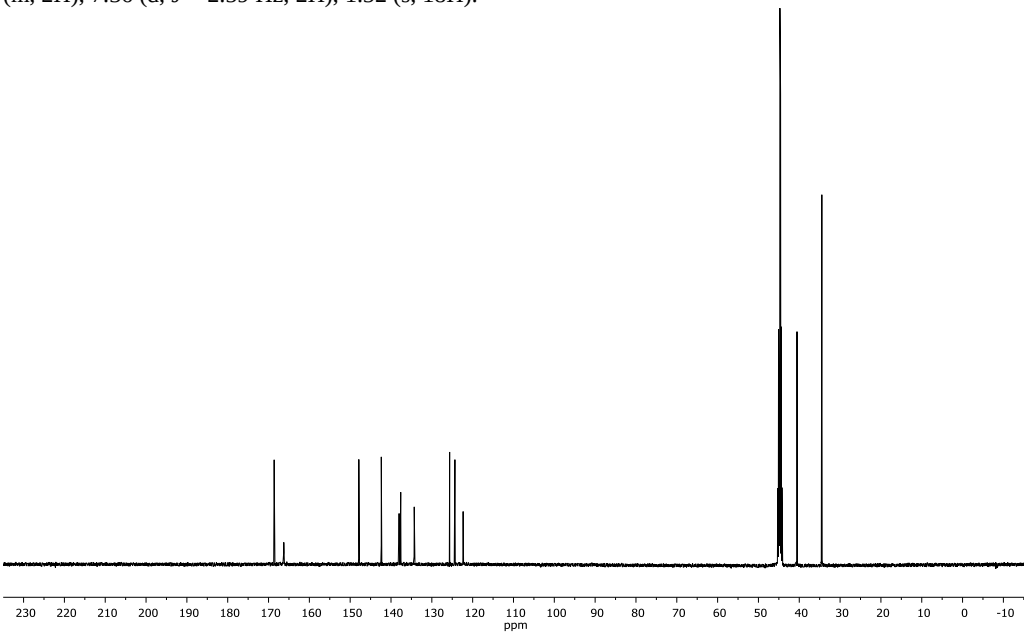

^{13}C NMR (125 MHz, DMSO-d6): δ 163.40, 161.01, 142.66, 137.16, 132.80, 132.39, 129.09, 120.41, 119.13, 117.11, 35.33, 29.25

HRMS (DART-MS): *m/z* calculated for $C_{28}H_{30}N_2O_3AlCl_2$ ($M-Cl^-+H_2O$) 539.14434; found 539.14680.

2.4.8 ^{1}H and ^{13}C NMR spectra for cyclic anhydrides

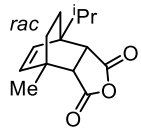

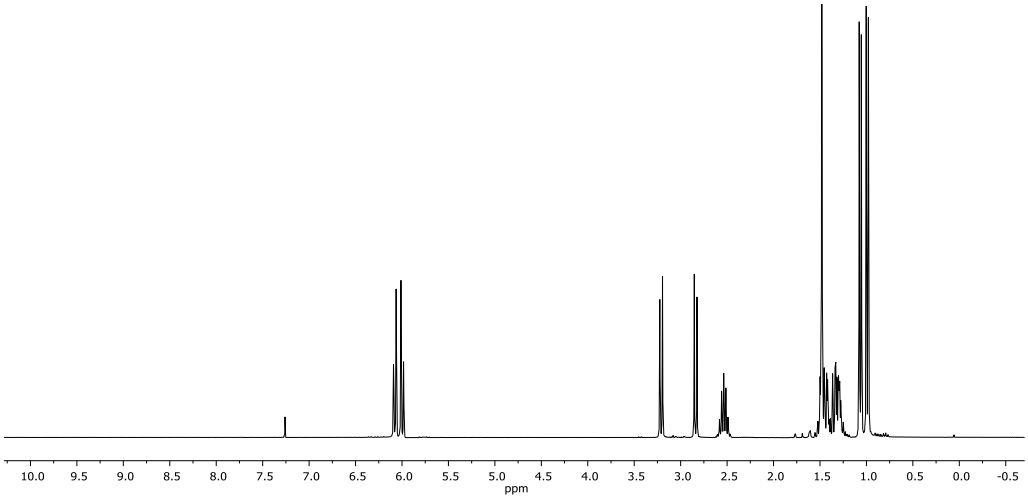

^{1}H NMR (500 MHz, $CDCl_3$): δ 6.10 (d, 1H), 6.03 (d, 1H), 3.23 (d, 1H), 2.86 (d, 1H), 2.57 (sept, 1H), 1.41–1.55 (m, 5H), 1.28–1.40 (m, 2H), 1.09 (d, 3H), 1.02 (d, 3H).

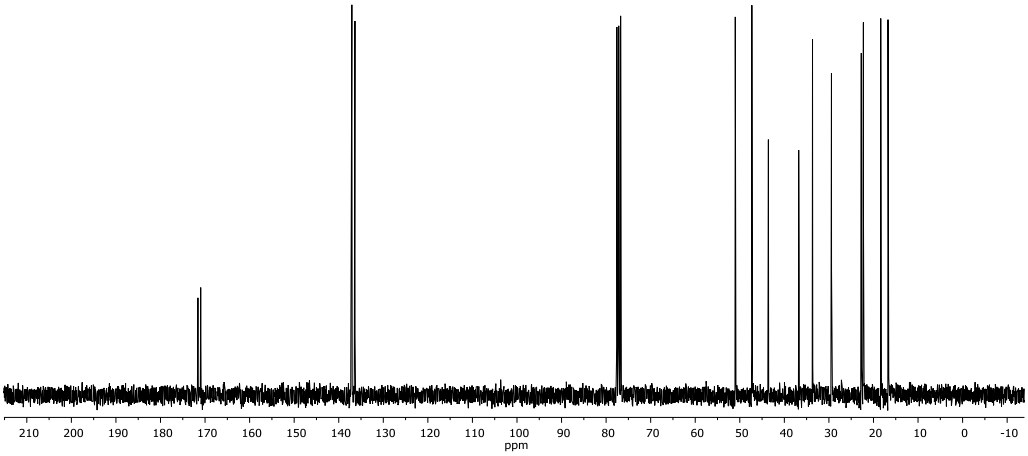

^{13}C NMR (75 MHz, $CDCl_3$) δ 171.60, 170.98, 137.05, 136.36, 51.02, 47.29, 43.58, 36.78, 33.68, 29.43, 22.74, 22.27, 18.37, 16.74.

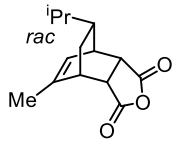

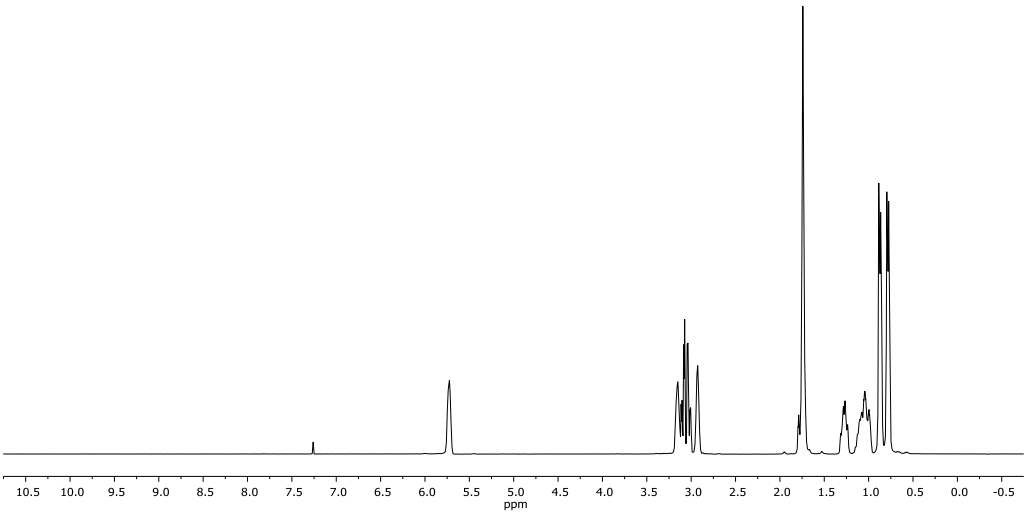

^{1}H NMR (500 MHz, $CDCl_3$): δ 5.76 (s, 1H), 3.18–3.22 (m, 1H), 3.08–3.12 (m, 1H), 3.02–3.07 (m, 1H), 2.95–2.99 (m, 1H), 1.74–1.81 (m, 4H), 1.25-1.32 (m, 1H), 1.02–1.16 (m, 2H), 0.90 (d, 3H), 0.81 (d, 3H).

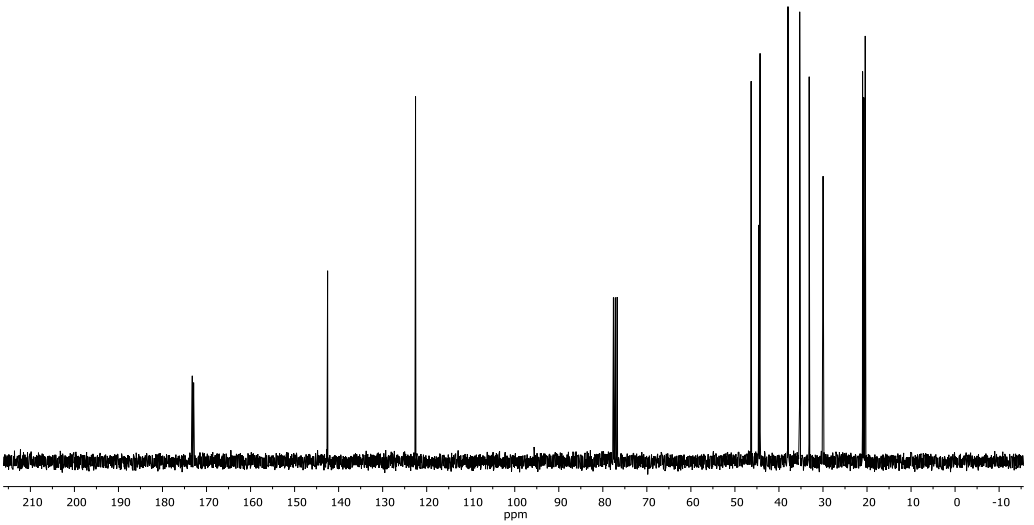

^{13}C NMR (75 MHz, $CDCl_3$) δ 173.22, 172.93, 142.50, 122.54, 46.32, 44.56, 44.29, 37.94, 35.29, 33.13, 29.98, 21.00, 20.75, 20.40.

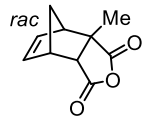

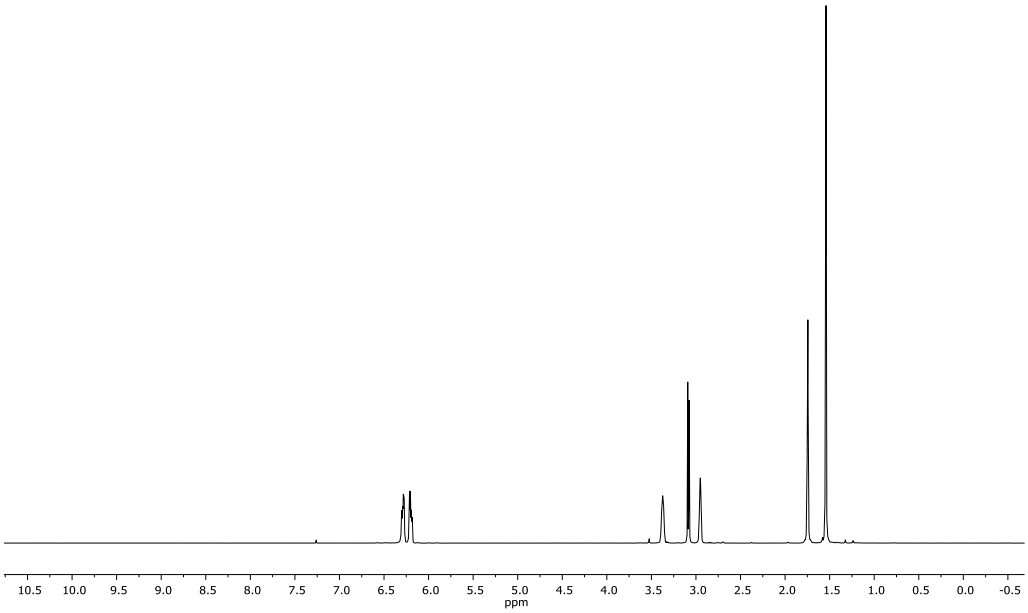

^{1}H NMR (400 MHz, $CDCl_3$): δ = 6.39 (dd, 1H), 6.29 (dd, 1H), 3.47–3.44 (m, 1H), 3.13 (d, 1H), 3.04–3.03 (m, 1H), 1.84 (dt, 1H), 1.80 (dt, 1H), 1.62 (s, 3H).

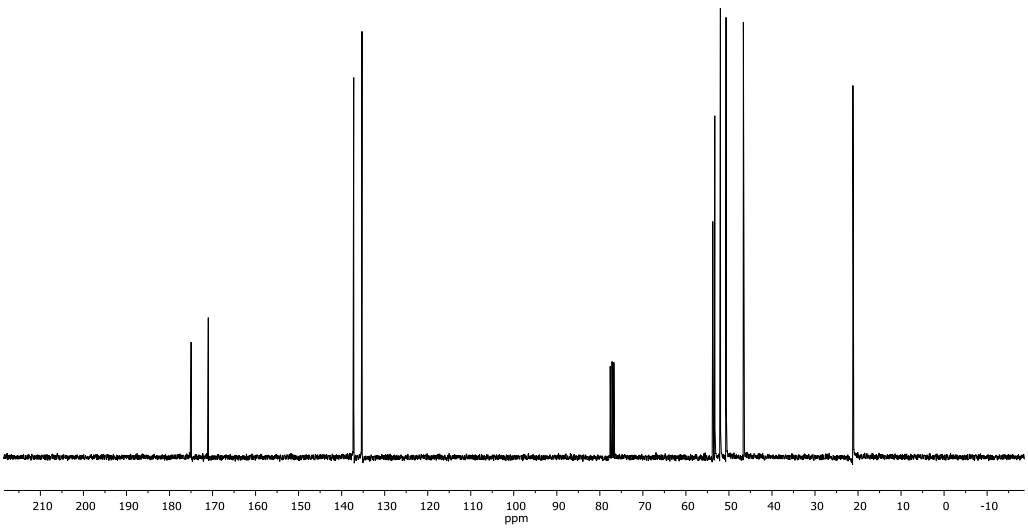

13C NMR (75 MHz, $CDCl_3$) δ 174.98, 170.99, 137.19, 135.27, 53.75, 53.29, 51.99, 50.66, 46.65, 21.19.

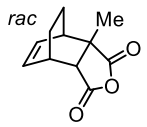

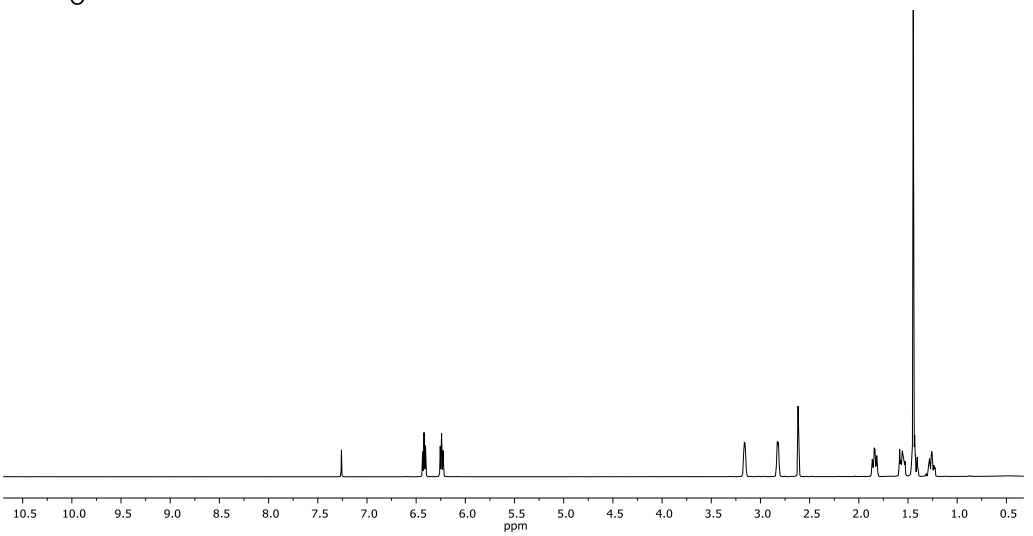

^{1}H NMR (500 MHz, $CDCl_3$): δ 6.42 (t, *J* = 7.3 Hz, 1H), 6.24 (t, *J* = 7.3 Hz, 1H), 3.16 (s,1H), 2.83 (s, 1H), 2.62 (d, *J* = 3.2 Hz, 1H), 1.84 (m, 1H), 1.55 (m, 1H), 1.45 (m, 1H), 1.26 (m, 1H).

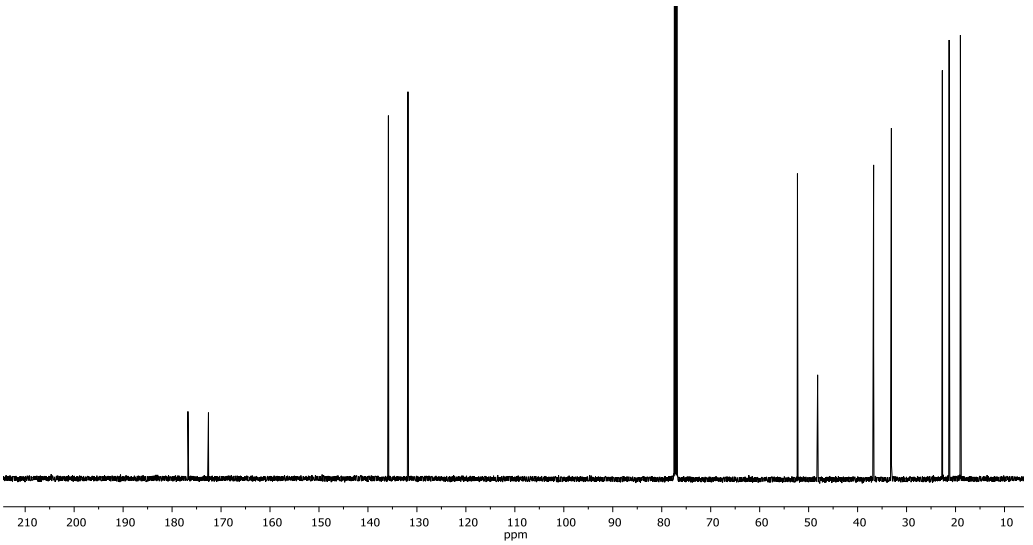

^{13}C NMR (125MHz, $CDCl_3$): δ 176.76, 172.57, 135.82, 131.83, 52.29, 48.16, 36.73, 33.10, 22.70, 21.31, 19.01.

HRMS (DART-MS): *m/z* calculated for $C_{11}H_{13}O_3$ (M+H) 193.0865; found 193.0850.

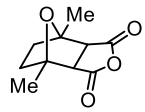

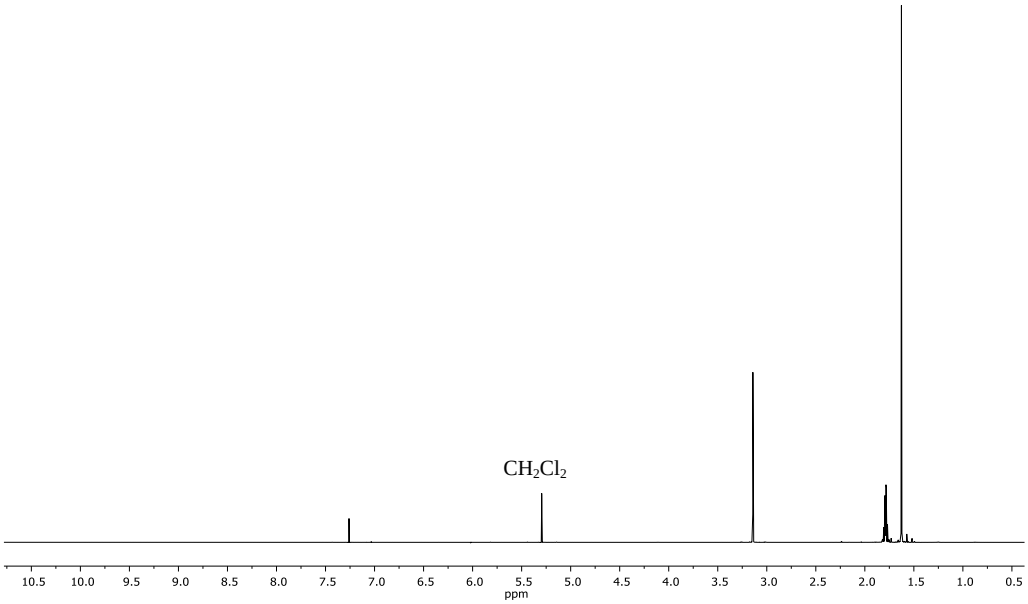

^{1}H NMR (500 MHz, $CDCl_3$): δ 3.14 (s, 2 H), 1.78 (m, 4 H), 1.63 (s, 6H).

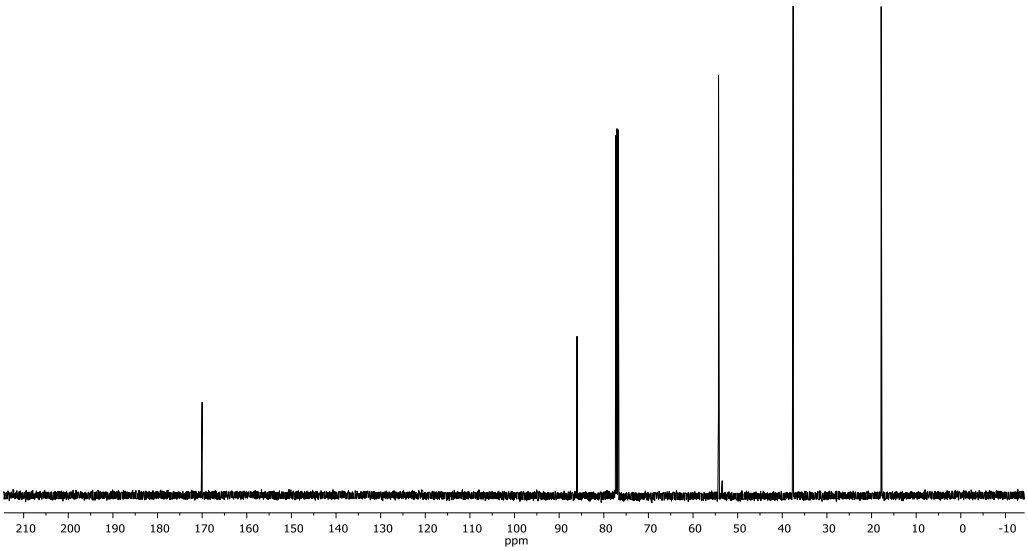

^{13}C NMR (125 MHz, $CDCl_3$): δ 170.13, 86.12, 54.41, 37.69, 17.96.

HRMS (DART-MS): *m/z* calculated for $C_{10}H_{13}O_4$ (M+H) 197.0808; found 197.0808.

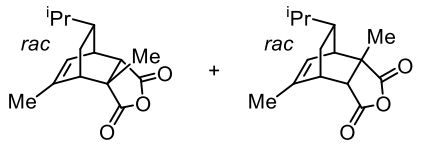

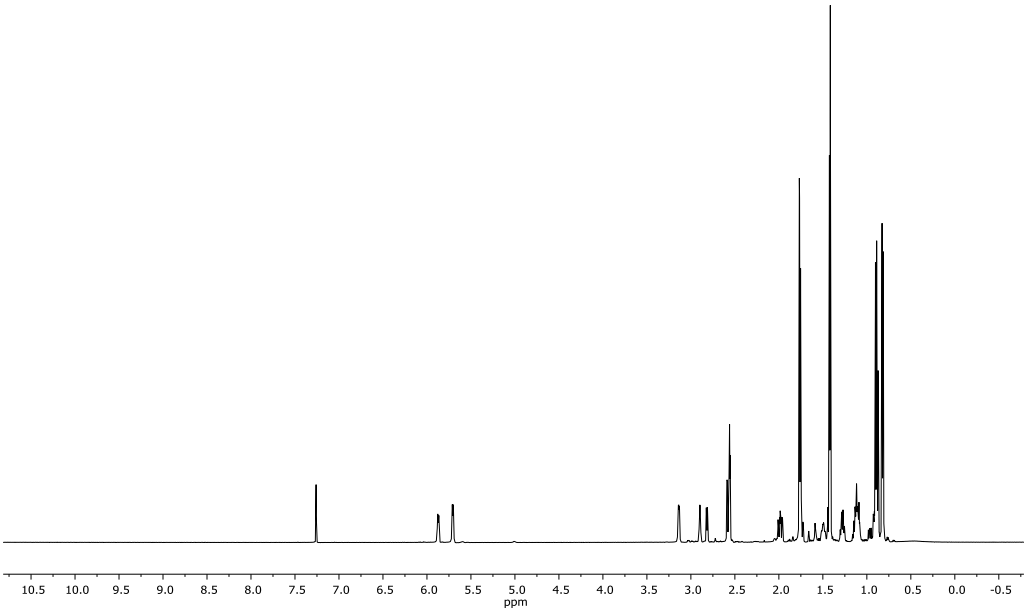

^{1}H NMR (600 MHz, $CDCl_3$): δ 5.88 (d, *J* = 6.39, 1H), 5.70 (d, *J* = 6.39 Hz, 1H), 3.13 (m, 1H), 2.90 (s, 1H), 2.81 (dd, *J* = 2.01, 6.31 Hz, 1H) 2.56 (m, 4H), 1.99 (m, 2H), 1.77 (m, 9H), 1.49 (m, 1H), 1.43 (m, 8H), 1.27 (m, 2H), 1.12 (m, 4H), 0.90 (m, 10H), 0.83 (m, 8H).

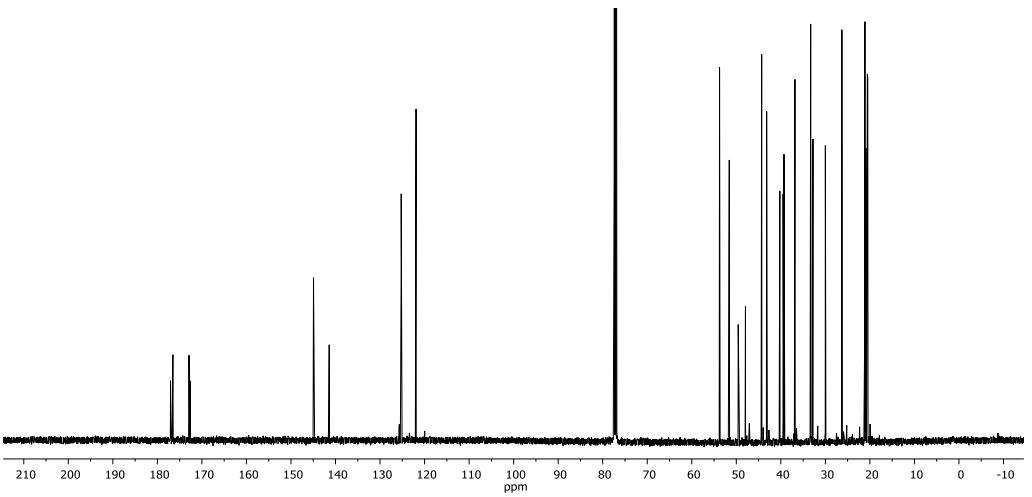

^{13}C NMR (125 MHz, $CDCl_3$): δ 177.05, 176.52, 172.90, 172.60, 144.94, 141.41, 125.25, 121.91, 53.76, 51.58, 49.57, 47.94, 44.30, 43.18, 40.22, 39.49, 39.29, 36.83, 33.30, 32.78, 30.00, 26.29, 21.17, 21.12, 21.10, 20.92, 20.70, 20.68, 20.57, 20.48**.**

HRMS (DART-MS): *m/z* calculated for $C_{15}H_{21}O_3$ (M+H) 249.1485; found 249.1481.

2.4.9 ^{1}H and ^{13}C NMR spectra for *cis* and *trans* diol model compounds

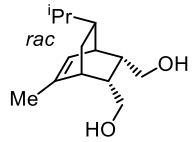

^{1}H NMR (400 MHz, $CDCl_3$): δ 5.59 (d, *J* = 6.67 Hz, 1H), 3.64 (m, 2H), 3.55 (m, 2H), 2.43 (m, 1H) 2.20 (m, 2H), 2.10 (m, 2H), 1.72 (m, 4H), 1.25 (m, 3H), 1.04 (m, 1H), 0.86 (m, 5 H), 0.77 (m, 3H).

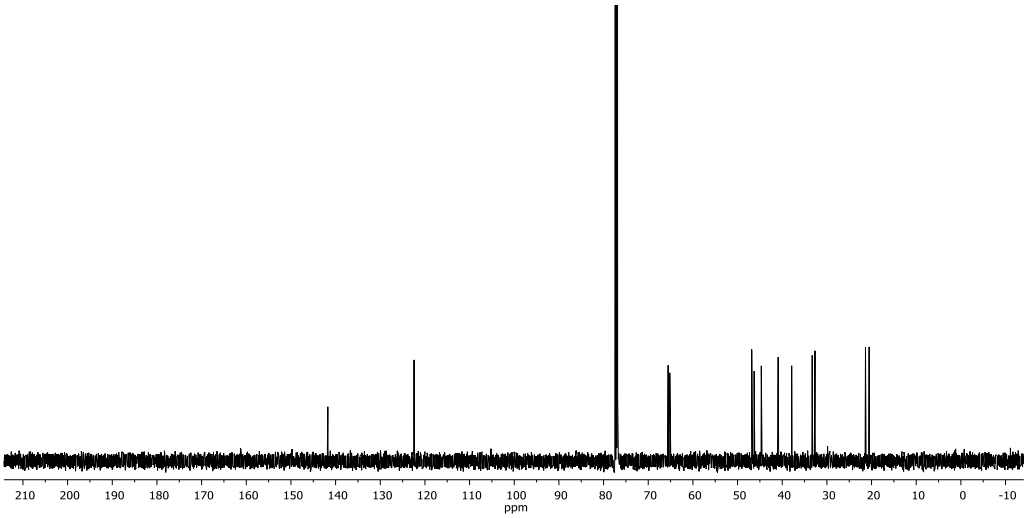

^{13}C NMR (125MHz, $CDCl_3$): δ 141.73, 122.43, 65.54, 65.17, 46.83, 46.29, 44.69, 40.91, 37.88, 33.29, 32.67, 21.43, 21.36, 20.54.

HRMS (DART-MS): *m/z* calculated for $C_{14}H_{25}O_2$ (M+H): 225.1855; found 225.1841.

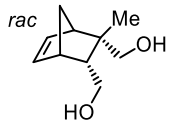

^{1}H NMR (400 MHz, $CDCl_3$): δ 6.06 (m, 1H), 5.97 (m, 1H), 4.67 (br s, 2H), 3.46 (m, 2H), 3.24 (m, 2H), 2.64 (s, 1H), 2.28 (s, 1H), 2.00 (m, 1H), 1.66 (d, J = 8.19 Hz, 1H), 1.32 (d, J = 8.19 Hz, 1H), 1.25 (s, 3H).

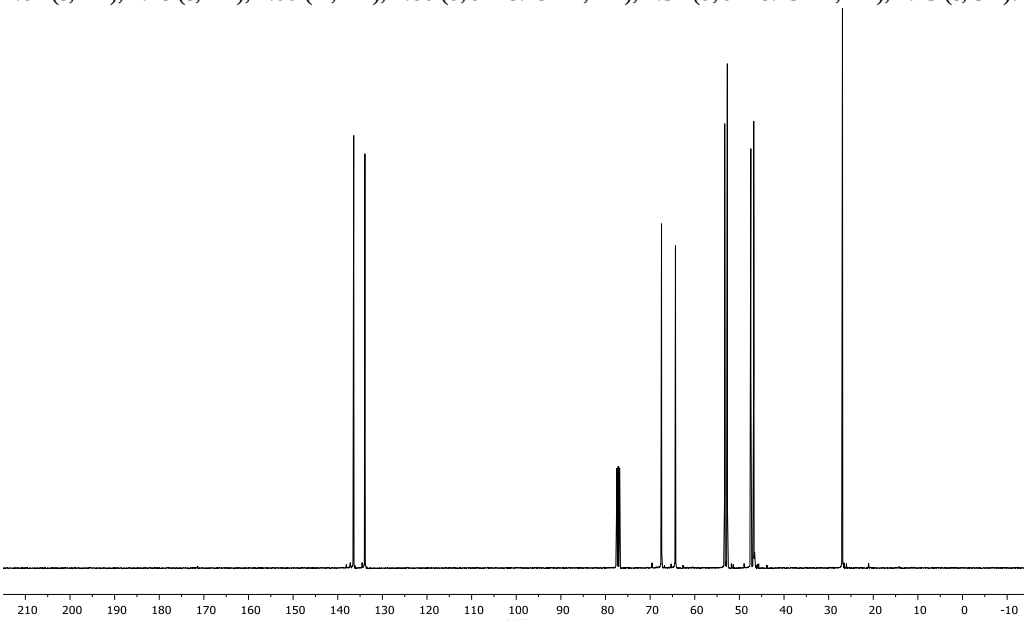

^{13}C NMR (125MHz, $CDCl_3$): δ 136.42, 133.91, 67.45, 64.33, 53.29, 52.70, 47.44, 46.78, 46.62, 29.90.

HRMS (DART-MS): *m/z* calculated for $C_{10}H_{17}O_2$ (M+H): 169.1229; found 169.1218.

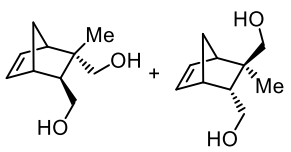

^{1}H NMR (400 MHz, $CDCl_3$): δ 6.04 (d, 2H), 5.93 (d, 2H), 4.22 (br s, 4H), 3.45 (t, *J* = 8.74 Hz, 1H), 3.35 (m, 3H), 3.12 (m, 3H), 2.98 (d, *J* = 10.26 Hz, 1H) 2.69 (s, 1H), 2.49 (s, 1H), 2.33 (s, 1H), 2.27 (s,1H), 1.78 (s, 1H), 1.52 (d, *J* = 8.57 Hz, 1H), 1.43 (d, *J* = 8.57 Hz, 1H), 1.23 (t, *J* = 7.99 Hz, 2H), 1.06 (t, *J* = 8.20 Hz, 1H), 1.01 (s, 3H), 0.69 (s, 3H).

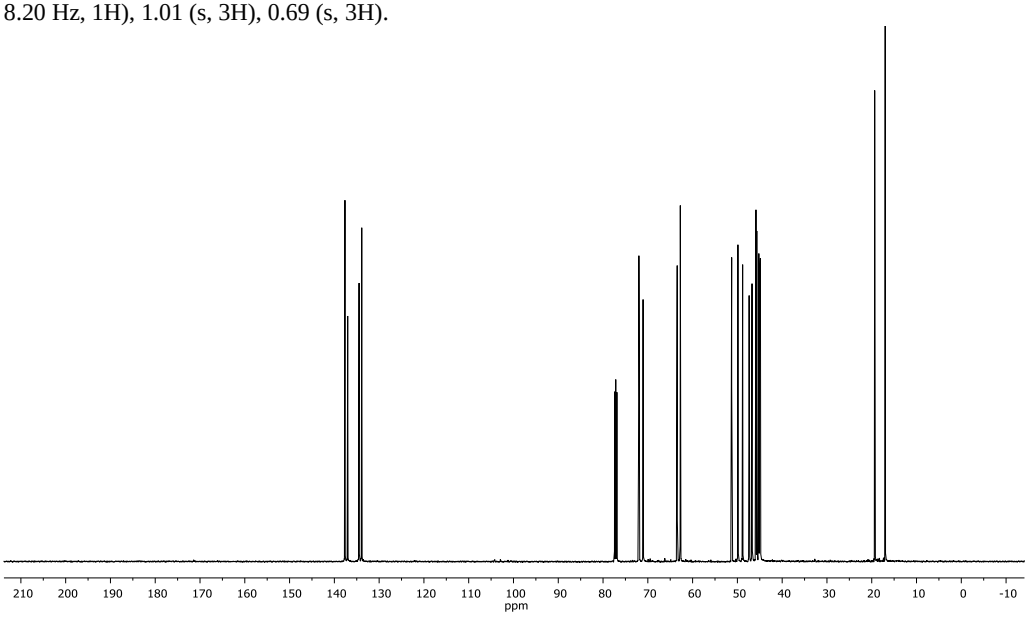

^{13}C NMR (125MHz, $CDCl_3$): δ 137.63, 137.02, 134.48, 133.88, 72.00, 71.06, 63.44, 62.75, 51.27, 49.88, 48.83, 47.38, 46.73, 45.85, 45.66, 45.21, 45.04, 44.86, 19.34, 17.00.

HRMS (DART-MS): *m/z* calculated for $C_{10}H_{17}O_2$ (M+H): 169.1229; found 169.1218.

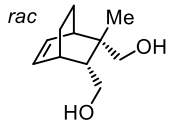

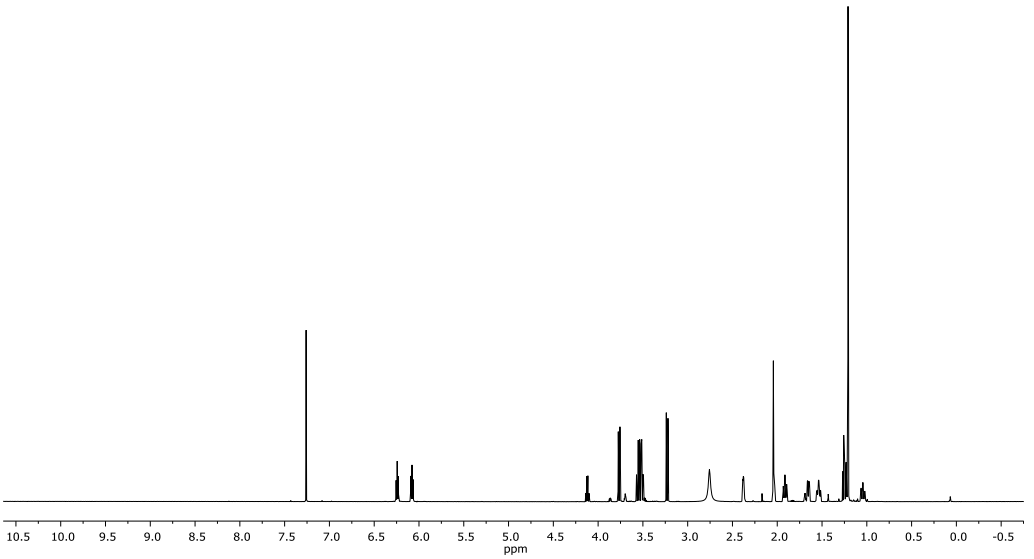

^{1}H NMR (500 MHz, $CDCl_3$): δ 6.24 (t, *J* = 7.3 Hz, 1H), 6.08 (t, *J* = 7.3 Hz, 1H), 3.77 (d, *J* = 12.0 Hz, 1H), 3.54 (m, 2H), 3.24 (d, *J* = 12.0 Hz, 1H), 2.76 (br s, 1H), 2.38 (s, 1H), 1.91 (m,1H), 1.65 (ddd, *J* = 1.5, 4.2, 10.2 Hz, 1H), 1.54 (m, 1H), 1.25 (m, 1H), 1.21 (s, 3H), 1.04 (m,1H).

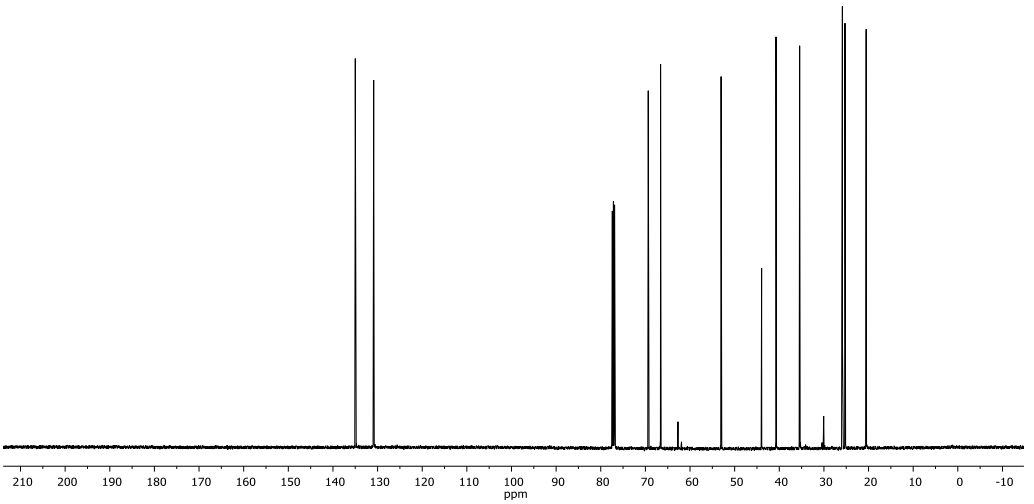

^{13}C NMR (125MHz, $CDCl_3$): δ 135.00, 130.87, 69.36, 66.59, 53.04, 43.96, 40.73, 35.44, 25.86, 25.28, 20.54**.**

HRMS (DART-MS): *m/z* calculated for $C_{11}H_{19}O_2$ (M+H): 183.1380; found 183.1379.

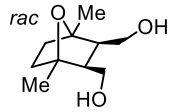

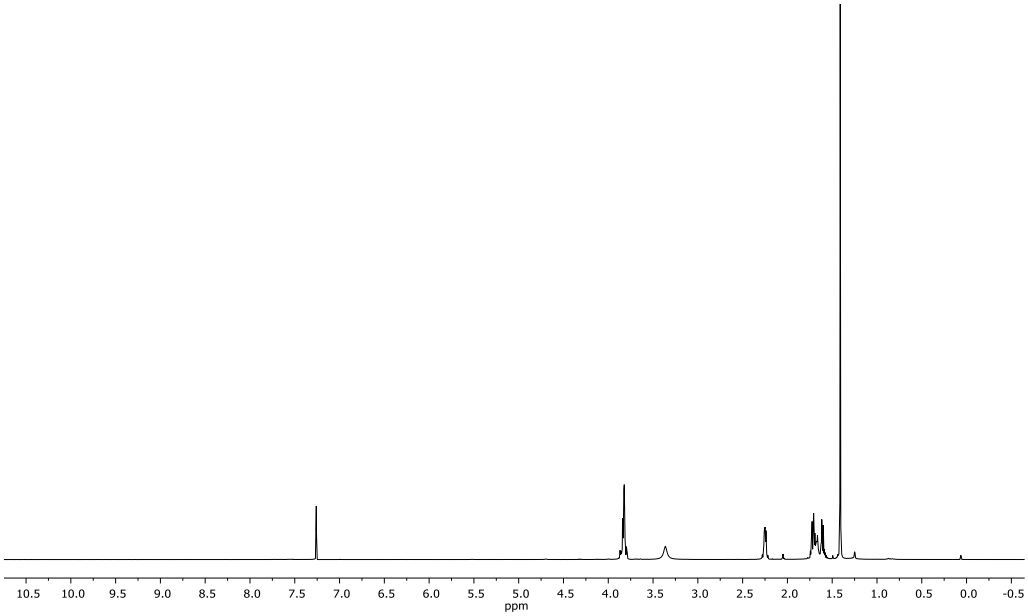

^{1}H NMR (400 MHz, $CDCl_3$): δ 3.82 (m, 4H), 3.39 (br s, 2H), 2.25 (m, 2H), 1.66 (m, 6H), 1.41 (s, 6H).

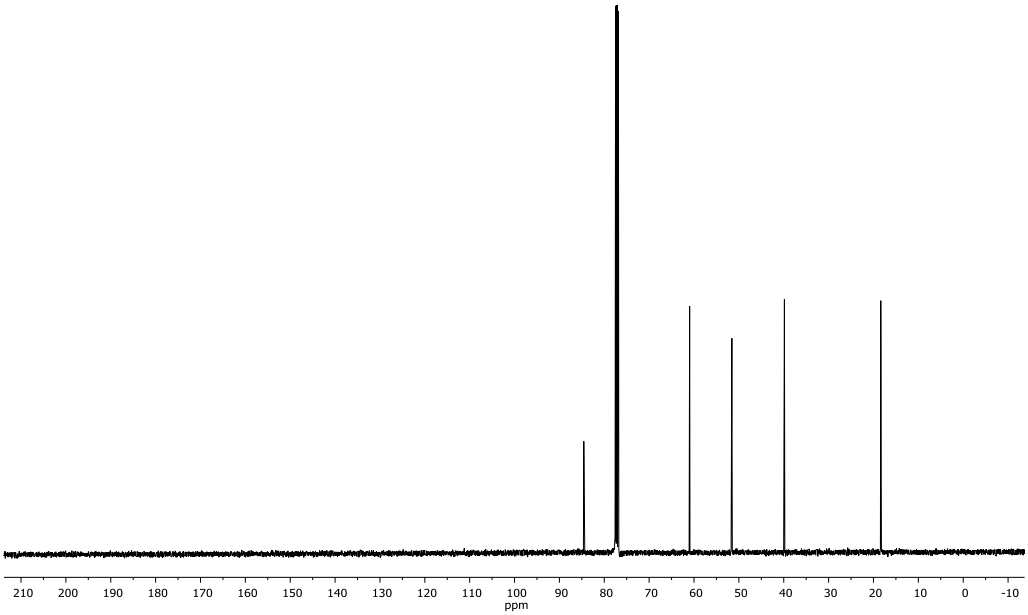

^{13}C NMR (125MHz, $CDCl_3$): δ 84.56, 60.97, 51.56, 39.85, 18.37.

HRMS (DART-MS): *m/z* calculated for $C_{10}H_{19}O_3$ (M+H): 187.1334; found 187.1323.

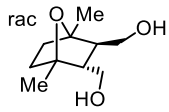

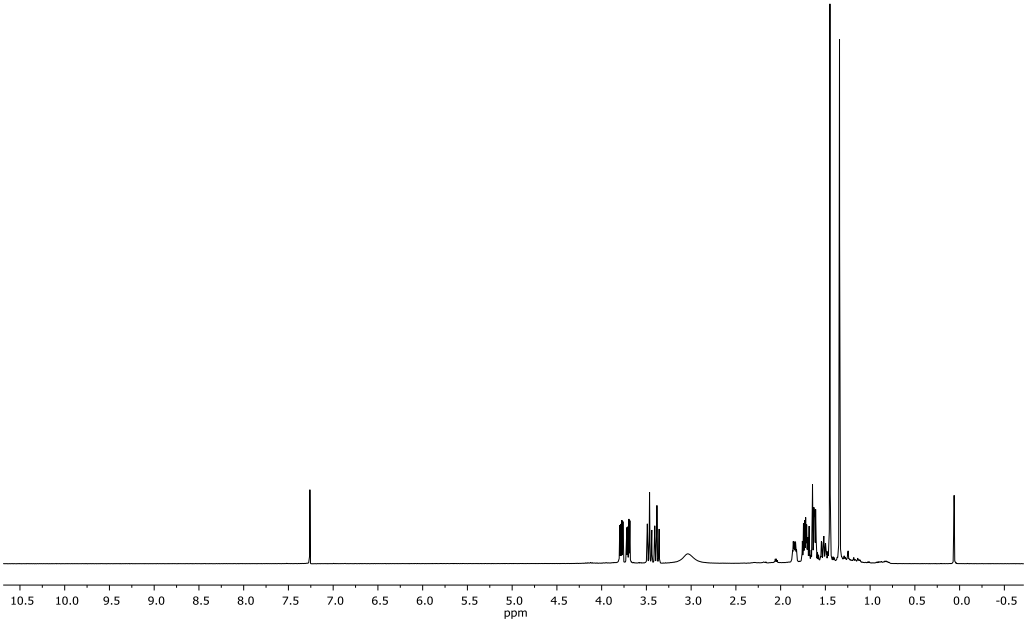

^{1}H NMR (400 MHz, $CDCl_3$): δ 3.77 (dd, *J* = 4.60, 9.39 Hz, 1H) 3.70 (dd, *J* = 4.60, 9.39 Hz, 1H) , 3.04 (br s, 2H), 1.85 (m, 1H), 1.72 (m, 2H), 1.63 (m, 3H), 1.52 (m, 3H), 1.45 (s, 3H), 1.34 (s, 3H).

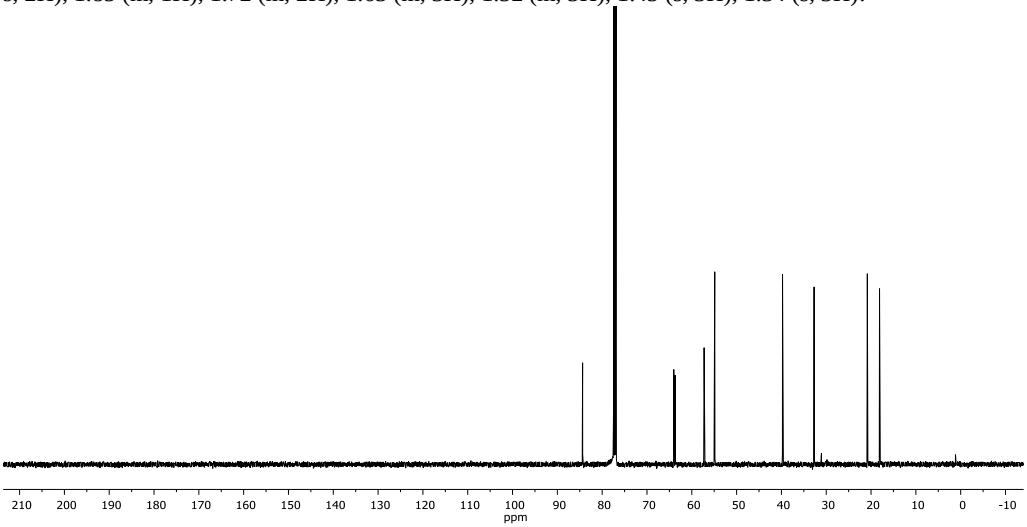

^{13}C NMR (125MHz, $CDCl_3$): δ 84.51, 84.36, 64.02, 63.68, 57.25, 54.88, 39.75, 32.70, 20.83, 18.11.

HRMS (DART-MS): *m/z* calculated for $C_{10}H_{19}O_3$ (M+H): 187.1334; found 187.1324.

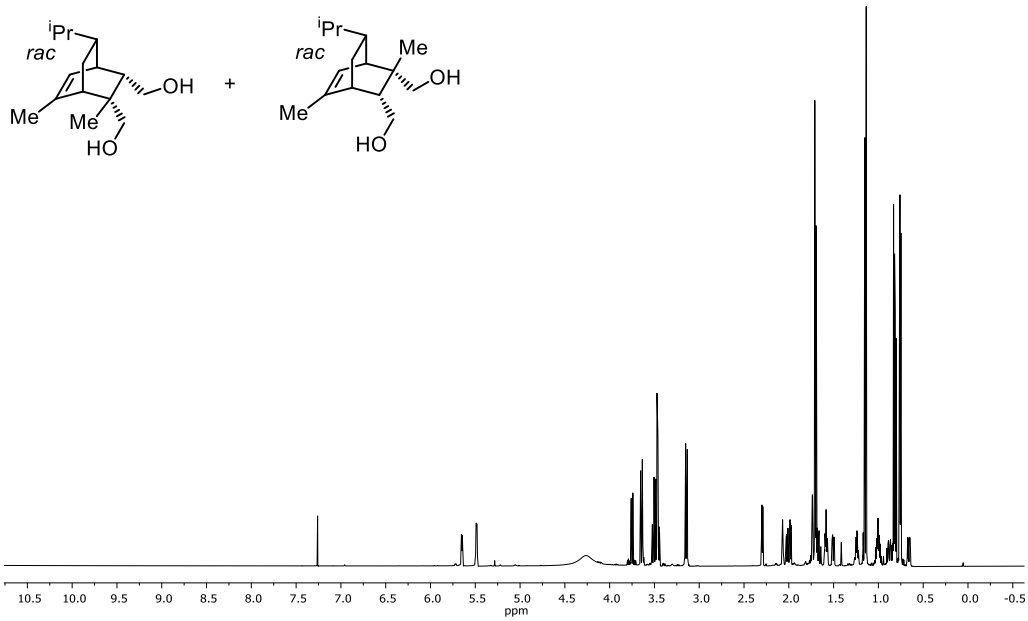

^{1}H NMR (500 MHz, $CDCl_3$): δ, 5.65 (d, *J* = 6.95 Hz, 1H), 5.49 (d, *J* = 6.95 Hz, 1H), 4.27 (br s, 4H), 3.76 (m, 1H), 3.65(m, 2H), 3.47 (m, 5H), 3.15 (dd, *J* = 4.1, 11.05 Hz, 3H), 2.30 (m, 1H), 2.07 (s, 1H), 2.01 (m, 1H), 1.71 (m, 11H), 1.58 (m, 2H), 1.51 (m, 1H), 1.24 (m, 2H), 1.15 (m, 8H), 1.00(m, 3H), 0.92–0.79 (m, 10H), 0.76 (dd, *J* = 2.84, 6.65 Hz, 8H), 0.66 (m, 1H).

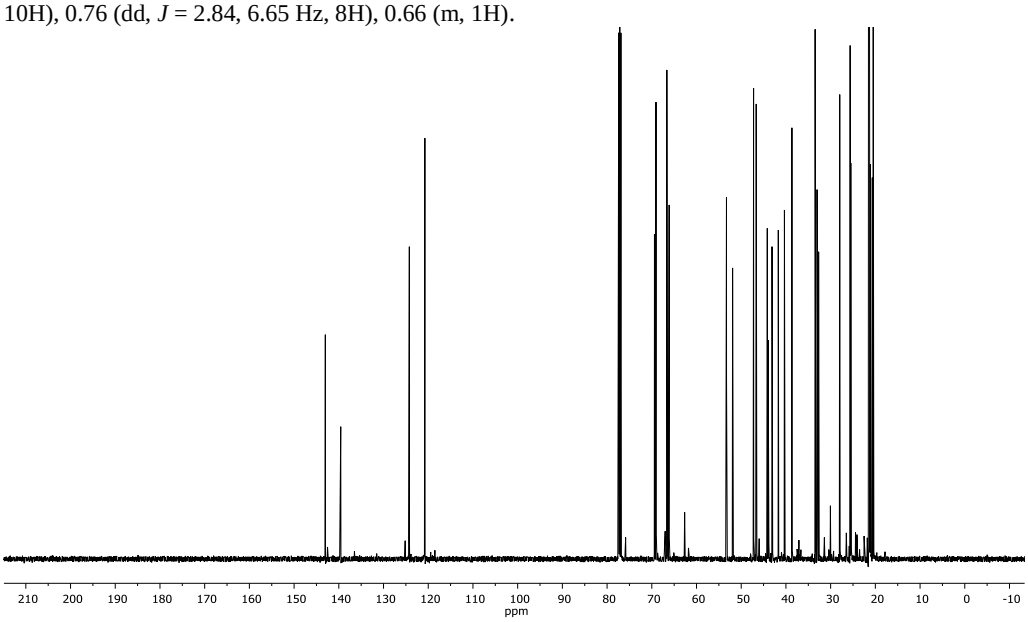

^{13}C NMR (125MHz, $CDCl_3$): δ 143.01, 139.57, 124.23, 120.75, 69.40, 69.06, 66.63, 66.12, 53.30, 51.93, 47.23, 46.65, 44.17, 43.97, 43.11, 41.71, 40.34, 38.66, 33.47, 33.04, 32.68, 27.96, 25.64, 25.49, 21.54, 21.40, 21.30, 21.09, 20.69, 20.48.

HRMS (DART-MS): *m/z* calculated for $C_{15}H_{27}O_2$ (M+H): 239.2006; found: 239.2005.

2.4.10 Assigned ^{1}H and ^{13}C NMR spectra of polymers

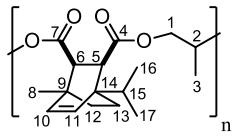

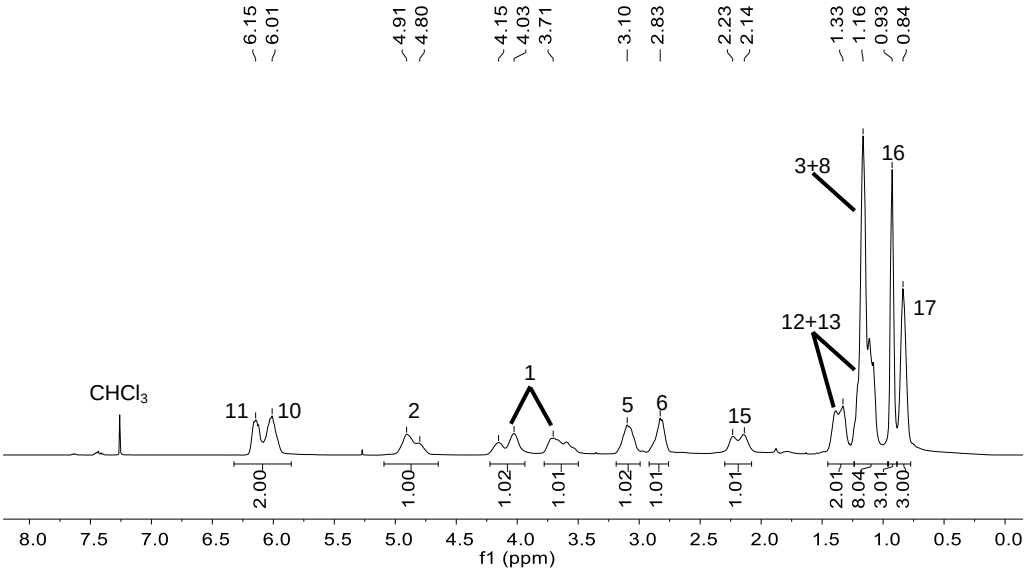

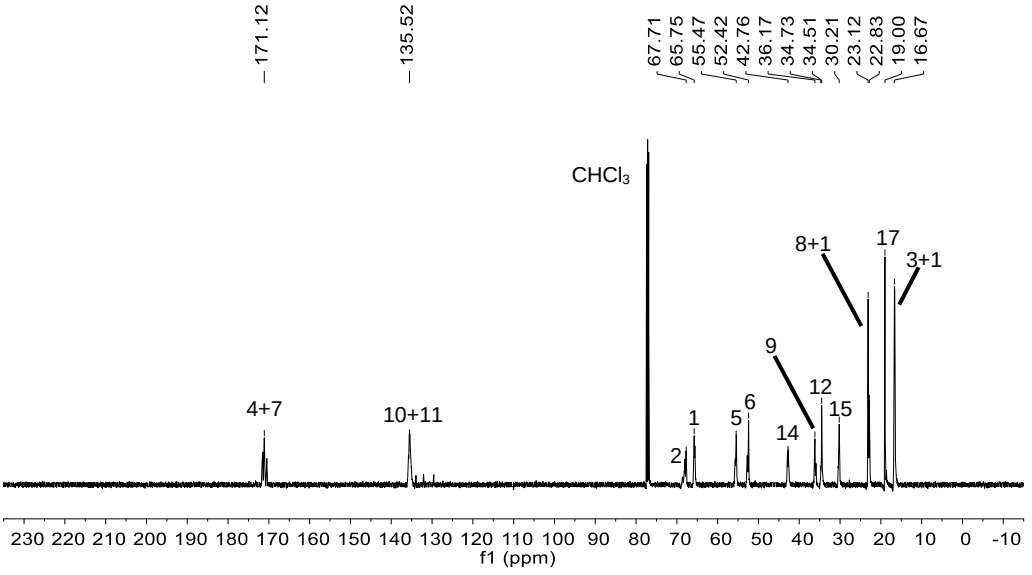

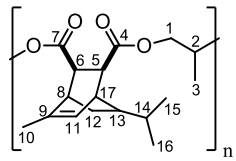
O
O
O
O
O
1
2
3
4
5
6
7
8
9
10
11
12
13
14
15
16
17
n

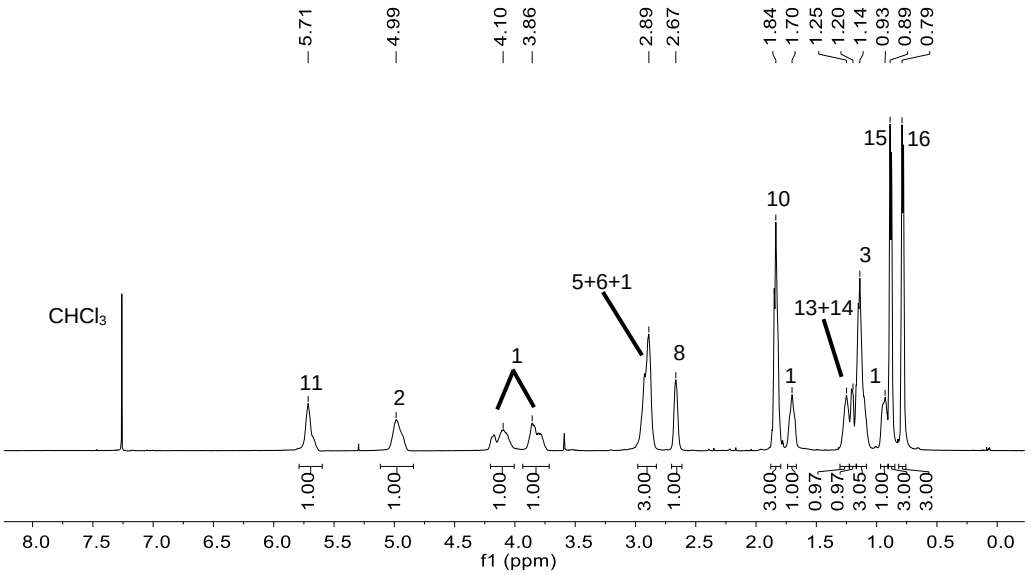
5.71
4.99
4.10
3.86
2.89
2.67
1.84
1.70
1.25
1.20
1.14
0.93
0.89
0.79
CHCl3
11
2
1
5+6+1
8
10
1
13+14
3
1
15
16
1.00
1.00
1.00
1.00
3.00
1.00
3.00
1.00
0.97
0.97
3.05
1.00
3.00
3.00
f1 (ppm)

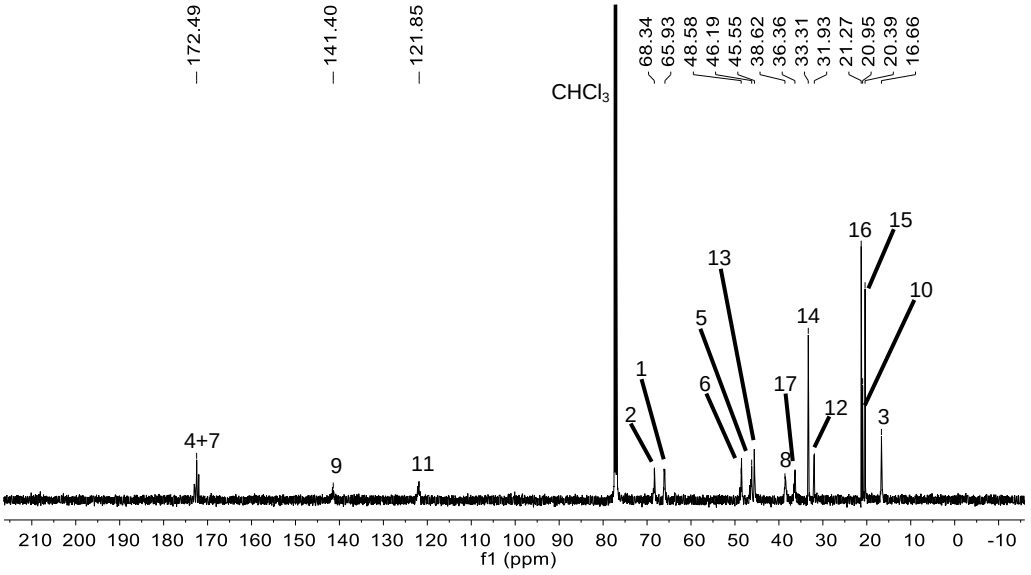
172.49
141.40
121.85
68.34
65.93
48.58
46.19
45.55
38.62
36.36
33.31
31.93
21.27
20.95
20.39
16.66
CHCl3
4+7
9
11
2
1
6
5
13
8
17
14
12
3
16
15
10
f1 (ppm)

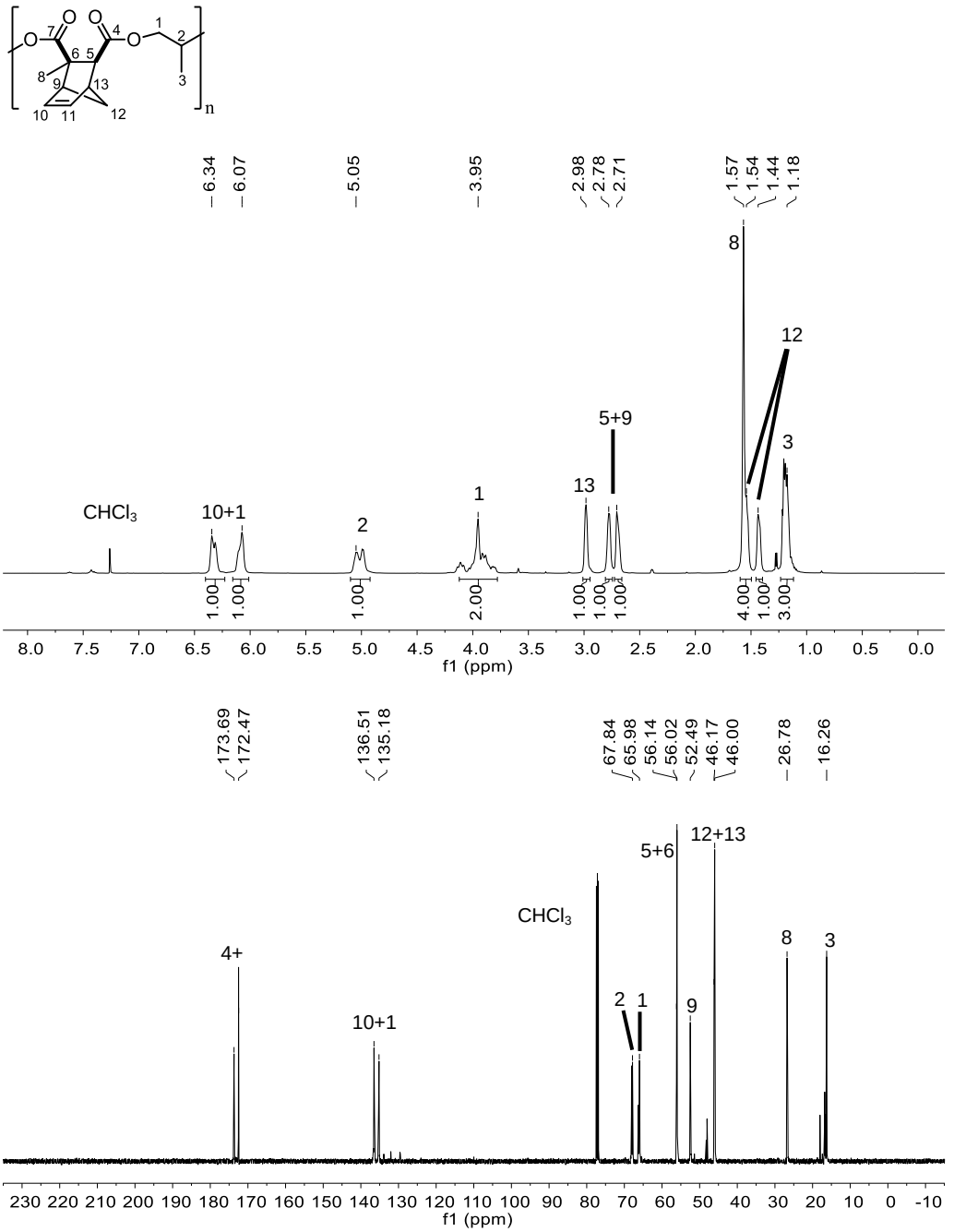
6.34
6.07
5.05
3.95
2.98
2.78
2.71
1.57
1.54
1.44
1.18
8
12
5+9
3
13
1
CHCl3
10+1
2
1.00
1.00
1.00
2.00
1.00
1.00
1.00
4.00
1.00
3.00
f1 (ppm)
173.69
172.47
136.51
135.18
67.84
65.98
56.14
56.02
52.49
46.17
46.00
26.78
16.26
5+6
12+13
CHCl3
8
3
4+
2
1
9
10+1
f1 (ppm)

Alternating copolymerization of propylene oxide and cyclohexene oxide with partially renewable tricyclic anhydrides

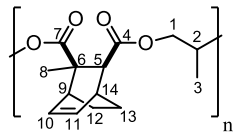

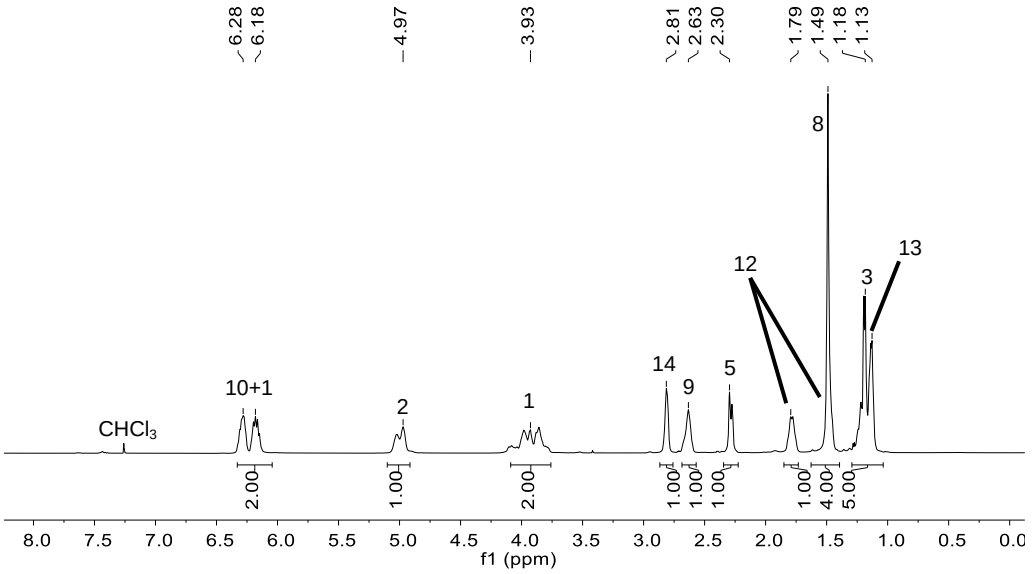

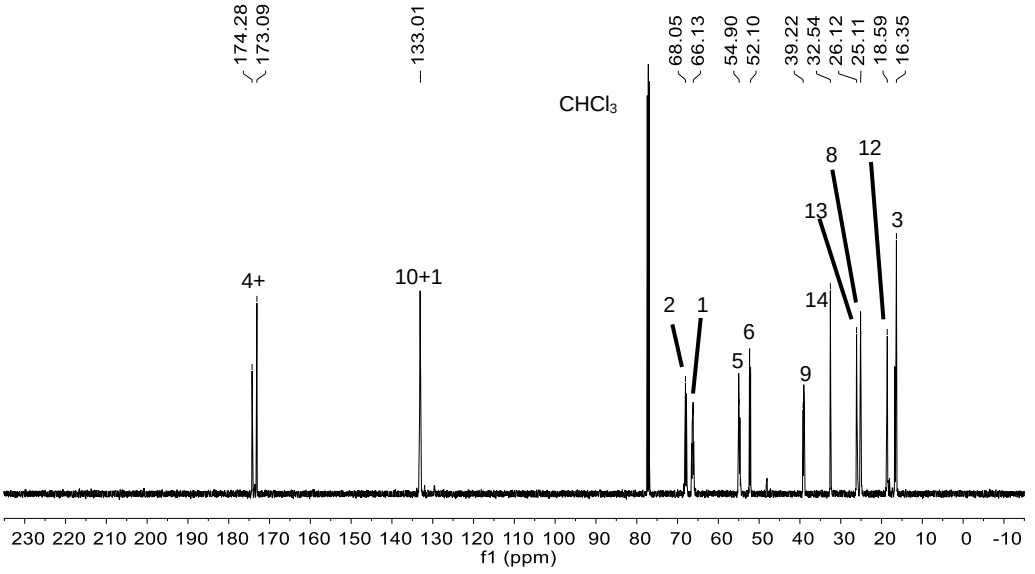

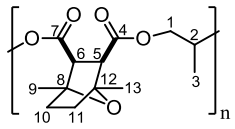
O
O
O
O
1
2
3
4
5
6
7
8
9
10
11
12
13
n

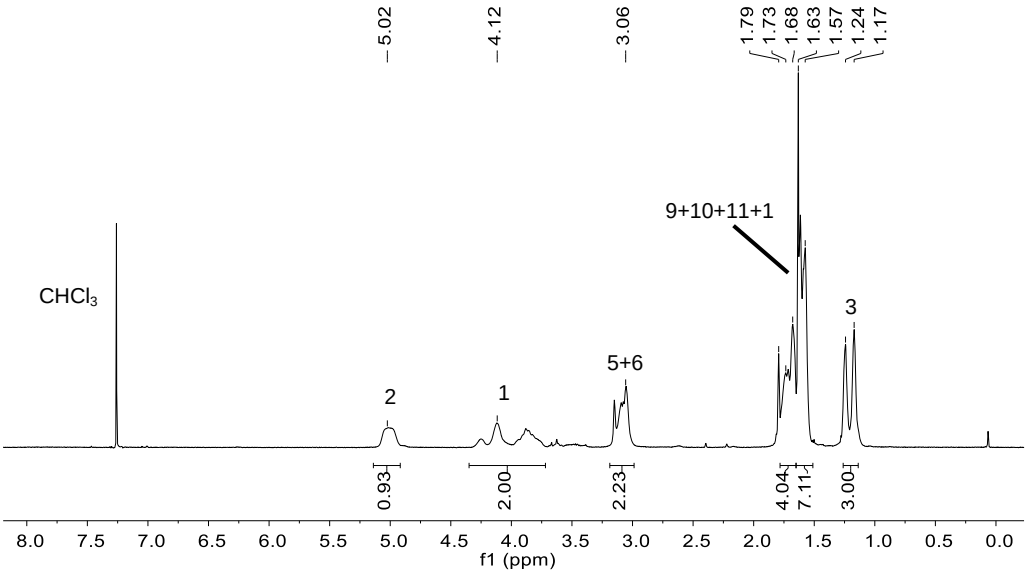
5.02
4.12
3.06
1.79
1.73
1.68
1.63
1.57
1.24
1.17
CHCl3
9+10+11+1
3
5+6
2
1
0.93
2.00
2.23
4.04
7.11
3.00
f1 (ppm)

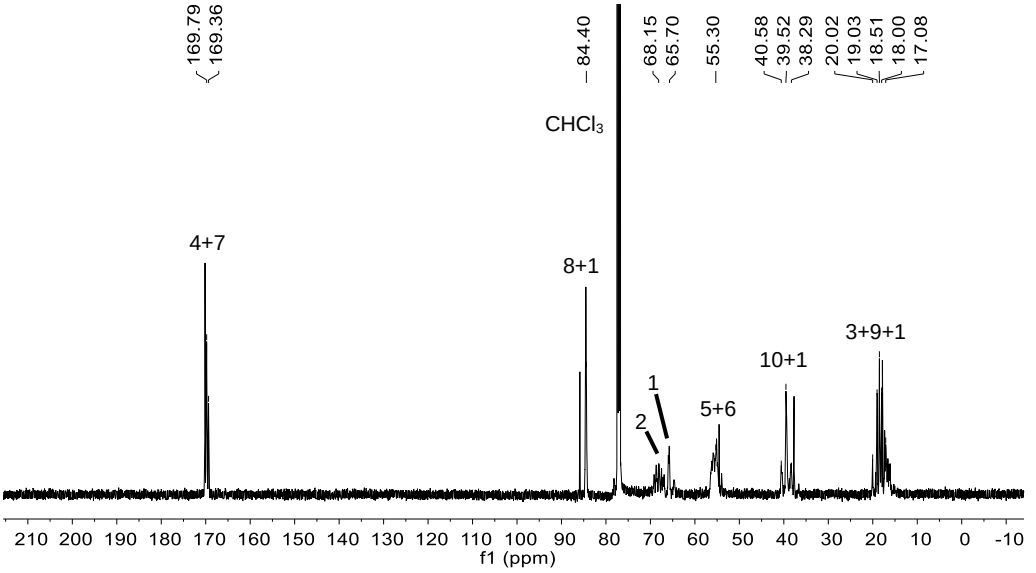
169.79
169.36
84.40
68.15
65.70
55.30
40.58
39.52
38.29
20.02
19.03
18.51
18.00
17.08
CHCl3
4+7
8+1
3+9+1
10+1
1
2
5+6
f1 (ppm)

Alternating copolymerization of propylene oxide and cyclohexene oxide with partially renewable tricyclic anhydrides

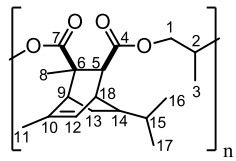

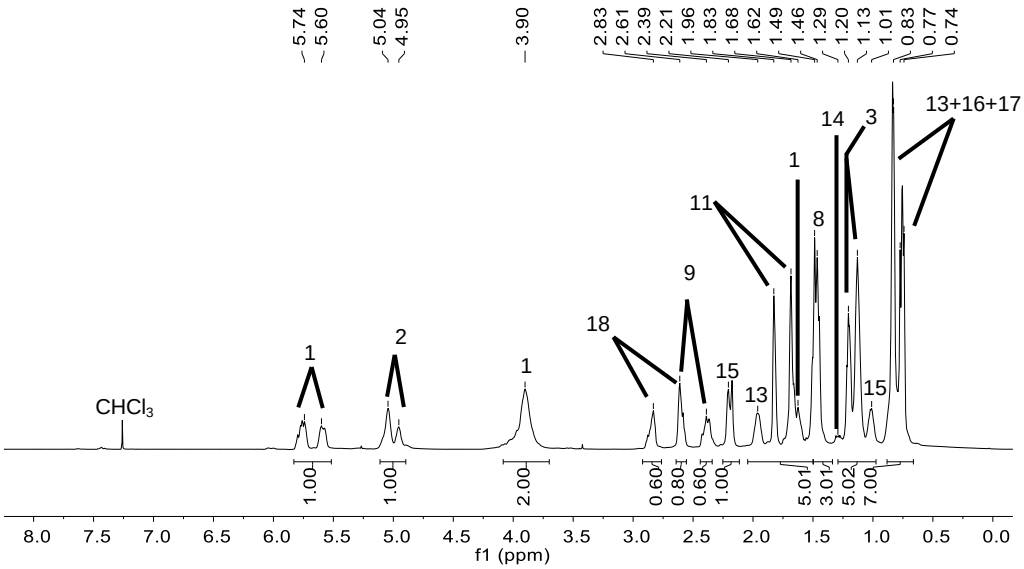

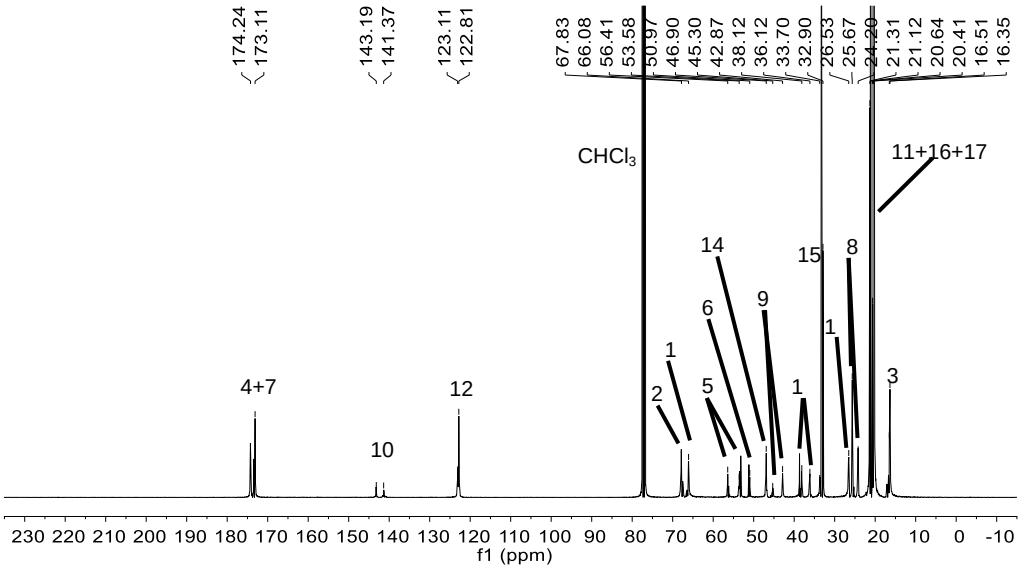

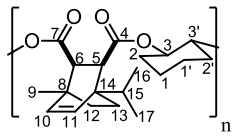
O
O
O
O
7
6
5
4
3
3'
2
1
1'
2'
16
8
14
15
9
10
11
12
13
17
n

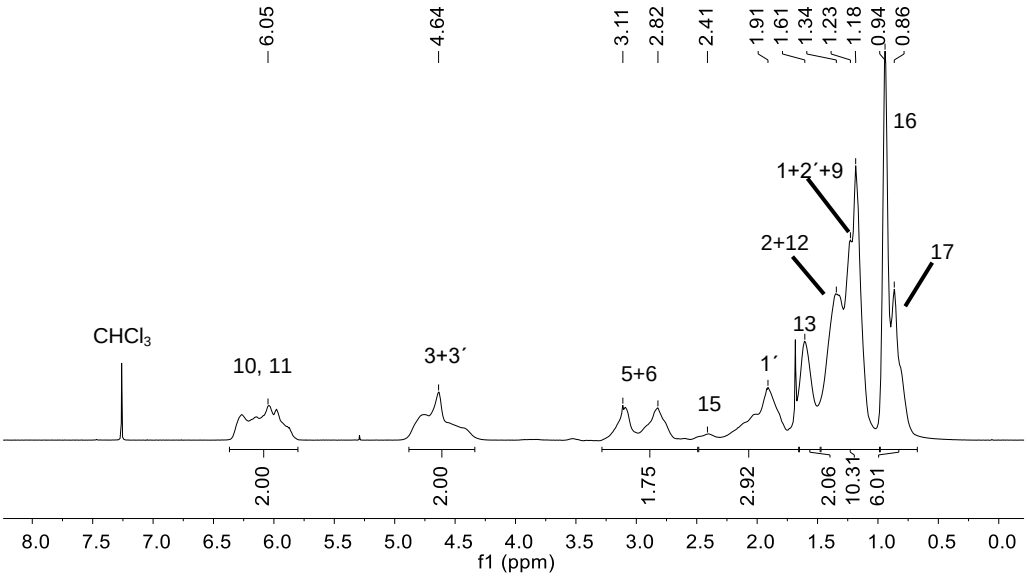
6.05
4.64
3.11
2.82
2.41
1.91
1.61
1.34
1.23
1.18
0.94
0.86
16
1+2´+9
2+12
17
13
CHCl3
10, 11
3+3´
5+6
1´
15
2.00
2.00
1.75
2.92
2.06
10.31
6.01
8.0 7.5 7.0 6.5 6.0 5.5 5.0 4.5 4.0 3.5 3.0 2.5 2.0 1.5 1.0 0.5 0.0
f1 (ppm)

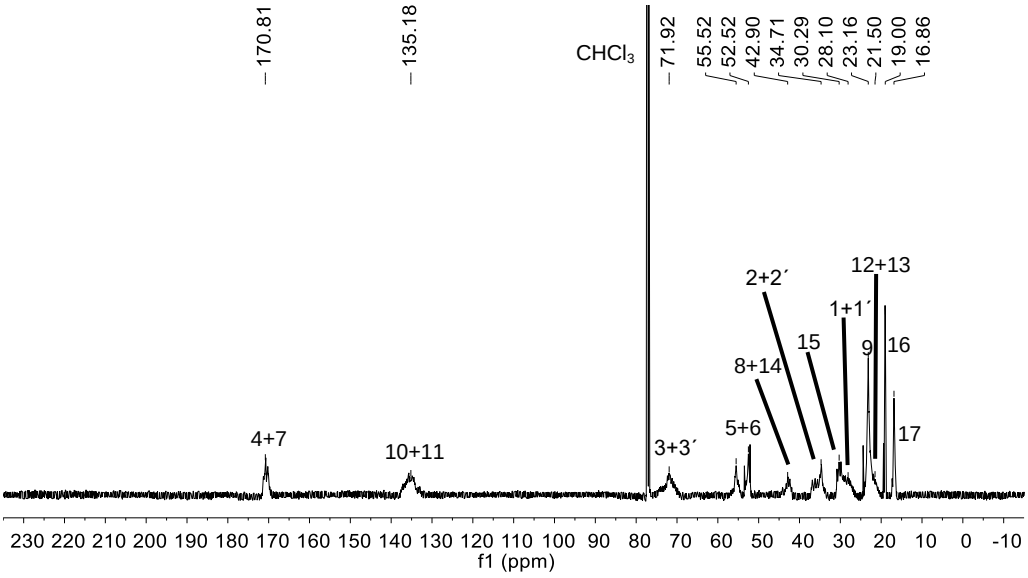
170.81
135.18
CHCl3
71.92
55.52
52.52
42.90
34.71
30.29
28.10
23.16
21.50
19.00
16.86
2+2´
12+13
1+1´
15
9
16
8+14
5+6
17
4+7
10+11
3+3´
230 220 210 200 190 180 170 160 150 140 130 120 110 100 90 80 70 60 50 40 30 20 10 0 -10
f1 (ppm)

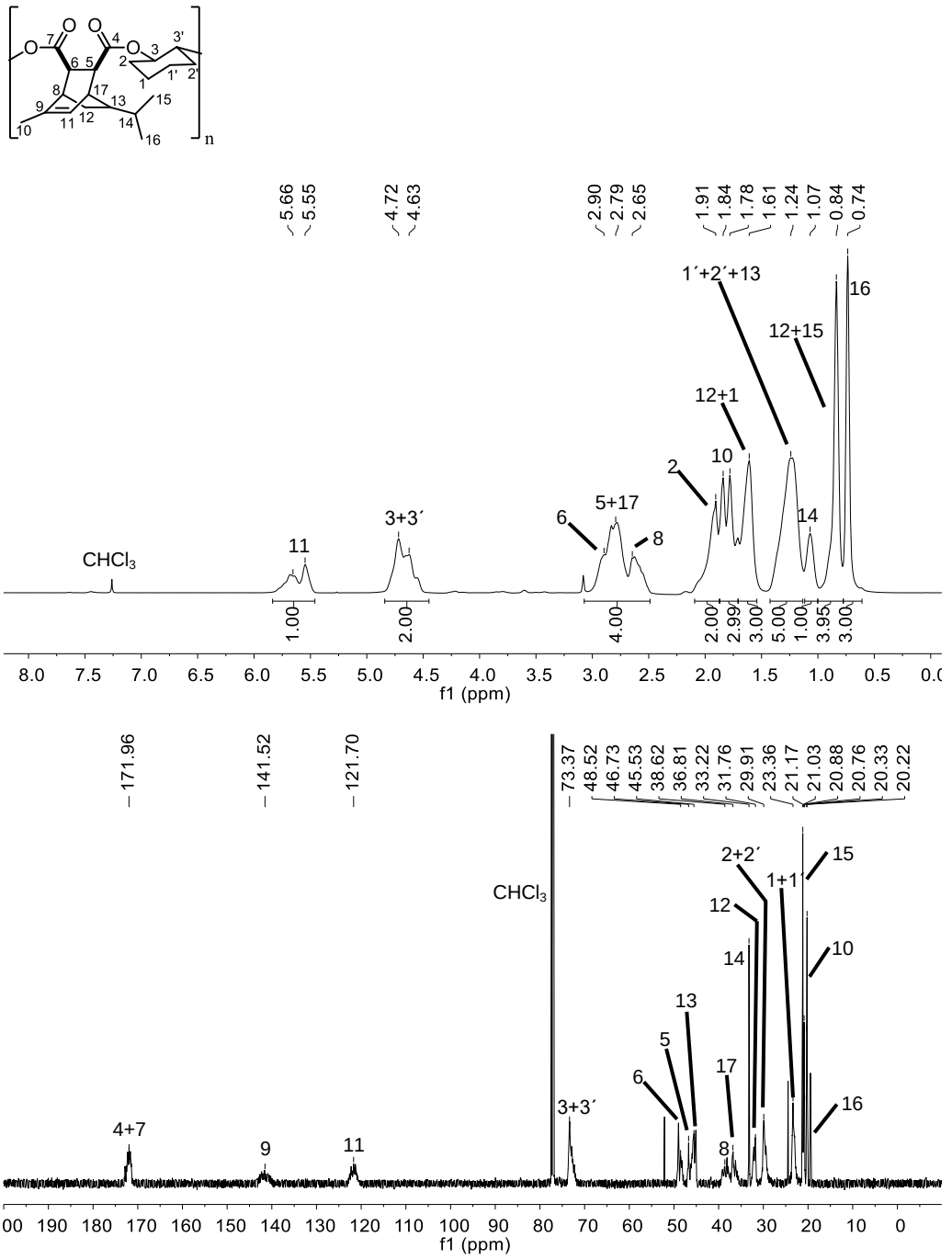
5.66
5.55
4.72
4.63
2.90
2.79
2.65
1.91
1.84
1.78
1.61
1.24
1.07
0.84
0.74
1´+2´+13
16
12+15
12+1
10
2
5+17
3+3´
6
14
8
11
CHCl3
1.00
2.00
4.00
2.00
2.99
3.00
5.00
1.00
3.95
3.00
f1 (ppm)
171.96
141.52
121.70
73.37
48.52
46.73
45.53
38.62
36.81
33.22
31.76
29.91
23.36
21.17
21.03
20.88
20.76
20.33
20.22
2+2´
1+1´
15
CHCl3
12
14
10
13
5
17
6
16
3+3´
4+7
9
11
8
f1 (ppm)

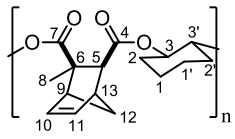
O
O
O
O
O
7
6
5
4
3
3'
2
2'
1
1'
8
9
13
10
11
12
n

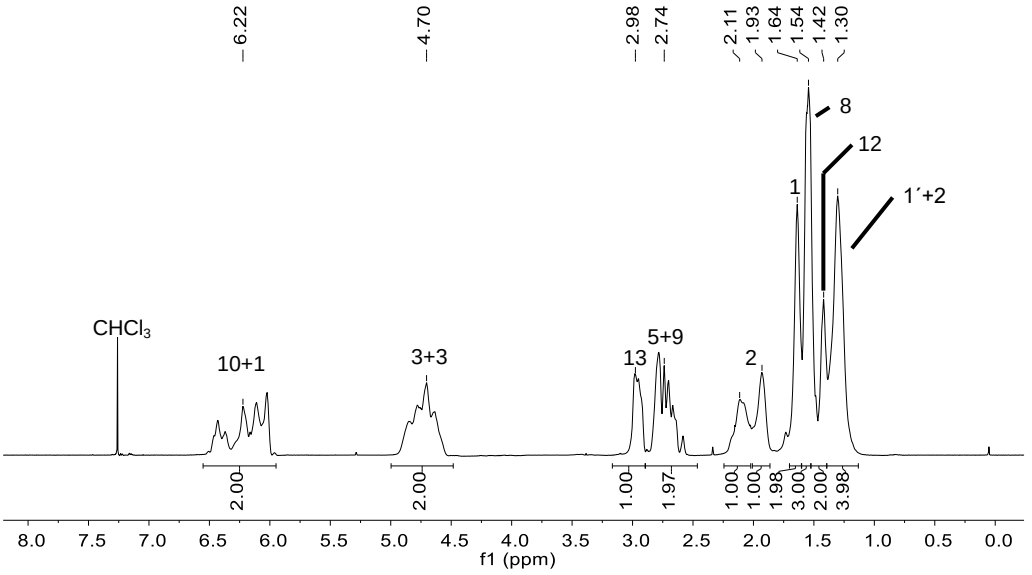
6.22
4.70
2.98
2.74
2.11
1.93
1.64
1.54
1.42
1.30
8
12
1
1´+2
CHCl3
10+1
3+3
13
5+9
2
2.00
2.00
1.00
1.97
1.00
1.00
1.98
3.00
2.00
3.98
8.0 7.5 7.0 6.5 6.0 5.5 5.0 4.5 4.0 3.5 3.0 2.5 2.0 1.5 1.0 0.5 0.0
f1 (ppm)

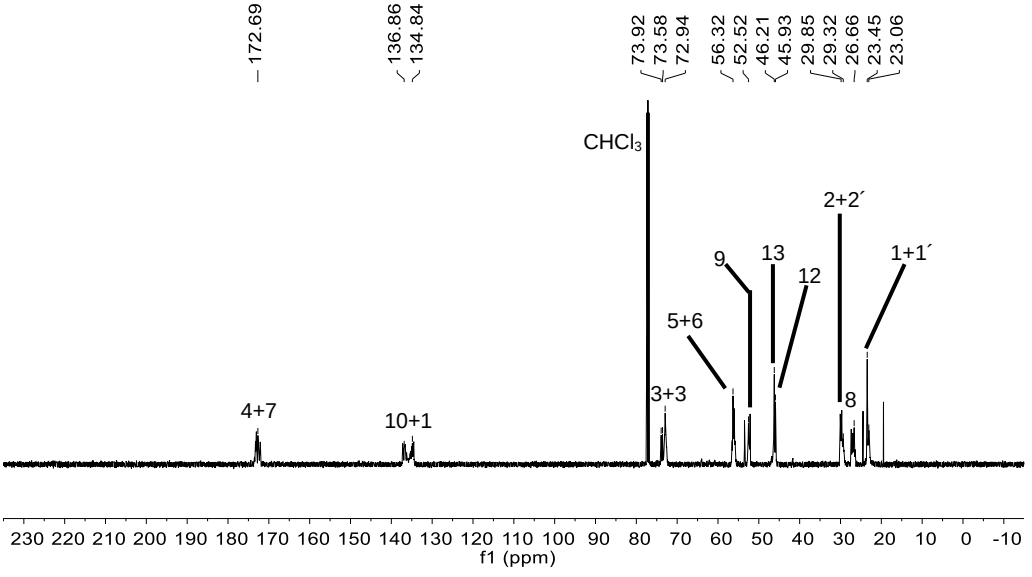
172.69
136.86
134.84
73.92
73.58
72.94
56.32
52.52
46.21
45.93
29.85
29.32
26.66
23.45
23.06
CHCl3
2+2´
9
13
12
1+1´
5+6
3+3
8
4+7
10+1
230 220 210 200 190 180 170 160 150 140 130 120 110 100 90 80 70 60 50 40 30 20 10 0 -10
f1 (ppm)

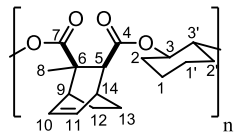
O
O
O
O
O
7
4
3'
6
5
3
2
8
1'
2'
9
14
1
10
11
12
13
n

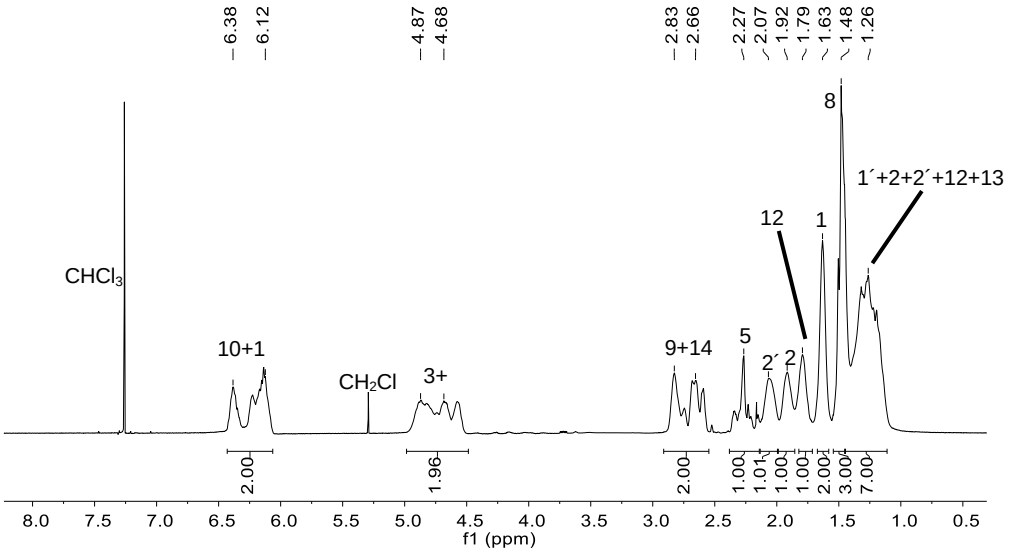
6.38
6.12
4.87
4.68
2.83
2.66
2.27
2.07
1.92
1.79
1.63
1.48
1.26
CHCl3
10+1
CH2Cl
3+
9+14
5
2´
2
12
1
8
1´+2+2´+12+13
2.00
1.96
2.00
1.00
1.01
1.00
1.00
2.00
3.00
7.00
f1 (ppm)

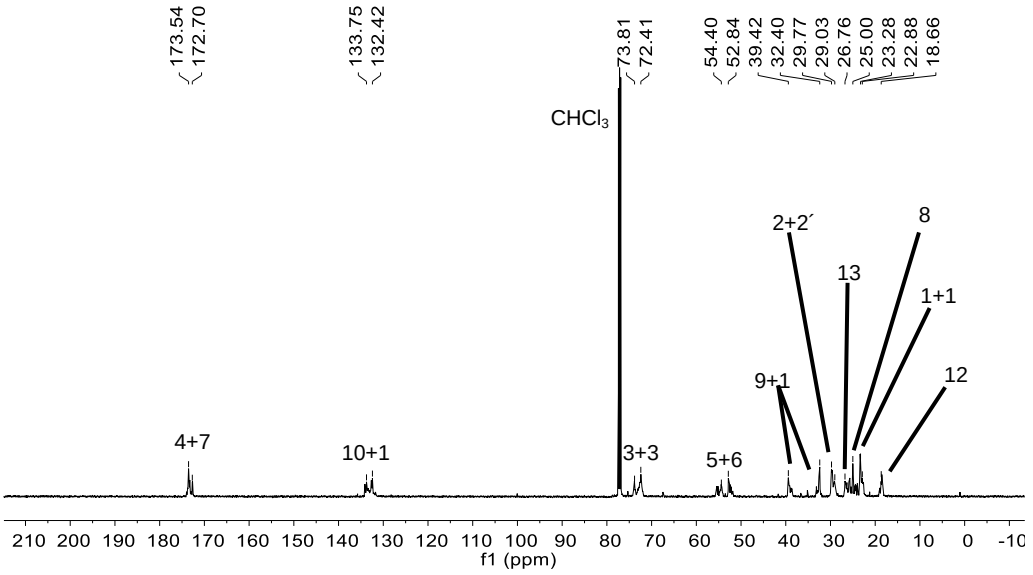
173.54
172.70
133.75
132.42
73.81
72.41
54.40
52.84
39.42
32.40
29.77
29.03
26.76
25.00
23.28
22.88
18.66
CHCl3
2+2´
8
13
1+1
9+1
12
4+7
10+1
3+3
5+6
f1 (ppm)

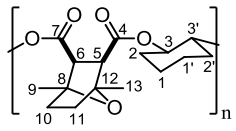
O
O
O
O
O
7
6
5
4
3
3'
2
1'
2'
1
8
12
13
9
10
11
n

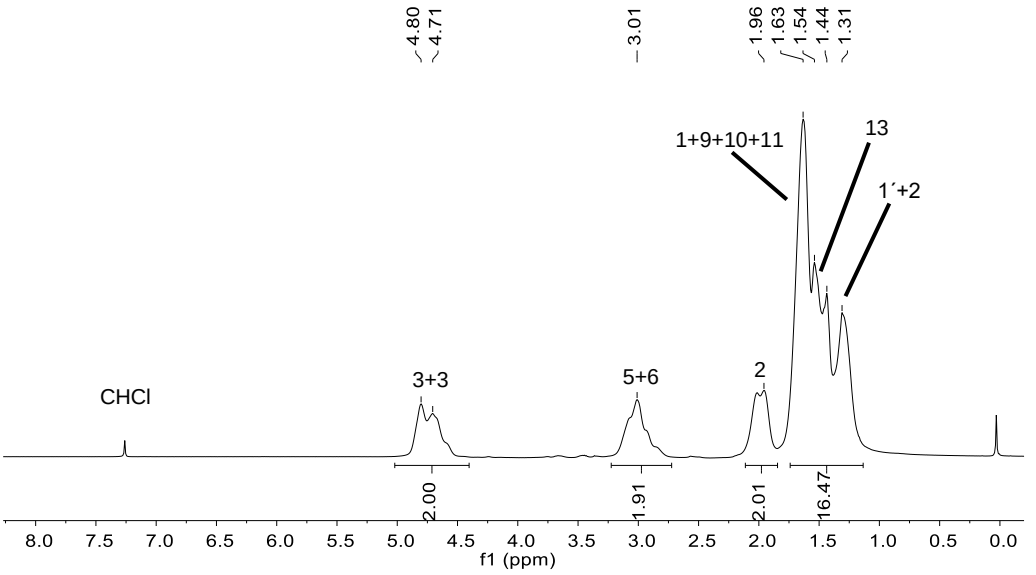
4.80
4.71
3.01
1.96
1.63
1.54
1.44
1.31
1+9+10+11
13
1´+2
CHCl
3+3
5+6
2
2.00
1.91
2.01
16.47
8.0 7.5 7.0 6.5 6.0 5.5 5.0 4.5 4.0 3.5 3.0 2.5 2.0 1.5 1.0 0.5 0.0
f1 (ppm)

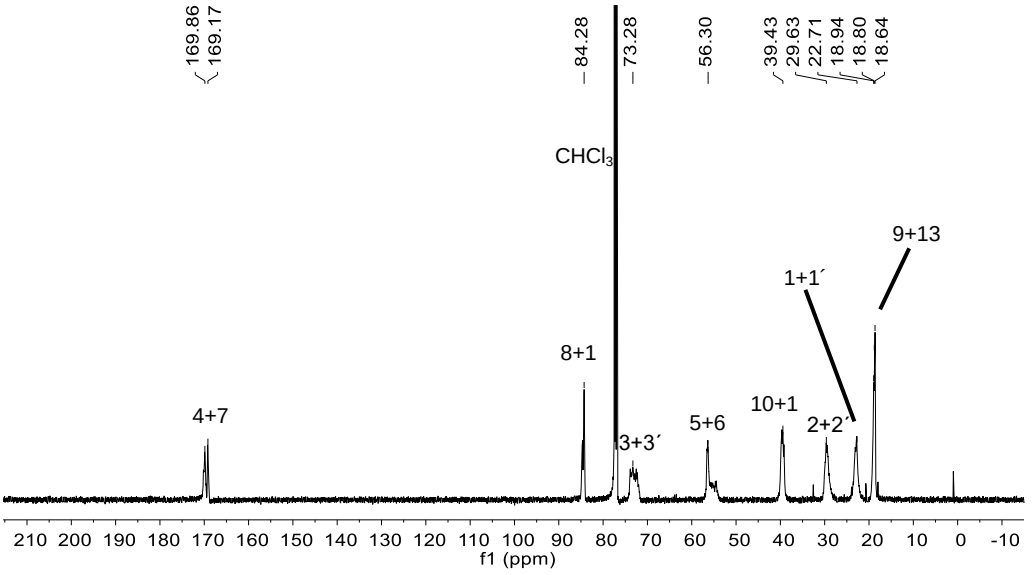
169.86
169.17
84.28
73.28
56.30
39.43
29.63
22.71
18.94
18.80
18.64
CHCl3
9+13
1+1´
8+1
10+1
4+7
5+6
2+2´
3+3´
210 200 190 180 170 160 150 140 130 120 110 100 90 80 70 60 50 40 30 20 10 0 -10
f1 (ppm)

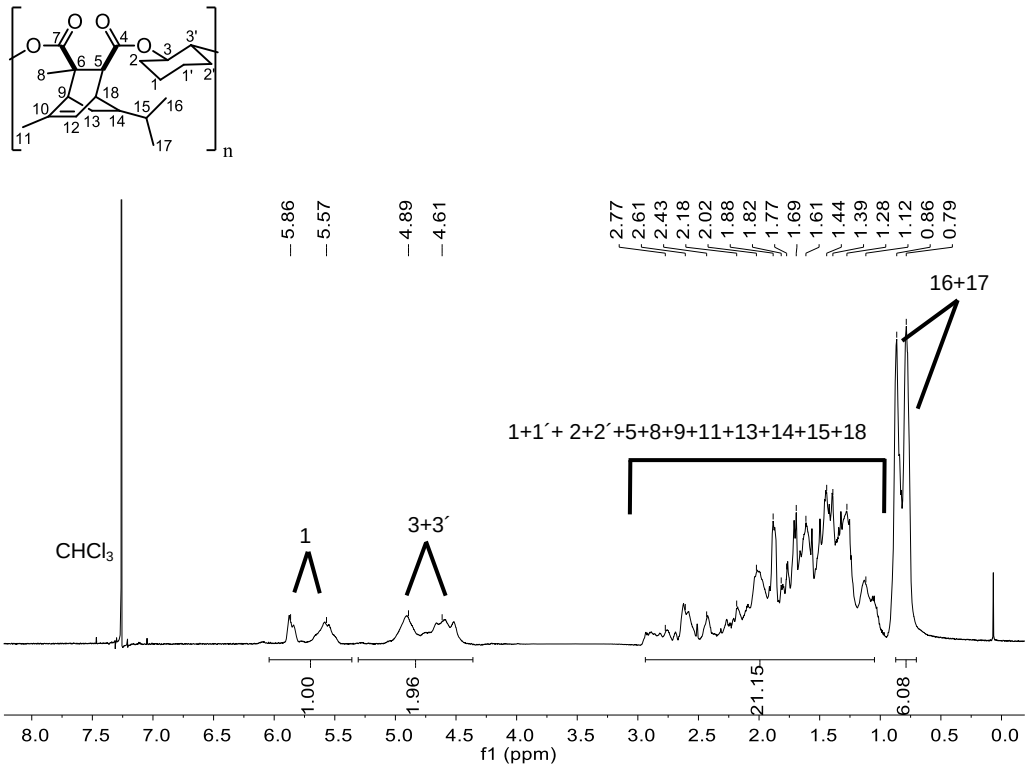
5.86
5.57
4.89
4.61
2.77
2.61
2.43
2.18
2.02
1.88
1.82
1.77
1.69
1.61
1.44
1.39
1.28
1.12
0.86
0.79
16+17
1+1´+ 2+2´+5+8+9+11+13+14+15+18
CHCl3
1
3+3´
1.00
1.96
21.15
6.08
f1 (ppm)

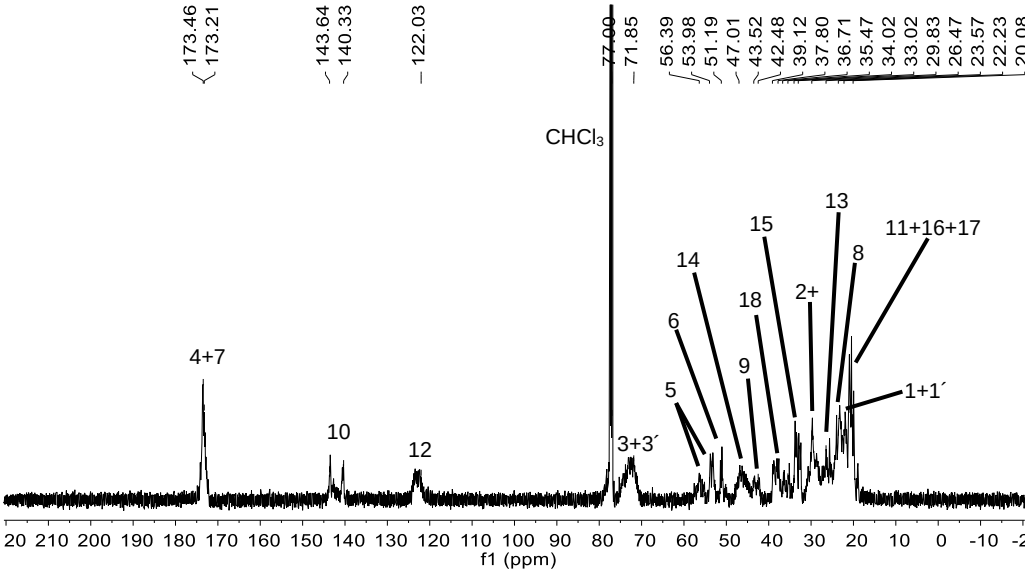
173.46
173.21
143.64
140.33
122.03
77.00
71.85
56.39
53.98
51.19
47.01
43.52
42.48
39.12
37.80
36.71
35.47
34.02
33.02
29.83
26.47
23.57
22.23
CHCl3
13
15
11+16+17
14
8
18
2+
6
9
4+7
5
1+1´
10
12
3+3´
f1 (ppm)

2.5 References

[1] A. Gandini, *Green Chem.* **2011**, *13*, 1061–1083.

[2] A. J. Ragauskas, C. K. Williams, B. H. Davison, G. Britovsek, J. Cairney, C. A. Eckert, W. J. Frederick, J. P. Hallett, D. J. Leak, C. L. Liotta, et al., *Science* **2006**, *311*, 484–489.

[3] S. Mecking, *Angew. Chem. Int. Ed.* **2004**, *43*, 1078–1085.

[4] R. A. Gross, *Science* **2002**, *297*, 803–807.

[5] M. A. Hillmyer, W. B. Tolman, *Acc. Chem. Res.* **2014**, *47*, 2390–2396.

[6] M. Vert, *Biomacromolecules* **2005**, *6*, 538–546.

[7] W. Amass, a Amass, B. Tighe, *Polym. Int.* **1998**, *47*, 89–144.

[8] D. A. Olson, S. E. A. Gratton, J. M. DeSimone, V. V. Sheares, *J. Am. Chem. Soc.* **2006**, *128*, 13625–13633.

[9] R. J. Müller, I. Kleeberg, W. D. Deckwer, *J. Biotechnol.* **2001**, *86*, 87–95.

[10] A. H. Brown, V. V. Sheares, *Macromolecules* **2007**, *40*, 4848–4853.

[11] B. Rieger, A. Künkel, G. W. Coates, R. Reichardt, E. Dinjus, A. T. Zevaco, *Synthetic Biodegradable Polymers*, Springer, Berlin, **2012**.

[12] H.-W. Engels, H.-G. Pirkl, R. Albers, R. W. Albach, J. Krause, A. Hoffmann, H. Casselmann, J. Dormish, *Angew. Chem. Int. Ed.* **2013**, *52*, 9422–9441.

[13] A. P. Gupta, V. Kumar, *Eur. Polym. J.* **2007**, *43*, 4053–4074.

[14] X. . W. Zhao L.; Liu, D., *J. Chem. Technol. Biotechnol.* **2007**, *82*, 1115–1121.

[15] R. Auras, B. Harte, S. Selke, *Macromol. Biosci.* **2004**, *4*, 835–864.

[16] E. T. H. Vink, K. R. Rábago, D. A. Glassner, P. R. Gruber, *Polym. Degrad. Stab.* **2003**, *80*, 403–419.

[17] Y. Ikada, H. Tsuji, *Macromol. Rapid Commun.* **2000**, *21*, 117–132.

[18] S. Paul, Y. Zhu, C. Romain, R. Brooks, P. K. Saini, C. K. Williams, *Chem. Commun.* **2015**, *51*, 6459–6479.

[19] F. Fenouillot, A. Rousseau, G. Colomines, R. Saint-Loup, J. P. Pascault, *Prog. Polym. Sci.* **2010**, *35*, 578–622.

[20] R. Storbeck, M. Ballauff, *Polym. (United Kingdom)* **1993**, *34*, 5003–5006.

[21] G. L. Fiore, F. Jing, V. G. Young, Jr., C. J. Cramer, M. a. Hillmyer, *Polym. Chem.* **2010**, *1*, 870–877.

[22] C. Lavilla, A. Alla, A. Martínez De Ilarduya, S. Muñoz-Guerra, *Biomacromolecules* **2013**, *14*, 781–793.

[23] B. Han, L. Zhang, B. Liu, X. Dong, I. Kim, Z. Duan, P. Theato, *Macromolecules* **2015**, *48*, 3431–3437.

[24] L. Zhu, D. Liu, L. Wu, W. Feng, X. Zhang, J. Wu, D. Fan, X. Lü, R. Lu, Q. Shi, *Inorg. Chem. Commun.* **2013**, *37*, 182–185.

[25] D. F. Liu, L. Y. Wu, W. X. Feng, X. M. Zhang, J. Wu, L. Q. Zhu, D. Di Fan, X. Q. Lü, Q. Shi, *J. Mol. Catal. A Chem.* **2014**, *382*, 136–145.

[26] Y. Liu, M. Xiao, S. Wang, L. Xia, D. Hang, G. Cui, Y. Meng, *RSC Adv.* **2014**, *4*, 9503–9508.

[27] P. K. Saini, C. Romain, Y. Zhu, C. K. Williams, *Polym. Chem.* **2014**, *5*, 6068–6075.

[28] L. Y. Wu, D. Di Fan, X. Q. Lü, R. Lu, *Chinese J. Polym. Sci. (English Ed.* **2014**, *32*, 768–777.

[29] M. Winkler, C. Romain, M. A. R. Meier, C. K. Williams, *Green Chem.* **2015**, *17*, 300–306.

[30] Y. Zhu, C. Romain, C. K. Williams, *J. Am. Chem. Soc.* **2015**, *137*, 12179–12182.

[31] A. Thevenon, J. A. Garden, A. J. P. White, C. K. Williams, *Inorg. Chem.* **2015**, *54*, 11906–11915.

[32] J. A. Garden, P. K. Saini, C. K. Williams, *J. Am. Chem. Soc.* **2015**, *137*, 15078–15081.

[33] A. Takasu, M. Ito, Y. Inai, T. Hirabayashi, Y. Nishimura, *Polym. J.* **1999**, *31*, 961–969.

[34] S. Huijser, E. Hosseininejad, R. Sablong, C. De Jong, C. E. Koning, R. Duchateau, *Macromolecules* **2011**, *44*, 1132–1139.

[35] C. Robert, F. de Montigny, C. M. Thomas, *Nat. Commun.* **2011**, *2*, 586.

[36] D. J. Darensbourg, R. R. Poland, C. Escobedo, *Macromolecules* **2012**, *45*, 2242–2248.

[37] E. Hosseini Nejad, A. Paoniasari, C. E. Koning, R. Duchateau, *Polym. Chem.* **2012**, *3*, 1308–1313.

[38] E. Hosseini Nejad, C. G. W. Van Melis, T. J. Vermeer, C. E. Koning, R. Duchateau, *Macromolecules* **2012**, *45*, 1770–1776.

[39] A. Bernard, C. Chatterjee, M. H. Chisholm, *Polym. (United Kingdom)* **2013**, *54*, 2639–2646.

[40] N. D. Harrold, Y. Li, M. H. Chisholm, *Macromolecules* **2013**, *46*, 692–698.

[41] J. Liu, Y.-Y. Bao, Y. Liu, W.-M. Ren, X.-B. Lu, *Polym. Chem.* **2013**, *4*, 1439–1444.

[42] E. H. Nejad, A. Paoniasari, C. G. W. Van Melis, C. E. Koning, R. Duchateau, *Macromolecules* **2013**, *46*, 631–637.

[43] U. Biermann, A. Sehlinger, M. A. R. Meier, J. O. Metzger, *Eur. J. Lipid Sci. Technol.* **2016**, *118*, 104–110.

[44] A. M. DiCiccio, G. W. Coates, *J. Am. Chem. Soc.* **2011**, *133*, 10724–10727.

[45] J. M. Longo, A. M. DiCiccio, G. W. Coates, *J. Am. Chem. Soc.* **2014**, *136*, 15897–15900.

[46] C. Robert, T. Ohkawara, K. Nozaki, *Chem. - A Eur. J.* **2014**, *20*, 4789–4795.

[47] D.-F. Liu, L.-Q. Zhu, J. Wu, L.-Y. Wu, X.-Q. Lü, *RSC Adv.* **2015**, *5*, 3854–3859.

[48] D. Liu, Z. Zhang, X. Zhang, X. Lü, *Aust. J. Chem.* **2016**, *69*, 47–55.

[49] T. Aida, S. Inoue, *J. Am. Chem. Soc.* **1985**, *107*, 1358–1364.

[50] T. Aida, K. Sanuki, S. Inoue, *Macromolecules* **1985**, *18*, 1049–1055.

[51] N. J. Van Zee, G. W. Coates, *Angew. Chem. Int. Ed.* **2015**, *54*, 2665–2668.

[52] N. J. Van Zee, M. J. Sanford, G. W. Coates, *J. Am. Chem. Soc.* **2016**, *138*, 2755–2761.

[53] C. J. Whiteoak, B. Gjoka, E. Martin, M. M. Belmonte, E. C. Escudero-Adán, C. Zonta, G. Licini, A. W. Kleij, *Inorg. Chem.* **2012**, *51*, 10639–10649.

[54] M. Taherimehr, S. M. Al-Amsyar, C. J. Whiteoak, A. W. Kleij, P. P. Pescarmona, *Green Chem.* **2013**, *15*, 3083–3090.

[55] R. Mundil, Z. Hošťálek, I. Šeděnková, J. Merna, *Macromol. Res.* **2015**, *23*, 161–166.

[56] A. Behr, L. Johnen, *ChemSusChem* **2009**, *2*, 1072–1095.

[57] K. A. D. Swift, *Top. Catal.* **2004**, *27*, 143–155.

[58] D. Dakshinamoorthy, A. K. Weinstock, K. Damodaran, D. F. Iwig, R. T. Mathers, *ChemSusChem* **2014**, *7*, 2923–2929.

[59] P. A. Wilbon, F. Chu, C. Tang, *Macromol. Rapid Commun.* **2013**, *34*, 8–37.

[60] J. Zhao, H. Schlaad, in *Bio-Synthetic Polym. Conjug.* (Ed.: H. Schlaad), Springer Berlin Heidelberg, Berlin, Heidelberg, **2013**, pp. 151–190.

[61] M.-Y. Chen, C.-B. Chen, B. Zada, Y. Fu, *Green Chem.* **2016**, *18*, 3858–3866.

[62] Y. Román-Leshkov, C. J. Barrett, Z. Y. Liu, J. a Dumesic, *Nature* **2007**, *447*, 982.

[63] H. Rasmussen, H. R. Sørensen, A. S. Meyer, *Carbohydr. Res.* **2014**, *385*, 45–57.

[64] The Merck Index, *14th ed. Merck Co., Ins. Whitehouse Station. NJ* **2006**.

[65] H. Hajian, W. Mohtar, W. Yusoff, *Curr. Res. J. Biol. Sci.* **2015**, *7*, 37–42.

[66] R. T. Mathers, M. J. Shreve, E. Meyler, K. Damodaran, D. F. Iwig, D. J. Kelley, *Macromol. Rapid Commun.* **2011**, *32*, 1338–1342.

[67] G. W. Coates, D. R. Moore, *Angew. Chem. Int. Ed.* **2004**, *43*, 6618–6639.

[68] M. R. Kember, A. Buchard, C. K. Williams, *Chem. Commun.* **2011**, *47*, 141–163.

[69] L. P. C. Nielsen, C. P. Stevenson, D. G. Blackmond, E. N. Jacobsen, *J. Am. Chem. Soc.* **2004**, *126*, 1360–1362.

[70] S. Inoue, *J. Polym. Sci. A Polym. Chem.* **2000**, *38*, 2861–2871.

[71] W. J. Van Meerendonk, R. Duchateau, C. E. Koning, G. J. M. Gruter, *Macromolecules* **2005**, *38*, 7306–7313.

[72] T. Kurahashi, H. Fujii, *J. Am. Chem. Soc.* **2011**, *133*, 8307–8316.

[73] A. Coletti, P. Galloni, A. Sartorel, V. Conte, B. Floris, *Catal. Today* **2012**, *192*, 44–55.

[74] D. Rutherford, D. a. Atwood, *Organometallics* **1996**, *15*, 4417–4422.

[75] C. A. Citron, S. M. Wickel, B. Schulz, S. Draeger, J. S. Dickschat, *European J. Org. Chem.* **2012**, 6636–6646.

[76] Y. Hayashi, M. Nakamura, S. Nakao, T. Inoue, M. Shoji, *Communications* **2002**, *91*, 4079–4082.

Chapter 3

Semi-aromatic polyesters derived from renewable terpene oxides with high glass transitions

UNIVERSITAT ROVIRA I VIRGILI
AVANCES EN SISTEMAS INTERACTIVOS PARA PERSONAS CON PARÁLISIS CEREBRAL
Leticia Peña Carrodeguas

3.1 Introduction

Synthetic polymers are essential for the production of a range of consumer-based products that focus on improving the quality of life. Due to an increasing demand to prepare such polymers in a sustainable fashion and to make use of renewable monomers derived from biomass,[1–4] there has been an upsurge in the development of partially to fully bioderived polymers.[5–12] Such biobased macromolecules represent more benign alternatives towards conventional polymers that for the larger part are prepared from petroleum based resources.[13–15] In the context of biopolymer synthesis, terpene compounds have been frequently considered as functional monomers towards the construction of a variety of polymer structures including polyterpenes[16–19] and polycarbonates.[20–27] However, examples of polyesters derived from terpene-based monomers remain scarce,[28–34] despite their abundance and structural diversity, and potential for post-modification and curing.

The ring-opening polymerization (ROP) of cyclic esters in the presence of suitable organic or metal-based initiators produces polyesters such as poly(lactide) and is an attractive and easy method to control the polymerization process.[35–38] However, the diversity in cyclic ester structures and limitations in functional group presence in these polyesters may limit the properties that can be attained through the use of these monomers. Therefore, complementary polyester preparation strategies offer a way to produce polymers with a wider range of properties modulated by the nature of the monomers, and ring-opening copolymerization (ROCOP) of epoxides and cyclic anhydrides[39–41] has been recognized as highly versatile route to further extend the (thermal) properties of polyesters.

Early work in this area showed the potential of ROCOP when using Al(III) centered porphyrins as catalysts,[39] whereas a major advancement in the development of this process was not noted until the use of a β-diiminate Zn-catalyst was reported.[28] Apart from this seminal report, other catalysts have also been reported in this context as highly efficient mediators of ROCOP using a variety of cyclic anhydrides and epoxides.[42–44] The thermal properties of polyesters can be easily regulated through ROCOP and this approach can provide macromolecular structures with long side chains and/or extremely flexible backbones providing consequently low T_g values (typically below 0 ºC) with potential towards the development of new thermoplastic elastomers.[45,46]

Many renewable monomers for epoxide and anhydride ROCOP have been explored, resulting in a range of renewably sourced aliphatic and semi-aromatic polyesters with desirable

properties. The development of higher T_g, purely aliphatic polyester variants from renewable sources with values beyond 100 ºC still remains in its infancy, though important progress was recently reported by Coates and coworkers,[32,34] who used a rigid terpene-based tricyclic anhydride and propylene oxide (PO) to yield a polyester (M_n = 55 kg/mol) with a T_g of 109 ºC. Analogous to the approach from Coates, also using a based renewable anhydride, Theato and coworkers considered organocatalytic ROCOP of a norbornene-based tricyclic anhydride monomer and cyclohexene oxide (CHO) giving also high T_g (up to 130 ºC) polyesters though with significantly lower M_n values.[47] The highest T_g´s for aliphatic polyesters (up to 184 ºC) derived from a series of partially renewable cyclic anhydrides combined with PO or CHO under Al(III) or Fe(III) catalysis were reported by Coates and Kleij, showing the importance of selecting more rigid monomer combinations to further extend and modify the thermal properties.[31][A]

Scheme 3.1 Anhydrides copolymerized with renewable based epoxides.

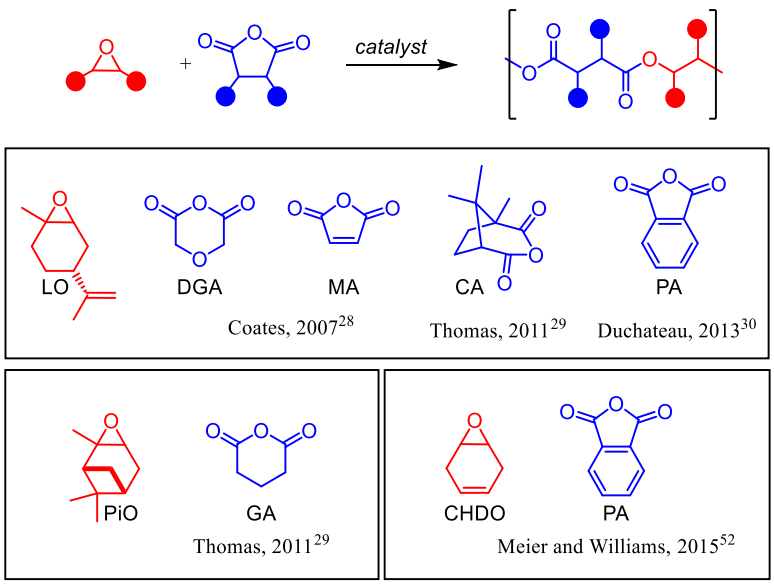

In 2007, Coates[28] and co-workers reported the copolymerization of limonene oxide (LO) with diglycolic anhydride (DGA) and with maleic anhydride (MA) to produce aliphatic polyesters with M_n = 36 Kg/mol and 12 Kg/mol respectively. Besides, Thomas *et al.* reported

[A] For a detailed explanation of ROCOP with terpene based tricyclic anhydride monomers, we refer to Chapter 2 "*Alternating copolymerization of propylene oxide and cyclohexene oxide with partially renewable tricyclic anhydrides*"

the use of limonene oxide (LO) and pinene oxide (PiO) monomers in the preparation of aliphatic polyesters using a tandem approach involving *in situ* cyclic anhydride synthesis from a dicarboxylic acid precursor and a dicarbonate reagent followed by a ROCOP at 100 ºC under metal-salen catalysis.[29]

Semi-aromatic polyesters, *i.e.* polyesters constructed from one aromatic monomer, either the epoxide[48,49], the anhydride[46,50,51] or both[49], also have good potential to produce polymers with higher T_g values. In this context, phthalic anhydride (PA) is the most commonly used monomer and when this monomer is copolymerized in the presence of (substituted) cyclohexene oxides[46] or cyclohexadiene oxide[52] it produces polyesters with T_g values of 146 ºC (M_n = 13.2 kg/mol) and 128 ºC (M_n = 7.5 kg/mol), respectively.

Inspired by these results and our ongoing interest in the use of renewable terpene-based feedstocks,[23,26,53] we considered the ROCOP of PA and various terpene oxides as a useful approach towards semi-aromatic polyesters with modular thermal properties by a proper selection of the combination of monomers, catalyst and reaction conditions. Additionally, although phthalic anhydride (PA) is currently not renewable sourced, a recent report suggests that a bio-derived version may be accessible in the future.[54] As far as we know, there are only few successful examples of ROCOP between aromatic cyclic anhydrides and terpene oxides. Duchateau and coworkers used M(salen)s as catalysts (M = Al, Cr, Mn and Co) and DMAP as a nucleophilic co-catalyst to mediate the ROCOP of PA and LO at 130 ºC under neat conditions. The polyesters produced this way had M_n values up to 9.7 kg/mol ($Đ$ = 1.4), and they further reported a moderately high T_g of 82 ºC for a polyester having a molecular weight of 7.2 kg/mol.[30] Therefore, further expansion of the potential of terpene oxide monomers in the synthesis of high T_g semiaromatic polyesters is still a challenging but inspiring objective in the realm of biobased polymer development.

Herein we present an Fe(III) based catalyst[55–57] derived from an aminotriphenolate ligand that, in the presence of a suitable initiator, mediates the ROCOP of various terpene-based monomers towards the preparation of semi-aromatic polyesters under comparatively mild reaction conditions.

3.2 Results and discussion

3.2.1 ROCOP of phthalic anhydride and limonene oxide

Based on our previous experience and success with Fe-centered aminotriphenolate complexes in the activation of sterically more demanding epoxide substrates,[58,59] we selected Fe-complex (**Fe^{MeMe}**) as activator and bis(triphenylphosphine)iminium chloride (PPNCl) as initiator[B],[31] of the ROCOP of phthalic anhydride PA and the trisubstituted monomer limonene oxide (commercial *cis*/*trans*-**1a**, *cis*/*trans* = 40:60) as benchmark reaction. For comparative reasons, we also employed Al(III) complex **Al^{MeMe}** and DMAP (4-dimethylamino-pyridine) as epoxide activator and initiator, respectively. We envisioned that the conformationally more flexible complexes **Fe^{MeMe}** and **Al^{MeMe}** should be able to mediate the alternating copolymerization of **1a** and PA under milder reaction conditions. Thus, initial trials were carried out at a relatively low reaction temperature of 65 ºC in various solvents (Table 3.1; entries 1–6) using first **Fe^{MeMe}** and DMAP at low loading (0.5 mol %).

Fortunately, the copolymerization of **1a** and PA proceeded though relatively slow and provided a high quality of poly(PA-*alt*-**1a**) under excellent control (≥ 98% ester bonds) and with reasonable molecular weight (M_n = 10.7 kg/mol; $Đ$ = 1.24). Interestingly, the isolated polymer from Table 3.1, entry 1 exhibited a high T_g value of 135 ºC which is significantly higher than the value reported by Duchateau and coworkers (82 ºC).[30] The use of PPNCl as initiator (

Table **3.1**, entry 2) gave fairly similar results in terms of M_n, $Đ$ and T_g data, but proved to be significantly faster. Then, other solvents (Table 3.1, entries 3–6; DCM, CH_3CN, DMF and toluene) were probed but these copolymerization attempts all gave poorer results.

Next we focused on further improving the formation of poly(PA-*alt*-**1a**) by performing the reactions under solvent-free conditions though using a larger excess of **1a** (Table 3.1, entries 7 and 8; 2 and 5 equiv, respectively). Particularly, the use of 2 equiv. of **1a** (Table 3.1, entry 7) gave full conversion of the PA in 24 h and the molecular weight and dispersity were comparable to the ones obtained in the solution phase process (Table 3.1, entry 2) despite the lower T_g value (115 ºC) measured. Alternatively, the use of **Al^{MeMe}** as catalyst for the solution phase copolymerization leading to poly(PA-*alt*-**1a**) (Table 3.1, entries 9–12) showed somewhat lower

[B] The choice for PPNCl as initiator is base done our recent observation that aliphatic polyesters are best prepared using this additive in the presence of complex **Fe^{MeMe}**.

PA conversions and inferior molecular weights compared to the use of **Fe^{MeMe}**, and therefore further studies were conducted using the latter complex.

Table 3.1 ROCOP of **1a** and PA using **Fe^{MeMe}** or **Al^{MeMe}** as catalysts and PPNCl or DMAP as initiators.[a] Nu stands for nucleophile.

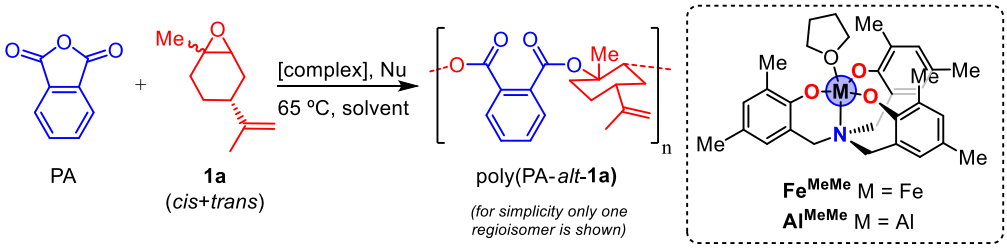

entry	complex	[Nu]	solv.	t (h)	conv.(%)[b]	M_n (Kg/mol)[c]	$Đ$[c,d]	T_g (°C)[e]
1	**Fe^{MeMe}**	DMAP	THF	48	92	10.7	1.24	135
2	**Fe^{MeMe}**	PPNCl	THF	24	84	10.5	1.24	131
3	**Fe^{MeMe}**	PPNCl	DCM	24	49	5.6	1.39	110
4	**Fe^{MeMe}**	PPNCl	Tol	24	46	5.6	1.28	111
5[f]	**Fe^{MeMe}**	PPNCl	DMF	24	10	–	–	–
6[f]	**Fe^{MeMe}**	PPNCl	ACN	24	25	–	–	–
7[g]	**Fe^{MeMe}**	PPNCl	–	24	>99	9.5	1.21	115
8[h]	**Fe^{MeMe}**	PPNCl	–	24	>99	5.5	1.24	95
9	**Al^{MeMe}**	DMAP	THF	48	87	4.3	1.24	104
10	**Al^{MeMe}**	PPNCl	THF	48	71	5.5	1.21	124
11[i]	**Al^{MeMe}**	DMAP	THF	48	62	8.0	1.24	120
12[i]	**Al^{MeMe}**	PPNCl	THF	48	46	6.9	1.26	124

[a]Reaction conditions: 1.5 mmol PA, [complex] = 0.50 mol%, [Nu] = 0.50 mol%, solvent (0.50 mL), T = 65 ºC, [PA]:[**1a**] = 1:1.1. [b]Conversion of PA determined by ^{1}H NMR ($CDCl_3$); selectivity for the alternating polymer ≥ 98%, regioselectivity not determined. [c]Determined by GPC in THF (30 ºC) using polystyrene standards for calibration. [d]$Đ = M_w/M_n$. [e]Determined by differential scanning calorimetry (DSC), the data refer to the second heating cycle. [f]Polymer not isolated. [g][PA]:[**1a**] = 1:2. [h][PA]:[**1a**] = 1:5. [i] 0.25 mol% [complex], 0.25 mol% [Nu].

3.2.2 ROCOP of various terpene oxides and phthalic anhydride

The use of various terpene oxides including *cis*/*trans*-LO **1a**, *cis*-LO **1b**, carene oxide (**3b**), menthene oxide (**3c**) and the bifunctional limonene dioxide (**3d**) was examined in the ROCOP using PA as the cyclic anhydride substrate. For comparative reasons, some of the best results obtained with the **1a** substrate (Table 3.1) are listed here as well (Table 3.2, entries 1 and 2).

While the use of *cis/trans* limonene oxide (**1a**) under attractive conditions (65 ºC, 0.50 mol% of both complex **Fe^{MeMe}** and PPNCl) provided appreciable molecular weight poly(PA-*alt*-**1a**), the ROCOP of **1b** (Table 3.2, entries 3 and 4) and PA gave a superior grade polyester with M_n values of up to 16.4 kg/mol. As observed throughout the copolymerization reactions, the solution phase experiments consistently gave better results in terms of polymer quality. Interestingly, the use of the diastereo-isomerically pure **1b** monomer resulted in a polyester with an improved and high T_g value of 141 ºC (Table 3.2, entry 3).

The promising results obtained using limonene oxide as a renewable terpene-based monomer in polyester synthesis prompted us to consider other terpene oxide monomers including those based on carene (carene oxide: **3b**) and menthene (menthene oxide: **3c**). Apart from these two monomers, we also selected cyclohexadiene oxide (**3a**; a monomer that can be derived from cyclohexadiene, a byproduct from oleochemical olefin metathesis),[52] and the bisepoxide from limonene (**3d**).[53,60,61] The most prominent results were obtained in the ROCOP using **3a** or **3c** as monomers (Table 3.2, entries 5–6 and 10–11, respectively). In the case of **3a**, high molecular weight poly(PA-*alt*-**3a**) was obtained up to 25 kg/mol ($Đ$ = 1.54) in the solution phase polymerization, though the reaction times required for high monomer (PA) conversion were typically longer (40–48 h; Table 3.2, entries 5 and 6) compared to the copolymerizations carried out with **1a** or **1b**. The highest T_g value (132 ºC) for poly(PA-*alt*-**3a**) is slightly above the value reported by Williams, Meier and coworkers (T_g = 128 ºC, M_n = 7.5 kg/mol, $Đ$ = 1.17)[52] despite the much higher molecular weights produced by our binary catalyst system **Fe^{MeMe}**/PPNCl.

The conversion of the bulky monomer carene oxide (**3b**) was a challenge and long reaction times were needed for high PA conversion under solution phase conditions (Table 3.2, entry 7). Though a shorter reaction time was required when applying bulk copolymerization (Table 3.2, entry 8), a higher reaction temperature was needed (95 ºC). The solution phase experiment provided slightly better quality poly(PA-*alt*-**3b**) (M_n = 3.7 kg/mol, $Đ$ = 1.39) with a relatively high T_g value of 130 ºC. The use of menthene oxide (**3c**) in the ROCOP process provided poly(PA-*alt*-**3c**) grades with molecular weights of up to 12.7 kg/mol (Table 3.2, entries 9–11)

and to our delight a very high T_g of 165 ºC (see **Error! Reference source not found.**, b). As far as we know, this is the highest T_g value reported for a semi-aromatic polyester based on PA.

Table 3.2 ROCOP of various terpene oxides and PA using **Fe^{MeMe}** as catalyst and PPNCl as initiator.

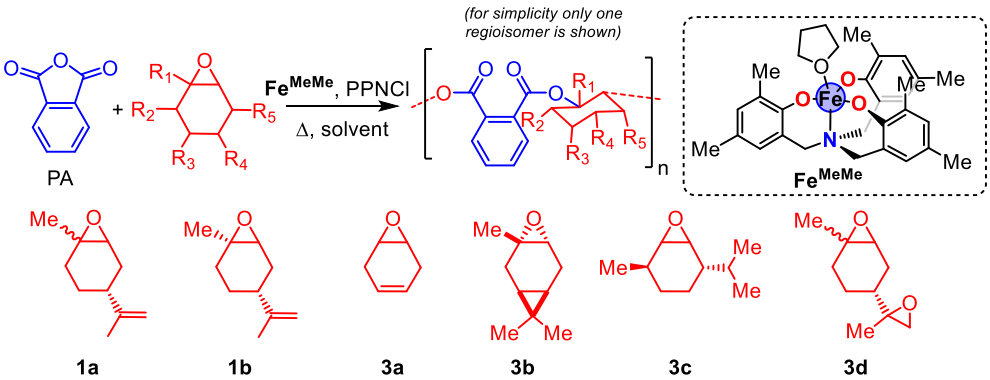

entry	epox.	Solv.	t (h)	conv.(%)[b]	M_n (Kg/mol)[c]	$Đ$[c,d]	T_g (°C)[e]
1	**1a**	THF	24	84	10.5	1.24	131
2[f]	**1a**	–	24	>99	9.5	1.21	115
3	**1b**	THF	24	>99	16.4	1.33	141
4[f]	**1b**	–	24	>99	9.2	1.44	129
5	**3a**	THF	40	85	24.9	1.54	132
6	**3a**	–	48	>99	19.6	1.42	105
7	**3b**	THF	100	79	3.7	1.39	130
8[f,g]	**3b**	–	48	89	3.3	1.52	112
9	**3c**	THF	24	56	3.2	1.24	155
10[f]	**3c**	–	24	75	5.1	1.28	161
11[f,h]	**3c**	–	72	75	12.7	1.20	165
12[i]	**3d**	THF	24	33	8.7	1.94	59
13[i]	**3d**	–	24	52	6.7	2.41	53

[a]Reaction conditions: 1.5 mmol PA, 0.50 mol% [**Fe^{MeMe}**], 0.50 mol% [PPNCl], solvent (0.50 mL), T = 65 ºC unless stated otherwise, [PA]:[Epox.] = 1:1.1. [b]Conversion of PA determined by ^{1}H NMR ($CDCl_3$); selectivity for the alternating polymer ≥ 98%, regioselectivity not determinated. [c]Determined by GPC in THF (30 ºC) using polystyrene standards for calibration. [d]$Đ = M_w/M_n$. [e]Determined by differential scanning calorimetry (DSC), the data refer to the second heating cycle. [f][PA]:[epox] = 1:2. [g]Reaction performed at 95 ºC. [h] 0.3 mol% [**Fe^{MeMe}**], 0.3 mol% [Nu] [i]Reaction performed at 45 ºC.

The bifunctional monomer limonene dioxide (**3d**; Table 3.2, entries 12 and 13) was also copolymerized with PA to afford poly(PA-*alt*-**3d**) at low reaction temperature (45 ºC): at higher reaction temperatures insoluble (presumably highly cross-linked materials) were produced. Though reasonable molecular weights of 6.7 and 8.7 kg/mol were attained for poly(PA-*alt*-**3d**), the polydispersities for these copolymers were quite high ($Đ$ = 1.9–2.4) which can be attributed to a low degree of control over the site-specific alternating copolymerization with PA in this bifunctional monomer. Apparently, when the copolymerization of **3d** and PA is carried out at 45 ºC using the binary system **Fe^{MeMe}**/PPNCl both epoxide groups are involved in "at random" ester formation reactions and no site-specific selectivity can be induced. Importantly, all polyesters described in Table 3.2 exhibited decomposition onsets (T_d^{10}) typically 110–120 ºC higher than their respective T_g values[C] which should allow to easily process these polyesters in coating preparations.

Figure 3.1. Selected regions of the DSC traces of (a) poly(PA-*alt*-**1a**), Table 3.2, entry 1, (b) poly(PA-*alt*-**3c**), Table 3.2, entry 11 (c) poly(NA-*alt*-**CHO**), Table 3.3, entry 1 and (d) poly(NA-*alt*-**1a**), Table 3.3, entry 5. In all cases, the traces refer to the second heating cycle.

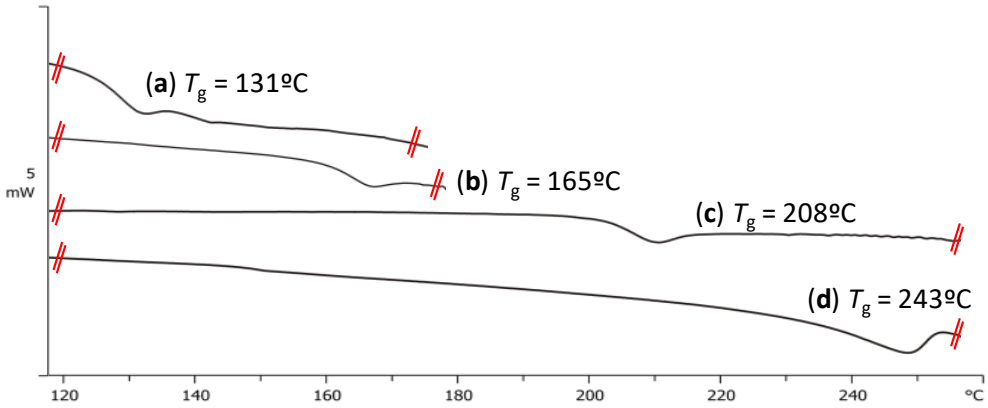

[C] See section 3.2.5 "*Thermogravimetric analysis of polymers*" in this chapter.

3.2.3 ROCOP of cyclohexene oxide and limonene oxide with 1,8-naphthalic anhydride

Having successfully developed high T_g semi-aromatic polyesters based on various terpene monomers, we then selected a more rigid and commercially available cyclic anhydride (1,8-naphthalic anhydride, NA) and investigated the ROCOP with both cyclohexene oxide **CHO** and limonene oxide **1a** (Table 3.3).

Table 3.3 ROCOP of **CHO** or *cis/trans*-**1a** and 1,8-naphthalic anhydride (NA) using **Fe^{MeMe}** as catalyst and PPNCl as initiator.

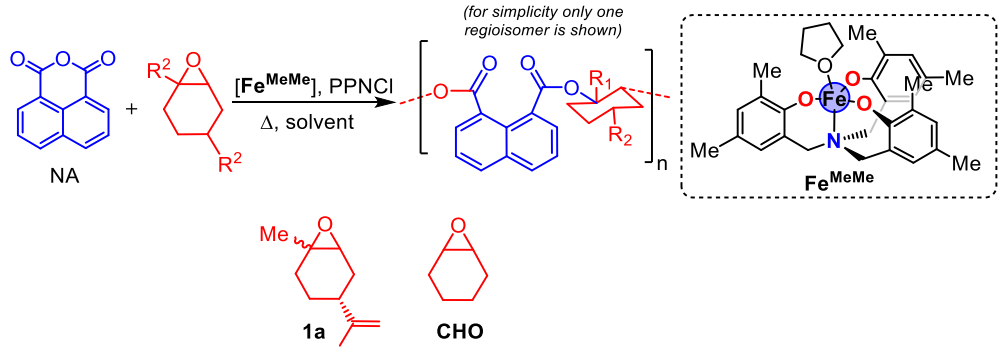

entry	epox.	solv.	T (°C)	t (h)	conv.(%)[b]	M_n (Kg/mol)[c]	$Đ$[c,d]	T_g (°C)[e]
1	**CHO**	THF	65	72	79	11.4	1.25	208
2	**CHO**	DCM	65	72	>99	2.5	2.35	182
3	**CHO**	Tol	65	72	31	2.3	1.81	190
4[f]	**CHO**	–	95	72	>99	6.9	1.71	182
5	**1a**	THF	65	72	50	2.2	1.36	243
6[f]	**1a**	–	95	72	50	1.6	1.52	227

[a]Reaction conditions: 1.5 mmol NA, solvent (0.50 mL), [NA]:[epox.] = 1:1.1, [Fe^{MeMe}]: 0.50 mol%, PPNCl: 0.50 mol%. [b]Conversion of NA determined by ^{1}H NMR ($CDCl_3$); selectivity for the alternating polymer ≥ 98%, regioselectivity not determined. [c]Determined by GPC in THF (30 °C) using polystyrene standards for calibration. [d]$Đ = M_w/M_n$. [e]Determined by differential scanning calorimetry (DSC), the data refer to the second heating cycle. [f][NA]:[LO] = 1:2.

In principle, the more rigid character of NA should provide increased rigidity in alternating polyesters, and first copolymerization experiments were conducted with the more reactive monomer **CHO** (Table 3.3, entries 1–4) under catalysis of the binary system **Fe^{MeMe}**/PPNCl at

65 ºC. The use of a solvent in these copolymerization experiments was warranted due to the rather insoluble nature of the NA. The solution phase reactions carried out with **CHO** and NA were performed in THF, DCM and toluene and compared with the bulk polymerization at an elevated reaction temperature (Table 3.3, entry 4, 95 ºC). As may be expected for the coupling of the sterically more crowded anhydride NA, in all cases the copolymerization was comparatively slow and longer reaction times were needed for high NA conversion. Under these conditions, the use of toluene was not beneficial as only a rather low NA conversion of 31% was achieved in 72 h. The use of DCM facilitated much higher NA conversion but the polyester quality (Table 3.3, entry 2; M_n = 2.5 kg/mol, $Đ$ = 2.35) was significantly lower than observed when THF was used as solvent (Table 3.3, entry 1; M_n = 11.4 kg/mol, $Đ$ = 1.25). Remarkably, the glass transitions determined for these poly(NA-*alt*-**CHO**) were high and the T_g´s of these polymers reached up to 208 ºC (**Error! Reference source not found.**, c). Despite the fact that the bulk copolymerization (Table 3.3, entry 4) provided quantitative NA conversion, the polymer properties of the poly(NA-*alt*-**CHO**) were inferior to the ones from the solution phase ROCOP of **CHO** and NA carried out in THF.

Next, the use of **1a** was probed and similar reactions conditions as reported in Table 3.3, entries 1 and 4 were taken as a starting point towards the preparation of poly(NA-*alt*-**1a**) (*cf.*, Table 3.3, entries 5 and 6). As opposed to the use of **CHO**, the lower reactive **1a** monomer provides only moderate NA conversion of around 50% in 72 h, and low molecular weights of up to 2.2 kg/mol with a calculated degree of polymerization (DP) of 7. However, the analysis of the thermal behavior of these oligomeric macromolecules reveals a high level of rigidity as testified by the T_g values of up to 243 ºC (see **Error! Reference source not found.**, d). Thus, by a proper selection of terpene oxide and anhydride monomers the glass transitions of semi-aromatic polyesters can be tuned over a wide range spanning more than 100 ºC.

3.2.4 MALDI-TOF analysis of polyesters

As we expected, most polymers showed major distributions attributable to α,ω-Cl,OH end-groups and monomodal GPC traces. Poly(PA-*alt*-**3a**) (Table 3.2, entry 5) and poly(NA-*alt*-**CHO**) (Table 3.3, entry 1) show bimodal GPC traces which two distinct distributions. The higher molecular weight distribution shows the presence of polymeric species with a molecular weight roughly two times higher (2X) than the ones found within the other distribution (X). We propose that (X) is attributable to chains intiated by chloride (α,ω-Cl,OH end-groups), whereas the other distribution of higher molecular weight (2X) is assigned to chains initiated by adventitious

water,[31] or chain shuttling leading to polymer chains with *α,ω*-OH,OH terminal groups having roughly a double molecuar weight compared to those initiated by chloride.[D]

MALDI-TOF-MS analysis of poly(PA-*alt*-**3a**) (Table 3.2, entry 5) and poly(NA-*alt*-**CHO**) (Table 3.3, entry 1) are shown in

Figure **3.2** and Figure **3.3**. Only one distribution was found for these two samples and their relatively high molecular weight [M_n = 24.9 Kg/mol for poly(PA-*alt*-**3a**) and M_n = 11.4 Kg/mol for poly(NA-*alt*-**CHO**)] did not allow to obtain better quality MALDI spectra.

Figure 3.2 MALDI-TOF mass spectrum of polyester poly(NA-*alt*-**CHO**).

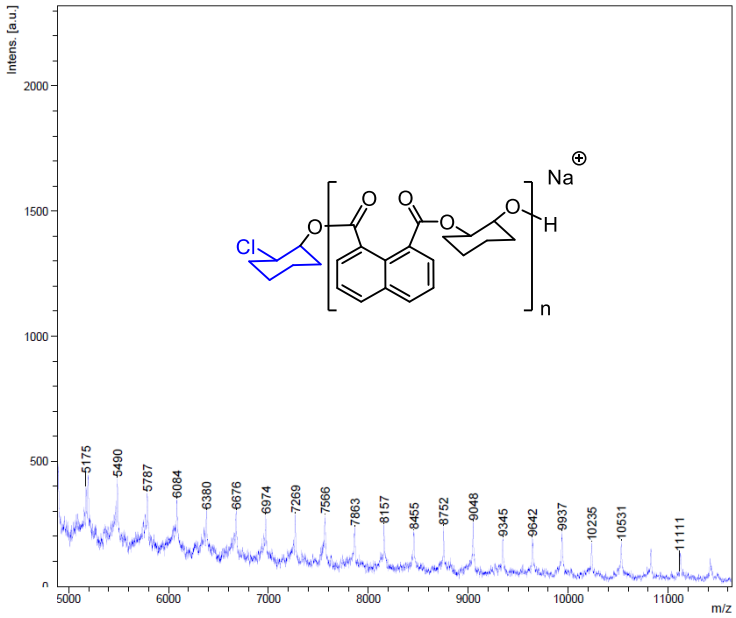

The MALDI-TOF spectrum for poly(NA-*alt*-**CHO**) in

Figure **3.2** shows a major distribution attributable to *α,ω*-Cl,OH end-groups. Contrary, polymer poly(PA-*alt*-**3a**) shows a major distribution with ω-OH end-groups (Figure 3.3). This end-group could be generated through a MPVO reaction[E] of the starting **3a** epoxide:[30,62] another possibility is the elimination of chloride from these polymers by a polymer alkoxide.[31]

[D] For a detailed explanation of initiation by water and chain shuttling with water, we refer to section 2.2.4 "*Comparison of GPC traces*" in Chapter 2.
[E] For a detailed explanation of MPVO reaction, we refer to section 2.2.5 "*MALDI-TOF-MS analysis*" in Chapter 2 where the mechanism is explained in more detail.

Figure 3.3 MALDI-TOF mass spectrum of polyester poly(PA-*alt*-**3a**)

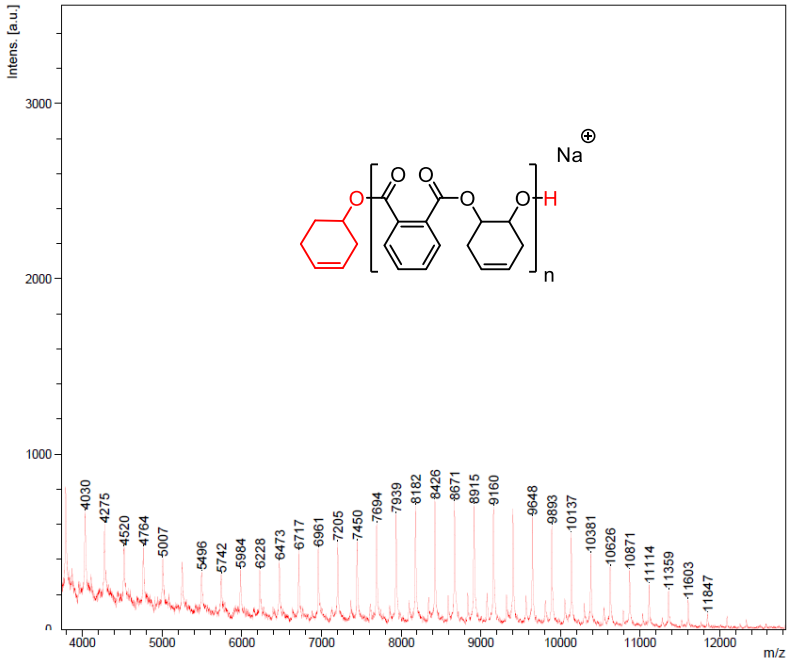

3.2.5 Thermogravimetric analysis of polymers

Samples prepared under the conditions reported in

Table **3.2** and Table **3.3** were analyzed using a Mettler Toledo Thermogravimetric Analyzer (TGA), model TGA/SDTA851. The heating program was 20 ºC to 500 ºC at 10 ºC/min under a nitrogen atmosphere. The onset thermal decomposition temperatures are reported in Table 3.4. It can be clearly deduced that the decomposition temperatures T_d^{10} are significantly higher (typically >100ºC) than the corresponding T_g values, an aspect of importance for potential practical applications and polymer processing.

Table 3.4 Thermal degradation data for all polymers.

Polymer	Sample	T_d^{10} (°C)[a]
Poly(PA-*alt*-**1a**)	Table 3.2, entry 1	255
Poly(PA-*alt*-**1b**)	Table 3.2, entry 3	258
Poly(PA-*alt*-**3a**)	Table 3.2, entry 5	309
Poly(PA-*alt*-**3b**)	Table 3.2, entry 7	210
Poly(PA-*alt*-**3c**)	Table 3.2, entry 11	297
Poly(PA-*alt*-**3d**)	Table 3.2, entry 12	298
Poly(NA-*alt*-**CHO**)	Table 3.3, entry 1	330
Poly(NA-*alt*-**1a**)	Table 3.3, entry 5	268

[a] Reported T_d data refer to T_d^{10} values at 10% wt loss.

3.3 Conclusions

In summary, we present here an effective catalyst based on a Fe(III) complex (**Fe^{MeMe}**) that mediates the ROCOP of various renewable/terpene oxides and cyclic anhydrides giving access to semi-aromatic polyesters with molecular weights of up to 25 kg/mol, low polydispersities and typically excellent chemo-selectivity control with exclusive ester bond formation (≥98% ester bonds). Moreover, the polyesters formed from limonene oxide, cyclohexadiene oxide and menthene oxide show promise towards the formation of highly rigid phthalate-based polymers with T_g´s of up to 165 ºC and T_d^{10} values at least 110–120 ºC above the determined glass transitions. The use of the highly rigid monomer naphthalic anhydride further allowed for tuning the glass transition behavior of these partially renewable polyesters to values far beyond 200 ºC.

The used ROCOP catalyst is a rare case of a system that can effectively produce terpene oxide based polyesters for which the T_g´s can be tuned over a wide and high temperature range. The thermal properties of the developed polyesters should be of interest towards the formation of di-block copolymers of potential importance in coatings for a range of (new) applications.

3.4 Experimental section

3.4.1. General considerations

All water sensitive operations were carried out under nitrogen atmosphere using an Mbraun glovebox, standard vacuum-line and Schlenk techniques. Solvents were purchased from Sigma-Aldrich (HPLC grade) and dried using an MBraun MBSPS800 purification system. All reagents were purchased from commercial suppliers (Aldrich and Acros) and used as received.

NMR spectra were recorded on a Bruker AV-400 spectrometer and referenced to the residual NMR solvent signals. Assignment of the signals in the NMR spectra of all polyesters was based on 2D NMR experiments.

Glass transition temperatures (T_g) were measured under an N_2 atmosphere using a Mettler Toledo equipped, model DSC822e. Samples were weighed into 40 μL aluminum crucibles and subjected to three heating cycles at a heating rate of 5 ºC/min. Thermo-gravimetric analyses were recorded under a N_2 atmosphere using Mettler Toledo equipment (model TGA/SDTA851) with a heating rate of 10 °C/min. Gel permeation chromatography (GPC) measurements were performed in tetrahydrofuran at 40 ºC at a flow rate of 1 mL·min^{-1}. Samples were analyzed at a concentration of 3 mg·mL^{-1} after filtration through a 0.45 μm pore-size membrane. The

separation was carried out on three polystyrene/divinylbenzene columns from Agilent: PLgel 5 μm MIXED-C, 300 × 7.5 mm. The setup (Viscotek TDA305) was equipped with a refractive index (RI) detector (λ = 670 nm). M_n, M_w and M_w/M_n ($Đ$) were derived from the RI signal by a calibration curve based on polystyrene standards (PS from Polymer Standards Service) for the analysis of the polymers. GPC measurements for the polymers were performed by the Instituto de Ciencia y Tecnologia de Polímeros de Madrid.

Matrix-assisted laser desorption/ionization time-of-flight mass spectrometry (MALDI-TOF) was performed by the Research Support Group at ICIQ on a BRUKER Autoflex spectrometer using dithranol as a matrix and CF_3COONa as an additive.

3.4.2 Reagents and catalysts

The anhydride substrates PA and NA are commercially available and were used after purification (recrystallization from hot chloroform) and dried under vacuum for 24 h.

Commercially available initiators bis(triphenylphosphine)iminium chloride, PPNCl, and 4-dimethylaminopyridine, DMAP, were purified by recrystallization from dichloromethane and dried under vacuum at 40 ºC for 24 h. The complexes **Fe^{MeMe}**[56] and **Al^{MeMe}** [63,64] were prepared following previously reported procedures.[F] Limonene oxide (*cis* and *trans* mixture), cyclohexene oxide, cyclohexadiene oxide, 3-carene and (-)-menthol were purchased from Aldrich.

Cyclohexadiene oxide (CHDO, **3a**),[65] carene oxide (CA, **3b**)[66] and limonene dioxide (LDO, **3d**)[60,61] were synthesized from their alkene precursors which are commercially available. CHDO **3a** was synthesized from 1,4-cyclohexadiene, while CA **3b** was obtained after the epoxidation of 3-carene. LDO **3d** was synthesized using the *cis/trans* limonene oxide mixture commercially available. Menthene oxide (MEO) was obtained from (−)-menthol and prepared following literature procedures.[53]

3.4.2 Synthesis of epoxides

Limonene oxide (**1a**) (*cis/trans* mixture 40:60) and cyclohexene oxide (**CHO**) are commercially available. *Cis*-limonene oxide (**1b**) was isolated from the commercially available *cis/trans* limonene oxide mixture through kinetic resolution.[67][G]

[F] For more information see section 1.4.2 "*Synthesis of complexes*" in chapter 1.
[G] Kinetic resolution of *cis*-LO is described in section 1.4.5 "*Kinetic resolution of cis- and trans-1,2-limonene oxide*" in Chapter 1.

Synthesis of menthene from (-)-menthol

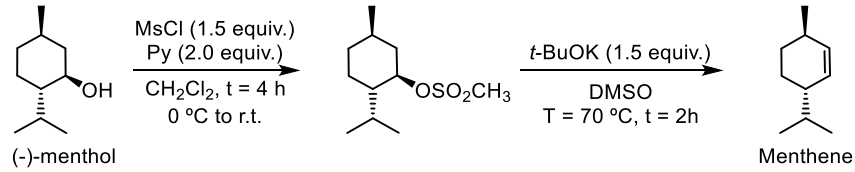

Step 1*:* 12.0 g (77 mmol, 1.0 equiv) of (–)-menthol was solubilized in 40 mL of CH_2Cl_2 and added dropwise to a solution containing 12 mL (154 mmol, 2.0 equiv) of pyridine and 9 mL (115.5 mmol, 1.5 equiv.) of methansulfonyl chloride dissolved in 40 mL of CH_2Cl_2; the solution was kept at 0 ºC. The resulting mixture was allowed to reach r.t. while kept under vigorous stirring, until formation of a white precipitate was observed (t = 4 h). The reaction mixture was then concentrated at a rotary evaporator, obtaining a white paste. The paste was suspended in 100 mL of AcOEt and washed with 2 × 20 ml HCl 1 M, 1 × 20 mL sat. aq. $NaHCO_3$ and 1 × 20 ml of brine. The organic phase was dried over $MgSO_4$, concentrated at a rotary evaporator and dried *in vacuo* (heating at T = 90 ºC), obtaining 17.6 g (75 mmol) of menthyl mesylate (98 %). The product was used for the following step without additional purification.

Step 2: Menthyl mesylate was dissolved into 60 mL of DMSO and the solution kept at T = 0 ºC. Then 12.8 g (113 mmol, 1.5 equiv) of *t*-BuOK was added in small portions. Once the *t*-BuOK was completely added, the mixture was heated at 50 ºC for 24 h, obtaining an orange gel. Once cooled, the quasi-solid gel was disrupted adding 110 mL of deionized H_2O and isolating the organic phase. The aqueous solution was further extracted with 3 × 80 mL of pentane; the combined organic phases were washed with 1 × 100 mL of brine. The organic phase was dried over $MgSO_4$, filtered and concentrated at a rotary evaporator to yield 8.9 g (64 mmol) of 3-isopropyl-6-methylcyclohex-1-ene as a pale yellow oil with a strong mint smell (85 %). The product was used for the following step (general epoxidation method) without additional purification.

General epoxidation method

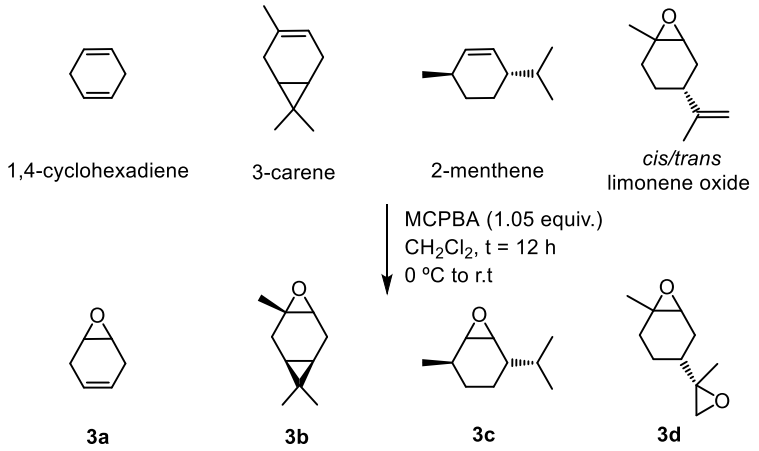

1 g of the respective alkene was dissolved into CH_2Cl_2 (40 mL) and cooled to 0 ºC. Then metachloroperbenzoic acid (1.2 equiv.) was slowly added to the solution. The solution was left stirring for 12 h at ambient temperature. The solution was washed with 1 M Na_2SO_3 (3 × 30 mL, 1 M), a saturated solution of $NaHCO_3$ (3 × 30 mL) and brine. The organic phase was dried over sodium sulfate and the product obtained after removal of the solvent *in vacuo* (rotary evaporator).

Drying process of epoxides

The epoxides were stirred over freshly ground CaH_2 for one night, vacuum distilled onto a new portion of freshly ground CaH_2 in a dry roundbotton flask with Strauss adapter, stirred one day and then vacuum distilled again before being degassed by three freeze–pump–thaw cycles. After that, they were stored in a glove box *prior to* use.

3.4.3 Procedure for the ROCOP reactions.

All reaction mixtures were prepared in a glove box under moisture-free conditions. The catalyst (metal complex and initiator) and 1.5 mmol of the corresponding anhydride were placed in an oven-dried 4 mL vial equipped with a magnetic stir bar. The appropriate amount of epoxide and solvent were added and the vial was sealed with a Teflon-lined cap. The reaction mixture was then removed from the glove box and placed in an aluminum heating block preheated at the desired reaction temperature. The reaction progress was monitored by ^1H NMR spectroscopy. After the ROCOP reaction, the volatiles were removed under vacuum. The crude product was dissolved in a minimal amount of dichloromethane and precipitated with a solution of HCl (1

M) in methanol. This latter procedure was repeated three times and finally the polymer was washed with methanol (three times) and dried under vacuum.

3.4.4 ^{1}H and ^{13}C NMR analysis of epoxides

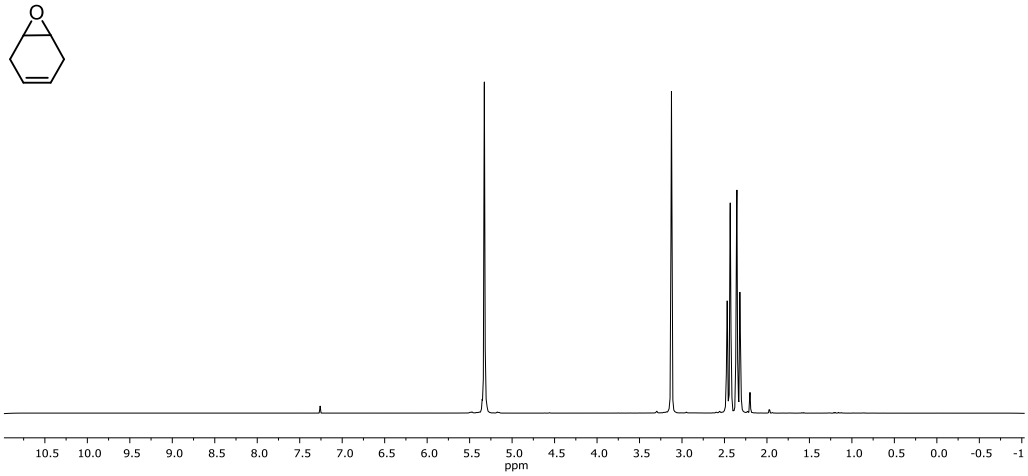

^{1}H NMR (400 MHz, $CDCl_3$) δ = 5.43 (s, 2H), 3.24 (s, 2H), 2.50 (m, 4H).

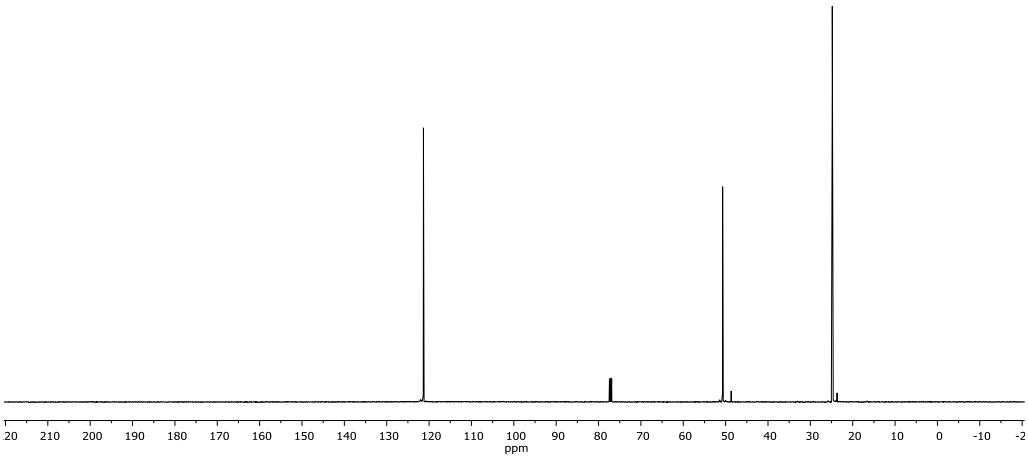

^{13}C NMR (126 MHz, $CDCl_3$) δ = 121.33, 50.70, 24.82.

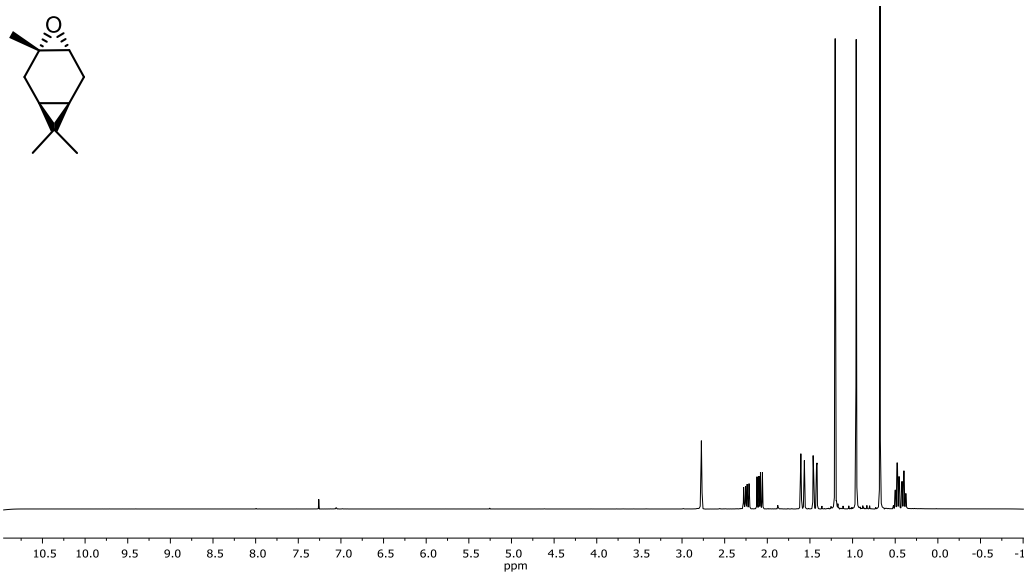

^{1}H NMR (400 MHz, $CDCl_3$) δ = 2.84 (s, 1H), 2.30 (dd, *J* = 9.1, 18.4 Hz, 1H), 2.15 (dd, *J* = 9.2, 16.1 Hz, 1H), 1.65 (dd, *J* = 2.3, 16.5 Hz, 1H), 1.51 (dd, *J* = 2.3, 16.2 Hz, 1H), 1.27 (s, 3H), 1.03 (s, 3H), 0.75 (s, 3H), 0.55 (td, *J* = 2.3, 9.1 Hz, 1H), 0.47 (td, *J* = 2.2, 9.1 Hz, 1H).

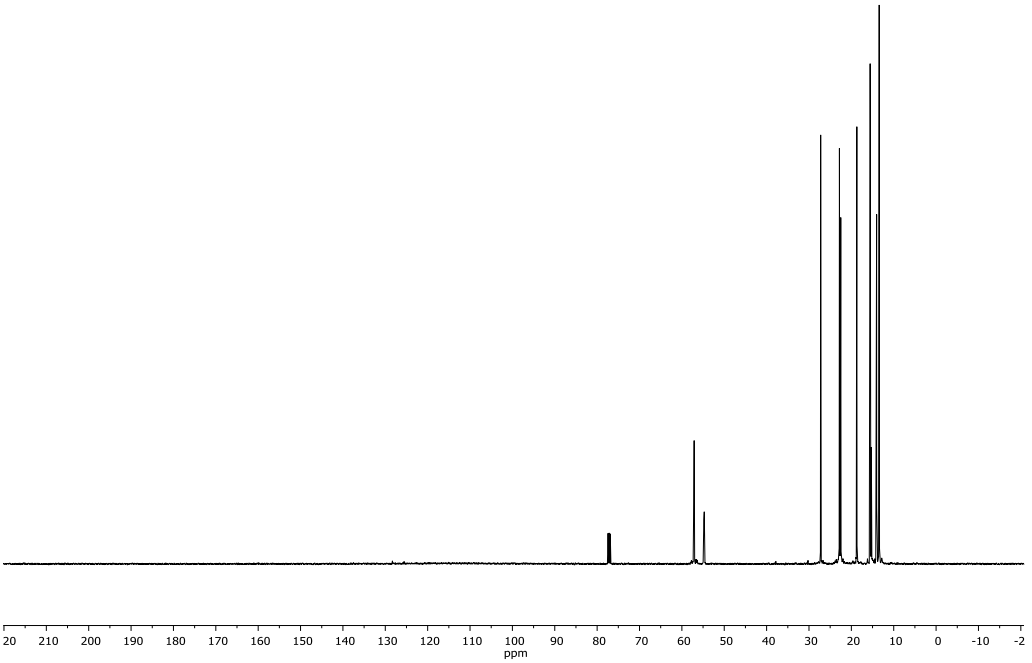

^{13}C NMR (126 MHz, $CDCl_3$) δ 57.18, 54.72, 27.24, 22.82, 22.50, 18.71, 15.56, 15.28, 14.04, 13.43.

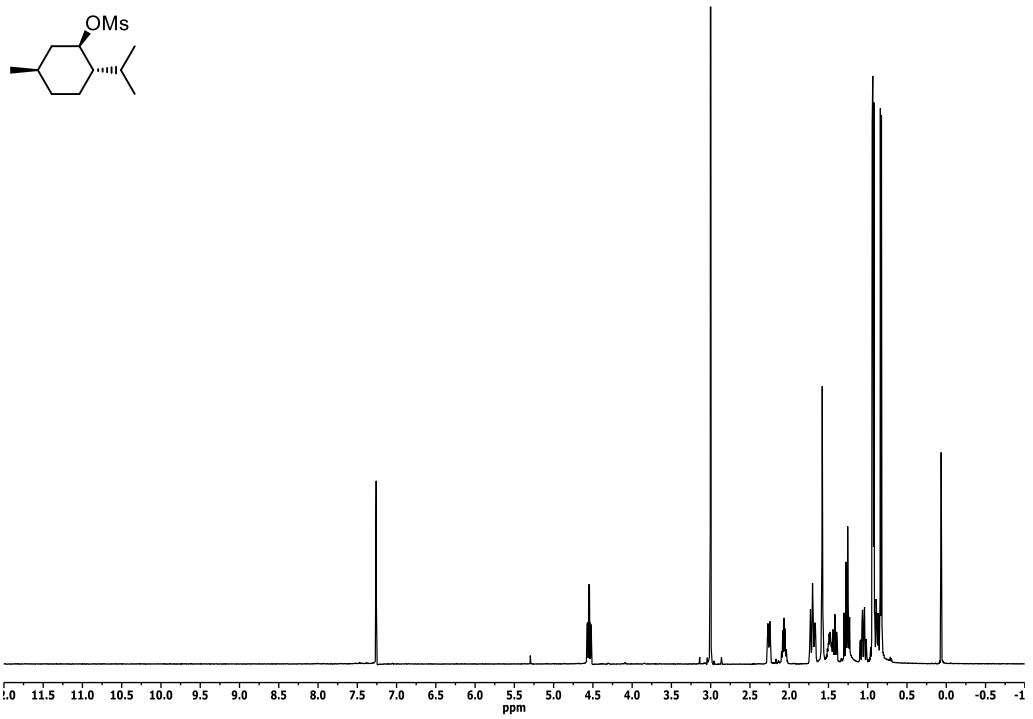

^{1}H NMR (500 MHz, $CDCl_3$): δ = 4.55 (d, *J* = 4.6, 10.9 Hz, 1H), 3.00 (s, 3H), 2.26 (m, 1H), 2.07 (m, 1H), 1.70 (m, 2H), 1.37-1.53 (m, 2H), 1.21-1.31 (m, 2H), 1.06 (m, 1H), 0.93 (dd, *J* = 4.2, 6.8 Hz, 6H), 0.83(t, *J* = 6.9 Hz, 3H).

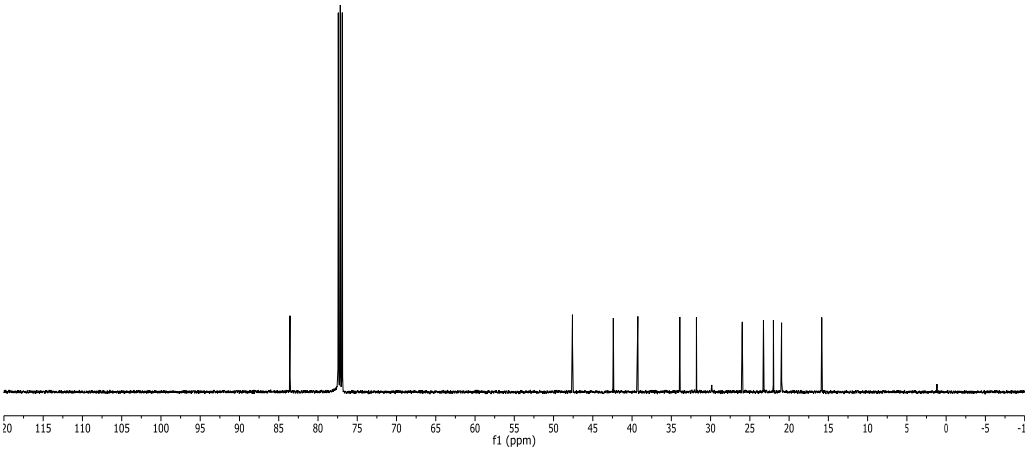

^{13}C NMR (125 MHz, $CDCl_3$): δ = 83.6, 47.6, 42.4, 39.3, 33.9, 31.8, 26.0, 23.7, 22.0, 21.0, 15.8.

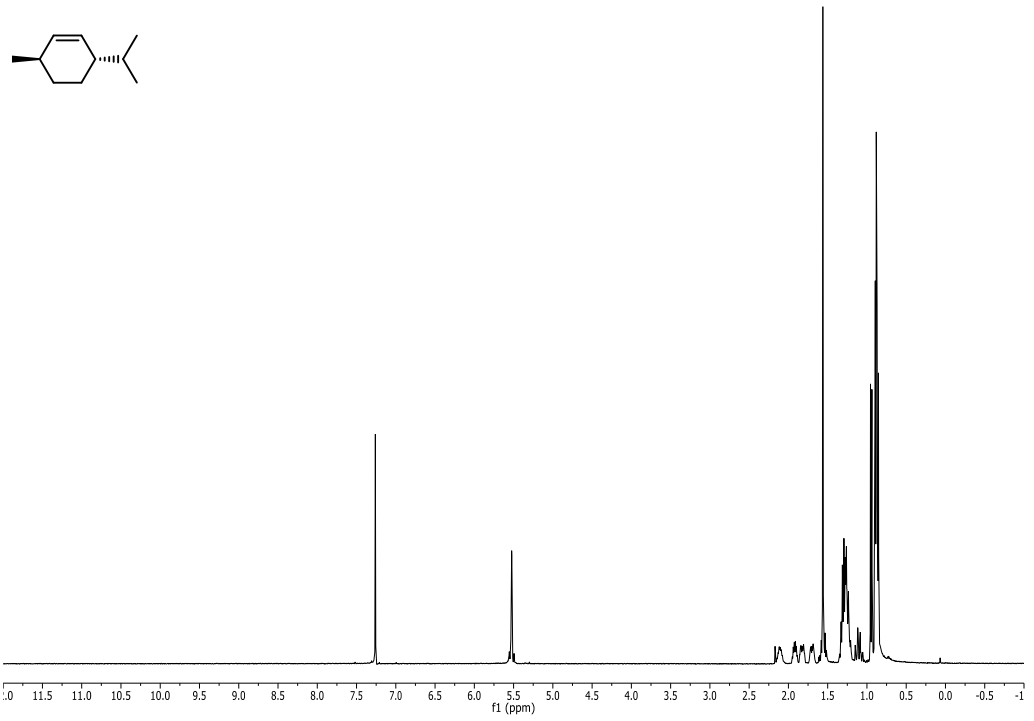

^{1}H NMR (500 MHz, $CDCl_3$): δ 5.52 (m, 2H), 2.04-2.17 (m, 1H), 1.77-1.97 (m, 2H), 1.65-1.75 (m, 1H), 1.19-1.26 (m, 2H), 1.06-1.18 (m, 1H), 0.95 (d, *J* = 7.0 Hz, 3H).

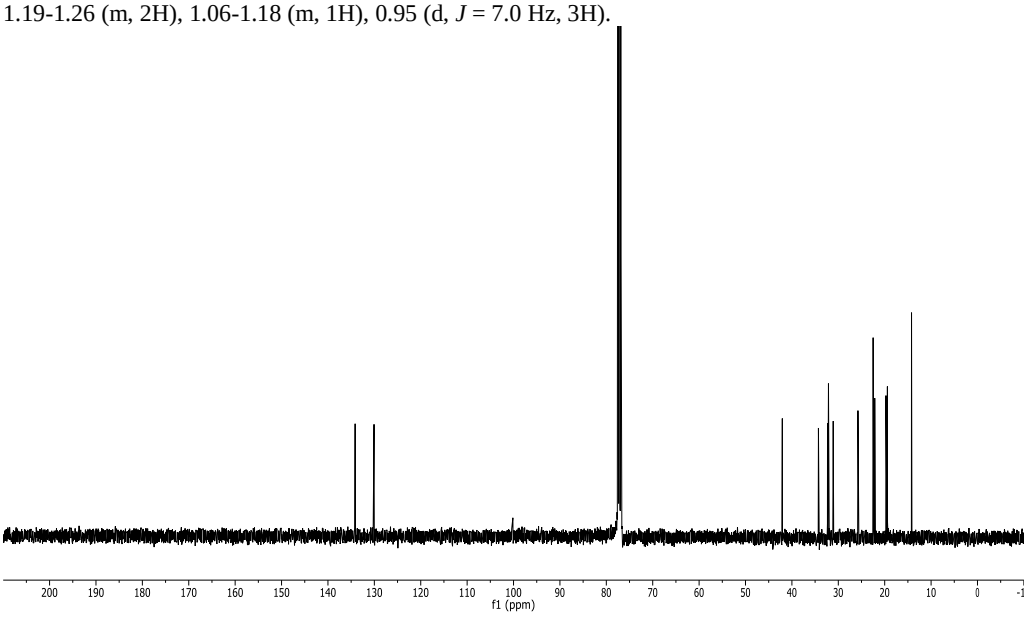

^{13}C NMR (125 MHz, $CDCl_3$): δ = 134.1, 130.0, 42.1, 34.3, 32.3, 31.6, 25.7, 22.1, 19.7, 19.4.

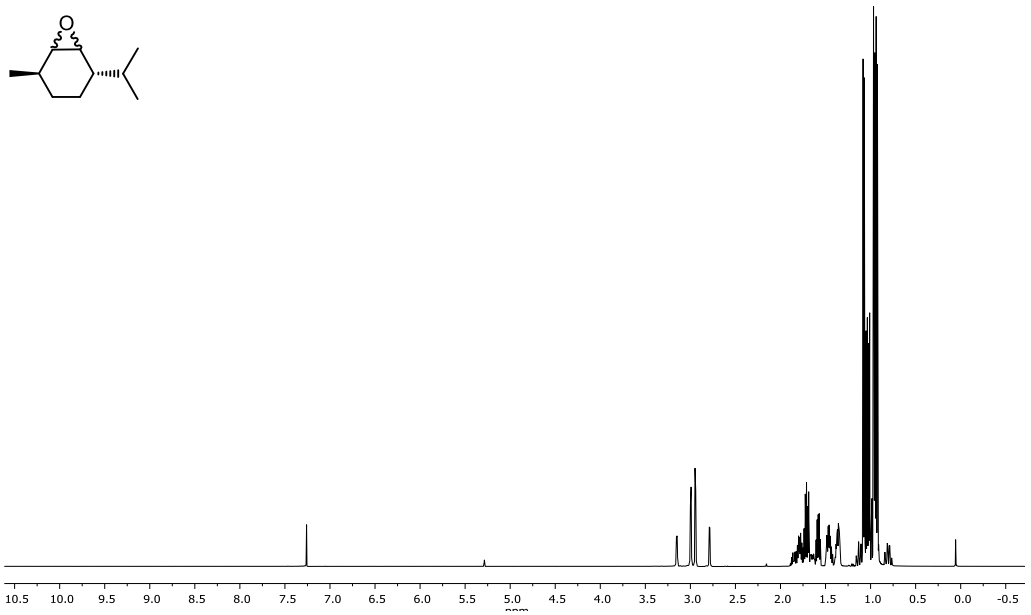

^{1}H NMR (500 MHz, $CDCl_3$): δ = 2.56–3.46 (m, 2H), 1.20–1.84 (m, 7H), 1.04 (d, *J* = 6.8 Hz, 3H), 0.95 (d, *J* = 7.0 Hz, 3H), 0.92 (d, *J* = 7.0 Hz, 3H). The *trans/cis* ratio was 72:28 by NMR integration.

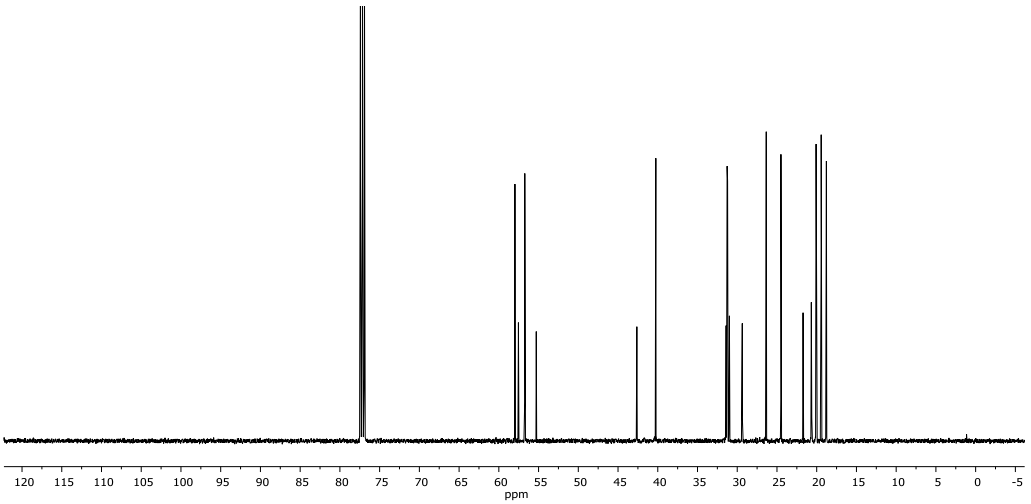

^{13}C NMR (125 MHz, $CDCl_3$; major isomer): δ = 58.1. 56.9, 40.8, 31.7, 31.6, 26.9, 24.9, 20.3, 19.6, 19.0. *minor cis*: 57.7, 55.4, 43.0, 31.9, 31.4, 30.0, 22.1, 20.9, 20.8, 20.2.

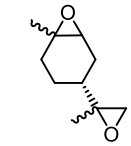

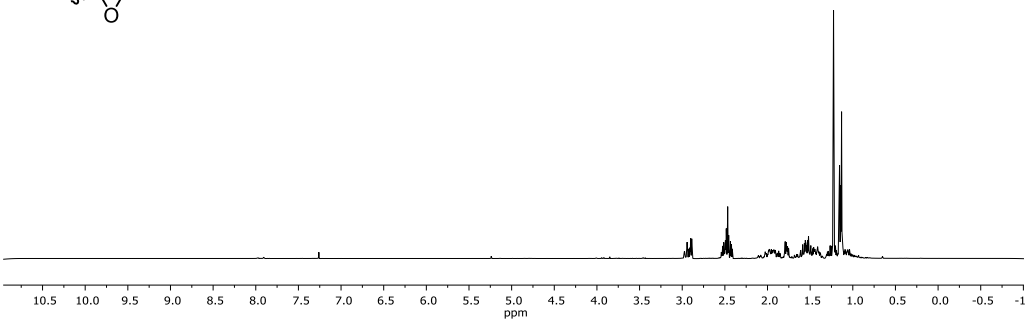

^{1}H NMR (400 MHz, $CDCl_3$) δ:3.06–2.93 (m, 1H), 2.65–2.46 (m, 2H), 2.22–1.33 (m, 6H), 1.30 (s, 3H), 1.26–0.96 (m, 4H). Note: mixture of isomers.

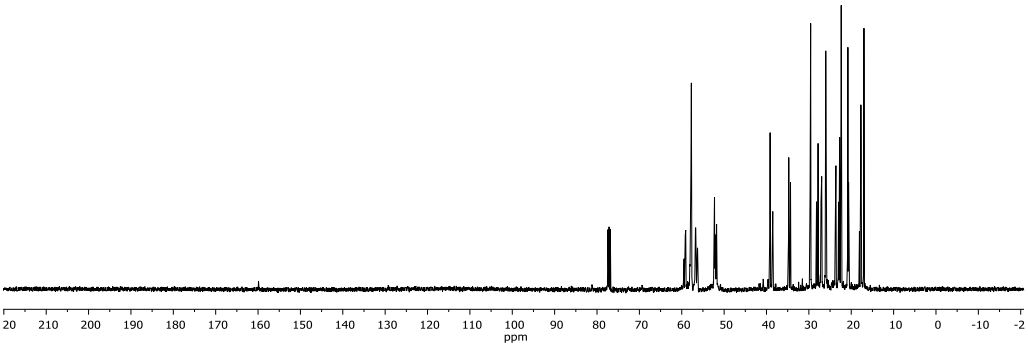

^{13}C NMR (126 MHz, $CDCl_3$) δ 59.38, 58.08, 57.07, 52.70, 52.57, 52.34, 52.06, 39.50, 38.83, 35.05, 34.64, 29.88, 28.50, 28.13, 27.27, 26.32, 23.92, 23.30, 23.05, 22.67, 21.09, 18.36, 18.03, 17.92, 17.30. Note: mixture of isomers.

3.4.5 Assigned ^{1}H and ^{13}C NMR spectra of polymers[H]

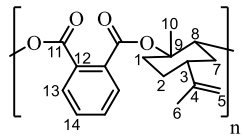

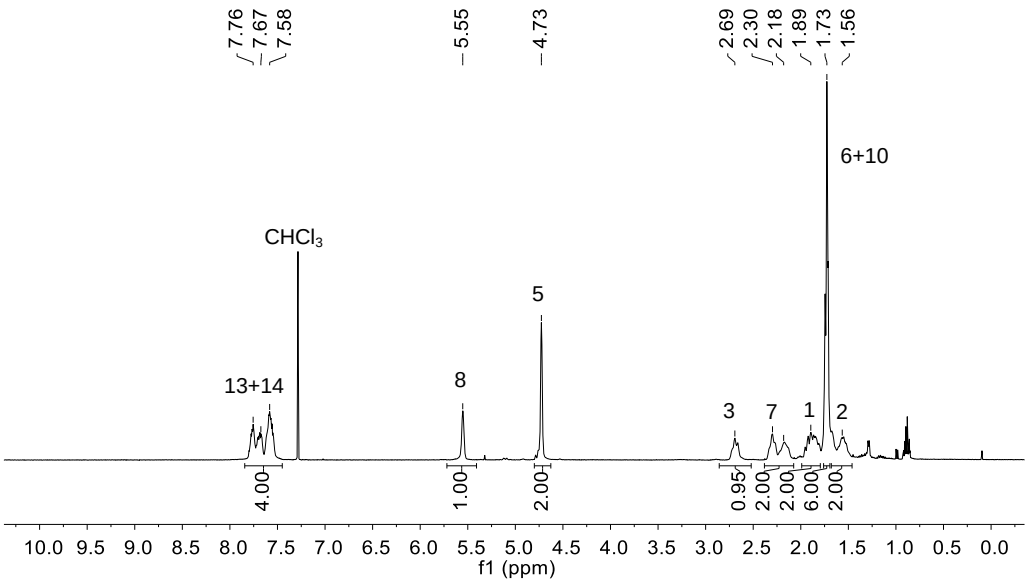

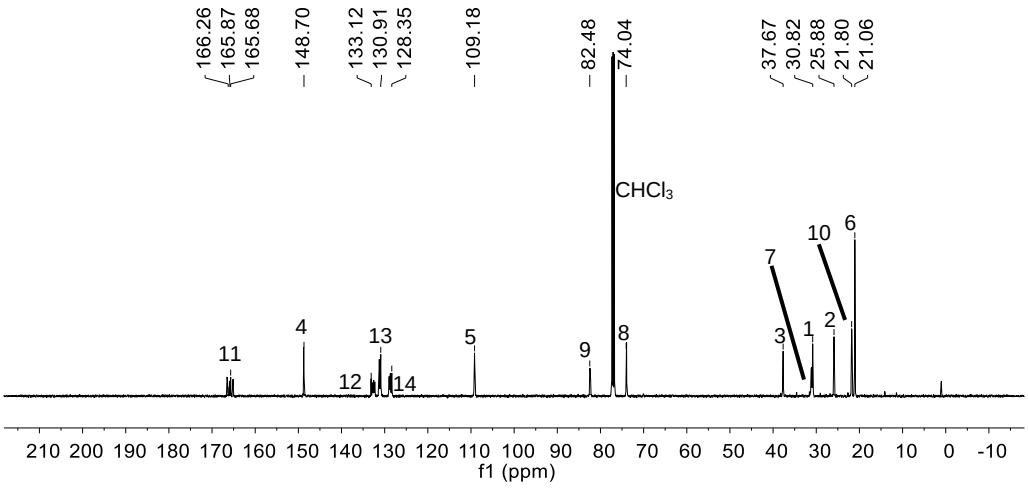

[H] Note that while there are multiple regioisomeric repeat units possible for most of the polymers [poly(PA-*alt*-**1a**), poly(PA-*alt*-**1b**), poly(PA-*alt*-**3b**), poly(PA-*alt*-**3c**), poly(PA-*alt*-**3d**) and poly(NA-*alt*-**1a**)], the peaks are overlapping and for simplicity only one of these isomeric repeat unit is drawn.

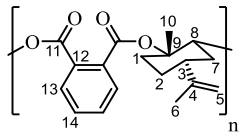
O
O
O
O
10
9
8
11
12
1
7
13
2
3
4
5
6
14
n

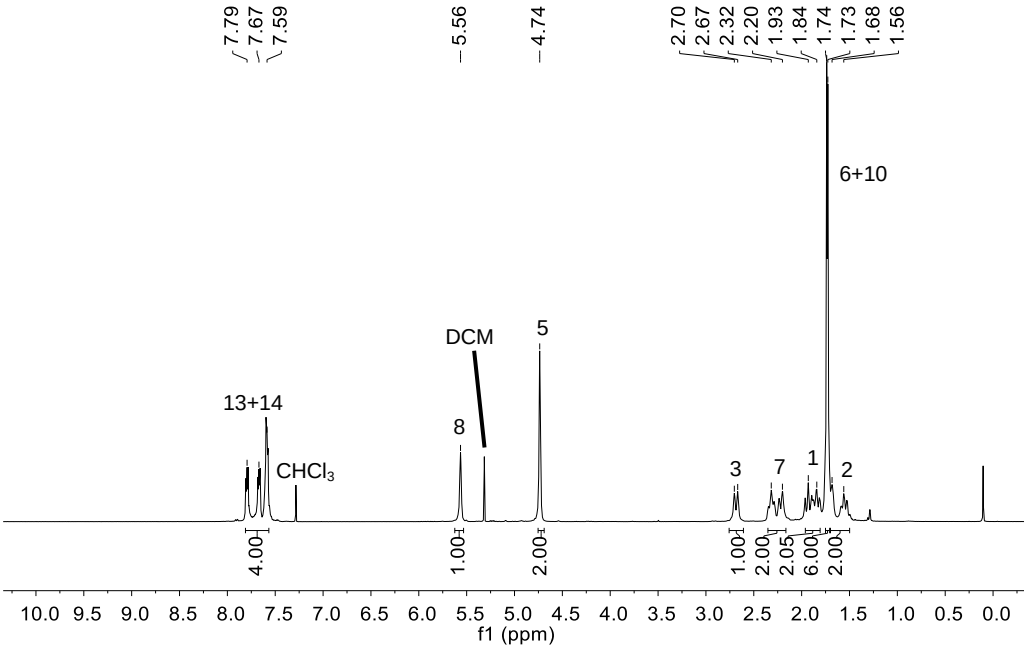
7.79
7.67
7.59
5.56
4.74
2.70
2.67
2.32
2.20
1.93
1.84
1.74
1.73
1.68
1.56
6+10
DCM
5
13+14
8
CHCl3
3
7
1
2
4.00
1.00
2.00
1.00
2.00
2.05
6.00
2.00
10.0 9.5 9.0 8.5 8.0 7.5 7.0 6.5 6.0 5.5 5.0 4.5 4.0 3.5 3.0 2.5 2.0 1.5 1.0 0.5 0.0
f1 (ppm)

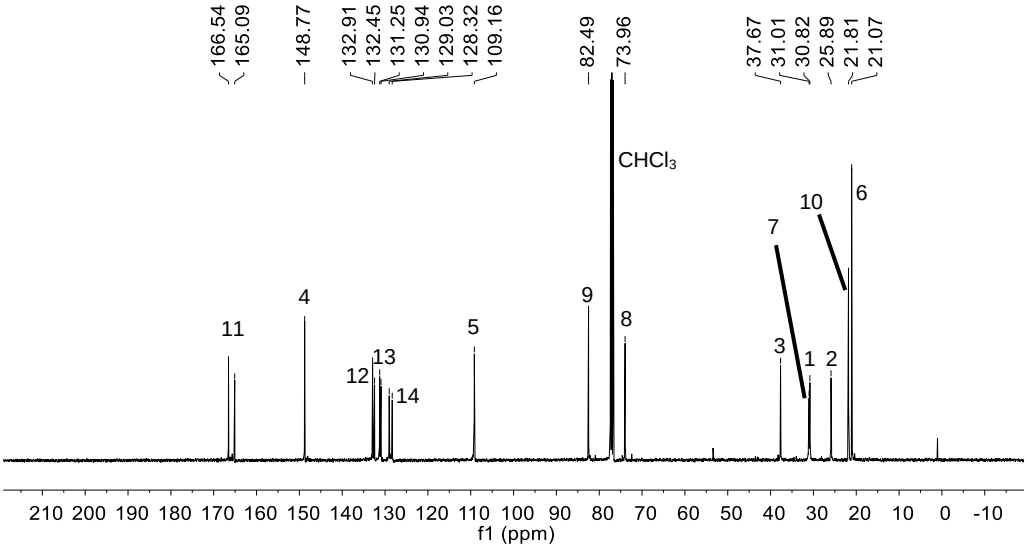
166.54
165.09
148.77
132.91
132.45
131.25
130.94
129.03
128.32
109.16
82.49
73.96
37.67
31.01
30.82
25.89
21.81
21.07
CHCl3
10
6
7
11
4
9
8
5
3
1
2
12
13
14
210 200 190 180 170 160 150 140 130 120 110 100 90 80 70 60 50 40 30 20 10 0 -10
f1 (ppm)

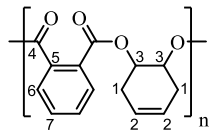
O
O
O
O
4
5
3
3
6
1
1
7
2
2
n

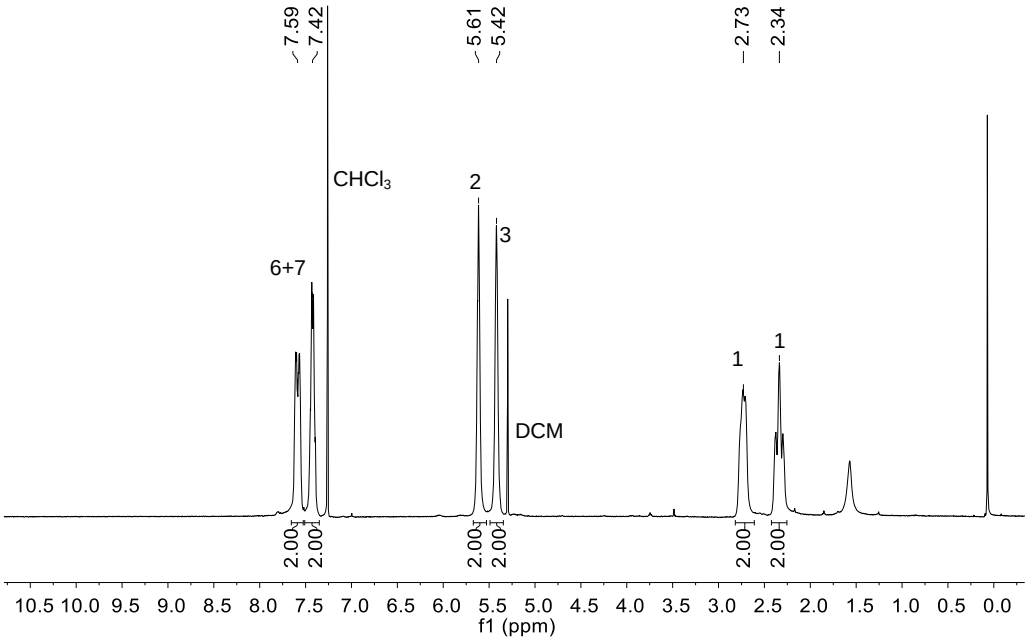
7.59
7.42
5.61
5.42
2.73
2.34
CHCl3
6+7
2
3
1
1
DCM
2.00
2.00
2.00
2.00
2.00
2.00
10.5 10.0 9.5 9.0 8.5 8.0 7.5 7.0 6.5 6.0 5.5 5.0 4.5 4.0 3.5 3.0 2.5 2.0 1.5 1.0 0.5 0.0
f1 (ppm)

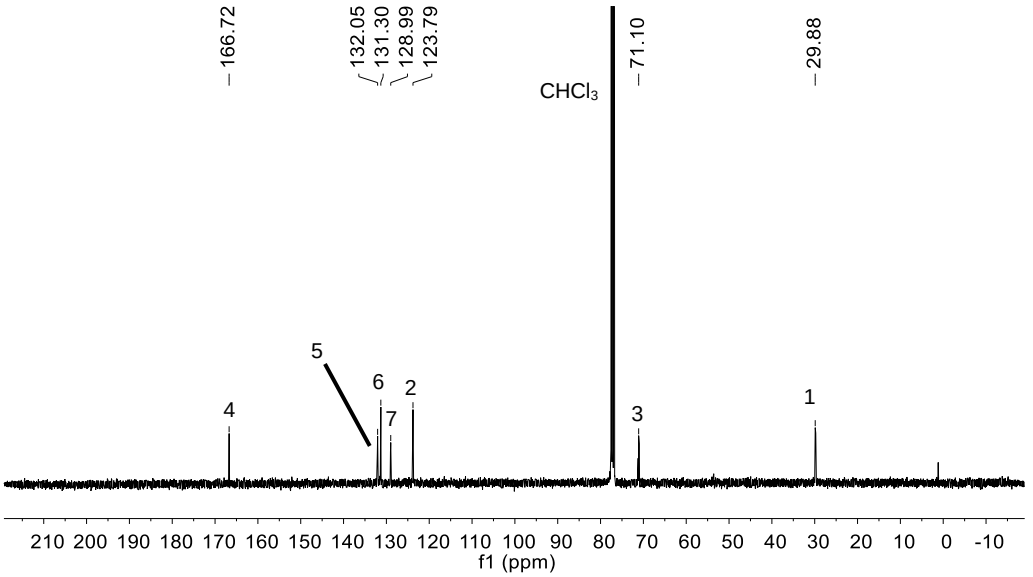
166.72
132.05
131.30
128.99
123.79
CHCl3
71.10
29.88
5
6
2
4
7
3
1
210 200 190 180 170 160 150 140 130 120 110 100 90 80 70 60 50 40 30 20 10 0 -10
f1 (ppm)

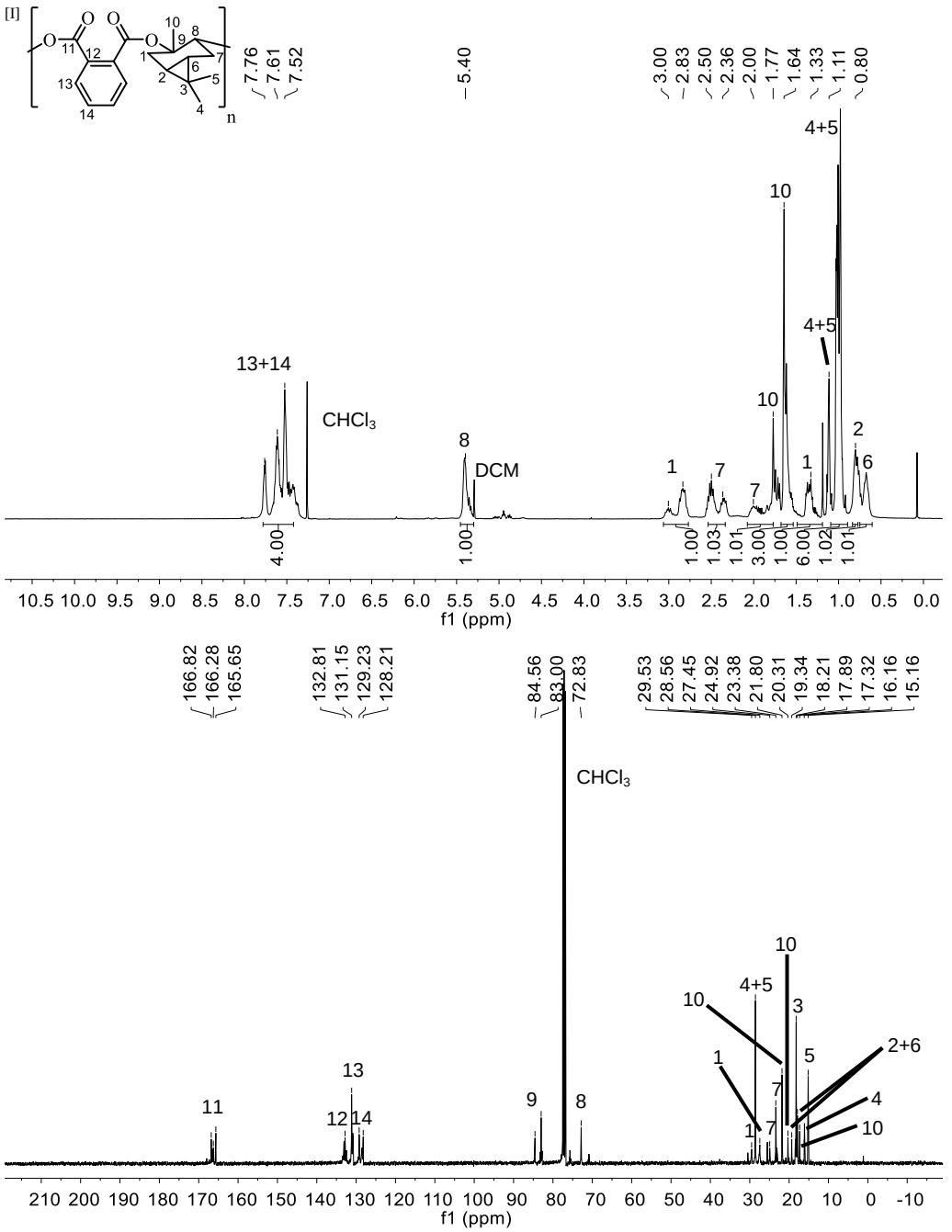

[I] The much lower molecular weight obtained for poly(PA-*alt*-**3b**) allows for detection of end-groups around 5.0 ppm.

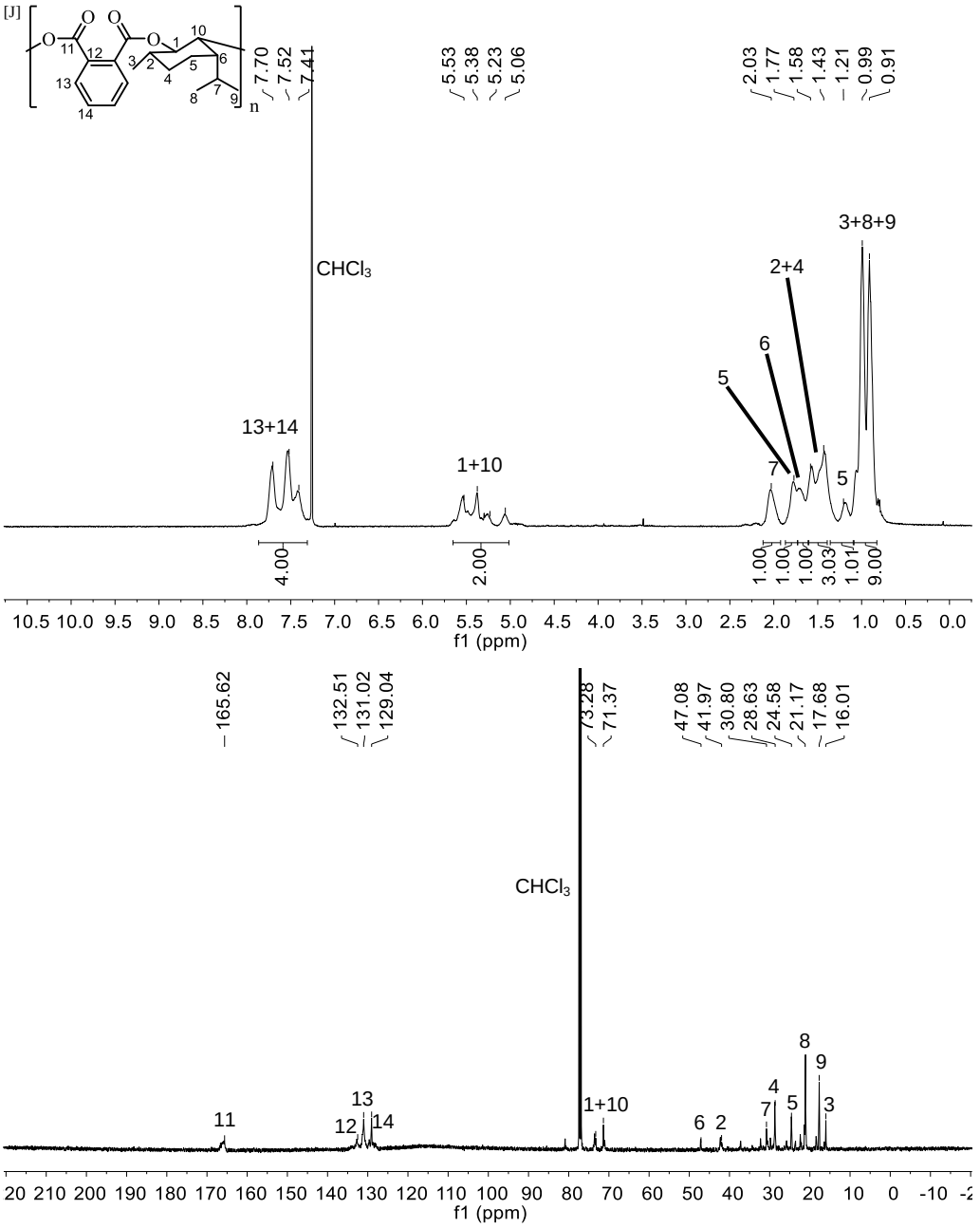

[J] After epoxidation of menthene, two diastereoisomers of **3c** are formed in an approximate 3:1 ratio. This feature is clearly maintained in the repeat units of the poly(PA-*alt*-**3c**) and the observed broadening of the peaks in the region 5.0–5.6 ppm is a result of protons **1** and **10** being inequivalent due to the asymmetric nature of the menthene backbone.

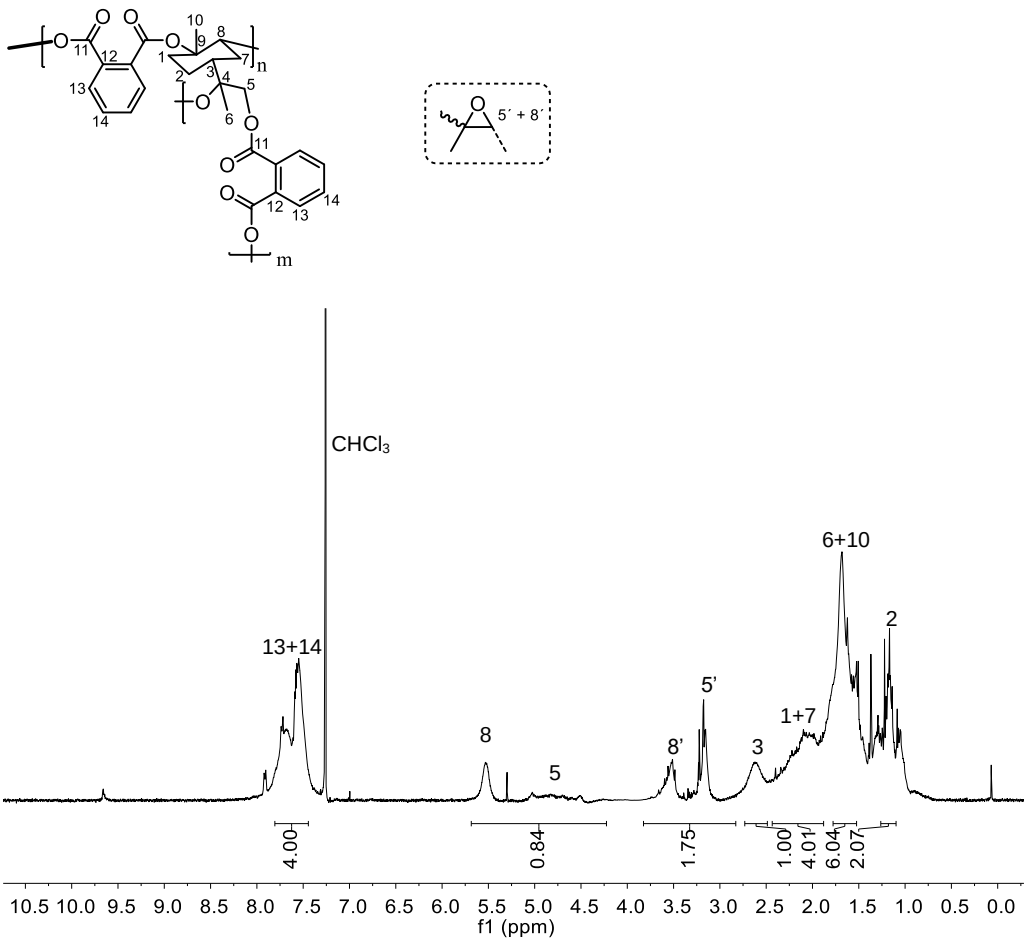
CHCl3
13+14
8
5
8'
5'
3
1+7
6+10
2
4.00
0.84
1.75
1.00
4.01
6.04
2.07
10.5 10.0 9.5 9.0 8.5 8.0 7.5 7.0 6.5 6.0 5.5 5.0 4.5 4.0 3.5 3.0 2.5 2.0 1.5 1.0 0.5 0.0
f1 (ppm)
5´ + 8´

Semi-aromatic polyesters derived from renewable terpene oxides with high glass transitions

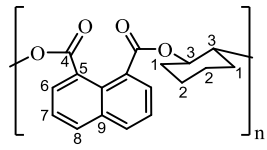

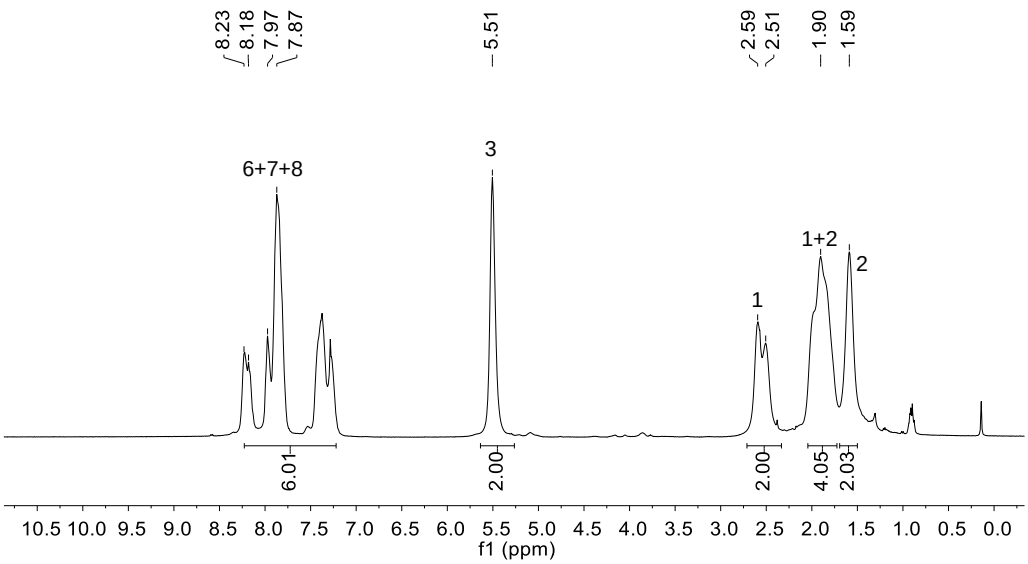

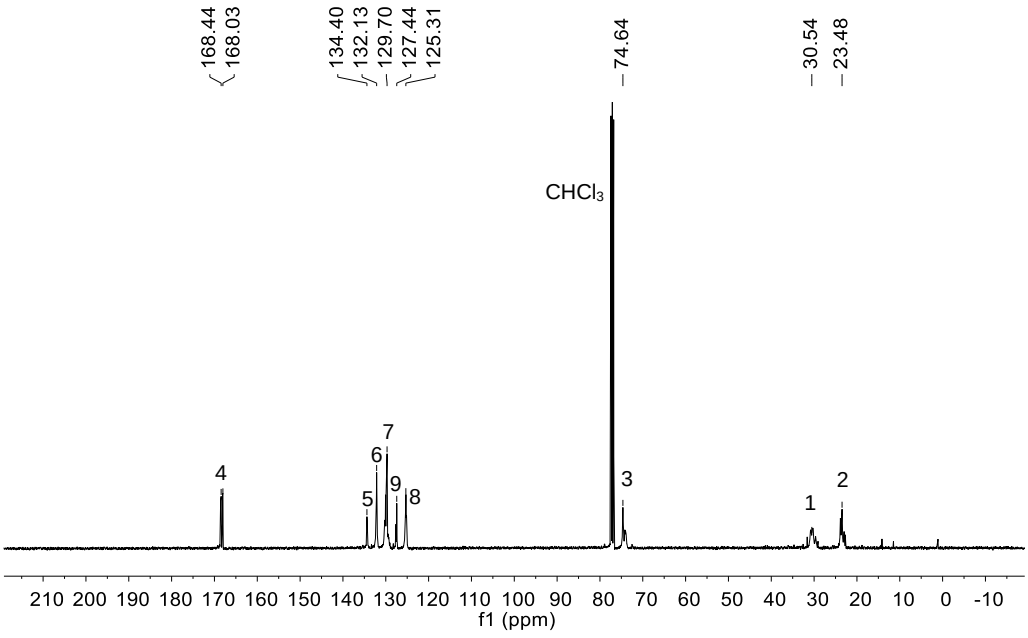

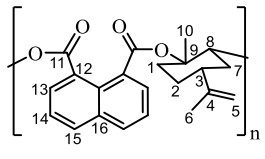
O
O
O
O
10
9
8
11
12
1
7
13
2
3
14
6
4
5
16
15
n

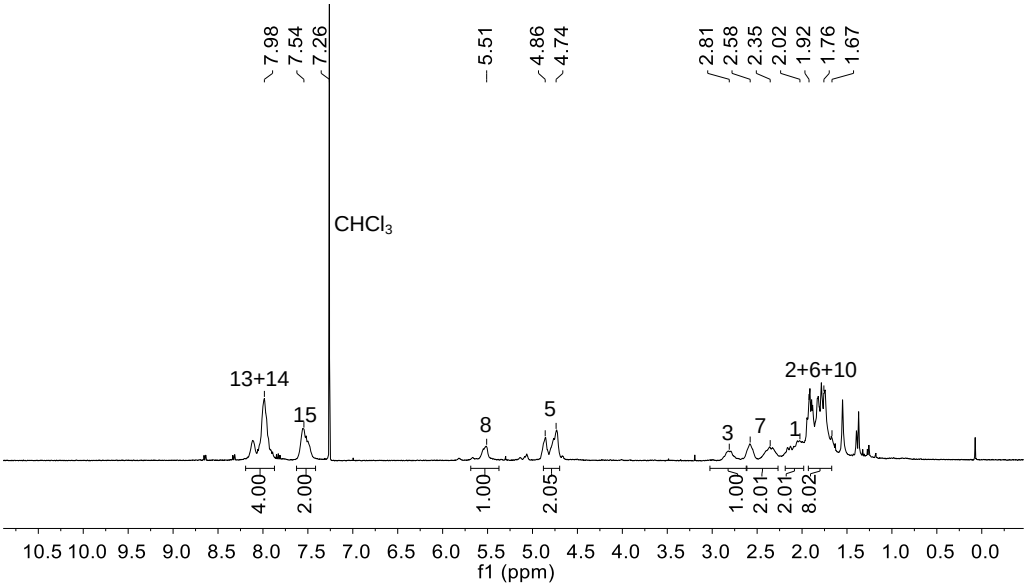
7.98
7.54
7.26
5.51
4.86
4.74
2.81
2.58
2.35
2.02
1.92
1.76
1.67
CHCl3
13+14
15
8
5
3
7
1
2+6+10
4.00
2.00
1.00
2.05
1.00
2.01
2.01
8.02
10.5 10.0 9.5 9.0 8.5 8.0 7.5 7.0 6.5 6.0 5.5 5.0 4.5 4.0 3.5 3.0 2.5 2.0 1.5 1.0 0.5 0.0
f1 (ppm)

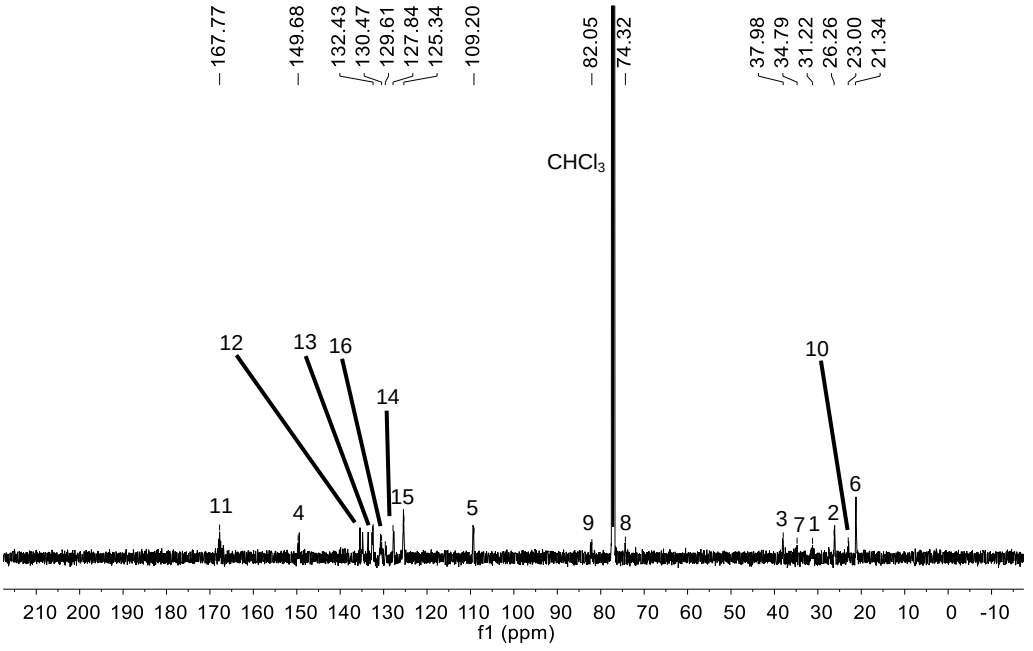
167.77
149.68
132.43
130.47
129.61
127.84
125.34
109.20
82.05
74.32
37.98
34.79
31.22
26.26
23.00
21.34
CHCl3
12
13
16
14
10
11
4
15
5
9
8
3
7
1
2
6
210 200 190 180 170 160 150 140 130 120 110 100 90 80 70 60 50 40 30 20 10 0 -10
f1 (ppm)

3.5 References

[1] E. L. Kunkes, D. A. Simonetti, R. M. West, J. C. Serrano-Ruiz, C. A. Gartner, J. A. Dumesic, *Science* **2008**, *322*, 417–421.

[2] G. W. Huber, S. Iborra, A. Corma, *Chem. Rev.* **2006**, *106*, 4044–4098.

[3] M. Besson, P. Gallezot, C. Pinel, *Chem. Rev.* **2014**, *114*, 1827–1870.

[4] P. C. a. Bruijnincx, B. M. Weckhuysen, *Nat. Chem.* **2014**, *6*, 1035.

[5] M. A. Hillmyer, W. B. Tolman, *Acc. Chem. Res.* **2014**, *47*, 2390–2396.

[6] M. G. A. Vieira, M. A. da Silva, L. O. dos Santos, M. M. Beppu, *Eur. Polym. J.* **2011**, *47*, 254–263.

[7] D. J. a Cameron, M. P. Shaver, *Chem. Soc. Rev.* **2011**, *40*, 1761–1776.

[8] H. Tian, Z. Tang, X. Zhuang, X. Chen, X. Jing, *Prog. Polym. Sci.* **2012**, *37*, 237–280.

[9] A. P. Gupta, V. Kumar, *Eur. Polym. J.* **2007**, *43*, 4053–4074.

[10] C. K. Williams, *Chem. Soc. Rev.* **2007**, *36*, 1573–1580.

[11] H. R. Kricheldorf, *Chem. Rev.* **2009**, *109*, 5579–5594.

[12] L. Jasinska, C. E. Koning, *J. Polym. Sci. Part A Polym. Chem.* **2010**, *48*, 5907–5915.

[13] D. J. Darensbourg, *Chem. Rev.* **2007**, *107*, 2388–2410.

[14] H.-W. Engels, H.-G. Pirkl, R. Albers, R. W. Albach, J. Krause, A. Hoffmann, H. Casselmann, J. Dormish, *Angew. Chem. Int. Ed.* **2013**, *52*, 9422–9441.

[15] L. N. Ji, *Appl. Mech. Mater.* **2013**, *312*, 406–410.

[16] J. Zhao, H. Schlaad, in *Bio-Synthetic Polym. Conjug.* (Ed.: H. Schlaad), Springer Berlin Heidelberg, Berlin, Heidelberg, **2013**, pp. 151–190.

[17] M. Firdaus, L. Montero de Espinosa, M. A. R. Meier, *Macromolecules* **2011**, *44*, 7253–7262.

[18] E. Grau, S. Mecking, *Green Chem.* **2013**, *15*, 1112–1115.

[19] P. A. Wilbon, F. Chu, C. Tang, *Macromol. Rapid Commun.* **2013**, *34*, 8–37.

[20] C. M. Byrne, S. D. Allen, E. B. Lobkovsky, G. W. Coates, *J. Am. Chem. Soc.* **2004**, *126*, 11404–11405.

[21] O. Hauenstein, S. Agarwal, A. Greiner, *Nat. Commun.* **2016**, *7*, 11862.

[22] O. Hauenstein, M. Reiter, S. Agarwal, B. Rieger, A. Greiner, *Green Chem.* **2016**, *18*, 760–770.

[23] L. Peña Carrodeguas, J. González-Fabra, F. Castro-Gómez, C. Bo, A. W. Kleij, *Chem. - Eur. J.* **2015**, *21*, 6115–6122.

[24] C. Li, R. J. Sablong, C. E. Koning, *Angew. Chem. Int. Ed.* **2016**, *55*, 11572–11576.

[25] M. Reiter, S. Vagin, A. Kronast, C. Jandl, B. Rieger, *Chem. Sci.* **2017**, *8*, 1876–1882.

[26] C. Martín, A. W. Kleij, *Macromolecules* **2016**, *49*, 6285–6295.

[27] F. Auriemma, C. De Rosa, M. R. Di Caprio, R. Di Girolamo, W. C. Ellis, G. W. Coates, *Angew. Chem. Int. Ed.* **2015**, *54*, 1215–1218.

[28] R. C. Jeske, A. M. DiCiccio, G. W. Coates, *J. Am. Chem. Soc.* **2007**, *129*, 11330–11331.

[29] C. Robert, F. de Montigny, C. M. Thomas, *Nat. Commun.* **2011**, *2*, 586.

[30] E. H. Nejad, A. Paoniasari, C. G. W. Van Melis, C. E. Koning, R. Duchateau, *Macromolecules* **2013**, *46*, 631–637.

[31] M. J. Sanford, L. Peña Carrodeguas, N. J. Van Zee, A. W. Kleij, G. W. Coates, *Macromolecules* **2016**, *49*, 6394–6400.

[32] N. J. Van Zee, G. W. Coates, *Angew. Chem. Int. Ed.* **2015**, *54*, 2665–2668.

[33] H. C. Quilter, M. Hutchby, M. G. Davidson, M. D. Jones, *Polym. Chem.* **2017**, *8*, 833–837.

[34] N. J. Van Zee, M. J. Sanford, G. W. Coates, *J. Am. Chem. Soc.* **2016**, *138*, 2755–2761.

[35] X. Lou, C. Detrembleur, R. Jérôme, *Macromol. Rapid Commun.* **2003**, *24*, 161–172.

[36] N. Ajellal, J.-F. Carpentier, C. Guillaume, S. M. Guillaume, M. Helou, V. Poirier, Y. Sarazin, A. Trifonov, *Dalton Trans.* **2010**, *39*, 8363–8376.

[37] B. Rieger, A. Künkel, G. W. Coates, R. Reichardt, E. Dinjus, A. T. Zevaco, *Synthetic Biodegradable Polymers*, Springer, Berlin, **2012**.

[38] Y. Sarazin, J. F. Carpentier, *Chem. Rev.* **2015**, *115*, 3564–3614.

[39] T. Aida, K. Sanuki, S. Inoue, *Macromolecules* **1985**, *18*, 1049–1055.

[40] S. Paul, Y. Zhu, C. Romain, R. Brooks, P. K. Saini, C. K. Williams, *Chem. Commun.* **2015**, *51*, 6459–6479.

[41] J. M. Longo, M. J. Sanford, G. W. Coates, *Chem. Rev.* **2016**, *116*, 15167–15197.

[42] D. J. Darensbourg, R. R. Poland, C. Escobedo, *Macromolecules* **2012**, *45*, 2242–2248.

[43] E. Hosseini Nejad, C. G. W. Van Melis, T. J. Vermeer, C. E. Koning, R. Duchateau, *Macromolecules* **2012**, *45*, 1770–1776.

[44] J. Liu, Y.-Y. Bao, Y. Liu, W.-M. Ren, X.-B. Lu, *Polym. Chem.* **2013**, *4*, 1439–1444.

[45] A. M. DiCiccio, G. W. Coates, *J. Am. Chem. Soc.* **2011**, *133*, 10724–10727.

[46] G. Si, L. Zhang, B. Han, Z. Duan, B. Li, J. Dong, X. Li, B. Liu, *Polym. Chem.* **2015**, *6*, 6372–6377.

[47] B. Han, L. Zhang, B. Liu, X. Dong, I. Kim, Z. Duan, P. Theato, *Macromolecules* **2015**, *48*, 3431–3437.

[48] N. D. Harrold, Y. Li, M. H. Chisholm, *Macromolecules* **2013**, *46*, 692–698.

[49] E. Hosseini Nejad, A. Paoniasari, C. E. Koning, R. Duchateau, *Polym. Chem.* **2012**, *3*, 1308–1313.

[50] P. K. Saini, C. Romain, Y. Zhu, C. K. Williams, *Polym. Chem.* **2014**, *5*, 6068–6075.

[51] T. Aida, S. Inoue, *J. Am. Chem. Soc.* **1985**, *107*, 1358–1364.

[52] M. Winkler, C. Romain, M. A. R. Meier, C. K. Williams, *Green Chem.* **2015**, *17*, 300–306.

[53] G. Fiorani, M. Stuck, C. Martín, M. M. Belmonte, E. Martin, E. C. Escudero-Adán, A. W. Kleij, *ChemSusChem* **2016**, *9*, 1304–1311.

[54] E. Mahmoud, D. A. Watson, R. F. Lobo, *Green Chem.* **2014**, *16*, 167–175.

[55] M. Taherimehr, S. M. Al-Amsyar, C. J. Whiteoak, A. W. Kleij, P. P. Pescarmona, *Green Chem.* **2013**, *15*, 3083–3090.

[56] C. J. Whiteoak, B. Gjoka, E. Martin, M. M. Belmonte, E. C. Escudero-Adán, C. Zonta, G. Licini, A. W. Kleij, *Inorg. Chem.* **2012**, *51*, 10639–10649.

[57] R. Mundil, Z. Hošt'álek, I. Šeděnková, J. Merna, *Macromol. Res.* **2015**, *23*, 161–166.

[58] C. J. Whiteoak, E. Martin, M. M. Belmonte, J. Benet-Buchholz, A. W. Kleij, *Adv. Synth. Catal.* **2012**, *354*, 469–476.

[59] C. J. Whiteoak, E. Martin, E. Escudero-Adán, A. W. Kleij, *Adv. Synth. Catal.* **2013**, *355*, 2233–2239.

[60] V. Schimpf, B. S. Ritter, P. Weis, K. Parison, R. Mülhaupt, *Macromolecules* **2017**, *50*, 944–955.

[61] M. Bähr, A. Bitto, R. Mülhaupt, *Green Chem.* **2012**, *14*, 1447–1454.

[62] W. J. Van Meerendonk, R. Duchateau, C. E. Koning, G. J. M. Gruter, *Macromolecules* **2005**, *38*, 7306–7313.

[63] C. J. Whiteoak, N. Kielland, V. Laserna, F. Castro-Gómez, E. Martin, E. C. Escudero-Adán, C. Bo, A. W. Kleij, *Chem. - A Eur. J.* **2014**, *20*, 2264–2275.

[64] A. Chandrasekaran, R. O. Day, R. R. Holmes, *J. Am. Chem. Soc.* **2000**, *122*, 1066–1072.

[65] Y. Belokon, D. Chusov, A. Peregudov, L. Yashkina, G. Timofeeva, V. Maleev, M. North, H. Kagan, *Adv. Synth. Catal.* **2009**, *351*, 3157–3167.

[66] L. a. Paquette, R. J. Ross, Y. J. Shi, *J. Org. Chem.* **1990**, *55*, 1589–1598.

[67] H. Mehrabi, *Can. J. Chem.* **2009**, *87*, 1117–1121.

UNIVERSITAT ROVIRA I VIRGILI
AVANCES EN SISTEMAS INTERACTIVOS PARA PERSONAS CON PARÁLISIS CEREBRAL
Leticia Peña Carrodeguas

Chapter 4

Fatty acid based biocarbonates: Al-mediated stereo-selective preparation of mono-, di- and tricarbonates

This chapter has been published in:
L. Peña Carrodeguas, A. Cristofol, J. M. Fraile, J. A. Mayoral, V. Dorado, C. I. Herrerías, A. W. Kleij, *Green Chem.* **2017**, DOI: 10.1039/C7GC01206C.

This work described in this chapter was carried out in collaboration with Prof. J. A. Mayoral and Prof. C. I. Hererrías from CSIC-Universidad de Zaragoza.

UNIVERSITAT ROVIRA I VIRGILI
AVANCES EN SISTEMAS INTERACTIVOS PARA PERSONAS CON PARÁLISIS CEREBRAL
Leticia Peña Carrodeguas

4.1 Introduction

The synthesis and use of cyclic organic carbonates (CCs) has witnessed a spectacular growth over the last years.[1–3] Nowadays, the single most used approach in CC synthesis is the coupling of epoxides and CO_2, representing a simple and efficient process when mediated by a suitable catalyst.[4–8] While their main application potential has primarily been recognized as green, non-protic solvents, electrolytes for Li-ion batteries and in some cases as monomers towards the formation of polycarbonates,[9–11] more recently various groups have used CCs as a prelude to more complex organic molecules including fine chemicals,[12–16] pharma-orientated structures[17–19] and (biobased) polymers.[20–23] In the latter context, the formation of organic molecules possessing more than one CC unit within the structural framework offers potential to use these molecules as a starting point for the preparation of isocyanate-free polyhydroxyurethanes.[24–28] Thus, such a new strategy improving the sustainability footprint of conventional polyurethane synthesis implemented in industrial processes[29] represents an attractive means to valorise CC structures into value-added materials.

In this respect, renewable olefin compounds based on fatty acids (also sometimes designated as oleochemicals) provide a widely available feed stock from the biodiesel industry. Medium to long-chain fatty acids such as oleic and linoleic acid comprise of *cis*-configured double bonds that can be converted in two steps into cyclic carbonates.[30] Recent work in this area has shown that such biocarbonates can be made easily through the use of suitable catalysts. For instance, Leitner and coworkers reported an effective binary system based on a polyoxometalate (POM) and an onium salt at 100ºC and around 13 MPa (130 bar) of CO_2 pressure for the conversion of various epoxidised fatty acids.[31] The use of the POM component was highly beneficial in terms of the overall kinetics; however, for a number of substrates containing multiple vicinal epoxide groups, the chemo-selectivity dropped significantly due to the occurrence of side-reactions such as epoxide hydrolysis. Site-isolation of multiple epoxide groups in other substrates restored the observed high chemo-selective conversion of the epoxide into cyclic carbonate groups noted for mono-epoxy fatty acids, and apparently the selective conversion of vicinal oxirane units is more challenging.

Beside the chemo-selectivity, controlling the stereoselective nature of these conversions (Scheme 4.1-a) can also be quite challenging as reported recently in various contributions.[30–36] Werner *et al*. reported on binary catalysts comprising of MoO_3[32] or $FeCl_3$[33] in combination with phosphonium salts, or bifunctional phosphorus-based organocatalysts[36] operated under

similar reaction conditions (80–100ºC, p = 25–50 bar, 20–24 h) giving the fatty acid based products typically as a mixture of *cis*/*trans* diastereoisomers (*cf*., in the carbonate units). As far as we know, no catalyst has been reported thus far that is able to efficiently convert mono-, di- and even tri-epoxidized fatty acid structures with both high stereo- and chemo-selectivity. In order to control these features, a catalyst is required able to combine epoxide activation potential while minimizing parasitic pathways comprising the overall selectivity.

Previous success while using binary catalysts based on the combination of trivalent or tetravalent metal-centred aminotriphenolate complexes (M = Al, Fe, V) and ammonium halides in the coupling of terminal and internal di/tri-substituted epoxides and CO_2 [4,12,37–41] motivated us to use these binary systems (Scheme 4.1-c) as catalysts for epoxy fatty acid conversion into their corresponding bio-carbonates. Further to this, the stereoselective preparation of disubstituted CCs using Fe(III) complexes[38] provided us with a useful starting point to control the selectivity features of these reactions.

4.2 Results and discussion

For the catalytic studies we selected six substrates **4a–4f** (Scheme 4.1-b) and Al(III) complexes **Al^{MeMe}**, **Al^{ClCl} and Al^{tButBu}** (Scheme 4.1-c) to investigate the CO_2/epoxide coupling reactions at different temperatures, different loadings of catalysts and different nucleophilic additives. All ester-protected fatty acid precursors were first epoxidised under standard conditions.[A]

[A] See section 4.4.3 "*Experimental procedure*" of this chapter for more information.

Scheme 4.1 (a) Schematic representation of the conversion of epoxidised fatty acids and the stereo-chemical implications. (b) Methyl esters of the epoxidized fatty acids **4a–4f** used as substrates in this work and the origin of these substrates. (c) Structures of the Al(III) aminotriphenolate complexes.

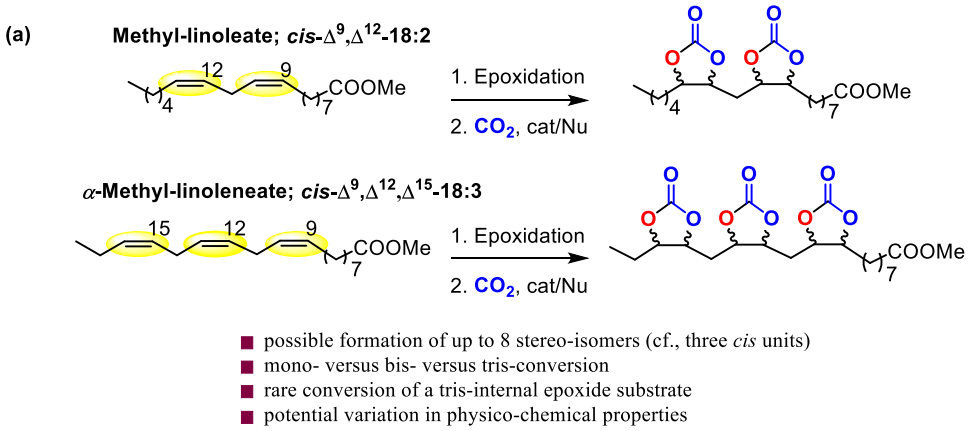

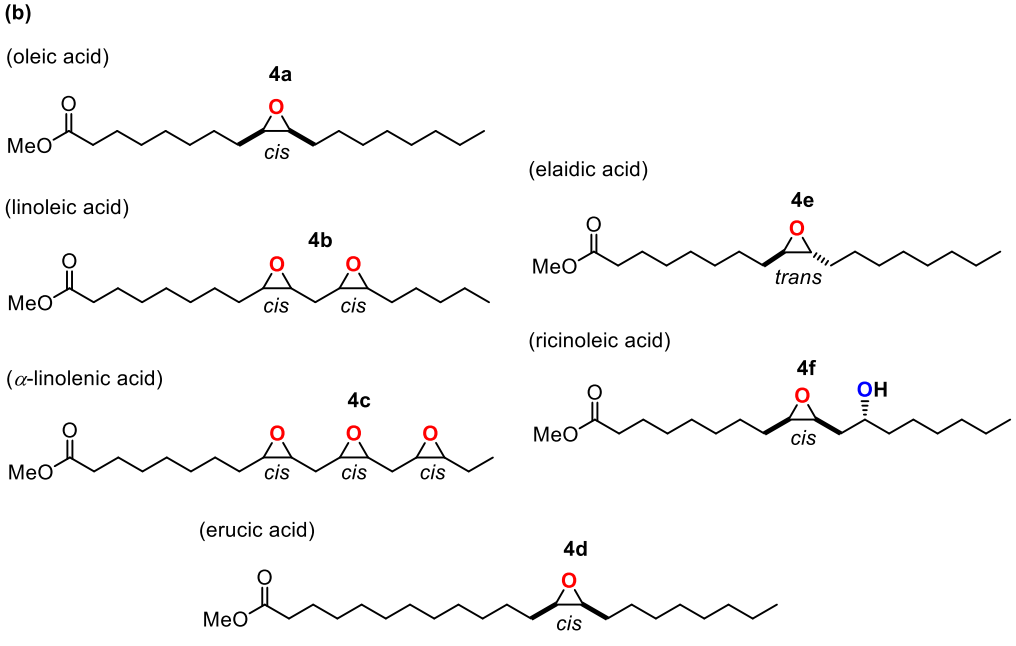

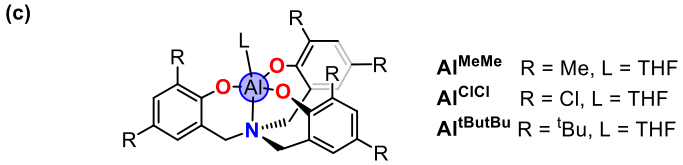

4.2.1 Oleic acid based cyclic carbonate

Substrate **4a** was then first examined under various catalytic conditions (see Table 4.1). Complexes **Al^{MeMe}** and **Al^{ClCl}** (1.0 mol%) were combined with a bromide based nucleophile (tetrabutylammonium bromide: TBAB; 5.0 mol%) at 70ºC and an initial CO_2 pressure of 10 bar (Table 4.1, entries 1–2). The conversion of internal epoxides in this area is typically probed with bromide based nucleophiles.[12,38] Under these conditions (nearly) quantitative and chemo-selective conversion of substrate **4a** into product **CC-4a** was achieved with a *cis*/*trans* ratio of up to 76:24. The use of 5.0 mol% of TBAB alone (Table 4.1, entry 3) also gave quantitative conversion but with a significantly reduced stereoselectivity (51:49). Further experiments conducted with Al-complex **Al^{MeMe}** and **Al^{ClCl}** in the presence of chloride based nucleophiles (PPNCl = bis(triphenylphosphine)iminium chloride, TBAC = tetrabutylammonium chloride; Table 4.1, entries 4–19) allowed to optimize the synthesis of **CC-4a** combining high conversion, chemo-selectivity and stereocontrol. Interestingly, the use of chloride based nucleophiles proved to be beneficial to produce almost exclusively the *cis*-configured **CC-4a**. The use of a solvent was less productive (Table 4.1, entries 8–11 and 14), and the best compromise between high conversion and selectivity with a minimal Al-complex and nucleophile loading proved to be the conditions reported in Table 4.1, entry 17 (0.5 mol% **Al^{ClCl}**, 3.0 mol% PPNCl; conversion/selectivity >99%, *cis*/*trans* = 97:3).[B] Using these optimized conditions, we isolated **CC-4a** in 97%.[C]

The conversion of epoxidised methyl oleate **4a** was chosen for a scaling up experiment using 2.5 g of starting material. We found that in the same reactor system, the kinetics of this conversion were slower than observed during the screening experiments carried out with 0.32 mmol of **4a** and the same amount of Al-complex **Al^{ClCl}** and PPNCl. After 48 h, the conversion of **4a** under neat conditions was 94% (isolated yield: 72%, *cis*/*trans* ratio 96:4) whereas the conversion was rather similar when using a solvent (toluene; 89%). Apparently the CO_2 dissolution kinetics were affected upon increasing the solvent volume to contact surface ratio. Nonetheless, the scaling experiment shows the potential of these fatty acid conversions to be carried out with larger quantities of material while maintaining similar levels of stereoselectivity.

[B] Though the use of PPNCl and TBAC gave fairly similar results, the latter is rather hydroscopic and less easy to handle when using small amounts and therefore PPNCl is preferred for practical reasons.
[C] The isolated yields of all fatty acid carbonates were obtained by using the optimal reaction conditions and scaling up five times the reactions (1.6 mmol of epoxide) utilizing an autoclave with a Teflon insert having an internal volume of 30 mL.

Table 4.1 Screening and optimisation of the coupling between epoxidised methyl oleate **4a** and CO_2.

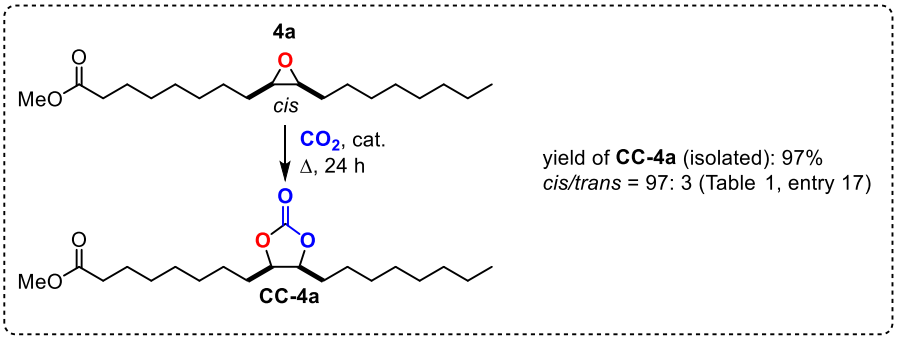

entry	[Al] (mol%)	Nu (mol%)	Solv.	conv.(%)[b]	Sel.(%)[b]	*cis*/*trans*[b]
1	**Al**^{MeMe}, 1.0	TBAB, 5.0	neat	>99	>99	72:28
2	**Al**^{ClCl}, 1.0	TBAB, 5.0	neat	94	>99	76:24
3	–	TBAB, 5.0	neat	>99	>99	51:49
4	**Al**^{MeMe}, 1.0	PPNCl, 5.0	neat	92	>99	98:2
5	**Al**^{MeMe}, 1.0	PPNCl, 3.0	neat	65	>99	98:2
6	–	PPNCl, 5.0	neat	53	>99	96:4
7	–	PPNCl, 3.0	neat	40	>99	98:2
8	–	PPNCl, 5.0	Tol	61	>99	96:4
9	–	PPNCl, 3.0	Tol	31	>99	99:1
10	**Al**^{MeMe}, 1.0	PPNCl, 5.0	Tol	90	>99	95:5
11	**Al**^{MeMe}, 1.0	PPNCl, 3.0	Tol	37	>99	97:3
12	**Al**^{MeMe}, 0.50	PPNCl, 3.0	neat	81	>99	95:5
13	**Al**^{MeMe}, 0.50	PPNCl, 2.0	neat	56	>99	>99:1
14	**Al**^{MeMe}, 0.50	PPNCl, 3.0	Tol	46	>99	98:2
15	**Al**^{ClCl}, 1.0	PPNCl, 5.0	neat	>99	>99	95:5
16	**Al**^{ClCl}, 0.50	PPNCl, 5.0	neat	>99	>99	96:4
17	**Al**^{ClCl}, 0.50	PPNCl, 3.0	neat	>99	>99	97:3
18	**Al**^{ClCl}, 1.0	TBAC, 5.0	neat	>99	>99	96:4
19	–	TBAC, 5.0	neat	6	>99	>99:1

[a]General conditions: 0.32 mmol **4a**, 70 ºC, 24 h, $p(CO_2)^o$ = 10 bar, medium indicated: neat or toluene (0.1 mL). [b]Conversion, selectivity and *cis/trans* ratio were determined by ^{1}H NMR ($CDCl_3$).

4.2.2 Linoleic acid based cyclic carbonate

The reaction conditions and preferred Al-complex/nucleophile combination **Al^{ClCl}**/PPNCl were then used as starting point for the catalytic coupling of the bis-epoxy derivative of methyl linoleate **4b** and CO_2 (Table 4.2).[D] Product **CC-4b** could also be attained in good yield, high chemoselectivity (>99%) and with excellent stereoselectivity (*cis*/*trans* = 97:3; Table 4.2, entry 21). From the catalytic data presented in Table 4.2 it can be inferred that higher reaction temperatures typically lead to a decrease in stereocontrol as previously also observed by other authors.[31–33,36] Fortunate, the use of binary catalysts comprising of **Al^{MeMe}** or **Al^{ClCl}** and chloride based nucleophiles allows for very high to quantitative conversions of substrate **4b** with excellent chemo- and stereo-selectivity (*cf*., Table 4.2, entries 9 and 21). Comparatively, the use of the chloride-substituted Al-complex **Al^{ClCl}** gave the best results and **CC-4b** was isolated in high yield (80%) using the optimized conditions of Table 4.2, entry 21.

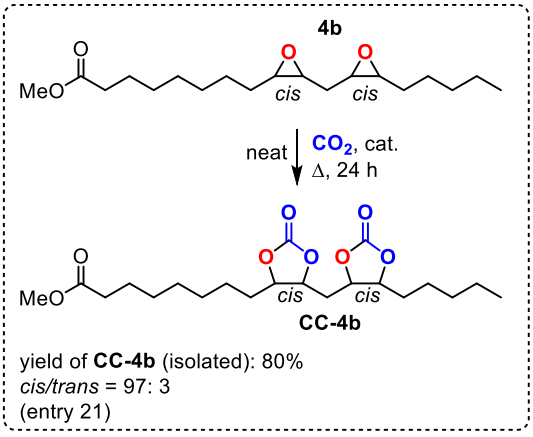

(Figure to Table 4.2)

[D] Note that this bis-epoxide may exist as a mixture of 4 stereoisomers (two pairs of enantiomers) having both epoxides with a *cis* configuration though with a different relative orientation of these units. For more information see section 4.2.7 "*Stereochemistry of fatty acid based epoxides and cyclic carbonates*" of this chapter.

Table 4.2 Screening and optimisation of the coupling between epoxidised methyl linoleate **4b** and CO_2

entry	[Al] (mol%)	Nu (mol%)	t (ºC)	conv.(%)[b]	Sel.(%)[b]	*cis/trans*[c]
1	**Al^{MeMe}**, 0.50	TBAC, 5.0	70	59	>99	99:1
2	–	TBAC, 5.0	70	80	>99	98:2
3	**Al^{MeMe}**, 1.0	PPNCl, 5.0	70	>99	>99	98:2
4	**Al^{MeMe}**, 1.0	PPNCl, 5.0	85	>99	>99	80:20
5	**Al^{MeMe}**, 0.50	PPNCl, 5.0	70	>99	>99	86:14
6	**Al^{MeMe}**, 0.50	PPNCl, 5.0	85	>99	>99	93:7
7	**Al^{MeMe}**, 0.50	PPNCl, 3.0	70	90	>99	76:24
8	**Al^{MeMe}**, 0.50	PPNCl, 3.0	85	>99	>99	79:21
9	**Al^{MeMe}**, 0.30	PPNCl, 5.0	70	85	>99	95:5
10	–	PPNCl, 3.0	70	47	>99	>99:1
11	–	PPNCl, 3.0	85	92	>99	96:4
12	–	PPNCl, 5.0	70	66	>99	>99:1
13	–	PPNCl, 5.0	85	95	>99	95:5
14	**Al^{ClCl}**, 1.0	TBAC, 5.0	70	97	>99	85:15
15	**Al^{ClCl}**, 1.0	PPNCl, 5.0	70	95	>99	82:18
16	**Al^{ClCl}**, 1.0	PPNCl, 5.0	85	>99	>99	83:17
17	**Al^{ClCl}**, 0.50	PPNCl, 5.0	70	>99	>99	83:17
18	**Al^{ClCl}**, 0.50	PPNCl, 5.0	85	>99	>99	92:8
19	**Al^{ClCl}**, 0.50	PPNCl, 3.0	70	87	>99	73:27
20	**Al^{ClCl}**, 0.50	PPNCl, 3.0	85	>99	>99	87:13
21	**Al^{ClCl}**, 0.30	PPNCl, 5.0	70	>99	>99	97:3
22	**Al^{ClCl}**, 0.20	PPNCl, 5.0	70	97	>99	94:6
23	**Al^{ClCl}**, 0.10	PPNCl, 5.0	70	87	>99	95:5
24	**Al^{ClCl}**, 0.30	PPNCl, 3.0	70	94	>99	92:8

[a]General conditions: 0.32 mmol **4b**, 70-85 ºC, 24 h, $p(CO_2)^o$ = 10 bar, neat. Note that the amount of [**Al**] or PPNCl is per epoxide unit. [b]Conversion/selectivity of epoxy groups was determined by ^{1}H NMR ($CDCl_3$). [c]*Cis*/*trans* ratios were determined by ^{1}H NMR and refer to the total % of *cis* and/or *trans* units in the product **CC-4b**.

4.2.3 Linolenic acid based cyclic carbonate

Inspired by the successful preparation of **CC-4a** and **CC-4b** from oleic and linoleic acid precursors, we then shifted our attention to the use of epoxidised methyl linolenate **4c** (Scheme 4.1-b)[E] to further challenge the binary catalyst system based on Al-complex $\mathbf{Al^{ClCl}}$ and PPNCl (Table 4.3). In general, the synthesis of tricarbonate product **CC-4c** proved to be more challenging, in particular the overall stereoselectivity control was markedly lower and the use of both Al-complexes $\mathbf{Al^{MeMe}}$ and $\mathbf{Al^{ClCl}}$ with PPNCl gave high to excellent conversions but with *cis*/*trans* ratios not exceeding 71:29 (Table 4.3, entry 4). Fortunate, the use of ^{t}Bu-substituted Al-complex $\mathbf{Al^{tButBu}}$ (Scheme 4.1-c) showed a significant improvement in the observed *cis*/*trans* ratio of 87:13 compared to the use of either $\mathbf{Al^{MeMe}}$ (Table 4.3, entry 9) or $\mathbf{Al^{ClCl}}$ (Table 4.3, entry 1) Further increase in the loading of Al-complex $\mathbf{Al^{tButBu}}$ (Table 4.3, entries 11 and 12; 1.0 mol%/epoxide unit) resulted in excellent stereo-control (*dr* = 96:4; Table 4.3, entry 11) and an improved conversion rate. As far as we know, the selective formation of tricarbonate **CC-4c** (61% yield)[C] is a rare example of the challenging conversion of a substrate with three vicinal epoxide groups under excellent stereocontrol.

[E] The epoxidised methyl linolenate is a mixture of eight stereosiomers, *i.e*. four pairs of enantiomers. For more information see section 4.2.7 "*Stereochemistry of fatty acid based epoxides and cyclic carbonates*" of this chapter.

Table 4.3 Screening and optimisation of the coupling between epoxidised methyl linolenate **4c** and CO_2

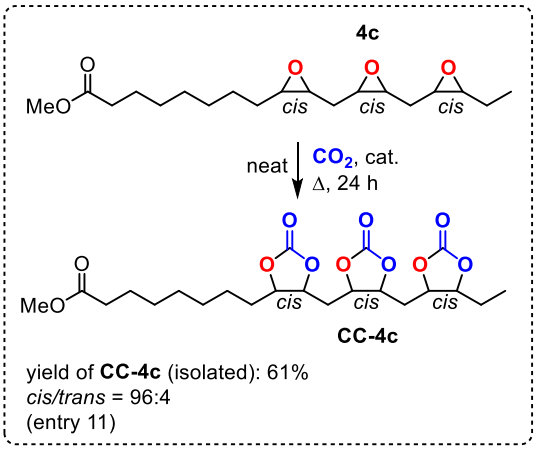

entry	[Al] (mol%)	Nu (mol%)	t (ºC)	conv.(%)[b]	Sel.(%)[b]	*cis/trans*[c]
1	**Al^{ClCl}**, 0.50	PPNCl, 5.0	70	>99	>99	53:47
2[d]	**Al^{ClCl}**, 0.50	PPNCl, 5.0	70	96	>99	61:39
3	**Al^{ClCl}**, 0.30	PPNCl, 5.0	70	90	>99	66:34
4[d]	**Al^{ClCl}**, 0.30	PPNCl, 5.0	70	81	>99	71:29
5	**Al^{ClCl}**, 0.30	PPNCl, 3.0	70	81	>99	67:33
6[d]	**Al^{ClCl}**, 0.30	PPNCl, 5.0	70	81	>99	73:27
7	**Al^{ClCl}**, 0.20	PPNCl, 5.0	70	>99	>99	68:32
8[d]	**Al^{ClCl}**, 0.20	PPNCl, 5.0	70	92	>99	69:31
9	**Al^{MeMe}**, 0.500	PPNCl, 5.0	70	>99	>99	62:38
10	**Al^{tButBu}**, 0.5	PPNCl, 5.0	70	75	>99	87:13
11	**Al^{tButBu}**, 1.0	PPNCl, 5.0	70	92	>99	96:4
12	**Al^{tButBu}**, 1.5	PPNCl, 5.0	70	91	>99	96:4
13	–	PPNCl, 5.0	70	75	>99	90:10

[a]General conditions: 0.32 mmol **4c**, 70 ºC, 24 h, $p(CO_2)^o$ = 10 bar, neat unless stated otherwise. Note that the amount of [**Al**] or PPNCl is per epoxide unit. [b]Conversion/selectivity of epoxy groups was determined by ^{1}H NMR ($CDCl_3$). [c]*Cis*/*trans* ratios were determined by ^{1}H NMR and refer to the total % of *cis* and/or *trans* units in the product **CC-4c**.[d]Toluene (0.1 mL) was added as solvent.

4.2.4 Erucic acid based cyclic carbonate

Next, we examined a longer alkyl tail fatty acid derivative (*i.e.*, the methyl ester of epoxidised erucic acid, **4d** in Scheme 4.1; see also Table 4.4). The presence of a longer alkyl chain significantly decreased the solubility of the nucleophilic additive PPNCl, and even in the presence of toluene as solvent no full dissolution was observed after the reaction mixture had been vented and cooled down to ambient temperature. Therefore, in these cases the total conversion remained very low (Table 4.4, entries 4–7). This was also the case when Al-complex **Al^{ClCl}** was combined with PPNCl at 70ºC, and only a low conversion (5%) of **4d** was achieved (Table 4.4, entry 1). Fortunately, in the presence of Al-complex **Al^{ClCl}** homogeneous mixtures were attained at 85ºC (Table 4.4, entries 2 and 3; the crude products were clear liquids) giving high conversion of substrate **4d** into the product **CC-4d** and importantly, also with high diastereoselectivity (*dr* = 96:4) towards the *cis*-configured product. The results with substrate **4d** help to confirm that binary catalysts derived from Al(III)aminotriphenolate complexes and chloride-based nucleophiles are efficient catalysts for a wider range of stereoselective fatty acid conversions, and apparently, the mechanistic manifold involves two sequential S_N2 reactions (*cf.*, a double inversion pathway).[31,38]

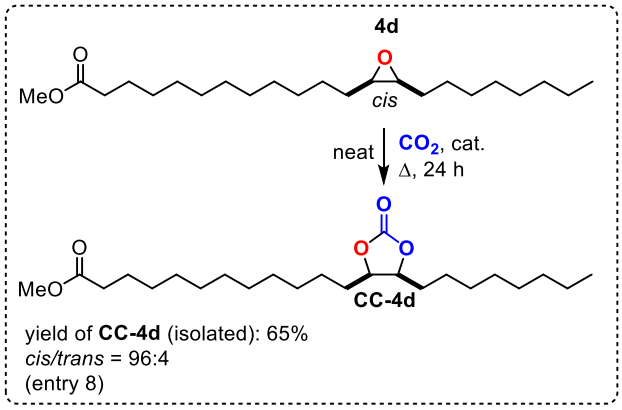

(Figure to Table 4.4)

Table 4.4 Screening and optimisation of the coupling between epoxidised methyl erucate **4d** and CO_2

entry	[Al] (mol%)	Nu (mol%)	t (ºC)	conv.(%)[b]	Sel.(%)[b]	*cis/trans*[c]
1	**Al^{ClCl}**, 0.50	PPNCl, 5.0	70	5	>99	99:1
2[d]	**Al^{ClCl}**, 0.50	PPNCl, 5.0	85	>99	>99	96:4
3[d]	**Al^{ClCl}**, 0.50	PPNCl, 3.0	85	>99	>99	96:4
4[d]	–	PPNCl, 3.0	85	1[f]	>99	99:1
5[d]	–	PPNCl, 5.0	85	1[f]	>99	99:1
6[d,e]	–	PPNCl, 3.0	85	1[f]	>99	99:1
7[d,e]	–	PPNCl, 5.0	85	1[f]	>99	99:1
8[d,e]	**Al^{ClCl}**, 0.50	PPNCl, 3.0	85	>99	>99	96:4

[a]General conditions: 0.32 mmol **4d**, 70ºC, 24 h, $p(CO_2)$º = 10 bar, neat unless stated otherwise. [b]Conversion/selectivity was determined by ^{1}H NMR ($CDCl_3$). [c]*Cis*/*trans* ratios were determined by ^{1}H NMR and refer to the total % of *cis* and/or *trans* units in the product **CC-4d**. [d]Reaction time was 48 h. [e]Toluene (0.1 mL) was added as solvent. [f]The nucleophilic additive was not (fully) soluble.

4.2.5 Elaidic acid based cyclic carbonate

In order to examine further the existence of such a double inversion pathway, we used substrate **4e** derived from the *trans* configured elaidic acid (Scheme 4.1). The utilization of the binary catalysts **Al^{MeMe}** or **Al^{ClCl}** combined with PPNCl (Table 4.5, entries 1–3)[F] showed full retention of stereochemistry and the product **CC-4e** was formed exclusively as the *trans* isomer. Although the expected, thermodynamically most stable isomer of **CC-4e** is formed, the retention of configuration in the carbonate unit is in line with a double inversion pathway efficiently mediated by the combination of the Al-complex **Al^{ClCl}** and a chloride nucleophile. The preferential use of chloride nucleophiles with sterically more congested substrates has recently been described.[40,42]

[F] Under the conditions used, as noted for substrate **4d**, the PPNCl was not (fully) soluble giving no observable conversion. Note that the presence of the Al complex facilitated the dissolution of the PPNCl as after the reaction mixture had cooled down and was vented, a clear homogeneous mixture was obtained. Apparently, the solubility of the nucleophile is highly dependent on the nature of the fatty acid precursor.

Table 4.5 Screening and optimisation of the coupling between epoxidised methyl elaidate **4e** and CO_2.

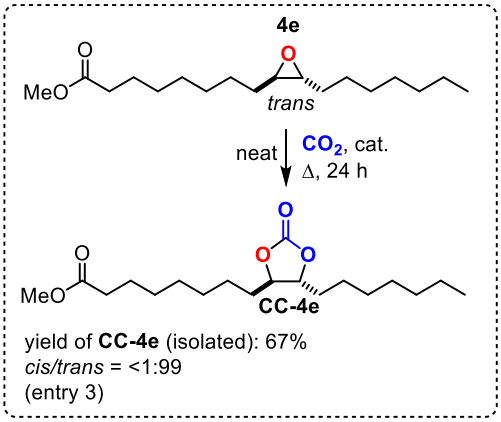

entry	[Al] (mol%)	Nu (mol%)	t (ºC)	conv.(%)[b]	Sel.(%)[b]	*cis/trans*[c]
1	**Al^{MeMe}**, 0.50	PPNCl, 5.0	70	28	>99	<1:99
2	**Al^{ClCl}**, 0.50	PPNCl, 5.0	70	65	>99	<1:99
3[d,e]	**Al^{ClCl}**, 0.50	PPNCl, 5.0	85	75	>99	<1:99
4	–	PPNCl, 5.0	70	0[f]	–	–
5[d,e]	–	PPNCl, 5.0	70	0[f]	–	–
6[d,e]	–	PPNCl, 5.0	85	0[f]	–	–

[a]General conditions: 0.32 mmol **4e**, 70ºC, 24 h, $p(CO_2)^o$ = 10 bar, neat unless stated otherwise. [b]Conversion/selectivity was determined by ^{1}H NMR ($CDCl_3$). [c]*Cis/trans* ratios were determined by ^{1}H NMR and refer to the total % of *cis* and/or *trans* units in the product **CC-4e**. [d]Reaction time was 48 h. [e]Toluene (0.1 mL) was added as solvent. [f]The nucleophilic additive was not (fully) soluble.

4.2.6 Ricinoleic acid based cyclic carbonate

As a more functional example, the conversion of epoxidised methyl ricinoleate **4f** was also studied in the presence of the binary catalyst **Al^{ClCl}**/PPNCl (Table 4.6). The stereochemical course of this conversion proved to be interesting as the binary catalyst system provided the product **CC-4f** with high inversion of configuration (*dr* = 90:10, *trans* isomer major product, Table 4.6, entry 2). The use of the nucleophile also gave high conversion towards the CC target but with significantly lower diastereoselectivity (Table 4.6, entries 4 and 5).

Table 4.6 Screening and optimisation of the coupling between epoxidised methyl ricinoleate **4f** and CO_2

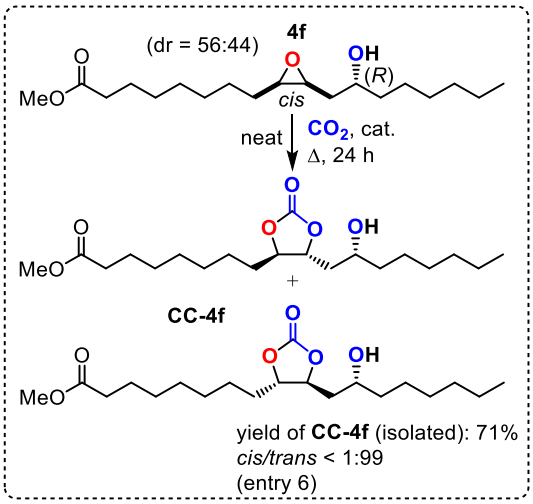

entry	[Al] (mol%)	Nu (mol%)	t (°C)	conv.(%)[b]	Sel.(%)[b]	*cis/trans*[c]
1	**Al^{MeMe}**, 0.50	PPNCl, 5.0	70	28	>99	<1:99
2	**Al^{ClCl}**, 0.50	PPNCl, 5.0	70	65	>99	<1:99
3[d]	**Al^{ClCl}**, 0.50	PPNCl, 5.0	85	75	>99	<1:99
4	–	PPNCl, 5.0	70	0[f]	–	–
5	–	PPNCl, 5.0	70	0[f]	–	–
6	–	PPNCl, 5.0	85	0[f]	–	–

[a]General conditions: 0.32 mmol **4f**, 70ºC, 24 h, $p(CO_2)^o$ = 10 bar, neat unless stated otherwise. [b]Conversion/selectivity was determined by ^{1}H NMR ($CDCl_3$). [c]*Cis*/*trans* ratios were determined by ^{1}H NMR and refer to the total % of *cis* and/or *trans* units in the product **CC-4f**. [d]Toluene (0.1 mL) was added as solvent.

Interestingly, in the absence of any nucleophile (Table 4.6, entry 6; using only Al-complex **Al^{ClCl}**) the reaction proceeds also well with exclusive formation of the *trans* product **CC-4f**. In order to explain this inversion of configuration, a mechanistic rationale based on a double inversion pathway can be discarded. Also, the occurrence of an overall "S_N1" type manifold is unlikely as the reactivity is controlled by the Al-complex **Al^{ClCl}** only. Therefore, a different mechanistic explanation is required. We recently reported that hydroxy-oxetanes[43] and epoxy alcohols[15] react with CO_2 in the absence of external nucleophiles but in the presence of Al(III) aminotriphenolate complexes to give either five- or six-membered CCs. In these cases, the Al(III) complex is able to stabilize a proposed hemi-ester of a linear carbonate

derived from initial reaction of the alcohol unit in the substrate and CO_2. Intramolecular proton-transfer from the hemi-carbonic ester to one of the phenolate O–donors of the ligand allows for the *in situ* formation of a carbonate species that acts as an intramolecular nucleophile towards epoxide ring-opening (Scheme 4.2 a). Such a manifold is also feasible with substrate **4f** that contains a homo-allylic alcohol unit (Scheme 4.2 b).

Scheme 4.2 (**a**) Previously reported mechanistic manifold in the conversion of epoxy-alcohol derivatives. (**b**) Proposed sequence of steps in the conversion of hydroxy-substituted substrate **4f** into its five-membered product **CC-4f**.

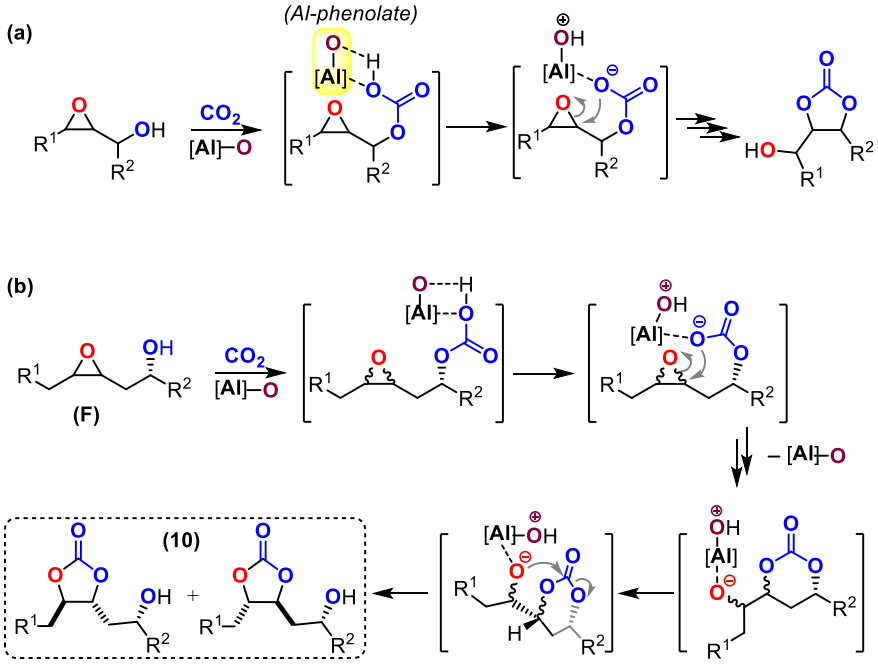

In this manifold, the alcohol unit reacts with CO_2 to form a carbonic acid like intermediate, and following a similar proton-shuttling to one of the phenolate donors of the Al-complex, a nucleophilic species is produced that attacks the oxirane unit with inversion of configuration. At this stage a six-membered CC is formed which is thermodynamically less stable than its five-membered analogue. Therefore, the alcoholate unit in the intermediate cyclic carbonate product stabilized by the Al complex, is involved in a nucleophilic attack onto the carbon center of the six-membered CC giving finally the five-membered product **CC-4f**. The overall process, according to this manifold, produces the product carbonate **CC-4f** with inversion of the initial *cis* configuration and fits the experimental observations. This alternative

mechanism gives additional potential to control the stereoselective conversion of more functional fatty acid precursors.

4.2.7 Stereochemistry of fatty acid-based epoxides and cyclic carbonates

It should be noted that in all cases the formation of several isomers is possible both for the fatty acid based epoxides and their derived cyclic carbonates. When considering the synthesis of the cyclic carbonate, only one diastereoisomer is formed during the epoxidation process (*cis* epoxide **4a**) from methyl oleate. The epoxidised *cis*-methyl oleate **4a** has two enantiomers which are shown in Scheme 4.3.

Scheme 4.3 Configuration of the enantiomeric epoxides derived from methyl oleate

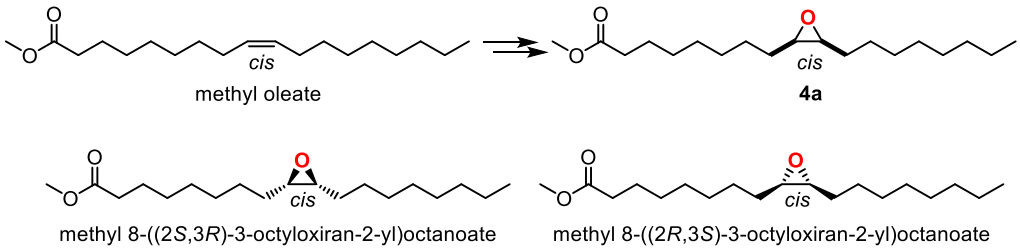

Two diastereoisomers (*cis* and *trans* CC) can be obtained during the formation of cyclic carbonate **CC-4a** though the catalytic conversion (Table 4.1) occurs with excellent diastereoselectivity (*cis/trans* = 97:3). Stereoisomeric forms of **CC-4a** include the two enantiomers of both ***cis*-CC-4a** and ***trans*-CC-4a** which are shown in Scheme 4.4.

Scheme 4.4 Configuration of all possible stereoisomeric cyclic carbonates derived from **4a**

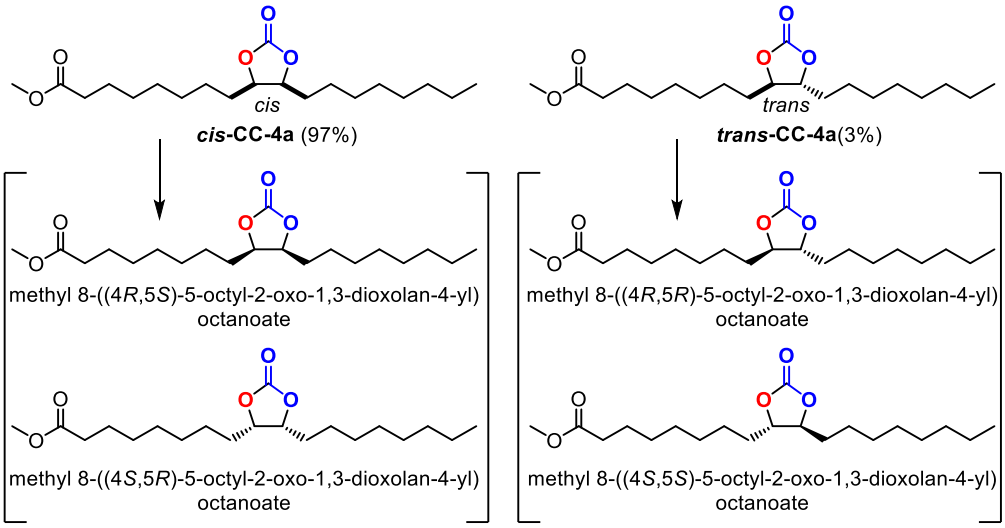

Scheme 4.5 Configuration of the *cis*-di-cyclocarbonate based on linoleic acid **4b.**

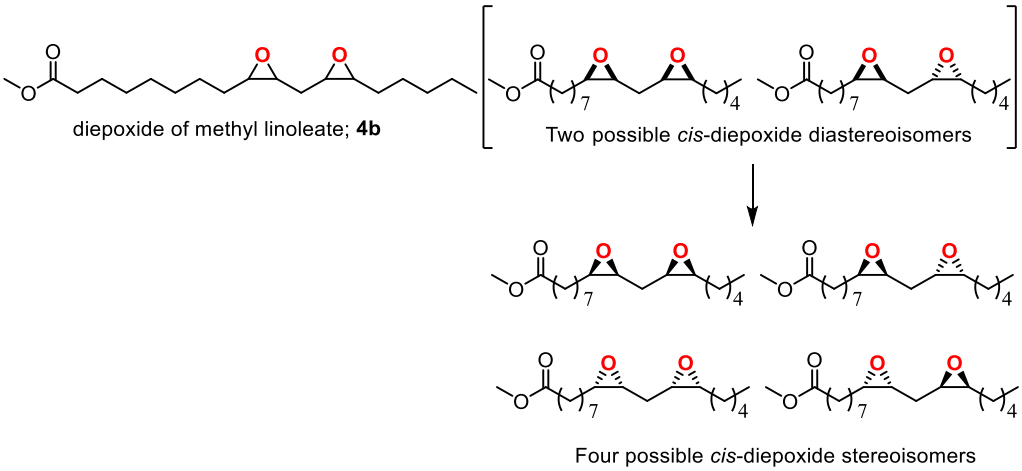

In the case of the diepoxide **4b** based on methyl linoleate two possible *cis*-diepoxide diastereoisomers can be formed as depicted in Scheme 4.5 and each diastereoisomer has a mirror image (*i.e*, two enantiomers) therefore in total four stereoisomers may be obtained. These four isomers should have a *cis* configuration within each epoxide unit, though different relative positions of the epoxide rings is feasible. All possible relative orientations are shown in Scheme 4.5, and for simplicity only the orientation of the epoxide ring is shown.

Formation of the corresponding bis-cyclic carbonate **CC-4b** from methyl linoleate **4b** occurs with high selectivity towards the *cis*-**CC** (*cis/trans* = 97:3), and Scheme 4.6 represents all possible stereoisomers of *cis*-**CC-4b**.

For the tris-epoxide based on methyl linolenate (**4c**) four possible *cis*-tris-epoxide diastereoisomers and eight possible stereoisomers can be formed as is shown in Scheme 4.7, and for simplicity only the orientation of the epoxide ring is shown. The possible stereochemical configurations for the all *cis* tris-**CC-4c** are the same as in the case of the tris-epoxide precursor, *i.e.* there are four diastereoisomers and eight possible stereoisomers.

Scheme 4.6 Configuration of the *cis* bis cyclic carbonate based on linoleic acid **CC-4b**

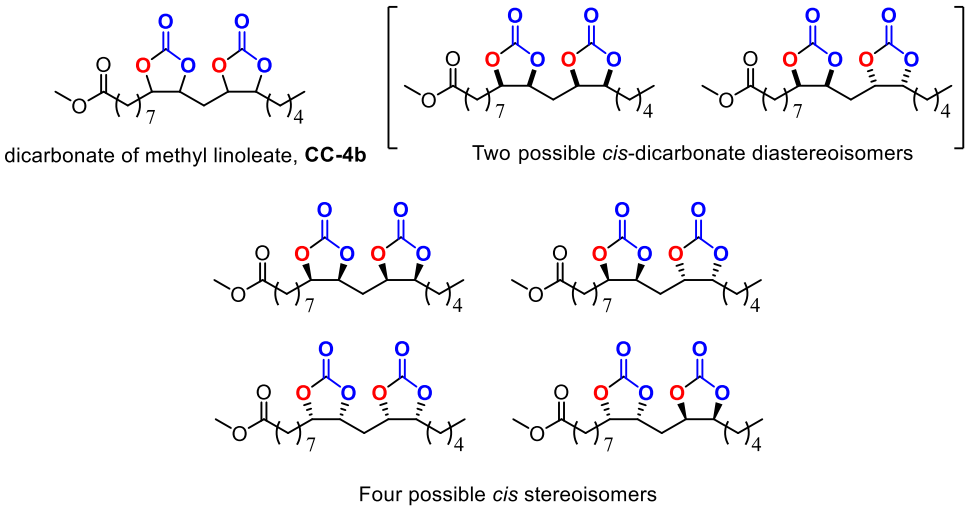

Scheme 4.7 Configuration of the *cis*-tri-cyclocarbonate based on linolenic acid **4c**.

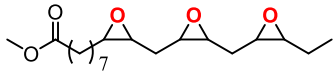

tris-epoxy of methyl linoleate (**4c**)

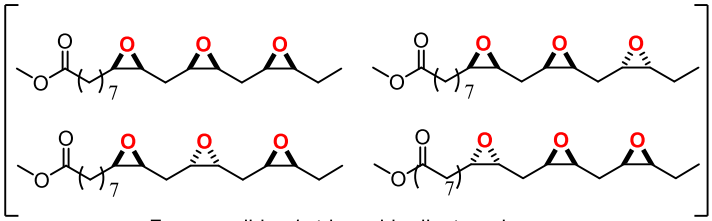

Four possible *cis*-triepoxide diastereoisomers

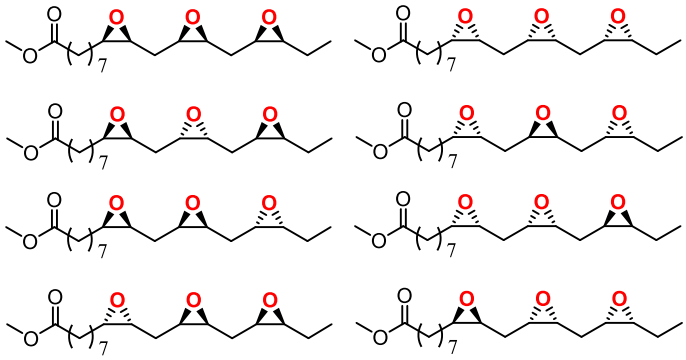

Eight possible *cis*-triepoxide stereoisomers

4.3 Conclusions

In summary, we here report the use of a binary catalyst comprising of an Al(III) aminotriphenolate complex that combined with PPNCl allows for the stereoselective conversion of methyl esters of various epoxy fatty acid derivatives under comparatively mild reaction conditions. Specifically, the selective conversion of mono- (oleate), di- (linoleate) and tris-epoxy (linolenate) substrates with sterically challenging combinations of vicinal epoxide groups has been achieved with the highest levels of stereocontrol (*dr´*s up to >99:1) reported to date. Furthermore, the conversion of hydroxy-functionalized substrates follows a different mechanistic manifold and opposed to the stereo-retention observed for substrates **4a–4e**, formal and quantitative inversion of configuration is noted when **4f** is coupled with CO_2 in the presence of Al-complex $\mathbf{Al^{ClCl}}$ but essentially in the absence of an external nucleophile. The developed protocol therefore represents an unprecedented example of chemo- and stereo-selective conversion of renewable oleochemical compounds into their CC derivatives that have shown potential in the sustainable formation of isocyanate-free polyhydroxyurethanes.

4.4 Experimental section

4.4.1 General information and instrumentation

Commercially available fatty acids (oleic acid, linoleic acid, α-linolenic acid, erucic acid, elaidic acid and ricinoleic acid) solvents, co-catalysts (PPNCl, TBAC, TBAB) and oxidants were purchased from various commercial sources (Acros, Aldrich and TCI) and used without further purification. Carbon dioxide (purchased from PRAXAIR) was used without further purification or drying *prior to* its use.

^{1}H NMR and ^{13}C NMR spectra were recorded at rt on a Bruker AV-300, AV-400 or AV-500 spectrometer and referenced to the residual deuterated solvent signals. Diastereo-isomeric ratios (*dr´*s) were calculated from the corresponding ^{1}H NMR spectra using signal integration where possible; alternatively, integrable ^{13}C NMR spectra were recorded with a 500 MHz AV-500 spectrometer. All reported NMR values are given in parts per million (ppm). Mass spectrometric analyses were performed by the Research Support Group at ICIQ.

4.4.2 Synthesis of complexes

The Al(III) aminotriphenolate complexes **Al^{MeMe}**[44,45] and **Al^{ClCl}**[4] and the starting ligands were synthesized according to reported literature procedures.[I]

Synthesis of amino triphenolate ligand H_3L^tBu

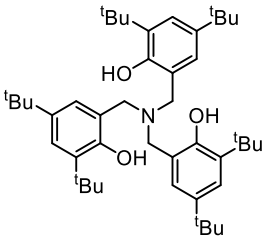

2,4-di-tertbutylphenol (8.25 g, 31 mmol), hexamethylene tetramine (HMTA; 1.2 g, 8.5 mmol) and *para*-toluenesulfonic acid (70 mg, 0.36 mmol) were heated at 110ºC for 24 h, after this an additional 2 g of 2,4 dimethylphenol were added to the reaction mixture and it was left stirring at 110ºC for another 18 h. Hereafter, the reaction was cooled down to rt and 20 mL of MeOH were added to the yellow slurry. The solution was sonicated until a pale yellow solid crashed out of solution. The solid was filtered off, washed with cold MeOH and dried under vacuum. The compound was recrystallized from acetone.[45] Spectroscopic characterization was consistent with the data reported in the literature.

^{1}H NMR (400 MHz, $CDCl_3$) δ 7.26 (d, *J* = 2.4 Hz, 3H), 7.00 (d, *J* = 2.4 Hz, 3H), 3.66 (s, 6H), 1.42 (s, 27H), 1.30 (s, 27H).
^{13}C NMR (101 MHz, $CDCl_3$) δ 151.40, 142.06, 136.40, 125.55, 123.95, 121.78, 56.51, 34.87, 34.18, 31.60, 29.66.

Synthesis of aluminum complex **Al^{tButBu}**

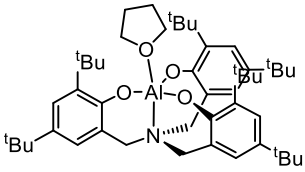

[$AlMe_3$] (2 M in heptane, 1.19 mL, 2.38 mmol) was slowly added to a solution of ligand H_3L^tBu (1.6 g, 2.38 mmol) in THF (20 mL). The solution was stirred at rt for 2 h and then concentrated. Hexane was added to the residue resulting in precipitation of the targeted

[I] For more information see section 1.4.2 "*Synthesis of complexes*" in chapter 1.

complex, which was isolated by filtration and further dried under vacuum to yield a white powder.[45]. Spectroscopic characterization was consistent with the data reported in the literature.

^{1}H NMR (400 MHz, $CDCl_3$) δ 7.23 (d, *J* = 2.5 Hz, 3H), 6.88 (d, *J* = 2.4 Hz, 3H), 4.30 (d, *J* = 13.1 Hz, 3H), 4.01 (m, 4H), 2.95 (d, *J* = 13.0 Hz, 3H), 1.98 (m, 4H) 1.43 (s, 27H), 1.29 (s, 27H).
^{13}C NMR (101 MHz, $CDCl_3$) δ 154.70, 139.20, 136.99, 123.77, 123.57, 121.26, 68.19, 59.03, 34.84, 34.05, 31.73, 29.58, 25.59.

4.4.3 Experimental procedures:

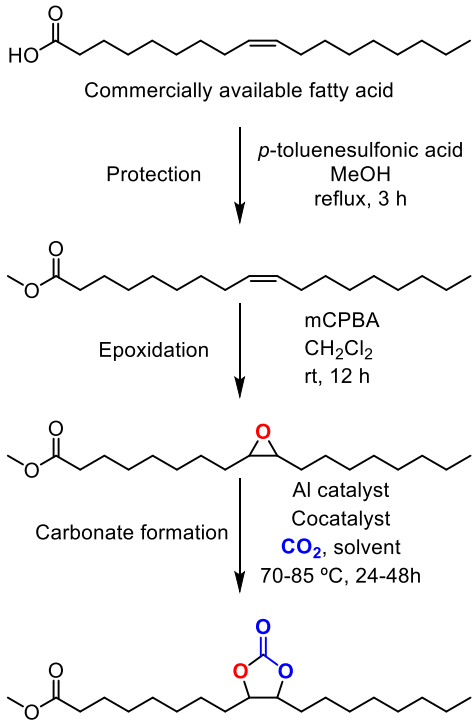

Acid protection method (typical procedure):

1 g of fatty acid and 5 mg of *para*-toluenesulfonic acid (mono-hydrate) were dissolved in MeOH (50 mL). The reaction mixture was heated to reflux for 3 h. Hereafter, the solvent was removed *in vacuo* (rotary evaporator) and the fatty ester product was used without further purification in the next step – *i.e.* epoxidation.

Epoxidation method (typical procedure):

1 g of the methyl ester was dissolved in CH_2Cl_2 (40 mL) and cooled to 0 ºC. Then *meta*-chloroperbenzoic acid (1.2 equiv) was slowly added to this solution. The reaction mixture was

left stirring for 12 h at rt. The solution was then washed with an aqueous solution of Na_2SO_3 (3 × 30 mL, 1 M), a saturated aqueous solution of $NaHCO_3$ (3 × 30 mL) and brine. The organic phase was dried over sodium sulfate and the product was obtained after removal of the solvent *in vacuo* using a rotary evaporator.

Carbonate formation (Screening experiments):

The screening experiments of all fatty acid carbonates were obtained by using a HEL pressure multi-reactor (HEL CAT[24]) with 24 vials of 10 × 75 mm. The epoxide substrate (0.32 mmol) was introduced into a vial of the HEL with a pre-selected loading of catalyst and co-catalyst and solvent where required. The HEL was pressurized to 10 bar with CO_2 and heated to the desired temperature. The reaction mixture was stirring for 24–48 h. After cooling to ambient temperature the crude product was analyzed by ^{1}H NMR ($CDCl_3$) to determinate the conversion, selectivity and *cis/trans* ratio.

Carbonate formation (scaled experiments):

The isolated yields of all fatty acid carbonates were obtained by using the optimal reaction conditions and scaling up five times the reactions (at 1.6 mmol of epoxide) The epoxide substrate was introduced into a 30 mL autoclave with a Teflon insert and with a pre-selected loading of catalyst (Al-complex) and co-catalyst (nucleophile) and solvent where required. The autoclave was heated to the desired temperature, pressurized to 10 bar with CO_2 and the reaction mixture left stirring for 24–48 h. Then, after cooling to ambient temperature, the reaction was carefully and slowly vented, and the crude product analyzed by ^{1}H NMR and ^{13}C NMR ($CDCl_3$). The product was purified by flash chromatography (silica gel, EtOAc/hexane) following subsequent removal of the solvent using rotary evaporation.

4.4.4 ^{1}H and ^{13}C-NMR data of epoxide products

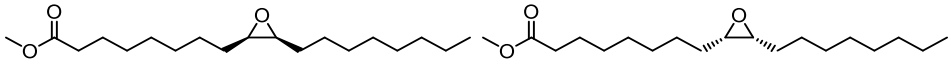

cis-Methyl 8-(3-octyloxiran-2-yl)octanoate **4a**

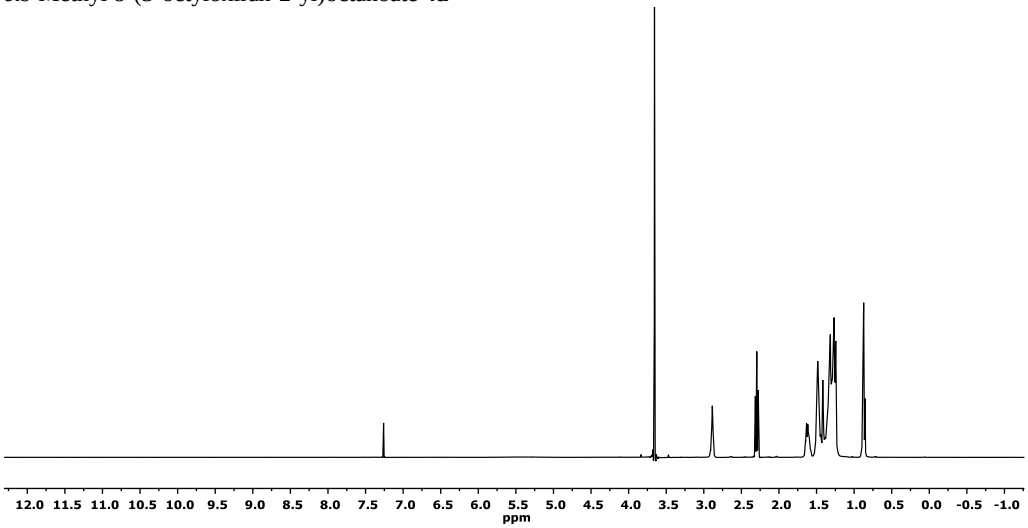

^{1}H NMR (400 MHz, $CDCl_3$) δ: 3.66 (s, 3H), 2.89 (m, 2H), 2.30 (t, $^{3}J_{H,H}$ = 7.5 Hz, 2H), 1.67-1.56 (m, 2H), 1.53-1.20 (m, 24H), 0.87 (t, $^{3}J_{H,H}$ = 6.7 Hz, 3H).

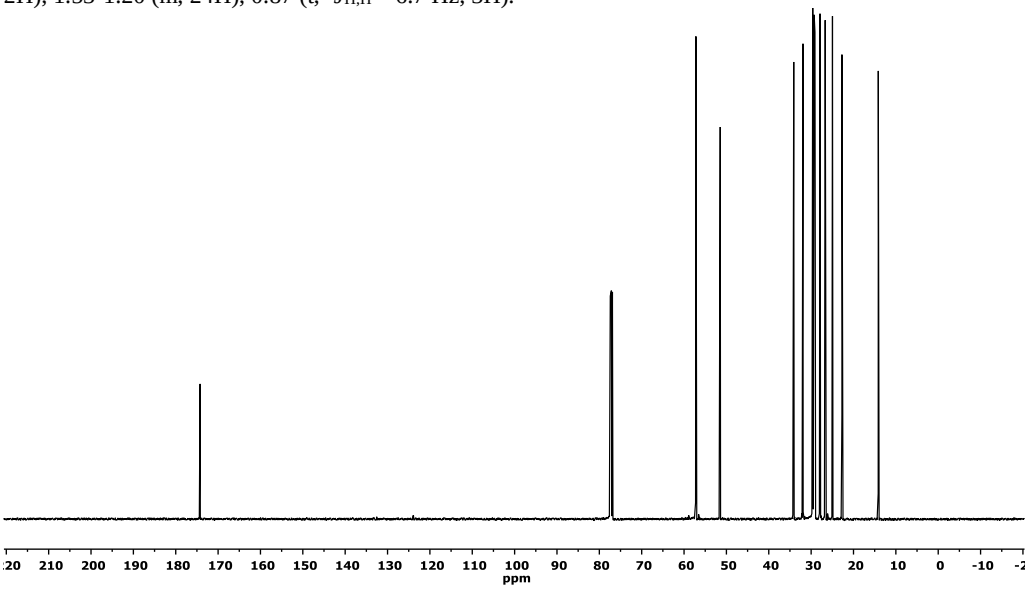

^{13}C NMR (126 MHz, $CDCl_3$) δ 174.24 (C=O), 57.25 (CH), 57.20 (CH), 51.46 (OCH_3), 34.11 (CH_2), 31.92 (CH_2), 29.62 (CH_2), 29.60 (CH_2), 29.40 (CH_2), 29.29 (CH_2), 29.24 (CH_2), 29.10 (CH_2), 27.91 (CH_2), 27.87 (CH_2), 26.68 (CH_2), 26.63 (CH_2), 24.96 (CH_2), 22.73 (CH_2), 14.14 (CH_3).

MS (ESI+, CH_3OH): *m/z* calcd. 335.3 $(M+Na)^+$; found: 335.3.[32]

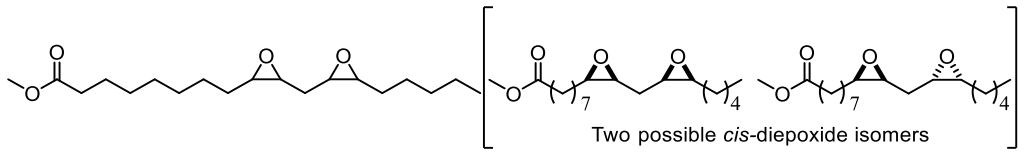

Methyl 8-(3-((3-pentyloxiran-2-yl)methyl)oxiran-2-yl)octanoate **4b**

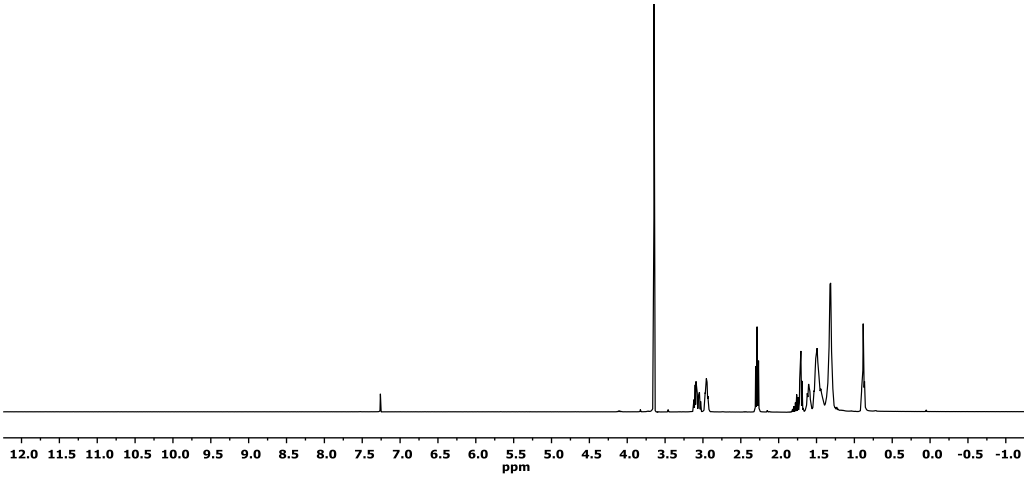

^{1}H NMR (400 MHz, $CDCl_3$) δ 3.65 (s, 3H), 3.12-3.02 (m, 2H), 2.99-2.92 (m, 2H) , 2.28 (t, $^{3}J_{H,H}$ = 7.5 Hz, 2H), 1.82-1.68 (m, 2H), 1.65-1.56 (m, 2H), 1.56-1.41 (m, 8H), 1.38-1.26 (m, 10H), 0.88 (t, $^{3}J_{H,H}$ = 6.9 Hz, 3H).

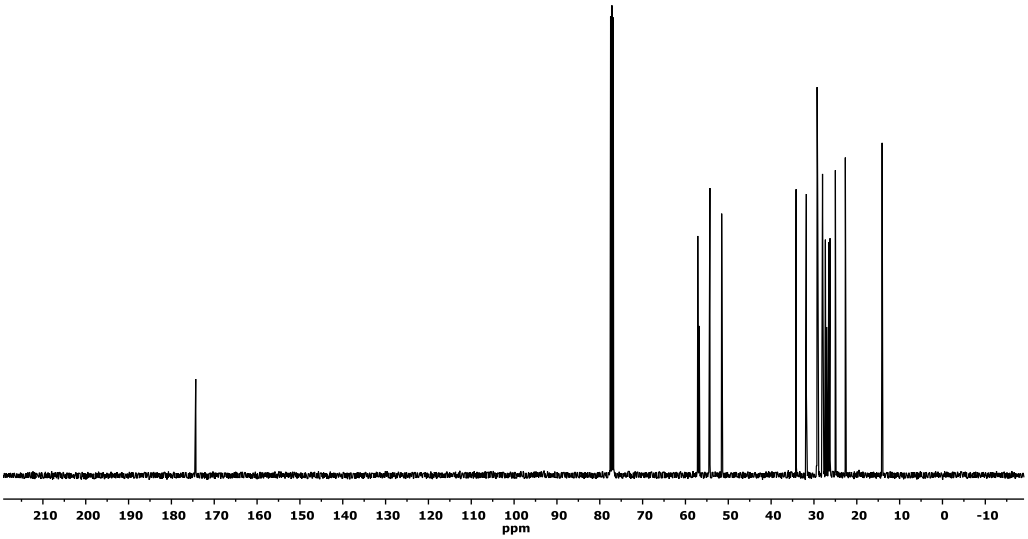

^{13}C NMR (101 MHz, $CDCl_3$) δ 174.32 (C=O), 57.12 (CH), 57.07 (CH), 56.84 (CH), 56.78 (CH), 54.47 (CH), 54.45 (CH), 54.29 (CH), 51.55 (OCH_3), 34.16 (CH_2), 31.78 (CH_2), 29.40 (CH_2), 29.26 (CH_2), 29.13 (CH_2), 28.01 (CH_2), 28.00 (CH_2), 27.93 (CH_2), 27.92 (CH_2), 27.33 (CH_2), 27.05 (CH_2), 26.64 (CH_2), 26.53 (CH_2), 26.36 (CH_2), 26.25 (CH_2), 25.00 (CH_2), 22.67 (CH_2), 14.09 (CH_3).

MS (ESI+, CH_3OH): *m/z* calcd. 349.2 $(M+Na)^+$; found: 349.2. [32]

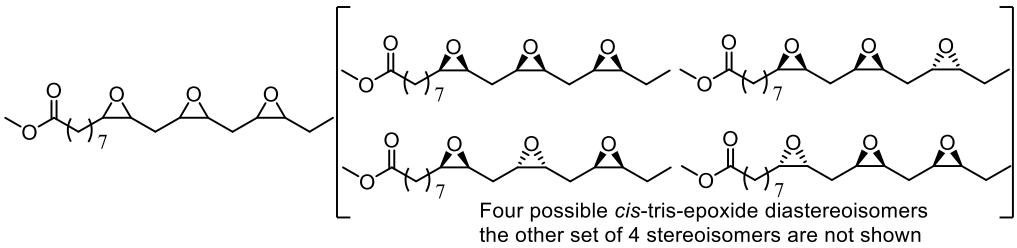

Methyl 8-(3-((3-((3-ethyloxiran-2-yl)methyl)oxiran-2-yl)methyl)oxiran-2-yl)octanoate **4c**

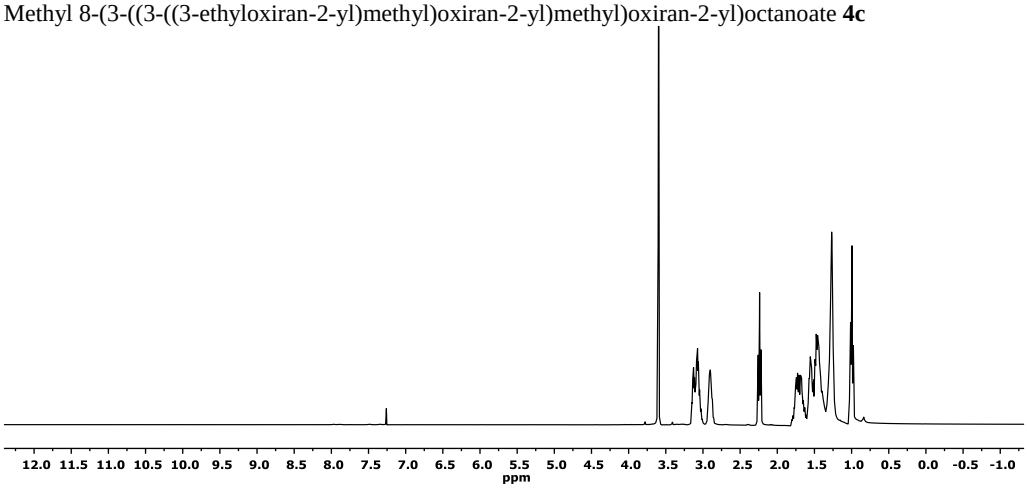

^{1}H NMR (400 MHz, $CDCl_3$) δ 3.60 (s, 3H), 3.16-3.01 (m, 4H), 2.96-2.86 (m, 2H), 2.24 (t, $^{3}J_{H,H}$ = 7.3 Hz, 2H), 1.82-1.61 (m, 4H), 1.60-1.35 (m, 8H), 1.34-1.22 (m, 6H), 1.04-0.97 (m, 3H).

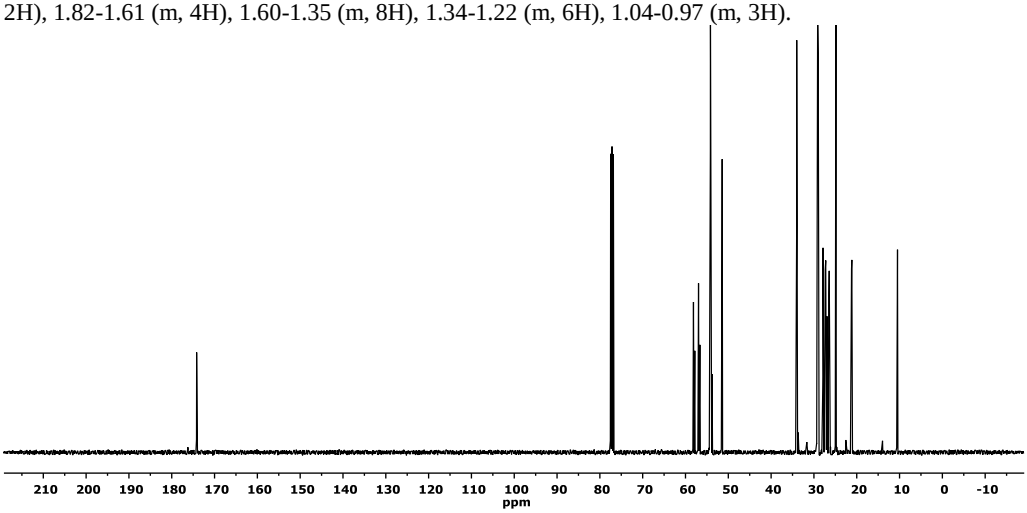

^{13}C NMR (101 MHz, $CDCl_3$) δ 174.19 (C=O), 58.14 (CH), 58.11 (CH), 57.83 (CH), 56.95 (CH), 56.93 (CH), 56.64 (CH), 54.26 (CH), 54.18 (CH), 54.11 (CH), 54.05 (CH), 53.99 (CH), 53.78 (CH), 51.42 (OCH_3), 34.02 (CH_2), 29.26 (CH_2), 29.13 (CH_2), 28.99 (CH_2), 27.88 (CH_2), 27.82 (CH_2), 27.36 (CH_2), 27.29 (CH_2), 27.24 (CH_2), 27.16 (CH_2), 27.03 (CH_2), 26.97 (CH_2), 26.92 (CH_2), 26.85 (CH_2), 26.51 (CH_2), 26.42 (CH_2), 26.40 (CH_2), 24.87 (CH_2), 21.25 (CH_2), 21.22 (CH_2), 21.14 (CH_2), 10.59 (CH_2), 10.48 (CH_3).

HRMS (ESI+, CH_3OH): *m/z* calcd. 363.2142 $(M+Na)^+$; found: 363.2147.

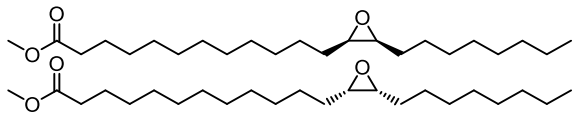

Methyl 12-3-octyloxiran-2-yl)dodecanoate **4d**

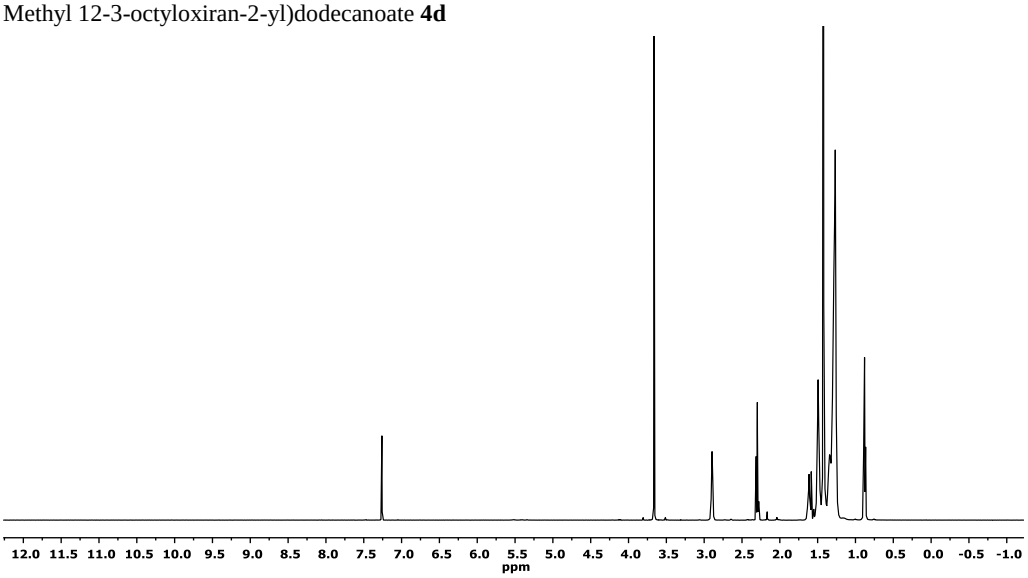

^{1}H NMR (500 MHz, $CDCl_3$) δ 3.66 (s, 3H), 2.92-2.87 (s, 2H), 2.30 (t, $^{3}J_{H,H}$ = 7.5 Hz, 2H), 1.65-1.59 (m, 2H), 1.53-1.45 (m, 6H), 1.39-1.19 (m, 26H), 0.88 (t, $^{3}J_{H,H}$ = 7.1 Hz, 3H).

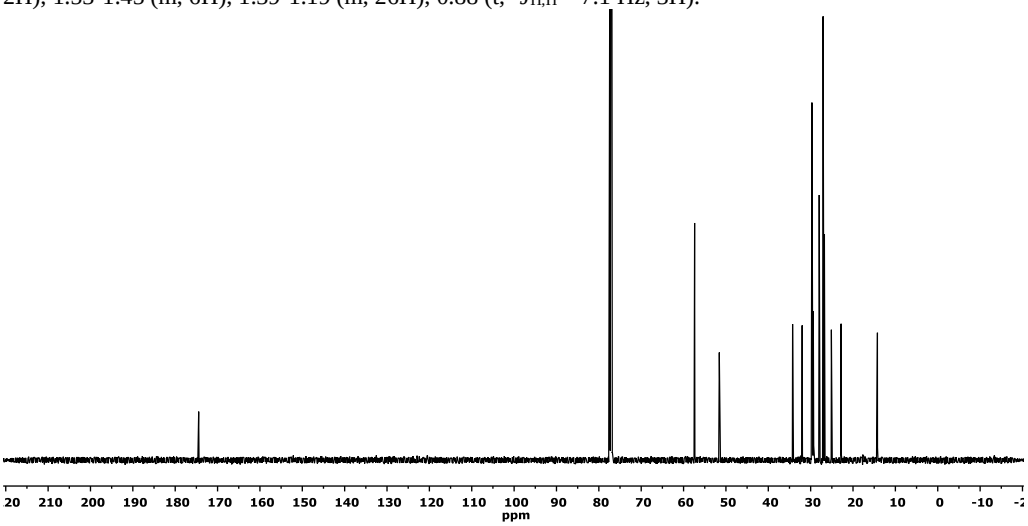

^{13}C NMR (126 MHz, $CDCl_3$) δ 174.46 (C=O), 57.39 (CH), 51.57 (OCH_3), 34.26 (CH_2), 31.01 (CH_2), 29.70 (CH_2), 29.68 (CH_2), 29.67 (CH_2), 29.58 (CH_2), 29.40 (CH_2), 29.37 (CH_2), 29.30 (CH_2), 27.98 (CH_2), 27.06 (CH_2), 26.75 (CH_2), 25.11 (CH_2), 22.81 (CH_2), 14.24 (CH_3).

MS (ESI+, CH_3OH): *m/z* calcd. 391.3 $(M+Na)^+$; found: 391.3.[32]

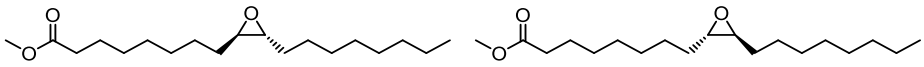

Methyl 8-3-octyloxiran-2-yl)octanoate **4e**

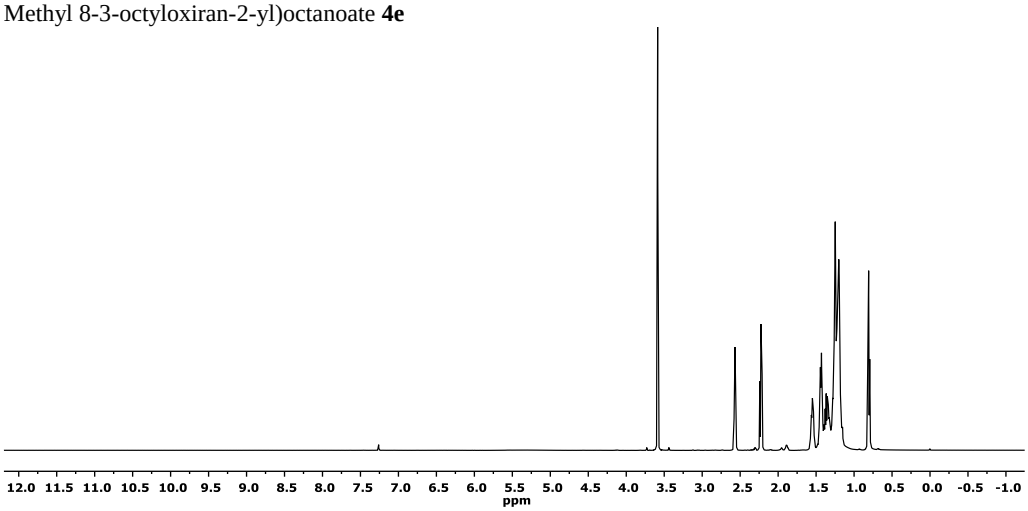

^{1}H NMR (500 MHz, $CDCl_3$) δ 3.59 (s, 3H), 2.57 (m, 2H), 2.23 (t, $^{3}J_{H,H}$ = 7.4 Hz, 2H), 1.58-1.51 (m, 2H), 1.47-1.40 (m, 4H), 1.40-1.31 (m, 4H), 1.30-1.16 (m, 16H), 0.81 (t, $^{3}J_{H,H}$ = 6.9 Hz, 3H).

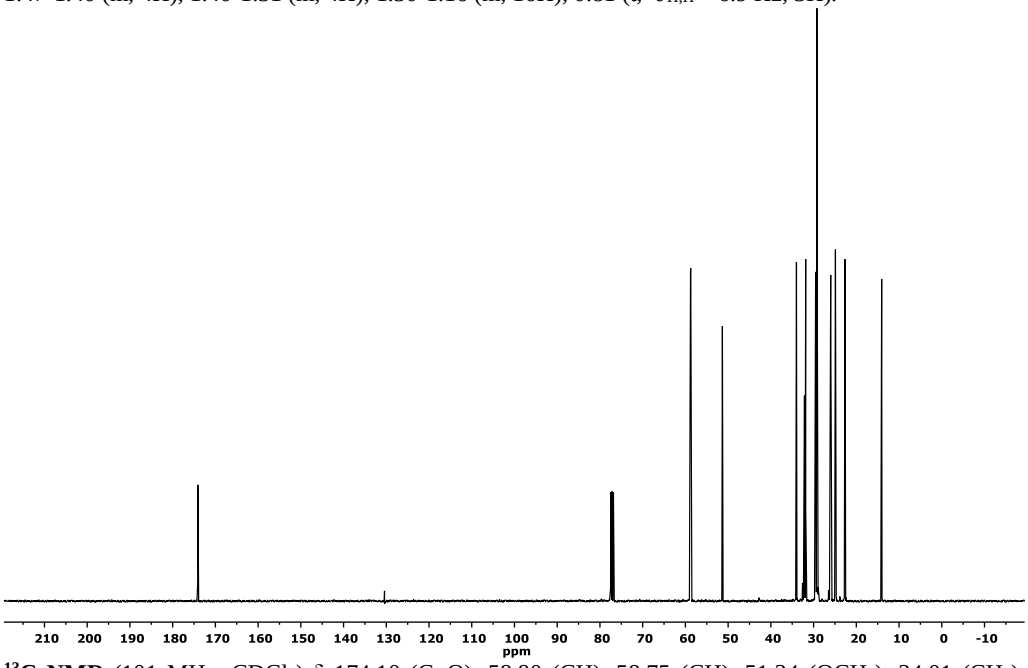

^{13}C NMR (101 MHz, $CDCl_3$) δ 174.10 (C=O), 58.80 (CH), 58.75 (CH), 51.34 (OCH_3), 34.01 (CH_2), 32.13 (CH_2), 32.09 (CH_2), 31.85 (CH_2), 29.52 (CH_2), 29.46 (CH_2), 29.23 (CH_2), 29.16 (CH_2), 29.02 (CH_2), 26.06 (CH_2), 25.99 (CH_2), 24.88 (CH_2), 22.65 (CH_2), 14.07 (CH_3).

HRMS (ESI+, CH_3OH): *m/z* calcd. 251.0526 $(M+Na)^+$; found: 251.0527.

Methyl 8-(3-(2-hydroxyoctyl)oxiran-2-yl)octanoate **4f** (*dr* = 56:44)

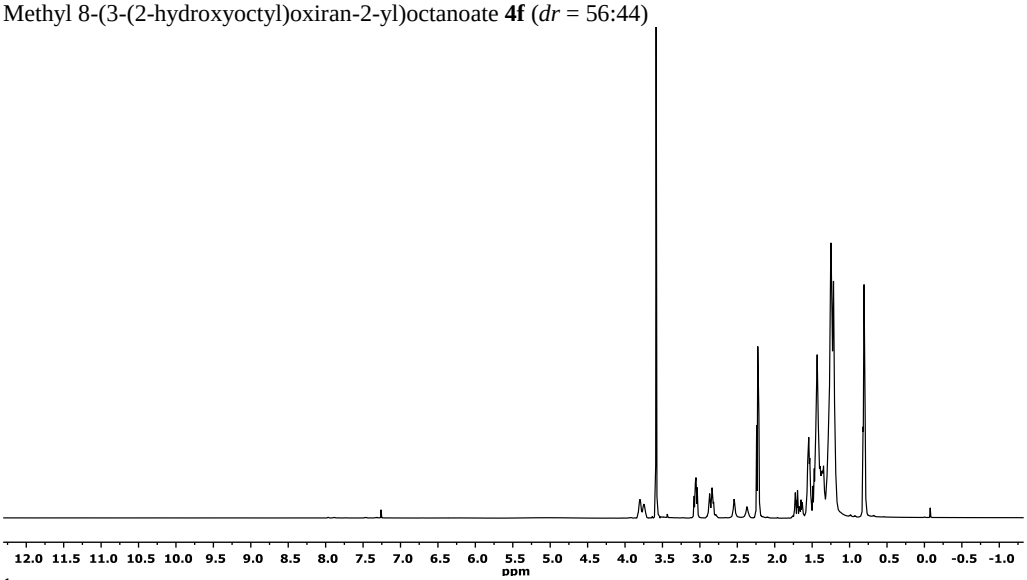

^{1}H NMR (500 MHz, $CDCl_3$) δ 3.86-3.74 (m, 1H), 3.61 (s, 3H), 3.11-3.05 (m, 1H), 2.93-2.82 (m, 1H), 2.60-2.35 (2 × br s, 1H, OH), 2.25 (t, $^{3}J_{H,H}$ = 7.5 Hz, 2H), 1.77-1.64 (m, 1H), 1.61-1.54 (m, 2H), 1.51-1.42 (m, 6H), 1.33-1.20 (m, 15H), 0.83 (t, $^{3}J_{H,H}$ = 6.8 Hz, 3H).

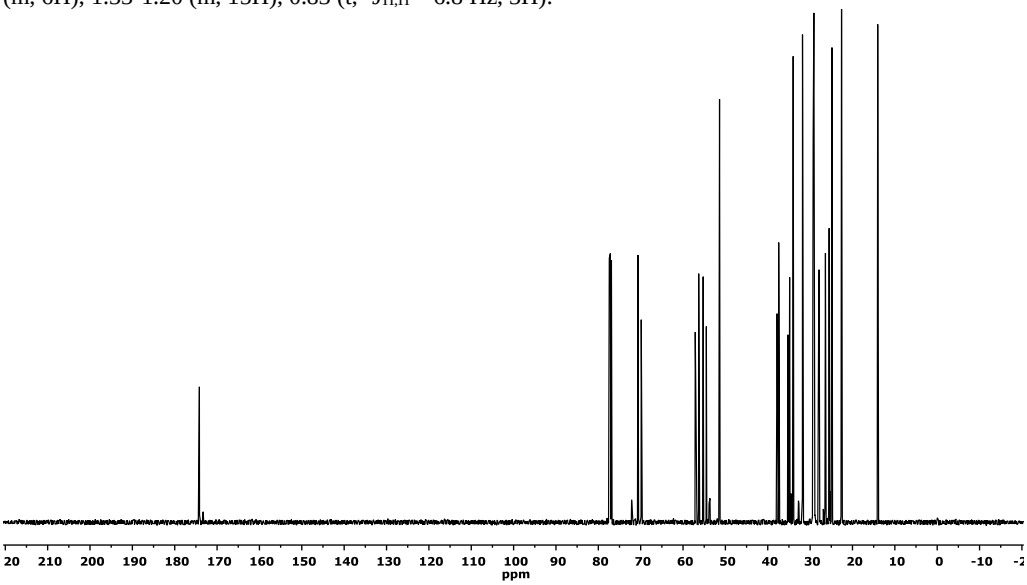

^{13}C NMR (126 MHz, $CDCl_3$) δ 174.19 (C=O), 174.18 (C=O), 70.65 (CH), 69.87 (CH), 57.12 (CH), 56.31 (CH), 55.25 (CH), 54.50 (CH), 51.38 (OCH_3), 37.79 (CH_2), 37.42 (CH_2), 35.25 (CH_2), 34.84 (CH_2), 34.00 (CH_2), 31.80 (CH_2), 29.28 (CH_2), 29.27 (CH_2), 29.25 (CH_2), 29.23 (CH_2), 29.12 (CH_2), 28.97 (CH_2), 28.00 (CH_2), 27.87 (CH_2), 26.41 (CH_2), 26.38 (CH_2), 25.58 (CH_2), 25.51 (CH_2), 24.85 (CH_2), 22.58 (CH_2), 14.04 (CH_3).

MS (ESI+, CH_3OH): *m/z* calcd. 351.3 $(M+Na)^+$; found: 351.3.[32]

4.4.5 ^{1}H and ^{13}C-NMR data of carbonate products and MS analysis

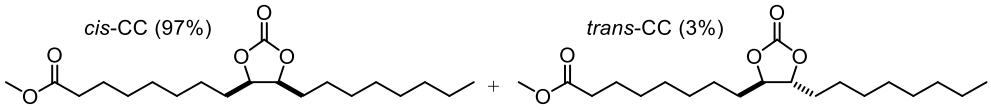

Methyl 8-(5-octyl-2-oxo-1,3-dioxolan-4-yl)octanoate **CC-4a**

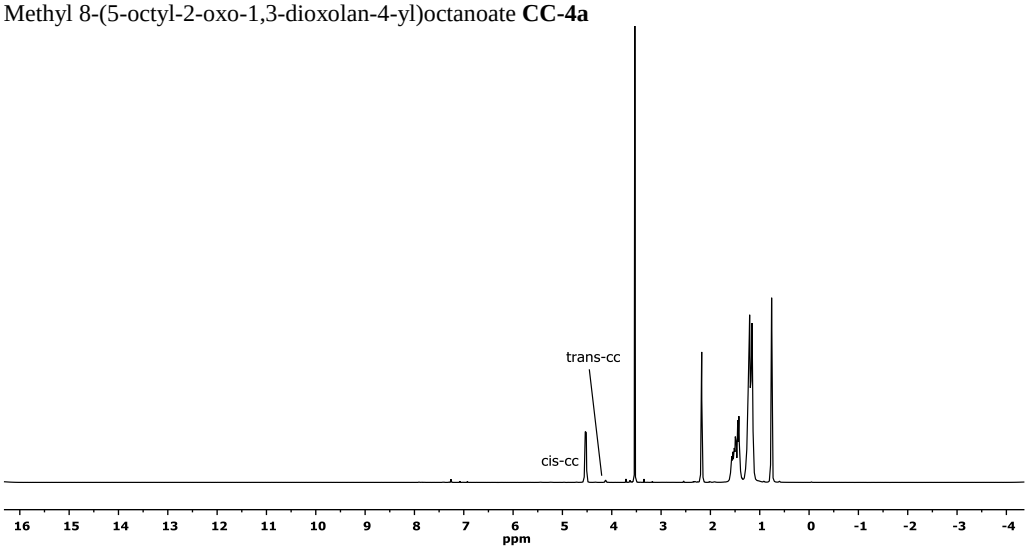

For the major isomer of CC-4a (*cis*): ^{1}H NMR (400 MHz, $CDCl_3$) δ 4.55-4.50 (m, 2H), 3.53 (s, 3H), 2.18 (t, $^{3}J_{H,H}$= 7.5 Hz, 2H), 1.60-1.40 (m, 8H), 1.30-1.10 (m, 18H), 0.76 (t, $^{3}J_{H,H}$ = 7.1 Hz, 3H). The peak at δ 4.14-4.11 (m) corresponds to ***trans*-CC-4a** (3%).

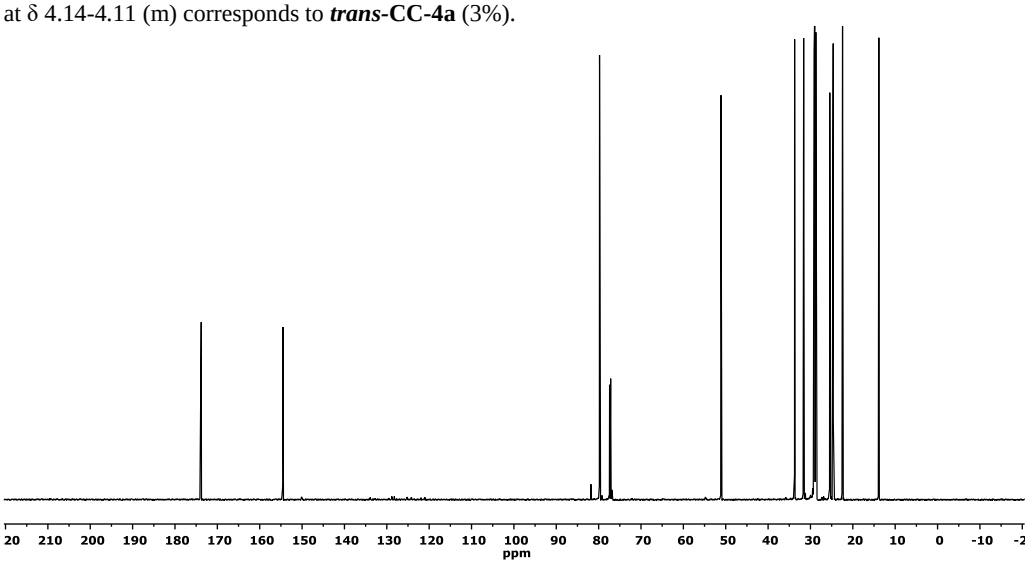

For the major isomer of CC-4a (*cis*): ^{13}C NMR (126 MHz, $CDCl_3$) δ 173.80 (C=O), 154.51 (C=O), 79.78 (CH), 79.75 (CH), 51.13 (OCH_3), 33.74 (CH_2), 31.61 (CH_2), 29.15 (CH_2), 29.05 (CH_2), 28.96 (CH_2), 28.82 (CH_2), 28.79 (CH_2), 28.73 (CH_2), 28.68 (CH_2), 28.64 (CH_2), 25.44 (CH_2), 25.37 (CH_2), 24.63 (CH_2), 22.43 (CH_2), 13.86 (CH_3).

MS (ESI+, CH_3OH): *m/z* calcd. 379.2 $(M+Na)^{+}$; found: 379.2. [32]

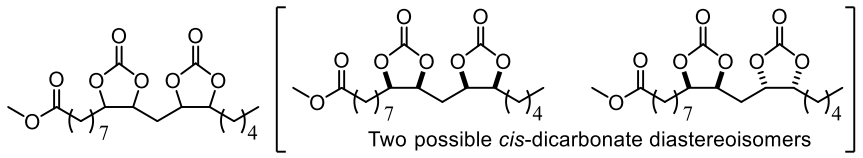

Methyl 8-(2-oxo-5-((2-oxo-5-pentyl-1,3-dioxolan-4-yl)methyl)-1,3-dioxolan-4-yl)octanoate **CC-4b.** Note: mixture of diastereo-isomers, two *cis* diastereo-isomers (97%) and two *trans* diastereo-isomers (3%).

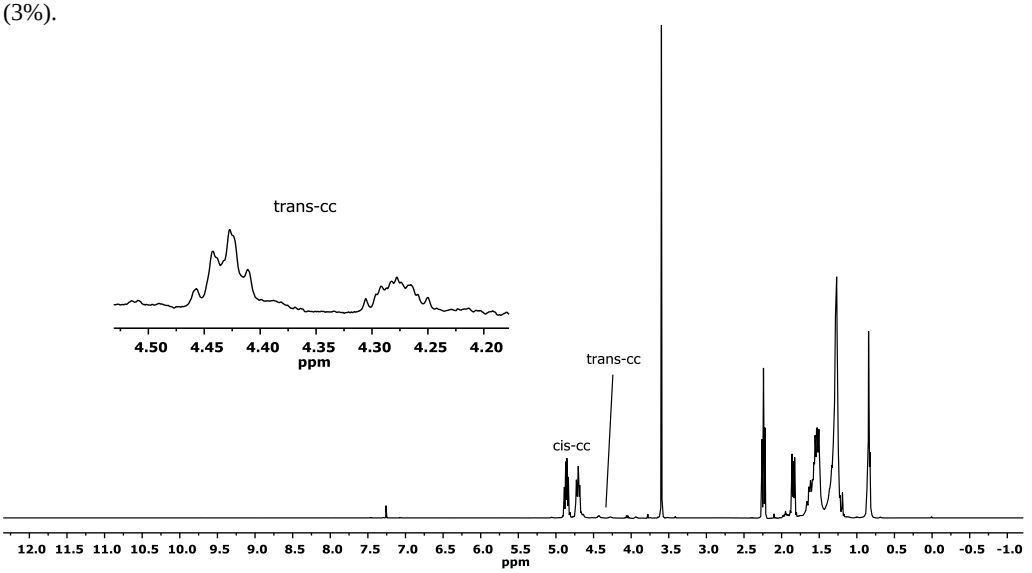

For the major isomers of CC-4b (*cis*): ^{1}H NMR (400 MHz, $CDCl_3$) δ 4.90-4.65 (m, 4H), 3.60 (s, 3H), 2.24 (t, $^{3}J_{H,H}$= 7.6 Hz, 2H), 1.88-1.81(m, 2H), 1.67-1.48 (m, 8H), 1.37-1.22 (m, 12H), 0.84 (t, $^{3}J_{H,H}$ = 7.2 Hz, 3H). The peaks at δ 4.47-4.25 (m) correspond to ***trans*-CC-4b** (3%).

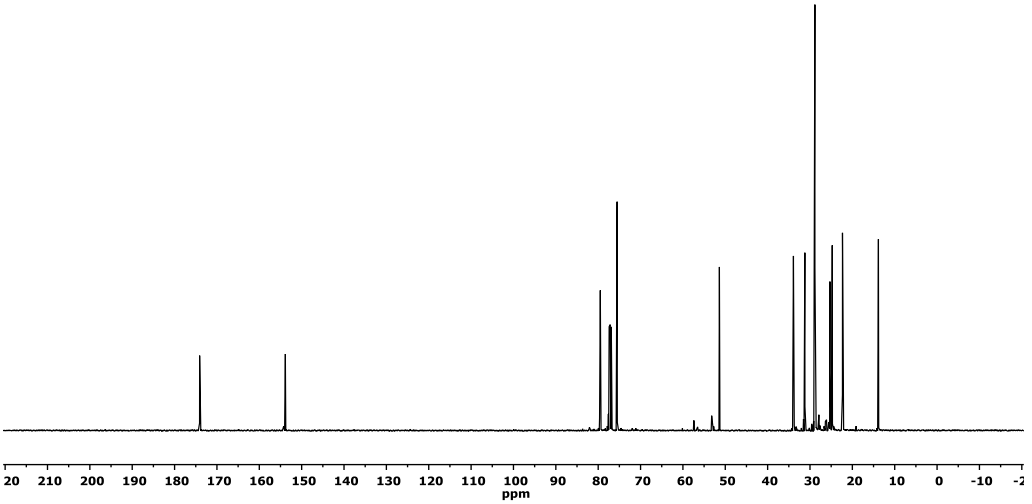

For the major isomers of CC-4b (*cis*): ^{13}C NMR (126 MHz, $CDCl_3$) δ 174.09 (C=O), 153.87 (C=O), 153.85 (C=O), 79.55 (CH), 79.50 (CH), 75.53 (CH), 51.39 (OCH_3), 33.91 (CH_2), 31.21 (CH_2), 28.89 (CH_2), 28.85 (CH_2), 28.77 (CH_2), 25.56 (CH_2), 25.30 (CH_2), 24.75 (CH_2), 22.33(CH_2), 13.85 (CH_3).
MS (ESI+, CH_3OH): *m/z* calcd. 437.2 $(M+Na)^+$; found: 437.2.[32]

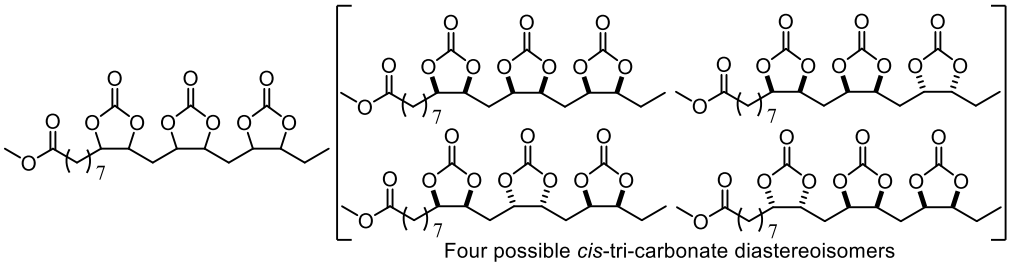

Methyl 8-(5-((5-((5-ethyl-2-oxo-1,3-dioxolan-4-yl)methyl)-2-oxo-1,3-dioxolan-4-yl)methyl)-2-oxo-1,3-dioxolan-4-yl)octanoate **CC-4c**. Note: mixture of diastereo-isomers, four *cis* diastereo-isomers (96%) and four *trans* diastereo-isomers (4%).

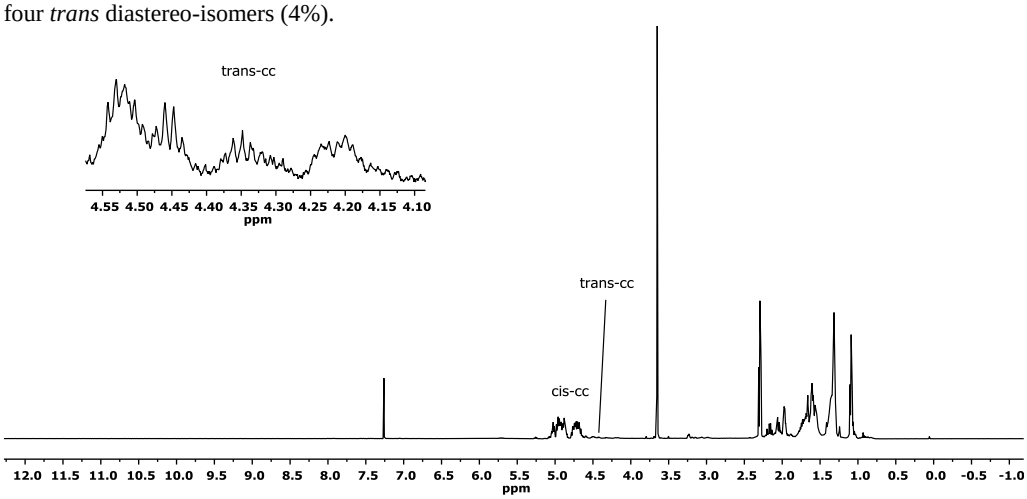

For the major isomers of CC-4c (*cis*): ^{1}H NMR (500 MHz, $CDCl_3$) δ 5.06-4.66 (m, 6H), 3.65 (s, 3H), 2.29 (t, $^{3}J_{H,H}$ = 7.4 Hz, 2H), 2.23-1.93 (m, 4H), 1.80-1.50 (m, 6H), 1.40-1.27 (m, 8H), 1.09 84 (t, $^{3}J_{H,H}$ = 7.2 Hz, 3H). The peaks at δ 4.55-4.15 (m) correspond to ***trans*-CC-4c** (4%).

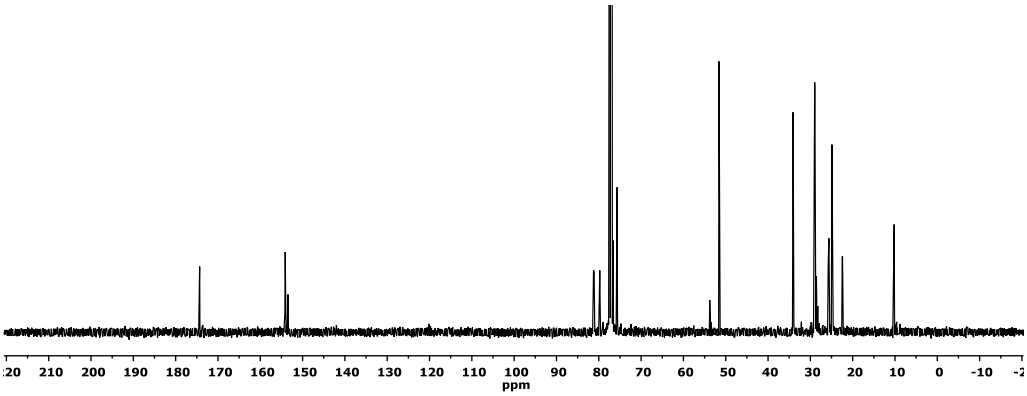

For the major isomers of CC-4c (*cis*): ^{13}C NMR (126 MHz, $CDCl_3$) δ 174.33 (C=O), 154.19 (C=O), 154.11 (C=O), 153.44 (C=O), 81.24 (CH), 81.10 (CH), 79.90 (CH), 79.77 (CH), 76.63 (CH), 75.68 (CH), 51.59 (OCH_3), 34.08 (CH_2), 29.03 (CH_2), 29.03 (CH_2), 28.95 (CH_2), 28.88 (CH_2), 28.53 (CH_2), 28.25 (CH_2), 25.79 (CH_2), 25.62 (CH_2), 24.89 (CH_2), 24.89 (CH_2), 22.47 (CH_2), 22.40 (CH_2), 10.33 (CH_3).

HRMS (ESI+, CH_3OH): *m/z* calcd. 495.1837 $(M+Na)^+$; found: 495.1848.

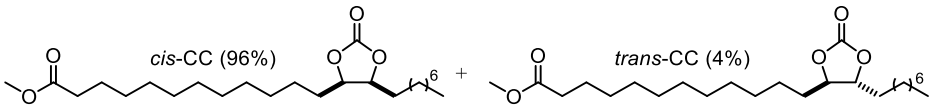

Methyl 12-(5-octyl-2-oxo-1,3-dioxolan-4-yl)dodecanoate **CC-4d**

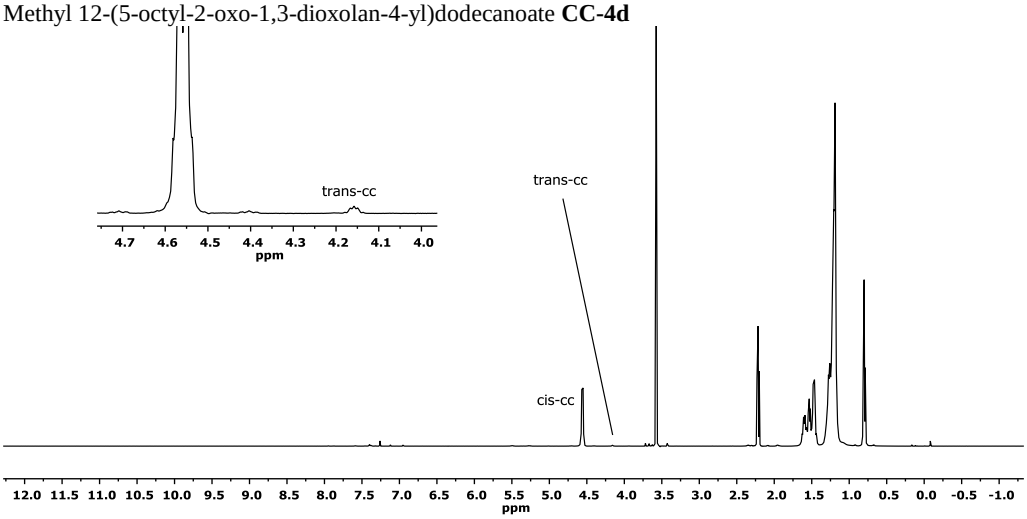

For the major isomer of CC-4d (*cis*): ^{1}H NMR (400 MHz, $CDCl_3$) δ 4.59-4.53 (m, 2H), 3.57 (s, 3H), 2.22 (t, $^{3}J_{H,H}$ = 7.5 Hz, 2H), 1.65-1.40 (m, 8H), 1.33-1.14 (m, 26H), 0.80 (t, $^{3}J_{H,H}$ = 7.1 Hz, 3H). The peak at δ 4.17-4.14 (m) corresponds to ***trans*-CC-4d** (4%).

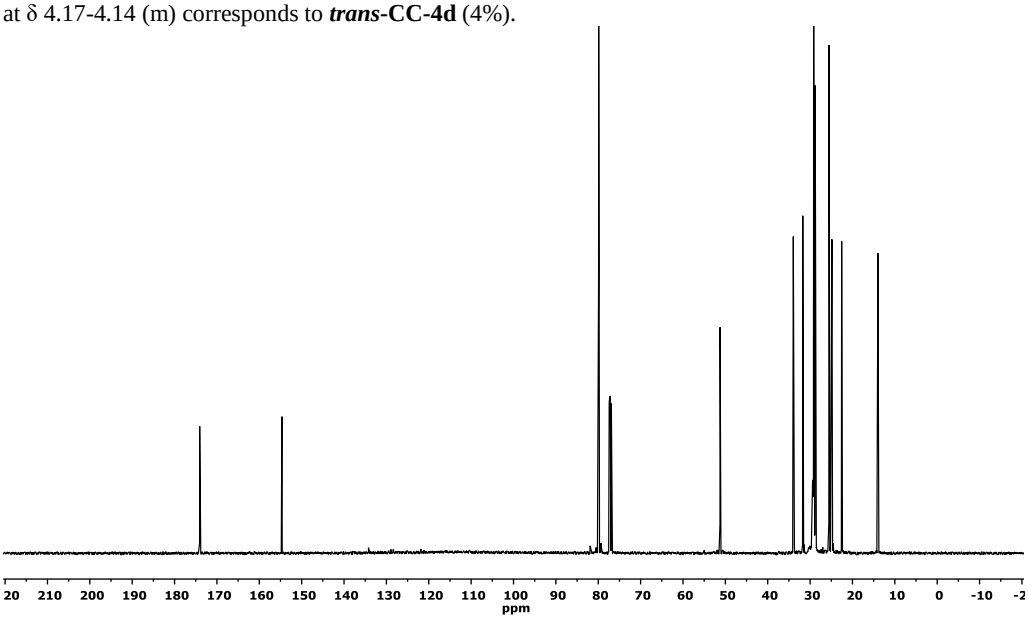

For the major isomer of CC-4d (*cis*): ^{13}C NMR (126 MHz, $CDCl_3$) δ 174.07 (C=O), 154.66 (C=O), 79.90 (CH), 51.25 (OCH_3), 33.96 (CH_2), 31.72 (CH_2), 29.40 (CH_2), 29.36 (CH_2), 29.31 (CH_2), 29.27 (CH_2), 29.26 (CH_2), 29.17 (CH_2), 29.15 (CH_2), 29.07 (CH_2), 29.03 (CH_2), 28.80 (CH_2), 25.54 (CH_2), 24.85 (CH_2), 22.55 (CH_2), 13.98 (CH_3).

MS (ESI+, CH_3OH): *m/z* calcd. 435.3 $(M+Na)^+$; found: 435.3. [32]

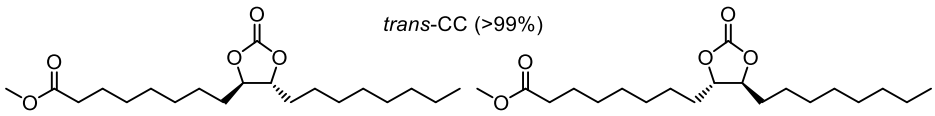

Methyl 8-5-octyl-2-oxo-1,3-dioxolan-4-yl)octanoate **CC-4e**

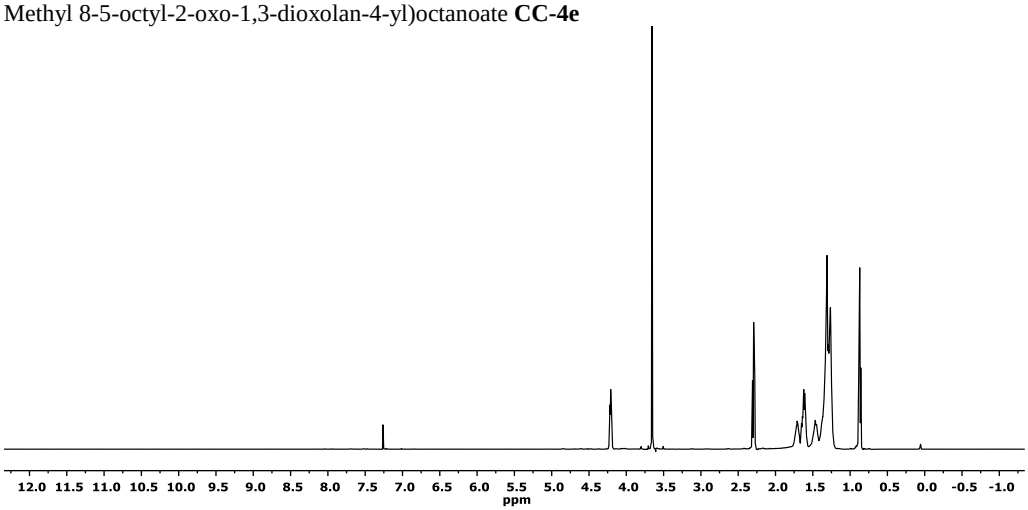

^{1}H NMR (500 MHz, $CDCl_3$) δ 4.22-4.19 (m, 2H), 3.66 (s, 3H), 2.29 (t, $^{3}J_{H,H}$ = 7.6 Hz, 2H), 1.76-1.67 (m, 2H), 1.66-1.56 (m, 4H), 1.52-1.41 (m, 2H), 1.35-1.24 (m, 18H), 0.87 (t, $^{3}J_{H,H}$ = 7.0 Hz, 3H).

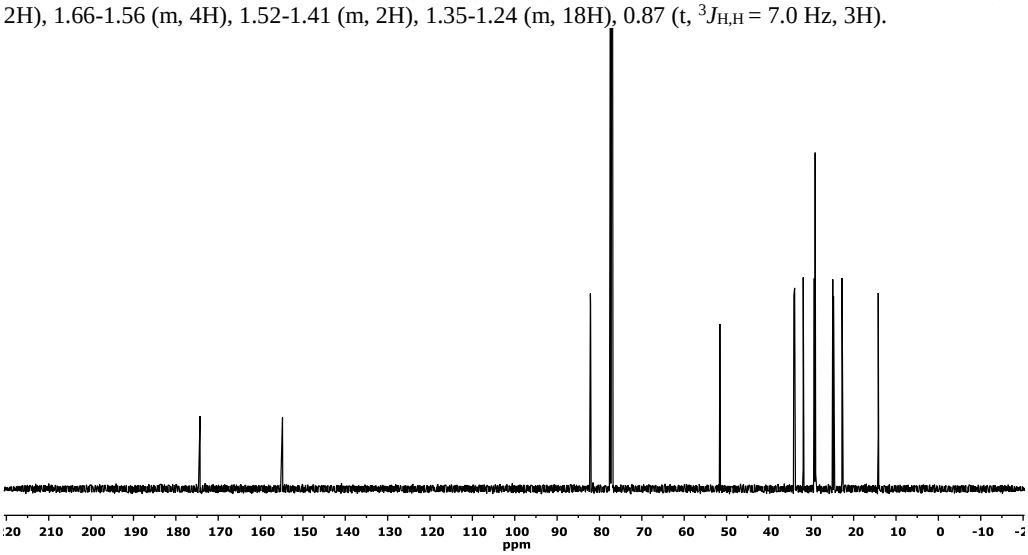

^{13}C NMR (126 MHz, $CDCl_3$) δ 174.29 (C=O), 154.82 (C=O), 82.14 (CH), 82.10 (CH), 51.58 (OCH_3), 34.11 (CH_2), 33.94 (CH_2), 33.93 (CH_2), 31.90 (CH_2), 29.42 (CH_2), 29.29 (CH_2), 29.23 (CH_2), 29.08 (CH_2), 29.03 (CH_2), 24.93 (CH_2), 24.76 (CH_2), 24.72 (CH_2), 22.74 (CH_2), 14.19 (CH_3).

HRMS (ESI+, CH_3OH): *m/z* calcd. 379.2455 $(M+Na)^+$; found: 379.2458.

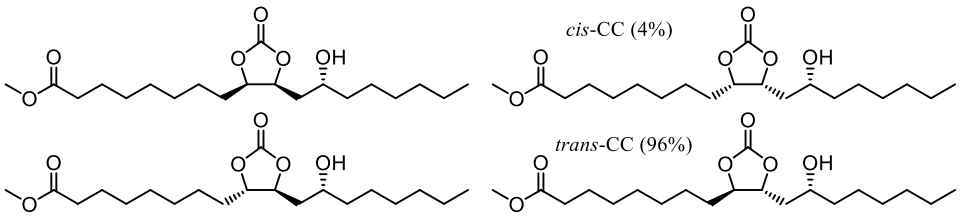

Methyl 8-(5-(2-hydroxyoctyl)-2-oxo-1,3-dioxolan-4-yl)octanoate **CC-4f**

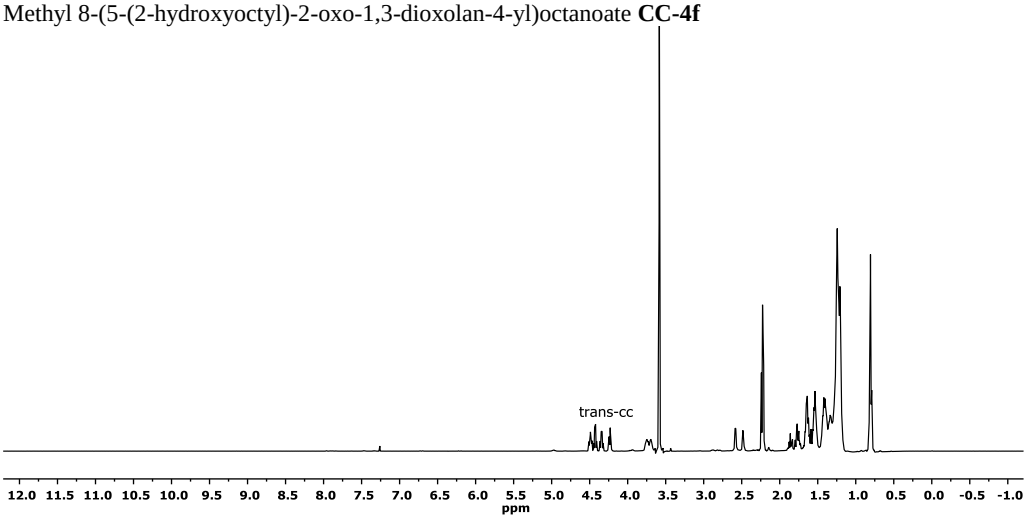

For the major isomers of CC-4f (*trans*): ^{1}H NMR (500 MHz, $CDCl_3$) δ 4.55-4.23 (m, 2H), 3.81-3.69 (m, 1H), 3.58 (s, 3H), 2.62-2.49 (2 × br s, 1H, OH), 2.23 (t, $^{3}J_{H,H}$ = 7.4 Hz, 2H), 1.91-1.19 (m, 24H), 0.81 (t, $^{3}J_{H,H}$ = 7.1 Hz, 3H).

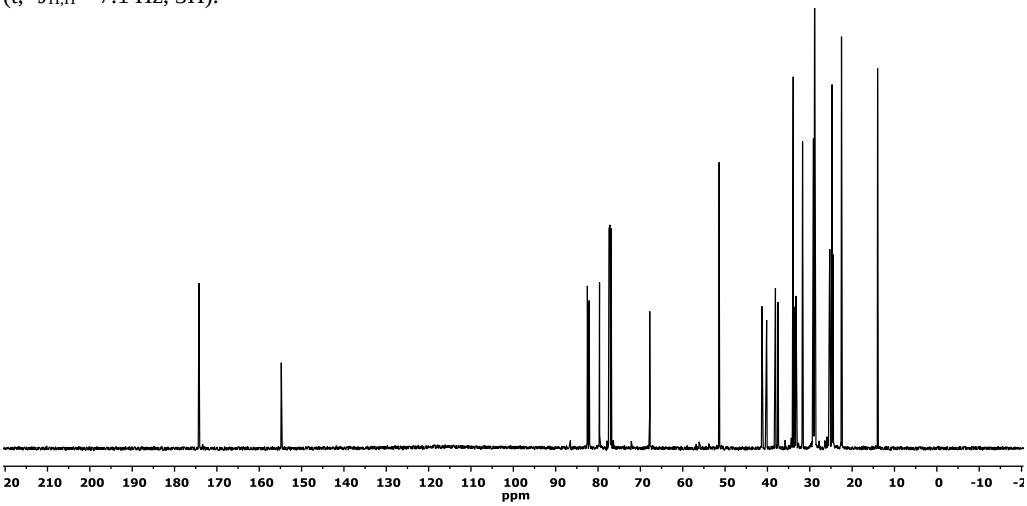

For the major isomers of CC-4f (*trans*): ^{13}C NMR (126 MHz, $CDCl_3$) δ 174.25 (C=O), 154.80 (C=O), 154.77 (C=O), 82.52 (CH), 82.10 (CH), 79.84 (CH), 79.64 (CH), 67.80 (CH), 67.61 (CH), 51.40(OCH_3), 41.29 (CH_2), 40.19 (CH_2), 38.10 (CH_2), 37.49 (CH_2), 33.91 (CH_2), 33.50 (CH_2), 33.25 (CH_2), 31.70 (CH_2), 29.14 (CH_2), 28.84 (CH_2), 28.80 (CH_2), 25.36 (CH_2), 25.27 (CH_2), 24.74 (CH_2), 24.48 (CH_2), 22.51 (CH_2), 13.99 (CH_3).

MS (ESI+, CH_3OH): *m/z* calcd. 395.2 $(M+Na)^+$; found: 395.2. [32]

4.4.6 ^{1}H-NMR analysis of the crude reaction mixture for CC-4a

Figure 4.1 ^{1}H NMR reaction crude of cyclic carbonate **CC-4a** (data for the product obtained using the conditions reported in Table 4.1, entry 18). The NMR analysis shows the high chemo-selectivity towards cyclic carbonate formation and the virtual absence of methyl 9-oxo-octadecanoate and methyl 10-oxo-octadecanoate.

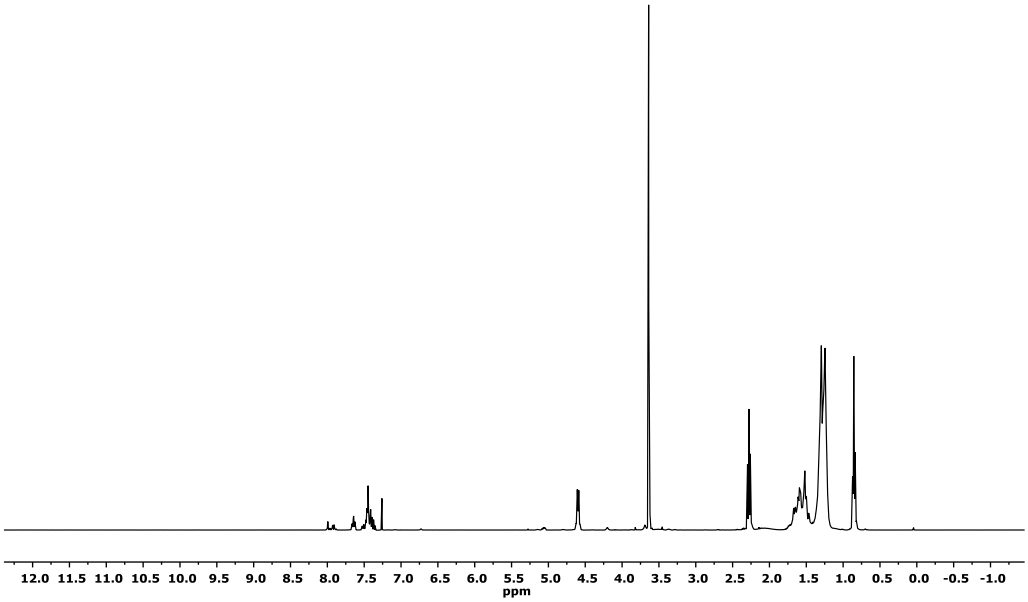

Figure 4.2 Methyl 9-oxooctadecanoate and methyl 10-oxooctadecanoate. Original data (^{1}H NMR and ^{13}C NMR data) for methyl 9-oxooctadecanoate and methyl 10-oxooctadecanoate can be found in the Supplementary Information of reference [32]

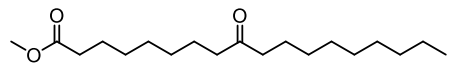

methyl 9-oxooctadecanoate

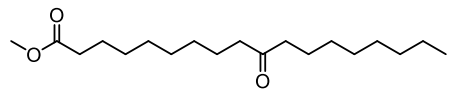

methyl 10-oxooctadecanoate

4.5 References

[1] C. Martín, G. Fiorani, A. W. Kleij, *ACS Catal.* **2015**, *5*, 1353–1370.

[2] J. W. Comerford, I. D. V. Ingram, M. North, X. Wu, *Green Chem.* **2015**, *17*, 1966–1987.

[3] G. Fiorani, W. Guo, A. W. Kleij, *Green Chem.* **2014**, *17*, 1375–1389.

[4] C. J. Whiteoak, N. Kielland, V. Laserna, E. C. Escudero-Adán, E. Martin, A. W. Kleij, *J. Am. Chem. Soc.* **2013**, *135*, 1228–1231.

[5] Y. Qin, H. Guo, X. Sheng, X. Wang, F. Wang, *Green Chem.* **2015**, *17*, 2853–2858.

[6] F. Della Monica, S. V. C. Vummaleti, A. Buonerba, A. De Nisi, M. Monari, S. Milione, A. Grassi, L. Cavallo, C. Capacchione, *Adv. Synth. Catal.* **2016**, *358*, 3231–3243.

[7] L. Martínez-Rodríguez, J. Otalora Garmilla, A. W. Kleij, *ChemSusChem* **2016**, *9*, 749–755.

[8] C. Maeda, J. Shimonishi, R. Miyazaki, J. Y. Hasegawa, T. Ema, *Chem.-Eur. J.* **2016**, *22*, 6556–6563.

[9] T. Sakakura, J. C. Choi, H. Yasuda, *Chem. Rev.* **2007**, *107*, 2365–2387.

[10] M. North, R. Pasquale, C. Young, *Green Chem.* **2010**, *12*, 1514.

[11] B. Schäffner, F. Schäffner, S. P. Verevkin, A. Börner, *Chem. Rev.* **2010**, *110*, 4554–4581.

[12] V. Laserna, G. Fiorani, C. J. Whiteoak, E. Martin, E. Escudero-Adán, A. W. Kleij, *Angew. Chem. Int. Ed.* **2014**, *53*, 10416–10419.

[13] A. Khan, L. Yang, J. Xu, L. Y. Jin, Y. J. Zhang, *Angew. Chem. Int. Ed.* **2014**, *53*, 11257–11260.

[14] W. Guo, L. Martínez-Rodríguez, R. Kuniyil, E. Martin, E. C. Escudero-Adán, F. Maseras, A. W. Kleij, *J. Am. Chem. Soc.* **2016**, *138*, 11970–11978.

[15] J. Rintjema, R. Epping, G. Fiorani, E. Martín, E. C. Escudero-Adán, A. W. Kleij, *Angew. Chem. Int. Ed.* **2016**, *55*, 3972–3976.

[16] W. Guo, L. Martínez-Rodríguez, E. Martin, E. C. Escudero-Adán, A. W. Kleij, *Angew. Chem. Int. Ed.* **2016**, *55*, 11037-11040.

[17] J. E. Gómez, W. Guo, A. W. Kleij, *Org. Lett.* **2016**, *18*, 6042–6045.

[18] A. Cai, W. Guo, L. Martínez-Rodríguez, A. W. Kleij, *J. Am. Chem. Soc.* **2016**, *138*, 14194–14197.

[19] W. Guo, V. Laserna, J. Rintjema, A. W. Kleij, *Adv. Synth. Catal.* **2016**, *358*, 1602–1607.

[20] G. L. Gregory, G. Kociok-Köhn, A. Buchard, *Polym. Chem.* **2017**, 2093–2104.

[21] G. L. Gregory, E. M. López-Vidal, A. Buchard, *Chem. Commun.* **2017**, *53*, 2198–2217.

[22] P. Brignou, M. Priebe Gil, O. Casagrande, J. F. Carpentier, S. M. Guillaume, *Macromolecules* **2010**, *43*, 8007–8017.

[23] N. Ajellal, J.-F. Carpentier, C. Guillaume, S. M. Guillaume, M. Helou, V. Poirier, Y. Sarazin, A. Trifonov, *Dalton Trans.* **2010**, *39*, 8363–8376.

[24] S. Schmidt, F. J. Gatti, M. Luitz, B. S. Ritter, B. Bruchmann, R. Mülhaupt, *Macromolecules* **2017**, *50*, 2296–2303.

[25] S. Schmidt, B. S. Ritter, D. Kratzert, B. Bruchmann, R. Mülhaupt, *Macromolecules* **2016**, *49*, 7268–7276.

[26] M. Bähr, R. Mülhaupt, *Green Chem.* **2012**, *14*, 483.

[27] B. Nohra, L. Candy, J. F. Blanco, C. Guerin, Y. Raoul, Z. Mouloungui, *Macromolecules* **2013**, *46*, 3771–3792.

[28] B. Grignard, J.-M. Thomassin, S. Gennen, L. Poussard, L. Bonnaud, J.-M. Raquez, P. Dubois, M.-P. Tran, C. B. Park, C. Jérôme, et al., *Green Chem.* **2016**, *18*, 2206–2215.

[29] H.-W. Engels, H.-G. Pirkl, R. Albers, R. W. Albach, J. Krause, A. Hoffmann, H. Casselmann, J. Dormish, *Angew. Chem. Int. Ed.* **2013**, *52*, 9422–9441.

[30] B. Schäffner, M. Blug, D. Kruse, M. Polyakov, A. Köckritz, A. Martin, P. Rajagopalan, U. Bentrup, A. Brückner, S. Jung, et al., *ChemSusChem* **2014**, *7*, 1133–1139.

[31] J. Langanke, L. Greiner, W. Leitner, *Green Chem.* **2013**, *15*, 1173–1182.

[32] N. Tenhumberg, H. Büttner, B. Schäffner, D. Kruse, M. Blumenstein, T. Werner, *Green Chem.* **2016**, *18*, 3775–3788.

[33] J. Großeheilmann, H. Büttner, C. Kohrt, U. Kragl, T. Werner, *ACS Sust. Chem. Engin.* **2015**, *3*, 2817–2822.

[34] M. Alves, B. Grignard, S. Gennen, C. Detrembleur, C. Jerome, T. Tassaing, *RSC Adv.* **2015**, *5*, 53629–53636.

[35] B. Tamami, S. Sohn, G. L. Wilkes, *J. Appl. Polym. Sci.* **2004**, *92*, 883–891.

[36] H. Büttner, J. Steinbauer, C. Wulf, M. Dindaroglu, H.-G. Schmalz, T. Werner, *ChemSusChem* **2017**, *10*, 1076–1079.

[37] C. J. Whiteoak, E. Martin, M. M. Belmonte, J. Benet-Buchholz, A. W. Kleij, *Adv. Synth. Catal.* **2012**, *354*, 469–476.

[38] C. J. Whiteoak, E. Martin, E. Escudero-Adán, A. W. Kleij, *Adv. Synth. Catal.* **2013**, *355*, 2233–2239.

[39] L. Peña Carrodeguas, J. González-Fabra, F. Castro-Gómez, C. Bo, A. W. Kleij, *Chem.-Eur. J.* **2015**, *21*, 6115–6122.

[40] G. Fiorani, M. Stuck, C. Martín, M. M. Belmonte, E. Martin, E. C. Escudero-Adán, A. W. Kleij, *ChemSusChem* **2016**, *9*, 1304–1311.

[41] C. Miceli, J. Rintjema, E. Martin, E. C. Escudero-Adán, C. Zonta, G. Licini, A. W. Kleij, *ACS Catal.* **2017**, 2367–2373.

[42] J. Rintjema, A. W. Kleij, *ChemSusChem* **2017**, *10*, 1274–1282.

[43] J. Rintjema, W. Guo, E. Martin, E. C. Escudero-Adán, A. W. Kleij, *Chem.-Eur. J.* **2015**, *21*, 10754–10762.

[44] A. Chandrasekaran, R. O. Day, R. R. Holmes, *J. Am. Chem. Soc.* **2000**, *122*, 1066–1072.

[45] C. J. Whiteoak, N. Kielland, V. Laserna, F. Castro-Gómez, E. Martin, E. C. Escudero-Adán, C. Bo, A. W. Kleij, *Chem.-Eur. J.* **2014**, *20*, 2264–2275.

UNIVERSITAT ROVIRA I VIRGILI
AVANCES EN SISTEMAS INTERACTIVOS PARA PERSONAS CON PARÁLISIS CEREBRAL
Leticia Peña Carrodeguas

List of Relevant Compounds

Catalysts

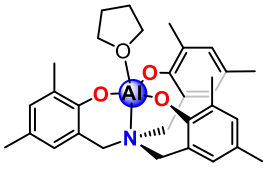

Al^{MeMe}

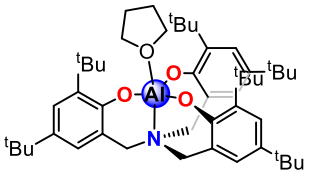

Al^{tButBu}

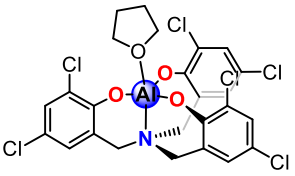

Al^{ClCl}

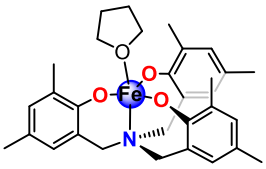

Fe^{MeMe}

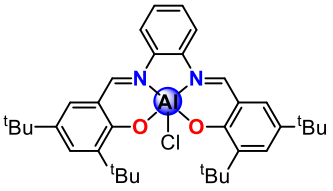

(salph-^{t}Bu)AlCl

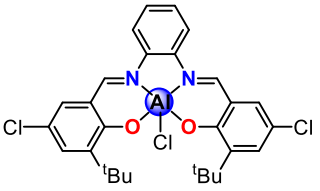

(salph-Cl)AlCl

Chapter 1

1a

1b

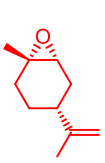

1c

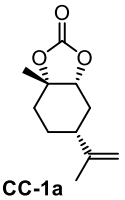

CC-1a

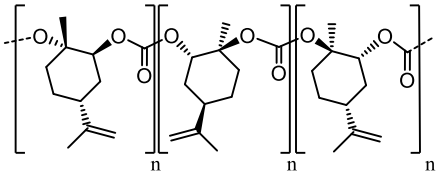

poly(CO_2-*alt*-**1a**)

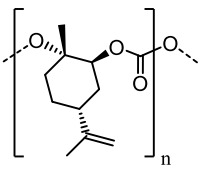

poly(CO_2-*alt*-**1b**)

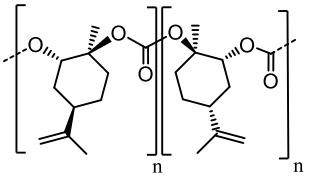

poly(CO_2-*alt*-**1c**)

Chapter 2

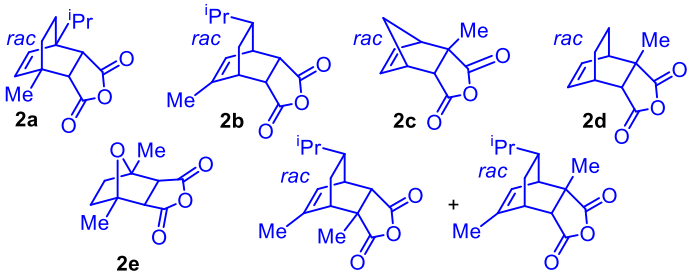

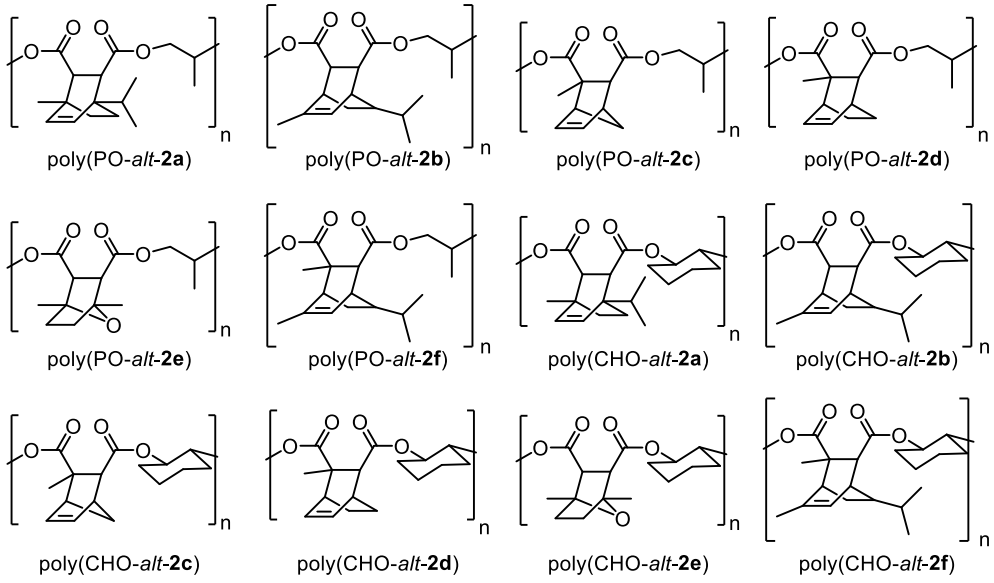

***cis* and *trans* diol model compounds (MC)**

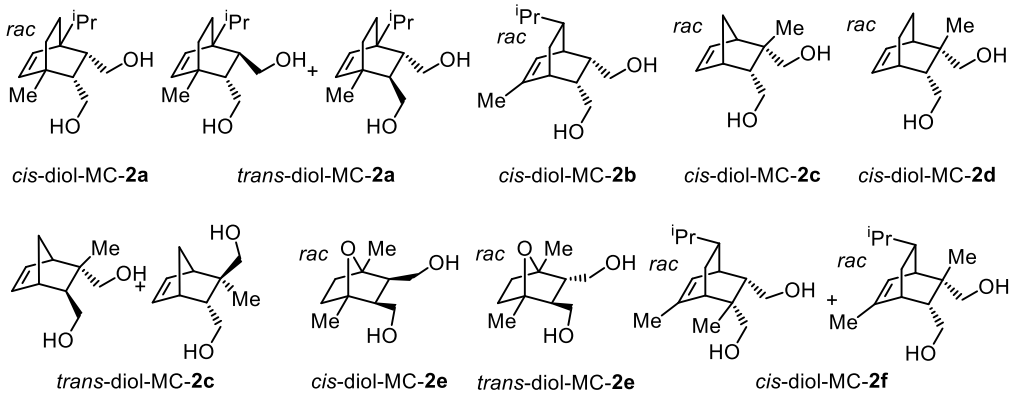

Chapter 3

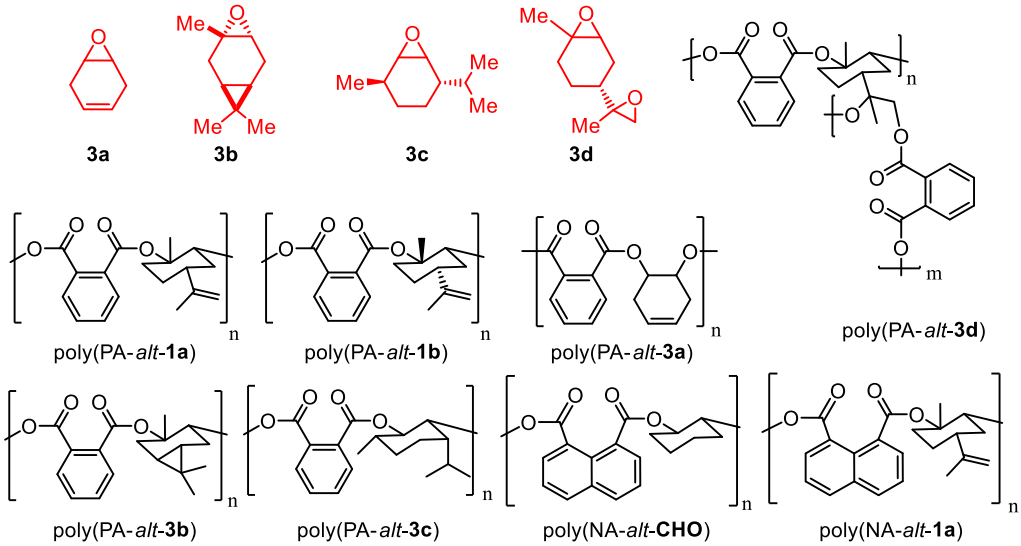

Chapter 4

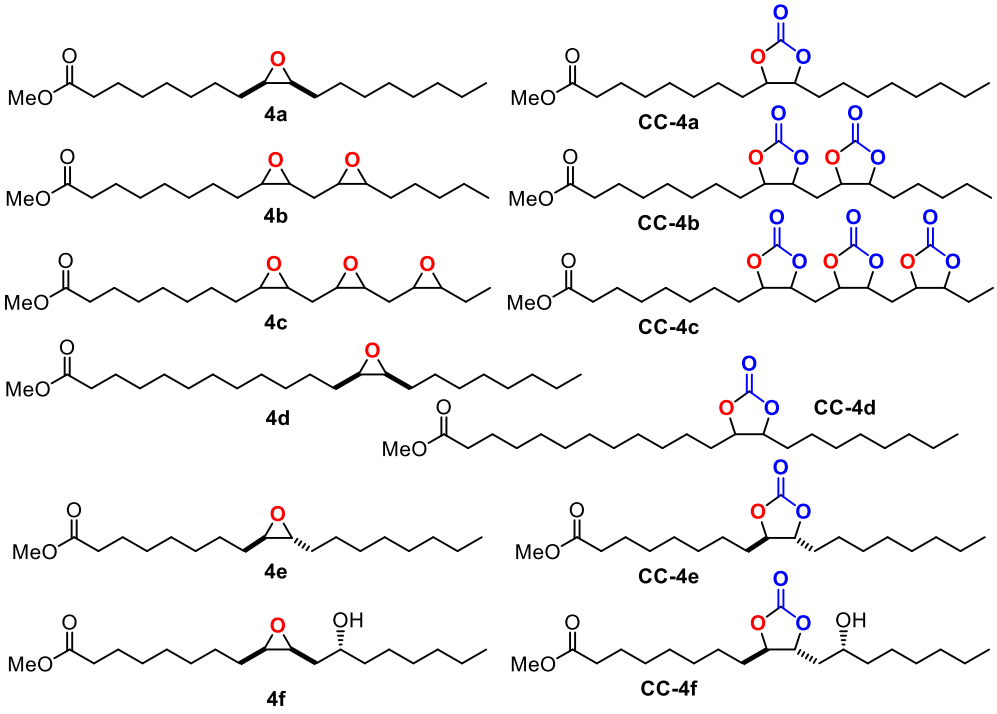

UNIVERSITAT ROVIRA I VIRGILI
AVANCES EN SISTEMAS INTERACTIVOS PARA PERSONAS CON PARÁLISIS CEREBRAL
Leticia Peña Carrodeguas

Conclusions

Plastics are important materials in modern life. However, due to concerns about fossil resources depletion, efforts have been made to provide bio-derived alternatives for conventional oil and gas based plastics. Although there is no straightforward solution for these complex environmental problems, ongoing efforts are made to develop more sustainable polymers. Research has mainly focused on replacing fossil raw materials with renewable alternatives and on developing materials that are suitable for recycling or biodegradation. In particular, monomers such as carbon dioxide, terpenes and vegetable oils have potential to be used as feedstocks for the production of sustainable materials.

One limiting factor in the development of bio-renewable polymers is that they must show similar, complementary or improved properties compared with the polymers available at present to be commercially viable. Furthermore, efficient catalysis is required to produce monomers and to facilitate selective polymerization reactions. This thesis has focused on the development of high T_g polymers from renewable sources, and catalysis design has been shown to be crucial. In particular, we have studied Al(III) and Fe(III) aminotriphenote complexes as modular catalysts for the synthesis of biobased polycarbonates and polyesters.

Aminotriphenolate derived Al(III) complexes combined with various nucleophiles have been used as binary catalysts for the coupling of limonene oxide and carbon dioxide to afford alternating polycarbonates. These Al(III) aminotriphenolate catalysts were able to produce stereo-regular, perfectly alternating *trans* polymers (*i.e.* in each repeat unit) from *cis* limonene oxide, whereas the pure *trans* isomer and *cis/trans* mixture gave rise to lower degrees of stereo-regularity. Since both *cis* and *trans* limonene oxide isomers were reactive, a regio-irregular polymer was produced with three different types of repeat units depending on the position where the nucleophilic attack occurs. Due to the regio-irregularity of the polycarbonate, the T_g obtained (around 78 °C) was rather low. However, using the pure *cis* isomer of limonene oxide as starting material, a regio-regular fully alternating polycarbonate could be prepared with 96% of *trans* repeat units incorporated in the polymer backbone, and this had a dramatic effect on the T_g value which increased from 78 °C to 112 °C. Therefore, by carefully selecting the catalyst (Al complex and type of nucleophile) and monomer structures both regio- and stereo-regularity of the polymer can be controlled and, as a consequence, also the T_g values (Scheme C.1).

The best Al(III) catalyst showed the potential to mediate the conversion of limonene oxide with high conversion levels of up to 71% under neat conditions, indicating a high degree of robustness and atom-efficiency of this catalytic process. Computational studies have revealed

unique features of the binary catalysts system, among which is the preferred nucleophilic attack on the quaternary carbon center in the limonene oxide substrate.

Scheme C.1 (a) A stereo-irregular poly(limonene)carbonate from *cis*/*trans* limonene oxide mixture. **(b)** A stereo-regular polymer from *cis* limonene oxide.

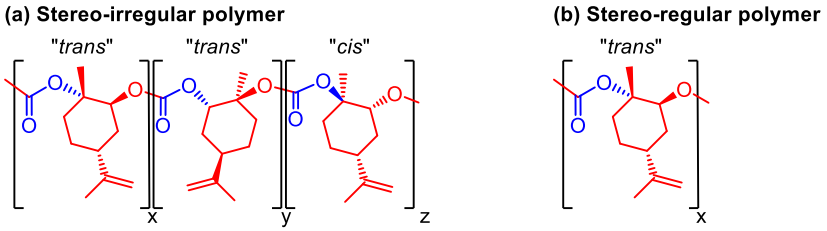

Other types of interesting polymers are aliphatic polyesters due their applications in biomedical devices. In order to obtain such renewable polyesters, a series of bio-sourced tricyclic anhydrides was prepared via Diels-Alder reactions. Six (partially) renewable tricyclic anhydrides based on terpenes, citraconic anhydride and 2,5-dimethylfuran were synthesized. These polymers were prepared using a Fe (III) aminotriphenolate catalyst as Lewis acid and PPNCl as nucleophile. Also, we investigated two Al(III) salphen catalysts and PPNCl as a binary catalytic system. First, propylene oxide (PO) was probed in the ROCOP of this epoxide with renewable or partially renewable anhydrides. Using the Fe(III) aminotriphenolate catalytic system full conversions in all cases was observed in less than 8 h. In the presence of (excess) PO, the six anhydrides (Scheme C.2) were converted into polyesters with perfectly alternating ester linkages and T_g values ranging from 66 to 108 ºC. Poly(PO-*alt*-**2a**), poly(PO-*alt*-**2b**) and poly(PO-*alt*-**2f**) are of particular interest as they have T_g values comparable to polystyrene. Then, the same series of six anhydrides was combined with a more rigid epoxide (cyclohexene oxide, CHO) and a significant increase in T_g compared to the corresponding polymers synthesized from PO was noted with T_g values ranging from 124 to 184 ºC. Similar to the PO based polymers, poly(CHO-*alt*-**2a**) displayed the highest T_g value (184 °C) which, to the best of our knowledge, is the highest reported T_g value for aliphatic polyesters prepared through chain-growth polymerization.

Scheme C.2 Partially renewable anhydrides (**2a–2e**) and fully renewable anhydride **2f**.

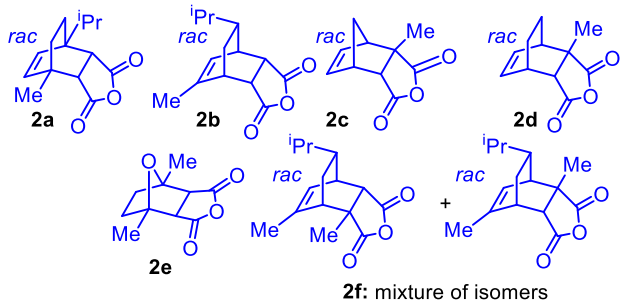

The use of terpene oxides as renewable monomers for the preparation of bio-based polymers remains rather limited. In order to advance the impact of such monomers, we have investigated the use of terpene derived epoxides (limonene oxide, carene oxide, limonene dioxide and menthene oxide, Scheme C.3) for the ring-opening copolymerization (ROCOP) in the presence of various aromatic anhydrides (phthalic anhydride and 1,8-naphthalic anhydride), and additionally the formation of semi-aromatic polyesters which are based on cyclohexadiene oxide. These copolymerization reactions were mostly performed under mild reaction conditions (65ºC, low loading of catalyst: 0.50 mol%) using a binary catalyst comprising of a Fe(III) based aminotriphenolate complex and PPNCl providing partially bio-based semi-aromatic polyesters with molecular weights of up to 25 kg/mol ($Đ$ = 1.54) and glass transitions spanning a wide range from 59 to 243 ºC. The copolymerization reactions proceeded with excellent selectivity towards fully alternating polyesters (≥ 98% ester bonds) with modular thermal properties that depend on the nature of the terpene oxide used, and are potentially useful towards the development of new coating and thermoset materials.

Scheme C.3 Renewable epoxides.

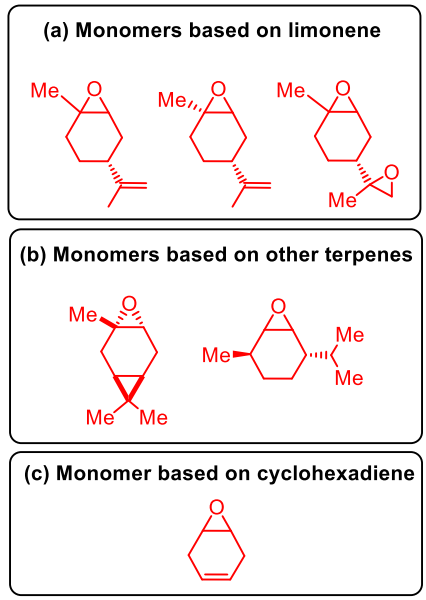

Finally, we investigated in collaboration with the group of Prof. José Mayoral and Prof. Clara Herrerías (University of Zaragoza) the development of renewable cyclic carbonates (cf., biocarbonates; Scheme C.4) from fatty acids. Various Al(III) aminotriphenolate/Nu binary catalyst systems (Nu = nucleophile) were examined with both oleic and linoleic based epoxides. Upon using an Al(III) aminotriphenolate as Lewis acid and PPNCl as nucleophile under mild operating conditions (10 bar of CO_2 and 70 °C) epoxidized methyl oleate was converted into the corresponding cyclic carbonate with a *cis:trans* selectivity of 97:3. Using the same mild conditions, we were able to prepare a bis-cyclic carbonate from the diepoxide based on methyl linoleate with a high *cis:trans* selectivity of 97:3. A challenging tris-cyclic carbonate based on epoxidized methyl linolenate was obtained with high *cis:trans* selectivity of 94:6. Three additional mono-cyclic carbonates were also synthesized based on other fatty acid precursors including elaidic acid, erucic acid and ricinoleic acid. An unexpected reactivity was found for epoxidized methyl ricinoleate, whose transformation to its corresponding mono-cyclic carbonate can be performed in the absence of externally added nucleophilic thereby generating selectively a *trans* cyclic carbonate. In this case, a different manifold is operative with the pendent alcohol unit present in the fatty acid backbone first involved in the activation of CO_2 leading to a six-membered carbonate intermediate. The six-membered carbonate is thermodynamically less stable than its five-membered analogues and therefore, the alcohol function present in the former allows for a nucleophilic attack onto the carbonate carbon center of the six-membered intermediate. This finally gave a five-membered product with formal inversion of the initial *cis* configuration present in the epoxide precursor. This alternative mechanism gives additional potential to control the stereoselective features in the conversion of more functional fatty acid precursors.

Scheme C.4 Mono-, bis- and tri-cyclic carbonates based on fatty acids.

(a) Cyclic carbonate based on oleic acid

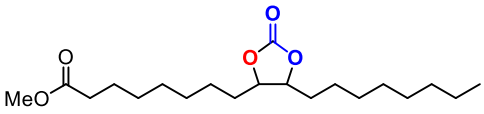

(b) Cyclic carbonate based on linoleic acid

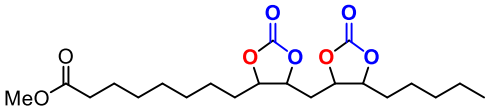

(c) Cyclic carbonate based on linolenic acid

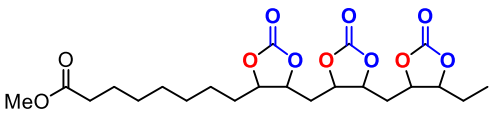

Acknowlegments

Curriculum Vitae

Leticia Peña Carrodeguas was born on August 18, 1986 in Ortigueira (Galicia). She started studying chemistry at the Universidade de Santiago de Compostela in October 2004 obtaining her BSc degree in September 2010. Her final research project in the field of organic chemistry was titled “Development of novel materials for hydrogen storage in ecological engines” in the group of Prof. Dr. Mercedes Torneiro Abuín. In September of 2012 she got her MSc degree in “Organic Chemistry” at the same university. After that, she started her PhD at the Institute of Chemical Research of Catalonia (ICIQ) under the supervision of Prof. Dr. Arjan W. Kleij in 2013 where she performed the research that is described in this thesis. Her PhD research was financially supported with a predoctoral fellowship FPI from the Spanish “Ministerio de economía y competitividad.” In 2015 she got a fellowship from the same Ministry to do a short stay at Cornell University under the supervision of Prof. Dr. Geoffrey Coates for three months. The resulting research is also described in this thesis. The results of this thesis have been communicated at CARISMA COST congress (Venecia, 2014), ICIQ's 10^{th} Anniversary Scientific Symposium (Tarragona, 2014), “Usos y conversión de CO_2: retos y oportunidades” (Madrid, 2015), INTECAT (Huelva, 2016) and International Conference on Carbon Dioxide Utilisation- ICCDU (Sheffield, 2016).

UNIVERSITAT ROVIRA I VIRGILI
AVANCES EN SISTEMAS INTERACTIVOS PARA PERSONAS CON PARÁLISIS CEREBRAL
Leticia Peña Carrodeguas

List of publications

- "*Semi-Aromatic Polyesters derived from Renewable Terpene Oxides with High Glass Transitions*"
  Peña Carrodeguas, L.; Kleij, Arjan W.
  2017, *under evaluation*.

- "*Fatty acid based biocarbonates: Al-mediated stereoselective preparation of mono-, di- and tricarbonates under mild and solvent-less conditions*"
  Peña Carrodeguas, L.; Cristofol, A.; Fraile, J. M.; Mayoral, J. A.; Dorado Horrillo, V.; Herrerías, C. I.; Kleij, A.W.
  Green Chem., **2017**, DOI 10.1039/C7GC01206C.

- "*Alternating Copolymerization of Propylene Oxide and Cyclohexene Oxide with Tricyclic Anhydrides: Access to Partially Renewable Aliphatic Polyesters with High Glass Transition Temperatures*"
  Sanford, M. J.; Peña Carrodeguas, L.; Van Zee, N. J.; Kleij, A. W.; Coates, G.W. *Macromolecules*, **2016**, *49*, 6394−6400.

- "*Al^{III} -Catalysed Formation of Poly(limonene)carbonate: DFT Analysis of the Origin of Stereoregularity*"
  Peña Carrodeguas, L.; González-Fabra, J.; Castro-Gómez, F.; Bo, C.; Kleij, A. W. *Chem. Eur.J.*, **2015**, *21*, 6115–6122.

- Book Chapter "*Metal Complexes Catalyzed Cyclization with CO_2*" in "*Carbon Dioxide and Organometallics*"
  Rintjema,J.; Peña Carrodeguas, L.; Laserna, V.; Sopeña,S.; Kleij, A. W. *Springer*, **2016**, *2*, 39-17 (ISBN: 1436-6002).

UNIVERSITAT ROVIRA I VIRGILI
AVANCES EN SISTEMAS INTERACTIVOS PARA PERSONAS CON PARÁLISIS CEREBRAL
Leticia Peña Carrodeguas

UNIVERSITAT ROVIRA I VIRGILI
AVANCES EN SISTEMAS INTERACTIVOS PARA PERSONAS CON PARÁLISIS CEREBRAL
Leticia Peña Carrodeguas

UNIVERSITAT ROVIRA I VIRGILI
AVANCES EN SISTEMAS INTERACTIVOS PARA PERSONAS CON PARÁLISIS CEREBRAL
Leticia Peña Carrodeguas

UNIVERSITAT ROVIRA I VIRGILI
AVANCES EN SISTEMAS INTERACTIVOS PARA PERSONAS CON PARÁLISIS CEREBRAL
Leticia Peña Carrodeguas